THE EVOLUTION OF FRONTS IN KPP-TYPE REACTION–DIFFUSION MODELS WITH CUT-OFF REACTION RATES

by

ALEX TISBURY

A thesis submitted to
The University of Birmingham
for the degree of
DOCTOR OF PHILOSOPHY

Joint Supervisors: Dr Alexandra Tzella and Professor David Needham
Internal Examiner: Dr John Meyer

School of Mathematics
College of Engineering and Physical Sciences
The University of Birmingham
February 2019

Abstract

This thesis concerns two closely related problems. Firstly, we consider Kolmogorov–Petrovskii–Piscounov (KPP) type models in the presence of an arbitrary cut-off in reaction rate at concentration $u = u_c$. For each fixed cut-off value $u_c \in (0, 1)$, we prove the existence of a unique permanent form travelling wave with a continuous and monotone decreasing propagation speed $v^*(u_c)$. We extend previous asymptotic results in the limit of small u_c and present new asymptotic results in the limit as u_c approaches 1, which are obtained via the systematic use of matched and regular asymptotic expansions, respectively. We then use the theory of matched asymptotic expansions to obtain a detailed description of the evolution of the asymptotic structure of the solution where, in particular, we establish the rate of convergence of the solution onto the permanent form travelling wave structure in large-time for arbitrary $u_c \in (0, 1)$. Secondly, we consider the impact of a heterogeneous environment enforced by a background shear flow on such fronts. We employ a two-scale asymptotic expansion to describe their speed of propagation in the limit of small Damköhler number (corresponding to slow reactions) and finite Péclet number (corresponding to similar strength of flow and molecular diffusivity).

I'd like to thank my supervisors without
whom this would of not been possible.
To my family and close friends, the
distraction you provided from allowing my
research to become all encompassing has
kept me sane for the last four years.
To my parents, you may not ever
understand what my work was on but at
least now you can show your friends this
and they can be equally as baffled.

CONTENTS

1 Introduction **1**

1.1 A class of homogeneous wave-fronts 1

1.1.1 The KPP model 2

1.1.2 The cut-off KPP model 7

1.1.3 From microscopic interactions to macroscopic kinetics 8

1.1.4 Aims and outline in relation to Chapters 2-5 13

1.2 A class of heterogeneous wave-fronts 14

1.2.1 The KPP model 14

1.2.2 The cut-off KPP model 19

1.2.3 Aims and outline in relation to Chapters 6-8 20

2 Formulation of the Problem **21**

3 Numerical solution to [QIVP] **25**

3.1 Numerical Method 25

3.2 Results 29

4 Permanent Form Travelling Wave Solution to [QIVP] **35**

4.1 Permanent Form Travelling Waves 35

4.2 The Existence and Uniqueness of a PTW Solution to [QIVP] 36

4.3 Asymptotic Structure of the PTW Solution when $u_c \to 0^+$ 46

4.4 Asymptotic Structure of the PTW Solution when $u_c \to 1^-$ 52

4.5 Numerical Example 56

4.6 Discussion and Conclusions . . . 59

5 Asymptotic Solution to [QIVP] 61

5.1 Asymptotic Solution to [QIVP] as $t \to 0^+$ . . . 61

5.2 Asymptotic Solution to [QIVP] as $|y| \to \infty$ . . . 71

5.3 Asymptotic Solution to [QIVP] as $t \to \infty$ . . . 74

5.4 Comparison with KPP asymptotics . . . 104

5.4.1 Formulation of the Problem . . . 104

5.4.2 Asymptotic Solution as $t \to 0^+$ . . . 105

5.4.3 Asymptotic Solution as $|y| \to \infty$ . . . 106

5.4.4 Asymptotic Solution as $t \to \infty$ . . . 106

5.5 Numerical Example . . . 108

5.5.1 Small time . . . 109

5.5.2 Large time . . . 110

5.6 Discussion and Conclusions . . . 113

6 Formulation of the Problem 116

7 Numerical solution to [IVPA] 122

7.1 Numerical Method . . . 122

7.1.1 The Advection Equation . . . 124

7.1.2 The Diffusion Equation . . . 129

7.1.3 The Reaction Equation . . . 135

7.1.4 Further Details . . . 135

7.2 Results . . . 136

8 Travelling Wave-Front Solutions to [QIVPA] 146

8.1 Travelling Wave-Fronts . . . 146

8.2 Homogenisation Limit . . . 148

8.2.1 Asymptotic solution for $\mathrm{Pe} = O(1)$ and $\mathrm{Da} = O(\epsilon^2)$ . . . 151

8.2.2 Numerical Example 160
8.3 Discussion and Conclusions 161

9 Future Work **164**

LIST OF FIGURES

1.1 (a) A sketch of a KPP-type reaction function. (b) A sketch of a cut-off KPP-type reaction function. 4

2.1 A sketch of the moving boundary problem. 23

3.1 A plot of the solution $u(y,t)$ to [QIVP] as it evolves over time. Results are obtained numerically for (a) $u_c = 0.1$, (b) $u_c = 0.5$ and (c) $u_c = 0.9$ for $t = 0$, 0.1, 1, 10 and $t = 30$ with the arrow pointing in the direction of increasing t. For panel (c), additional solutions obtained at $t = 100$, 200, 300, 350 and $t = 400$ are plotted. 31

3.2 A plot of $s(t)$ obtained numerically for $u_c = 0.1$ (top plot), $u_c = 0.5$ (middle plot) and $u_c = 0.9$ (bottom plot). 32

3.3 Comparison between $\dot{s}(t)$ (solid lines) and $v_\infty(u_c)$ (dashed lines). Results are obtained numerically for $u_c = 0.1$ (top plot), $u_c = 0.5$ (middle plot) and $u_c = 0.9$ (bottom plot) for (a) small time and (b) large time. 33

3.4 Comparison between $\dot{s}(t)$ (solid lines) and $v_\infty(u_c)$ (dashed lines). Results are obtained numerically for $u_c = 0.45$ (top plot) and $u_c = 0.55$ (bottom plot) for (a) small time and (b) large time. 34

3.5 A plot of $v_\infty(u_c)$ obtained numerically for selected values of $u_c \in (0,1)$. . . 34

4.1 The local phase portrait for the equilibrium points of the dynamical system (4.2.4). The thick black arrows denote the direction of the vector field $\boldsymbol{Q}(\alpha,\beta)$ along the line segments L_0, L_1 and on the boundary of D_-. . . . 39

4.2 The phase path $\mathcal{C}_0 = \mathcal{S}_1^+|_{v=0}$. 42

4.3 (a) Numerical solutions of $U_T(\bar{y})$ obtained from (4.3.5) for $u_c = 0.001, 0.01$ and 0.1, with the arrow pointing in the direction of increasing u_c (thick black lines), and exact solution derived from (4.2.29c) (thin black lines). These are plotted against the numerical solution of $U_m(\bar{y})$ (in red) obtained from (4.3.9). (b) Comparison between numerical and asymptotic results for $U_T(\bar{y})$ obtained for $\bar{y} \leq \bar{y}_c(u_c)$ for $u_c = 10^{-7}$ (in black) and $u_c = 10^{-5}$ (in blue). The numerical results are juxtaposed against the asymptotic expression (4.3.16) valid for $u_c \to 0^+$ and $\bar{y} \gg 1$ (dashed black and blue lines, respectively). These are plotted against the numerical solution of $U_m(\bar{y})$ (in solid red) and the large-$\bar{y}$ asymptotic expression (4.3.10) (dashed red line). 57

4.4 (a) Numerical solutions of $U_T(y)$ obtained from (4.2.3) for $u_c = 0.4$, 0.8, 0.9 and 0.99 (thick lines), with the arrow pointing in the direction of increasing u_c, and exact solution given by (4.2.29c) (thin lines). (b) Comparison between the numerical solutions of $U_T(y)$ and the asymptotic expression for $u_c \to 1^-$ derived from (4.4.16) (dashed black lines). 58

4.5 Comparison between asymptotic and numerical results of the speed for (a) small and (b) large cut-off values u_c. Numerical solutions of $v^*(u_c)$ derived from the boundary value problem (4.2.3) with f_c given by (4.5.1) are shown as solid lines. The dashed lines are the asymptotic predictions (4.3.27) and (4.4.17) of $v^*(u_c)$. In (a) the dotted line is expression (1.1.15) of Brunet and Derrida [14] and in (b) the red circles are the numerical solutions of $v_\infty(u_c)$ to [QIVP]. 59

5.1 A sketch of the structure of the solution to [QIVP] as $t \to 0^+$. 63

5.2 A sketch of $G_0(w)$. 77

5.3 A sketch of $\bar{G}_0(w)$. 79

5.4 A schematic representation of the location and thickness of the asymptotic regions in the solution to [QIVP] as $t \to \infty$. Here the exponents $G_0(w)$ and $\bar{G}_0(w)$ are given by (5.3.8) and (5.3.14), and there are thin transition regions at $w = -\sqrt{v^*(u_c)^2 - 4f'(1)}$ and at $w = v^*(u_c)$, respectively. Note that regions $\mathbf{III_L}$ and $\mathbf{III_R}$ are far field regions for $|w| \gg 1$ as $t \to \infty$. . . . 92

5.5 Sketches of the exponent in expansions (5.3.61) and (5.3.80), in regions $\mathbf{IV_L^a}$ and $\mathbf{IV_L^b}$, respectively, in brown; sketches of the exponent in expansions (5.3.33) and (5.3.44), in regions $\mathbf{IV_R^a}$ and $\mathbf{IV_R^b}$, respectively in blue; and sketches of the exponential corrections in regions $\mathbf{IV_L^b}$ ($a < w < 0$) and $\mathbf{IV_R^b}$ ($0 < w < v^*(u_c)$), respectively, in red. We have used the notation $a = -\sqrt{v^*(u_c)^2 - f'(1)}$ and $b = -2\sqrt{-f'(1)}$. 96

5.6 Comparison between numerical solutions of $\dot{s}(t)$ (solid lines) and the asymptotic expression (5.1.39) valid in small-time to leading order (dot-dashed lines) and to second order (dashed lines). Results are obtained for $u_c = 0.1$ (in black), $u_c = 0.5$ (in red) and $u_c = 0.9$ (in blue). 109

5.7 Comparison between numerical solutions of $u(y,t)$ (solid lines) and the asymptotic expressions (5.1.25), (5.1.33) and (5.1.38) valid in small-time (dashed lines). Results are obtained at time $t = 0.01$, $t = 0.1$ and $t = 1$ for (a) $u_c = 0.1$, (b) $u_c = 0.5$ and (c) $u_c = 0.9$ 110

5.8 Comparison between numerical solutions of $\dot{s}(t)$ (solid lines) and the two-term asymptotic expression (5.3.118) valid in large-time. Results are obtained for $u_c = 0.1$ (in black), $u_c = 0.5$ (in red) and $u_c = 0.9$ (in blue). . . . 111

5.9 Comparison between numerical solutions of $u(y,t)$ (black solid lines), numerical solutions of the PTW solution $U_T(y)$ (red solid lines) and the asymptotic expressions (5.3.33), (5.3.43), (5.3.50), (5.3.61), (5.3.79) and (5.3.93) valid in large-time (dashed lines). (a) Results are obtained at time $t = 1$ and $t = 5$ for $u_c = 0.1$, (b) at time $t = 1$ and $t = 10$ for $u_c = 0.5$ and (c) at time $t = 10$ and $t = 50$ for $u_c = 0.9$. 112

6.1 A sketch of the moving boundary problem at a fixed time t. 117

6.2 A sketch of the moving boundary problem at a fixed time t. 119

7.1 The solution $u(x, y, t)$ to (7.1.3) approximated numerically for shear flow $\boldsymbol{b} = (\sin(2y), 0)$ at time $t = 2$ for (a) a second order accurate flux function (7.1.9) and (b) a first order upwind flux function (7.1.11). 127

7.2 A sketch to illustrate which discrete mesh points are horizontally adjacent to the level curve $u = u_c$. 131

7.3 A sketch to illustrate which discrete mesh points are vertically adjacent to the level curve $u = u_c$. 131

7.4 A sketch of the discrete mesh points that are part of the set G_1 (circled in red) with $(i_1, j_1) = (i, j)$ and part of the set G_2 (circled in blue) with $(i_2, j_2) = (i - 1, j - 2)$. 133

7.5 Numerical approximation of $s_0(t)$ as it evolves over time for $u_c = 0.1$ (top plot), $u_c = 0.5$ (middle plot) and $u_c = 0.9$ (bottom plot). Results are obtained for Pe = 50 with (a) Da = 50, (b) Da = 1 and (c) Da = 1/50. . . 138

7.6 Numerical approximation of the profile of the moving boundary $s(y, t)$ as it evolves over time for Pe = 50 and Da = 50. Results are obtained for (a) $u_c = 0.1$, (b) $u_c = 0.5$ and (c) $u_c = 0.9$ for $t = 0$, $t = 0.1$, 1, 5, 10, 20 and $t = 30$ with the arrow pointing in the direction of increasing t. For panel (c), the axes have been increased so convergence can be observed. 139

7.7 Numerical approximation of the profile of the moving boundary $s(y, t)$ as it evolves over time for Pe = 50 and Da = 1. Results are obtained for (a) $u_c = 0.1$, (b) $u_c = 0.5$ and (c) $u_c = 0.9$ for $t = 0$, 0.1, 1, 10, 20, 30 and $t = 50$ with the arrow pointing in the direction of increasing t. For panel (c), additional solutions obtained at $t = 100$, 150, 200 and $t = 250$ are plotted and the axes have been increased so convergence can be observed. . 140

7.8 Numerical approximation of the profile of the moving boundary $s(y,t)$ as it evolves over time for Pe = 50 and Da = 1/50. Results are obtained for (a) $u_c = 0.1$, (b) $u_c = 0.5$ and (c) $u_c = 0.9$ for $t = 0$, $t = 1$, 10, 100, 200, 300, 400 and $t = 500$ with the arrow pointing in the direction of increasing t. 141

7.9 Numerical approximation of the large-time solution $u(x,y,t)$ to [IVPA] for Pe = 50 and Da = 50. Results are obtained for (a) $u_c = 0.1$ and (b) $u_c = 0.5$. 142

7.10 Numerical approximation of the large-time solution $u(x,y,t)$ to [IVPA] for Pe = 50 and Da = 1. Results are obtained for (a) $u_c = 0.1$ and (b) $u_c = 0.5$. 142

7.11 Numerical approximation of the large-time solution $u(x,y,t)$ to [IVPA] for Pe = 50 and Da = 1/50. Results are obtained for (a) $u_c = 0.1$ and (b) $u_c = 0.5$. 143

7.12 A plot of $c_\infty(u_c)$ obtained numerically for selected values of $u_c \in (0.05, 0.8)$. Results for Pe = 1 and Da = 1/25 are shown in black, Pe = Da = 1/10 are shown in red and Pe = 1/25 and Da = 1 are shown in blue. 145

8.1 Comparison between asymptotic and numerical results of the boundary $\phi_0(y)$ for $u_c = 0.1$ and Pe = 1. Numerical solutions derived from the large-time solution to [IVPA] are shown as solid lines with dashed lines representing the asymptotic prediction (8.2.38). Results are obtained for (a) Da = 1/25 and (b) Da = 1/50. 161

8.2 Comparison between asymptotic and numerical results of the speed for selected cut-off values $u_c \in (0,1)$ and Pe = 1. Numerical solutions of $c_\infty(u_c)$ derived from the large-time solution to [IVPA] are shown as circles with dashed lines representing the asymptotic prediction (8.2.40) of $c^*(u_c)$. The top plot is obtained for parameters Da = 1/25 and the bottom plot for Da = 1/50. 162

CHAPTER 1

INTRODUCTION

This thesis concerns two intimately related problems. The first problem concerns the evolution of wave-front solutions arising in a class of scalar homogeneous reaction–diffusion equations that are characterised by a cut-off in the reaction. The second problem considers the impact of a heterogeneous environment enforced by a background shear flow on these fronts. Consequently this introduction is in two parts. The first part (Section 1.1) introduces the homogeneous problem while the second part (Section 1.2) introduces the heterogeneous problem. Together these parts provide a review of both problems, a number of outstanding questions addressed in this thesis as well as an outline of the thesis.

1.1 A class of homogeneous wave-fronts

In the first part of the thesis we examine the evolution of travelling wave-fronts in homogeneous models of reaction–diffusion. These arise in a wide range of applications in mathematical chemistry, biology, ecology and genetics [13, 23, 43]. They describe the invasion of biological populations or chemical reactions and are usually established as a result of the interaction between molecular diffusion, local growth and saturation.

1.1.1 The KPP model

The simplest model that encapsulates this interaction is the KPP (or Fisher-KPP [25, 34]) model, named after the pioneering work by Fisher and Kolmogorov, Petrovskii and Piscounov. In one spatial dimension, this describes the evolution of the non-negative dimensional concentration $u(x,t)$ as

$$u_t = \kappa u_{xx} + \frac{1}{\tau} f(u), \qquad (x,t) \in \mathbb{R} \times \mathbb{R}^+, \tag{1.1.1a}$$

where the positive parameters τ and κ are the reaction time and molecular diffusivity. This is typically supplemented with Heaviside initial conditions

$$u(x,0) = \begin{cases} u_s, & \text{for } x < 0, \\ 0, & \text{for } x \geq 0, \end{cases} \tag{1.1.1b}$$

and boundary conditions

$$u(x,t) \to \begin{cases} u_s, & \text{as } x \to -\infty, \\ 0, & \text{as } x \to \infty, \end{cases} \tag{1.1.1c}$$

for a parameter $u_s > 0$ and with these limits being uniform for $t \in [0,T]$ and any $T > 0$. The function $f : \mathbb{R} \to \mathbb{R}$ is a KPP-type reaction function which satisfies conditions that $f \in C^1(\mathbb{R})$ with

$$f(0) = f(u_s) = 0, \quad f'(0) > 0, \quad f'(u_s) < 0, \tag{1.1.2a}$$

and in addition

$$0 < f(u) \leq u f'(0) \quad \forall u \in (0, u_s), \qquad f(u) < 0 \quad \forall u \in (u_s, \infty). \tag{1.1.2b}$$

We non-dimensionalise the initial-boundary value problem (1.1.1) for the KPP equation by introducing the following scalings

$$\hat{t} = \frac{f'(0)}{\tau}t, \quad \hat{x} = \sqrt{\frac{f'(0)}{\tau\kappa}}x, \quad \hat{u} = \frac{1}{u_s}u, \quad \hat{f} = \frac{1}{u_s f'(0)}f. \tag{1.1.3}$$

In terms of these scalings, the initial-boundary value problem (1.1.1) is reduced to (dropping hats for convenience)

$$u_t = u_{xx} + f(u), \qquad (x,t) \in \mathbb{R} \times \mathbb{R}^+, \tag{1.1.4a}$$

$$u(x,0) = \begin{cases} 1, & \text{for } x < 0, \\ 0, & \text{for } x \geq 0, \end{cases} \tag{1.1.4b}$$

$$u(x,t) \to \begin{cases} 1, & \text{as } x \to -\infty, \\ 0, & \text{as } x \to \infty, \end{cases} \tag{1.1.4c}$$

with these limits being uniform for $t \in [0,T]$ and any $T > 0$. The function $f : \mathbb{R} \to \mathbb{R}$ is a normalised KPP-type reaction function which satisfies conditions that $f \in C^1(\mathbb{R})$ with

$$f(0) = f(1) = 0, \quad f'(0) = 1, \quad f'(1) < 0, \tag{1.1.5a}$$

and in addition

$$0 < f(u) \leq u \quad \forall u \in (0,1), \qquad f(u) < 0 \quad \forall u \in (1,\infty). \tag{1.1.5b}$$

A prototypical example of such a KPP reaction is the Fisher reaction function [25] given by

$$f(u) = u(1-u). \tag{1.1.6}$$

An illustration of $f(u)$ against u is given in Figure 1.1(a).

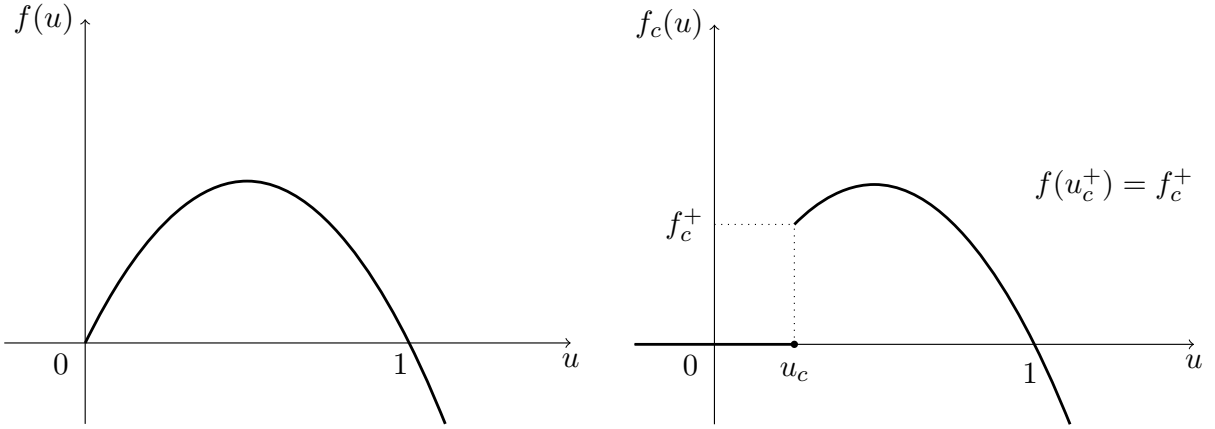

Figure 1.1: (a) A sketch of a KPP-type reaction function. (b) A sketch of a cut-off KPP-type reaction function.

Permanent form travelling wave solutions

It is well-known [23, 34, 3, 52] that the initial-boundary value problem (1.1.4) for the KPP equation supports a one-parameter family of non-negative permanent form travelling wave solutions of the form

$$u(x,t) = U(y) = U(x - vt) \quad \forall (x,t) \in \mathbb{R} \times \mathbb{R}^+. \tag{1.1.7}$$

These remain steady in time in a reference frame moving in the positive x-direction with speed $v \geq 0$ to be determined. Their existence and uniqueness (up to translation in origin) is established for

$$v \geq v_m = 2, \tag{1.1.8}$$

where v_m denotes the minimum speed of propagation. This is achieved by analysing the following nonlinear boundary value problem, namely,

$$U'' + vU' + f(U) = 0, \qquad -\infty < y < \infty, \tag{1.1.9a}$$

$$U(y) \geq 0, \qquad -\infty < y < \infty, \tag{1.1.9b}$$

$$U(y) \to \begin{cases} 1, & \text{as } y \to -\infty, \\ 0, & \text{as } y \to \infty, \end{cases} \tag{1.1.9c}$$

obtained by inserting (1.1.7) into equation (1.1.4a) and using (1.1.4c). The analysis is based on examining the existence of a unique heteroclinic orbit connecting the stable fixed point $(U, U') = (0, 0)$ to the unstable fixed point $(U, U') = (1, 0)$ in the (U, U') phase plane of the equivalent two-dimensional dynamical system obtained from (1.1.9). It is also used to establish that $U(y)$ is monotone decreasing in $y \in (-\infty, \infty)$, giving explicit expressions of the behaviour of the permanent form travelling wave near the two fixed points as

$$U(y) \sim \begin{cases} (A_\infty y + B_\infty)e^{-y}, & \text{as } y \to \infty, v = v_m = 2, \\ C_\infty e^{\alpha(v)y}, & \text{as } y \to \infty, v > v_m = 2, \end{cases} \tag{1.1.10a}$$

and for all $v \geq v_m = 2$,

$$U(y) \sim 1 - A_{-\infty}e^{\gamma y}, \qquad \text{as} \quad y \to -\infty, \tag{1.1.10b}$$

where

$$\alpha(v) = \frac{1}{2}(-v + \sqrt{v^2 - 4}) < 0, \qquad \gamma = (-1 + \sqrt{1 + |f'(1)|}) > 0, \tag{1.1.10c}$$

with $A_\infty(> 0)$, B_∞, $C_\infty(> 0)$ and $A_{-\infty}(> 0)$ being globally determined constants, dependent on the nonlinearity of the boundary value problem (1.1.9) (see, for example, [23, 30]).

Asymptotic solution to the initial-boundary value problem as $t \to \infty$

A central question is whether a permanent form travelling wave evolves in the solution to (1.1.4) at large times and if so what is its speed of propagation. It is well established [3, 24, 34] that the solution to (1.1.4) converges onto the permanent form travelling wave solution with minimum propagation speed $v = v_m = 2$ in the sense that there exists a function $s(t)$ such that as $t \to \infty$, $s(t)/t \to 2$ and

$$u(y + s(t), t) \to U(y), \tag{1.1.11}$$

uniformly in y. Here, $s(t)$ provides the location in the domain at which $u = u_c$, for $u_c \in (0, 1)$, specifically, $\{(s(t), t) \subset \mathbb{R} \times \mathbb{R}^+ : u(s(t), t) = u_c\}$; a usual choice is $u_c = 1/2$. A more detailed asymptotic description was provided by McKean [39, 40] and Bramson [11, 12] who, using a probabilistic approach, obtained that the rate of convergence of $u(y+s(t), t)$ onto $U(y)$ is algebraically small in t as $t \to \infty$, specifically $O(\dot{s}(t)-2)$, where

$$\dot{s}(t) = 2 - \frac{3}{2}t^{-1} + o(t^{-1}), \quad \text{as } t \to \infty, \tag{1.1.12}$$

with the dot denoting differentiation with respect to t. More recently, the same result has been established using a range of alternative approaches, based on a point patching procedure [14, 21], the theory of matched asymptotic expansions [10, 36] and rigorous bounds [31]. The advantage of the approach in [10, 36] is that the method is flexible and can be applied to a wider class of reactions.

The mechanism which selects the speed of propagation of the emerging permanent form travelling wave solution as well as the rate of convergence of the solution to the KPP equation (1.1.4a) onto the permanent form travelling wave solution is primarily based on the linearisation of (1.1.4a) at the leading edge of the travelling wave. There, the concentration u is small and the dynamics are unstable. As a result, any modification of the dynamics near the leading edge of the travelling wave would invalidate the mechanism

controlling the speed selection as well as the rate of convergence of the solution to the permanent form travelling wave solution.

1.1.2 The cut-off KPP model

This is precisely the case for the cut-off KPP model that Brunet and Derrida [14] proposed and considered. Motivated by the discrete nature of chemical and biological phenomena at the microscopic level, they took a reaction function that is effectively deactivated at points where the concentration u lies at or below a threshold value $u_c \in (0,1)$. This case corresponds to the cut-off KPP equation given by

$$u_t = u_{xx} + f_c(u), \qquad (x,t) \in \mathbb{R} \times \mathbb{R}^+, \tag{1.1.13a}$$

which is once more supplemented with Heaviside initial conditions

$$u(x,0) = \begin{cases} 1, & \text{for } x < 0, \\ 0, & \text{for } x \geq 0, \end{cases} \tag{1.1.13b}$$

and boundary conditions

$$u(x,t) \to \begin{cases} 1, & \text{as } x \to -\infty, \\ 0, & \text{as } x \to \infty, \end{cases} \tag{1.1.13c}$$

with these limits being uniform for $t \in [0,T]$ and any $T > 0$. The main difference is that the reaction function $f : \mathbb{R} \to \mathbb{R}$ in the KPP equation (1.1.4) is replaced with a cut-off reaction function $f_c : \mathbb{R} \to \mathbb{R}$ given by

$$f_c(u) = \begin{cases} f(u), & u \in (u_c, \infty), \\ 0, & u \in (-\infty, u_c], \end{cases} \tag{1.1.13d}$$

where $f(u)$ satisfies the KPP conditions (1.1.5). An illustration of $f_c(u)$ against u is given in Figure 1.1b, with $f_c^+ = f_c(u_c^+)$. The initial-boundary value problem (1.1.13) is the focus of the first part of this thesis. We henceforth refer to this initial-boundary value problem as [IVP].

Brunet and Derrida [14] considered the behaviour of permanent form travelling wave solutions arising for small values of u_c corresponding to a single particle cut-off for the specific case when

$$f(u) = u(1 - u^2). \tag{1.1.14}$$

Their main result is a prediction for the propagation speed $v^*(u_c)$ of the *unique* permanent form travelling wave given by

$$v^*(u_c) \approx 2 - \frac{\pi^2}{(\ln u_c)^2}, \quad \text{as} \quad u_c \to 0^+, \tag{1.1.15}$$

which they obtained using a point patching procedure. This significant result demonstrates the strong influence of a cut-off on the value of $v^*(u_c)$ for small values of u_c. Subsequently, a more rigorous approach was employed by Dumortier, Popovic and Kaper [19] who proved the existence and uniqueness of a permanent form travelling wave solution when u_c is small and used matched asymptotics in the phase plane to obtain that

$$v^*(u_c) \sim 2 - \frac{\pi^2}{(\ln u_c)^2} + O\left(\frac{1}{|\ln u_c|^3}\right), \quad \text{as} \quad u_c \to 0^+. \tag{1.1.16}$$

All these results have focused in the small u_c limit and the reaction function (1.1.14). There are no results describing how the solution to [IVP] evolves in time and whether this converges onto the permanenent form travelling wave solution.

1.1.3 From microscopic interactions to macroscopic kinetics

The cut-off KPP model is important as it attempts to go beyond the limitations of traditional 'mean field' or 'mass action' reaction kinetic theories. We here discuss in more

detail the assumptions behind the KPP model and the motivation behind the cut-off KPP model. This discussion is based on the review by Tesser and Doering [55] (see also [18]).

The 'mean field' or 'mass action' reaction kinetic theories offer a macroscopic description for the kinetics of the two-body reaction

$$\begin{aligned} A + B &\xrightarrow{k_+} B + B, \\ A + B &\xrightarrow{k_-} A + A, \end{aligned} \tag{1.1.17}$$

taking place inside a closed volume Ω, where A and B are two interacting particles and $k_+ > k_- \geq 0$ are the rate constants of the reaction. Let $N_A(t)$ and $N_B(t)$ denote the total number of A and B particles in Ω at time t. Then it is clear that the total number of particles in Ω

$$N = N_A(t) + N_B(t), \tag{1.1.18}$$

is conserved by this reaction.

In the mean field approach, the Law of Mass Action asserts that the rate at which a two-body reaction proceeds is proportional to the product of the number of reactants. For the autocatalytic reaction (1.1.17), this implies that

$$\frac{d}{dt}N_A = -\frac{(k_+ - k_-)}{\Omega}N_A N_B = -\frac{d}{dt}N_B. \tag{1.1.19}$$

It is convenient to consider the proportion of particles of type A. This is given by

$$U(t) = N_A(t)/N. \tag{1.1.20}$$

In this case (1.1.19) becomes the logistic equation

$$\frac{d}{dt}U = \frac{1}{\tau}U(1 - U). \tag{1.1.21}$$

where we have defined $\tau^{-1} = (k_+ - k_-)N/\Omega$. It is clear that as $N \to \infty$ and $\Omega \to \infty$, we

need $N/\Omega = O(1)$ for τ to remain finite.

The main assumption behind the mean field approach is that particles are well mixed (uniformly distributed) within the volume Ω at all times so that all A particles have a chance to interact with B particles at each time. This then means that we may further assume that particles A and B react at a rate that only depends on the density of reactants and not on their spatial distribution. When A and B particles move randomly, their spatial distribution becomes relevant. In this case we need to consider the evolution of the local proportions of particles of type A and B around position x at time t. In one spatial dimension, these are respectively denoted as $u(x,t)$ and $1-u(x,t)$ where

$$U(t) = \int_{-\infty}^{\infty} u(x,t)dx. \tag{1.1.22}$$

At the macroscopic level, Fick's Law [22] describes the random motion as a diffusion process. Combining reaction (1.1.17) with the process of diffusion leads to the KPP equation (1.1.1) with Fisher reaction function (1.1.6).

By design the mean field approach ignores chemical and biological fluctuations due to correlations that occur at the microscopic level. These are captured by considering a discrete microscopic Markov process. Let $p_n(t) = \text{Prob}(N_A(t) = n)$ where $n = 0, 1, \ldots, N$ and $p_{-1} = p_{N+1} = 0$. Then, the corresponding Master equation is given by

$$\begin{aligned} \frac{dp_n}{dt} = &-\frac{k_+}{\Omega} n(N-n)p_n + \frac{k_+}{\Omega}(n-1)(N-n+1)p_{n-1} \\ &-\frac{k_-}{\Omega} n(N-n)p_n + \frac{k_-}{\Omega}(n+1)(N-n-1)p_{n+1}. \end{aligned} \tag{1.1.23}$$

Let $u = n/N$ and define the function

$$P(u,t) = Np_n(t), \tag{1.1.24}$$

which converges onto the probability density function for the variable u with the discrete nature of the problem represented by $\epsilon = 1/N$. A continuum approximation is obtained

in the limit of $N \gg 1$ in which case individual jumps in $N_A(t)$ are small with $\epsilon \ll 1$. In the limit of $\epsilon \to 0$, equation (1.1.23) becomes

$$\begin{aligned}\epsilon^2 \frac{\partial P(u,t)}{\partial t} =& -\frac{k_+}{\Omega} u(1-u)P(u,t) + \frac{k_+}{\Omega}(u-\epsilon)(1-u+\epsilon)P(u-\epsilon,t) \\ & -\frac{k_-}{\Omega} u(1-u)P(u,t) + \frac{k_-}{\Omega}(u+\epsilon)(1-u-\epsilon)P(u+\epsilon,t),\end{aligned} \tag{1.1.25}$$

which simplifies to

$$\frac{\partial P(u,t)}{\partial t} = \frac{\partial}{\partial u}\left[-\frac{1}{\tau}u(1-u) + \frac{k_+ + k_-}{\Omega}\frac{\partial}{\partial u}u(1-u)\right]P(u,t) + O(\epsilon), \tag{1.1.26}$$

with boundary conditions $P(0,t) = P(1,t) = 0$. Ignoring $O(\epsilon)$ terms we obtain the Fokker-Planck equation. The Fokker-Planck equation is associated to the Itô stochastic differential equation for $U(t)$

$$dU(t) = \frac{1}{\tau}U(1-U)dt + \sigma\sqrt{U(1-U)}dW(t), \tag{1.1.27}$$

where $W(t)$ is the Wiener process used to represent random fluctuations in $U(t)$ in terms of a Gaussian white noise delta-correlated in time:

$$\langle W(t)W(s)\rangle = \delta(t-s).$$

The noise strength is given by $\sigma^2 = (k_+ + k_-)/\Omega$. As $\epsilon \to 0$, $\Omega = O(\epsilon^{-1})$ and $\sigma^2 = O(\epsilon)$. Therefore if U or $1-U$ are larger than $O(\epsilon) = O(N^{-1})$, then we recover the deterministic dynamics given by the logistic equation (1.1.21). However when U or $1-U$ are $O(\epsilon) = O(N^{-1})$, then both terms are important. Thus noise only matters when the number of A particles or the number of B particles is small compared to N. Including the process of diffusion leads to a stochastic version of the KPP equation (with Fisher reaction)

$$U_t = \kappa U_{xx} + \frac{1}{\tau}U(1-U) + \sqrt{\epsilon U(1-U)}W(x,t), \tag{1.1.28}$$

where $W(x,t)$ is a Gaussian white noise delta-correlated in time and space:

$$\langle W(x,t)W(y,s)\rangle = \delta(x-y)\delta(t-s).$$

Once again if U or $1-U$ are larger than $O(\epsilon) = O(N^{-1})$, then fluctuations are unimportant and we recover the deterministic KPP equation (1.1.4a). However when U or $1-U$ are $O(\epsilon) = O(N^{-1})$, then fluctuations are important and need to be taken into account. One expects that what happens for U close to 1 does not matter and instead it is the situation at the leading edge of the solution where U is small that controls the long-time properties of the solution.

One may now return to the Ito stochastic differential equation (1.1.27) and question how accurately does this represent the fluctuations that arise due to discreteness at the microscopic level. The Ito stochastic differential equation (1.1.27) is a continuum approximation. However, discreteness means that $U(t)$ is for all t an integer multiple of $1/N$. Thus, if $U(t)$ is non-zero, it cannot be smaller than $1/N$. It was this observation that led Brunet and Derrida [14] (see also [33]) to replace the classic logistic growth representing the reaction in equation (1.1.21) by a cut-off at $\epsilon = 1/N$ so that

$$\frac{d}{dt}U = \begin{cases} \frac{1}{\tau}U(1-U), & U \in (\epsilon, \infty), \\ 0, & U \in (-\infty, \epsilon]. \end{cases} \tag{1.1.29}$$

Using similar arguments as above we combine the cut-off reaction (1.1.29) with the process of diffusion from where we obtain the (non-dimensional) cut-off KPP equation (1.1.13) with $u_c = \epsilon$ and Fisher reaction function (1.1.6) where $u(x,t)$ is once more describing the local proportion of particles of type A.

1.1.4 Aims and outline in relation to Chapters 2-5

The aim of the first part of this thesis is to investigate the cut-off KPP model and address the number of fundamental questions that remain. The first question concerns the existence and uniqueness of a permanent form travelling wave solution for *arbitrary* threshold values u_c and KPP reaction functions $f(u)$. The second question concerns the propagation speed of such permanent form travelling wave solutions. The third question is with regard to the shape of the permanent form travelling wave solution. A final question concerns the evolution in time to the permanent form travelling wave solution. In this thesis we address all of these questions.

The outline of the first part of the thesis is as follows. In Chapter 2 we study classical solutions to [IVP] describing the cut-off KPP problem. We re-formulate [IVP] as a moving boundary problem. We then make a simple coordinate transformation to consider an equivalent initial-boundary value problem that we refer to as [QIVP]. In Chapter 3, we consider a numerical solution to [QIVP] with cut-off Fisher reaction function. The aim is to indicate whether the solution converges onto a permanent form travelling wave solution at large times. In Chapter 4, we examine the possibility that [QIVP] supports permanent form travelling wave solutions. We establish that for each cut-off value $u_c \in (0, 1)$, [QIVP] supports a unique permanent form travelling wave solution with a continuous and monotone decreasing propagation speed $v^*(u_c)$. We extend previous asymptotic results in the limit of small u_c and present new asymptotic results in the limit of large u_c which are respectively obtained via the systematic use of matched and regular asymptotic expansions. The asymptotic results are confirmed against numerical results obtained for the particular case of cut-off Fisher reaction function. In Chapter 5, we adapt the approach in [36] to obtain the detailed description of the large-t structure of the solution to [QIVP]. In particular, we use the theory of matched asymptotic expansions to establish that for all $u_c \in (0, 1)$, the solution to [QIVP] converges onto the permanent form travelling wave solution with propagation speed $v = v^*(u_c)$ at a rate that is linearly exponentially small

in t as $t \to \infty$, specifically $O(\dot{s}(t) - v^*(u_c))$, where

$$\dot{s}(t) = v^*(u_c) + O\left(t^\gamma \exp\left(-\frac{1}{4}v^*(u_c)^2 t\right)\right), \quad \text{as } t \to \infty, \tag{1.1.30}$$

(with $\gamma = -1/2$ or $-3/2$ depending on properties of $f_c(u)$) so that convergence slows down as u_c increases. Thus, introducing an arbitrary cut-off into the reaction function changes the rate of convergence of the large-time solution onto the permanent form travelling wave from algebraic (see, for example, [36]) to exponential. To conclude the chapter we illustrate the theory when applied for the specific case of cut-off Fisher reaction function.

1.2 A class of heterogeneous wave-fronts

In the second part of the thesis we examine the evolution of travelling waves in inhomogeneous models of reaction–diffusion. Inhomogeneities occur in many physical and biological systems, when the reactions take place in fluid or porous environments, with applications ranging from plankton blooms to combustion to groundwater contamination [54, 46, 17]. It is therefore fundamental to understand how inhomogeneities influence the evolution and propagation of fronts.

1.2.1 The KPP model

There has been a growing interest in analysing the impact of a background flow on the propagation of travelling waves. The main focus has been on incompressible periodic flows with KPP-type reactions. The approach is both theoretical see, for example, [28, 16, 53, 6, 5, 48, 8, 47, 62, 57] and experimental [50, 51, 56, 4].

The simplest model that incorporates the presence of a background heterogeneous flow is the KPP reaction–diffusion–advection equation

$$u_t + \boldsymbol{b} \cdot \nabla u = \kappa \Delta u + \frac{1}{\tau} f(u), \qquad (x, y, t) \in \mathbb{R} \times [0, \pi\ell] \times \mathbb{R}^+, \tag{1.2.1a}$$

with

$$\boldsymbol{b}(x,y) = (b(y), 0), \tag{1.2.1b}$$

representing a steady, shear flow with the function $b : [0, \pi l] \to \mathbb{R}$ satisfying $b \in C^1([0, \pi l])$ and, without loss of generality,

$$\int_0^{\pi\ell} b(y)dy = 0. \tag{1.2.1c}$$

Motivated by experiments, we consider the evolution of equation (1.2.1a) inside a two-dimensional channel domain. Equation (1.2.1a) is once again supplemented with the usual Heaviside initial conditions

$$u(x,y,0) = \begin{cases} u_s, & \text{for } x < 0, \\ 0, & \text{for } x \geq 0, \end{cases} \quad \text{for all } y \in [0, \pi\ell], \tag{1.2.1d}$$

and Neumann boundary conditions across the walls (i.e., the walls are impermeable) so that

$$\partial_y u(x,y,t) = 0, \qquad \text{at } y = 0, \pi\ell \text{ for all } (x,t) \in \mathbb{R} \times \mathbb{R}^+, \tag{1.2.1e}$$

as well as

$$u(x,y,t) \to \begin{cases} u_s, & \text{as } x \to -\infty, \\ 0, & \text{as } x \to \infty, \end{cases} \tag{1.2.1f}$$

with these limits being uniform for $y \in [0, \pi\ell]$, $t \in [0, T]$ and any $T > 0$. The function $f : \mathbb{R} \to \mathbb{R}$ is the KPP-type reaction function (see Section 1.1.1).

The initial-boundary value problem (1.2.1) for the KPP reaction–diffusion–advection equation can be non-dimensionalised by introducing the following scalings

$$\hat{t} = \frac{B}{\ell}t, \quad \hat{\boldsymbol{x}} = \frac{1}{\ell}\boldsymbol{x}, \quad \hat{u} = \frac{1}{u_s}u, \quad \hat{f} = \frac{1}{u_s f'(0)}f, \quad \hat{\boldsymbol{b}} = \frac{1}{B}\boldsymbol{b}, \tag{1.2.2}$$

where B is the maximum flow speed. In terms of these scalings, the initial-boundary

value problem (1.2.1) is reduced to (dropping hats for convenience)

$$u_t + \boldsymbol{b} \cdot \nabla u = \mathrm{Pe}^{-1} \Delta u + \mathrm{Da} f(u), \qquad (x, y, t) \in \mathbb{R} \times [0, \pi] \times \mathbb{R}^+, \tag{1.2.3a}$$

$$\boldsymbol{b}(x, y) = (b(y), 0), \quad \text{with} \quad b \in C^1([0, \pi]) \quad \text{and} \quad \int_0^\pi b(y) dy = 0, \tag{1.2.3b}$$

$$u(x, y, 0) = \begin{cases} 1, & \text{for } x < 0, \\ 0, & \text{for } x \geq 0, \end{cases} \quad \text{for all } y \in [0, \pi], \tag{1.2.3c}$$

$$\partial_y u(x, y, t) = 0, \qquad \text{at } y = 0, \pi \text{ and } (x, t) \in \mathbb{R} \times \mathbb{R}^+, \tag{1.2.3d}$$

$$u(x, y, t) \to \begin{cases} 1, & \text{as } x \to -\infty, \\ 0, & \text{as } x \to \infty, \end{cases} \tag{1.2.3e}$$

with these limits being uniform for $y \in [0, \pi]$, $t \in [0, T]$ and any $T > 0$. The two non-dimensional parameters are the Damköhler and Péclet numbers:

$$\mathrm{Da} = \frac{\ell f'(0)}{B\tau} \quad \text{and} \quad \mathrm{Pe} = \frac{B\ell}{\kappa}. \tag{1.2.4}$$

These respectively measure the strength of advection relative to reaction and to diffusion. Large values of Da and Pe correspond to strong reactions and flow when compared to diffusion.

Permanent form travelling wave solutions

In the presence of a background shear flow, permanent form travelling wave-front solutions are defined as solutions of the form

$$u(x, y, t) = U(\xi, y) = U(x - ct, y), \quad \forall (x, y, t) \in \mathbb{R} \times [0, \pi] \times \mathbb{R}^+. \tag{1.2.5}$$

These remain steady in time in a reference frame moving in the positive x-direction with speed $c \geq 0$ to be determined. Berestycki and Nirenberg [9] established their existence

and uniqueness (up to translation in origin) for

$$c \geq c_m, \tag{1.2.6}$$

where c_m denotes the minimum speed of propagation. This was achieved by analysing the nonlinear boundary value problem obtained by inserting (1.2.5) into equation (1.2.3a) and using (1.2.3c), (1.2.3d) and (1.2.3e). This is given by

$$\mathrm{Pe}^{-1}\Delta_{\xi,y}U + (c - b(y))\partial_\xi U + \mathrm{Da}f(U) = 0, \qquad (\xi, y) \in \mathbb{R} \times [0, \pi], \tag{1.2.7a}$$

$$b \in C^1([0,\pi]) \quad \text{and} \quad \int_0^\pi b(y)dy = 0, \tag{1.2.7b}$$

$$U(\xi, y) \geq 0, \qquad (\xi, y) \in \mathbb{R} \times [0, \pi], \tag{1.2.7c}$$

$$\partial_y U = 0, \qquad \text{at } y = 0, \pi \text{ and } \xi \in \mathbb{R}, \tag{1.2.7d}$$

$$U(\xi, y) \to \begin{cases} 1, & \text{as } \xi \to -\infty, \\ 0, & \text{as } \xi \to \infty, \end{cases} \tag{1.2.7e}$$

with these limits being uniform for $y \in [0, \pi]$. If the shear flow $b(y)$ does not have zero mean then the speed of propagation is changed proportionally by a constant amount, hence, we take the shear flow to satisfy condition (1.2.7b) without loss of generality. The analysis can no longer be based on a dynamical systems approach which requires establishing the existence of a unique heteroclinic orbit in phase space (Gardner's higher dimensional dynamical systems approach [27] is limited to constant b). The proof is intricate. It relies on establishing the precise exponential behaviour of U as $\xi \to \infty$ and $\xi \to -\infty$.

The precise value of c_m depends on the function $b(y)$ as well as the values of Pe and Da. It can be determined from the principal eigenvalue (that with maximum real part)

of the linear eigenvalue problem

$$\mathrm{Pe}^{-1}\Delta\psi + \left(b(y)q + \mathrm{Pe}^{-1}q^2\right)\psi = f(q)\psi, \qquad y \in [0,\pi], \tag{1.2.8a}$$

$$b \in C^1([0,\pi]) \quad \text{and} \quad \int_0^\pi b(y)dy = 0, \tag{1.2.8b}$$

$$\psi(y) \geq 0, \qquad \text{at } y = 0,\pi, \tag{1.2.8c}$$

$$\partial_y\psi = 0, \qquad \text{at } y = 0,\pi. \tag{1.2.8d}$$

This is obtained by looking for solutions of the form $U(\xi, y) = e^{-q\xi}\psi(y)$ for $q > 0$ and linearising around the leading edge of the front so that $f(U)$ is replaced by U. The Krein–Rutman theorem implies that this eigenvalue is unique, real and isolated. The front speed is then determined from the minimum speed condition

$$c_m = \inf_{q>0} \frac{f(q) + \mathrm{Da}}{q}. \tag{1.2.9}$$

The rigorous treatment in [9] confirms this to be the correct speed. The same formula was obtained by Gärtner and Freidlin [28] using an alternative probabilistic approach. When $b(y) = 0$, $f(q) = \mathrm{Pe}^{-1}q^2$, recovering the classical formula for the speed $c_m = v_m = 2B\sqrt{\mathrm{Da}/\mathrm{Pe}} = 2\sqrt{\kappa/\tau}$. When $b(y) \neq 0$, the eigenvalue problem (1.2.8) cannot be solved analytically. Numerically, it can be obtained by straightforward discretisation. Explicitly, it was obtained in the asymptotic limit of large Pe by Haynes and Vanneste [32] for the distinguished limits $q = O(\mathrm{Pe}^{-1})$ and $q = O(\mathrm{Pe})$.

Asymptotic solution to the initial-boundary value problem as $t \to \infty$

Freidlin and Gärtner [28] and Freidlin [26] were first to show that a permanent form travelling wave, with minimum propagation speed $c = c_m$, evolves in the solution of

(1.2.3) (see also [60, 7]) in the sense that

$$u(x-ct,y,t) \to \begin{cases} 1, & \text{if } 0 \le c < c_m, \\ 0, & \text{if } c > c_m, \end{cases} \quad \text{as } t \to \infty, \tag{1.2.10a}$$

locally with respect to the points $(x, y) \in \mathbb{R} \times [0, \pi]$. However, we are not aware of results providing a more detailed asymptotic description of the rate of convergence of $u(x-ct, y, t)$ onto $U(x - ct, y)$ as $t \to \infty$.

1.2.2 The cut-off KPP model

A natural question is what will happen when the KPP-type reaction is replaced by a cut-off KPP reaction. In this case, the cut-off KPP reaction–diffusion–advection equation reads as

$$u_t + \boldsymbol{b} \cdot \nabla u = \mathrm{Pe}^{-1} \Delta u + \mathrm{Da} f_c(u), \qquad (x, y, t) \in \mathbb{R} \times [0, \pi] \times \mathbb{R}^+, \tag{1.2.11a}$$

$$\boldsymbol{b}(x, y) = (b(y), 0), \quad \text{with} \quad b \in C^1([0, \pi]) \quad \text{and} \quad \int_0^\pi b(y)dy = 0, \tag{1.2.11b}$$

$$u(x, y, 0) = \begin{cases} 1, & \text{for } x < 0, \\ 0, & \text{for } x \ge 0, \end{cases} \quad \text{for all } y \in [0, \pi], \tag{1.2.11c}$$

$$\partial_y u(x, y, t) = 0, \qquad \text{at } y = 0, \pi \text{ and } (x, t) \in \mathbb{R} \times \mathbb{R}^+, \tag{1.2.11d}$$

$$u(x, y, t) \to \begin{cases} 1, & \text{as } x \to -\infty, \\ 0, & \text{as } x \to \infty, \end{cases} \tag{1.2.11e}$$

with these limits being uniform for $y \in [0, \pi]$, $t \in [0, T]$ and any $T > 0$. Here $f_c : \mathbb{R} \to \mathbb{R}$ is given by (1.1.13d). We are not aware of any rigorous results regarding this case. The initial-boundary value problem (1.2.11) is the focus of the second part of this thesis and is henceforth referred to as [IVPA]. In their work, Berestycki and Nirenberg [9] consider an ignition-type reaction (among other reactions) which, similar to the cut-off KPP reaction

f_c, is only switched on when the concentration passes a certain threshold value u_c. The difference between the two reactions is that in the ignition case, the reaction function is Lipschitz continuous on $[0, 1]$. This is not the case for the cut-off KPP reaction considered here.

1.2.3 Aims and outline in relation to Chapters 6-8

The aim of the second part of this thesis is to investigate the cut-off KPP reaction–diffusion–advection model. Our aim is to examine permanent form travelling wave solutions for arbitrary threshold values u_c and KPP reaction functions $f(u)$. We will employ a formal asymptotic approach to obtain the propagation speed of such permanent form travelling wave solutions.

The outline of the second part of the thesis is as follows. In Chapter 6 we study classical solutions to [IVPA] describing the cut-off KPP reaction–diffusion–advection problem. We re-formulate [IVPA] as a moving boundary problem. We then make a simple coordinate transformation to consider an equivalent initial-boundary value problem that we refer to as [QIVPA]. In Chapter 7, we consider a numerical solution to [IVPA] with cut-off Fisher reaction function. The aim is to determine whether it converges onto a permanent form travelling wave solution at large times. In Chapter 8, we assume that for each cut-off value $u_c \in (0, 1)$, [QIVPA] supports a unique permanent form travelling wave solution with a continuous propagation speed $c^*(u_c)$. We use homogenisation theory to approximate $c^*(u_c)$ as a function of u_c for $\mathrm{Pe} = O(1)$ and $\mathrm{PeDa} = O(\epsilon^2)$ where $\epsilon = o(1)$. The asymptotic results are confirmed against numerical results obtained for the particular case of cut-off Fisher reaction function.

CHAPTER 2

FORMULATION OF THE PROBLEM

Due to the discontinuity in $f_c(u)$ at $u = u_c$, it is convenient to re-structure [IVP] as a moving boundary problem. To this end, we introduce the domains:

$$D^L = \{(x,t) \in \mathbb{R} \times \mathbb{R}^+ : \quad x < s(t)\}, \tag{2.0.1a}$$

$$D^R = \{(x,t) \in \mathbb{R} \times \mathbb{R}^+ : \quad x > s(t)\}, \tag{2.0.1b}$$

and the curve

$$\mathcal{L} = \{(x,t) \in \mathbb{R} \times \mathbb{R}^+ : \quad x = s(t)\}, \tag{2.0.1c}$$

that describes the moving boundary between the two domains. The boundary is expressed in terms of $s(t)$ which satisfies $u(s(t),t) = u_c$, with $u \geq u_c$ in $\overline{D}^L$ and $u \leq u_c$ in $\overline{D}^R$. In this context, a classical solution will have $u : \mathbb{R} \times \overline{\mathbb{R}}^+ \to \mathbb{R}$ and $s : \overline{\mathbb{R}}^+ \to \mathbb{R}$ such that,

$$u \in C\left((\mathbb{R} \times \overline{\mathbb{R}}^+) \setminus \{(0,0)\}\right) \cap C^{1,1}\left(\mathbb{R} \times \mathbb{R}^+\right) \cap C^{2,1}\left(D^L \cup D^R\right), \tag{2.0.2}$$

$$s \in C\left(\mathbb{R}^+\right) \cap C^1\left(\mathbb{R}^+\right), \tag{2.0.3}$$

$$s(0^+) = 0. \tag{2.0.4}$$

The moving boundary problem is then formulated as follows,

$$u_t = u_{xx} + f_c(u), \quad (x,t) \in D^L \cup D^R, \tag{2.0.5a}$$

$$u \geq u_c \text{ in } \overline{D}^L, \quad u \leq u_c \text{ in } \overline{D}^R, \tag{2.0.5b}$$

$$u(x,0) = \begin{cases} 1, & x < 0, \\ 0, & x \geq 0, \end{cases} \tag{2.0.5c}$$

$$u(x,t) \to \begin{cases} 1 & \text{as} \quad x \to -\infty, \\ 0 & \text{as} \quad x \to \infty, \end{cases} \quad \text{uniformly for } t \in [0,T] \text{ for all } T > 0, \tag{2.0.5d}$$

$$u(s(t),t) = u_c, \quad t \in \mathbb{R}^+, \tag{2.0.5e}$$

$$u_x(s(t)^+,t) = u_x(s(t)^-,t), \quad t \in \mathbb{R}^+, \tag{2.0.5f}$$

$$s(0^+) = 0. \tag{2.0.5g}$$

The situation is illustrated in Figure 2.1. It is now convenient to make the simple coordinate transformation $(x,t) \to (y,t)$ with $y = x - s(t)$. We then introduce the following domains:

$$Q^L = \mathbb{R}^- \times \mathbb{R}^+, \qquad Q^R = \mathbb{R}^+ \times \mathbb{R}^+, \tag{2.0.6}$$

with $u : \mathbb{R} \times \overline{\mathbb{R}}^+ \to \mathbb{R}$ and $s : \overline{\mathbb{R}}^+ \to \mathbb{R}$ such that

$$u \in C\left((\mathbb{R} \times \overline{\mathbb{R}}^+) \setminus \{(0,0)\}\right) \cap C^{1,1}\left(\mathbb{R} \times \mathbb{R}^+\right) \cap C^{2,1}\left(Q^L \cup Q^R\right), \tag{2.0.7a}$$

$$s \in C\left(\mathbb{R}^+\right) \cap C^1\left(\mathbb{R}^+\right). \tag{2.0.7b}$$

The equivalent problem to (2.0.5) is then given by

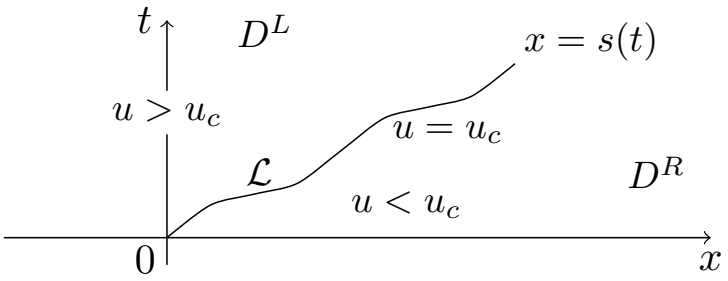

Figure 2.1: A sketch of the moving boundary problem.

$$u_t - \dot{s}(t)u_y = u_{yy} + f_c(u), \quad (y,t) \in Q^L \cup Q^R, \tag{2.0.8a}$$

$$u \geq u_c \text{ in } \overline{Q}^L, \quad u \leq u_c \text{ in } \overline{Q}^R, \tag{2.0.8b}$$

$$u(y,0) = \begin{cases} 1, & y < 0, \\ 0, & y \geq 0, \end{cases} \tag{2.0.8c}$$

$$u(y,t) \to \begin{cases} 1 & \text{as} \quad y \to -\infty, \\ 0 & \text{as} \quad y \to \infty, \end{cases} \quad \text{uniformly for } t \in [0,T] \text{ for all } T > 0, \tag{2.0.8d}$$

$$u(0,t) = u_c, \quad t \in \mathbb{R}^+, \tag{2.0.8e}$$

$$u_y(0^+,t) = u_y(0^-,t), \quad t \in \mathbb{R}^+, \tag{2.0.8f}$$

$$s(0^+) = 0, \tag{2.0.8g}$$

where the dot denotes differentiation with respect to time, t. This initial-boundary value problem will henceforth be referred to as [QIVP]. On using the classical maximum principle and comparison theorem (see, for example, [2] and [23]), together with translational invariance in y, and the regularity in (2.0.7), we can readily establish the following qualitative properties concerning [QIVP], namely,

(R1) $\quad 0 < u(y,t) < u_c \quad \forall (y,t) \in Q^R,$

(R2) $\quad u_c < u(y,t) < 1 \quad \forall (y,t) \in Q^L,$

(R3) $\quad u(y,t)$ is strictly monotone decreasing in $y \in \mathbb{R} \; \forall \; t \in \mathbb{R}^+$.

In addition, via the partial differential equation (2.0.8a) and the regularity conditions (2.0.7), we have

$$\text{(R4)} \qquad \begin{aligned} \lim_{y\to 0^+} u_{yy}(y,t) &= \lim_{y\to 0^+} \left(u_t(y,t) - \dot{s}(t)u_y(y,t)\right) \\ &= -\dot{s}(t)u_y(0,t) \quad \forall t \in \mathbb{R}^+, \end{aligned}$$

$$\text{(R5)} \qquad \begin{aligned} \lim_{y\to 0^-} u_{yy}(y,t) &= \lim_{y\to 0^-} \left(u_t(y,t) - \dot{s}(t)u_y(y,t) - f(u(y,t))\right) \\ &= -\dot{s}(t)u_y(0,t) - f_c^+ \quad \forall t \in \mathbb{R}^+, \end{aligned}$$

with the limits in (R4) and (R5) being uniform for $t \in [t_0, t_1]$ (for any $0 < t_0 < t_1$). It follows from (R4) and (R5) that

$$\text{(R6)} \qquad \left[u_{yy}(y,t)\right]_{y=0^-}^{y=0^+} = f_c^+ \quad \forall t \in \mathbb{R}^+,$$

whilst, (R3), (R5) and the regularity condition (2.0.7) establish

$$\text{(R7)} \qquad u_y(y,t) < 0 \quad \forall (y,t) \in \mathbb{R} \times \mathbb{R}^+.$$

Chapters 3, 4 and 5 concentrate on the analysis of [QIVP].

CHAPTER 3

NUMERICAL SOLUTION TO [QIVP]

In this chapter we consider a numerical solution to [QIVP]. We present results for the particular case of the cut-off Fisher reaction function, namely,

$$f_c(u) = \begin{cases} u(1-u), & u \in (u_c, \infty), \\ 0, & u \in (-\infty, u_c], \end{cases} \tag{3.0.1}$$

for fixed cut-off threshold $u_c \in (0,1)$. We adopt an explicit finite difference scheme to examine the large-time behaviour of $u(y,t)$ and $s(t)$, obtained numerically as a function of $u_c \in (0,1)$.

3.1 Numerical Method

We approximate $u(y,t)$ and $s(t)$ by piecewise linear functions defined on two evenly spaced space-time grids given by

$$y_i = -M + i\Delta y, \quad i \in \mathbb{I}, \qquad t_j = j\Delta t, \quad j \in \mathbb{J}, \tag{3.1.1}$$

where $\mathbb{I} = \{0, 1, \ldots, I-1, I+1, \ldots, 2I\}$ and $\mathbb{J} = \{0, 1, \ldots, J\}$, with $y_I = 0$ and $t_J = T$. We use $U_i^j \approx u_d(y_i, t_j)$ and $S^j \approx s_d(t_j)$ to approximate $u(y_i, t_j)$ and $s(t_j)$ for $i \in \mathbb{I}$ and $j \in \mathbb{J}$. We use explicit finite differences to approximate the derivatives in [QIVP] and then solve

the resulting differential equation. Specifically, we take first order forward differences to approximate the time derivatives and centred first and second differences to approximate the first and second space derivatives at all spatial points except at y_{I-1} and y_{I+1}. At these two points we use first order forward and backward differences to approximate the first order space derivative. This gives the following approximations,

$$\frac{\partial}{\partial t}U_i^j \approx \frac{U_i^{j+1}-U_i^j}{\Delta t}, \quad i \in \mathbb{I}, \qquad \frac{\partial}{\partial t}S^j \approx \frac{S^{j+1}-S^j}{\Delta t}, \tag{3.1.2}$$

$$\frac{\partial^2}{\partial y^2}U_i^j \approx \frac{U_{i+1}^j - 2U_i^j + U_{i-1}^j}{\Delta y^2}, \quad i \in \mathbb{I} \setminus \{0, 2I\}, \tag{3.1.3}$$

$$\frac{\partial}{\partial y}U_i^j \approx \frac{U_{i+1}^j - U_{i-1}^j}{2\Delta y}, \quad i \in \mathbb{I} \setminus \{0, I-1, I+1, 2I\}, \tag{3.1.4}$$

$$\frac{\partial}{\partial y}U_{I-1}^j \approx \frac{U_I^j - U_{I-1}^j}{\Delta y}, \qquad \frac{\partial}{\partial y}U_{I+1}^j \approx \frac{U_{I+1}^j - U_I^j}{\Delta y}, \tag{3.1.5}$$

for all $j \in \mathbb{J}$. On using (2.0.8e) to set $U_I^j = u_c$ for $j \in \mathbb{J} \setminus \{0\}$, these approximations lead to the following numerical scheme

$$\begin{aligned} U_i^{j+1} - U_i^j = {} & \mu\left(U_{i+1}^j - 2U_i^j + U_{i-1}^j\right) + \nu\left(S^{j+1} - S^j\right)\left(U_{i+1}^j - U_{i-1}^j\right) \\ & + \Delta t f_c(U_i^j), \quad i \in \mathbb{I} \setminus \{0, I-1, I+1, 2I\}, \end{aligned} \tag{3.1.6a}$$

$$\begin{aligned} U_{I-1}^{j+1} - U_{I-1}^j = {} & \mu\left(u_c - 2U_{I-1}^j + U_{I-2}^j\right) + 2\nu\left(S^{j+1} - S^j\right)\left(u_c - U_{I-1}^j\right) \\ & + \Delta t f_c(U_{I-1}^j), \end{aligned} \tag{3.1.6b}$$

$$U_{I+1}^{j+1} - U_{I+1}^j = \mu\left(U_{I+2}^j - 2U_{I+1}^j + u_c\right) + 2\nu\left(S^{j+1} - S^j\right)\left(U_{I+1}^j - u_c\right), \tag{3.1.6c}$$

for all $j \in \mathbb{J}$, with parameters $\mu = \Delta t/\Delta y^2$ and $\nu = 1/2\Delta y$. Using (2.0.8c) and (2.0.8g), we take as initial conditions

$$U_i^0 = \begin{cases} 1, & i = 0, 1, \ldots I-1, \\ 0, & i = I+1, \ldots, 2I, \end{cases} \qquad S^0 = 0, \tag{3.1.6d}$$

and use (2.0.8d) to set as boundary conditions

$$U_0^j = 1, \quad U_{2I}^j = 0, \quad j \in \mathbb{J}. \tag{3.1.6e}$$

The two space-time grids are coupled via the following condition

$$U_{I+1}^j + U_{I-1}^j = 2u_c, \quad j \in \mathbb{J} \setminus \{0\}, \tag{3.1.6f}$$

obtained using (2.0.8f). We use the discretised finite difference scheme (3.1.6), consisting of $2I-1$ linear equations, to solve for the unknowns U_i^j $(i \in \mathbb{I} \setminus \{0, 2I\})$ and S^j for each fixed $j \in \mathbb{J} \setminus \{0\}$. For ease of notation we define the $2I-1 \times 1$ vector $\boldsymbol{v}^j$ by

$$\boldsymbol{v}^j = \begin{bmatrix} U_1^j \\ \vdots \\ U_{I-1}^j \\ U_{I+1}^j \\ \vdots \\ U_{2I-1}^j \\ S^j \end{bmatrix}. \tag{3.1.7}$$

It follows from (3.1.6) that, for each fixed $j \in \mathbb{J}$, we obtain the large linear algebraic system

$$A\boldsymbol{v}^{j+1} = B\boldsymbol{v}^j + \boldsymbol{d}, \tag{3.1.8}$$

where A is a large, sparse almost tridiagonal matrix of dimension $2I-1 \times 2I-1$, B is a large, sparse almost block tridiagonal matrix of dimension $2I-1 \times 2I-1$ and $\boldsymbol{d}$ is a

$2I-1\times 1$ vector. In particular, the vector $\boldsymbol{d}$ is given by

$$d_i = \begin{cases} \mu, & i = 1, \\ \mu u_c, & i = I-1, I, \\ 2u_c, & i = 2I-1, \\ 0, & i \neq 1, I-1, I, 2I-1. \end{cases} \tag{3.1.9a}$$

The sparse matrices A and B are given by

$$A = \begin{bmatrix} 1 & 0 & \dots & & & & \cdots & 0 & g_1^j \\ 0 & \ddots & \ddots & & & & & \vdots & \vdots \\ \vdots & \ddots & & & & & & & \\ & & & & & & \ddots & \vdots & \vdots \\ \vdots & & & & & \ddots & \ddots & 0 & g_{2(I-1)}^j \\ 0 & \cdots & & & & \cdots & 0 & 1 & 0 \\ 0 & \cdots & 0 & 1 & 1 & 0 & \cdots & \cdots & 0 \end{bmatrix}, \tag{3.1.9b}$$

($I-1^{\text{th}}$ and I^{th} columns)

$$B = \begin{bmatrix} \bar{\mu}+b_1^j & \mu & 0 & \cdots & & & \cdots & 0 & g_1^j \\ \mu & \ddots & \ddots & \ddots & & & & \vdots & \vdots \\ 0 & \ddots & & \mu & & & & & \vdots \\ \vdots & \ddots & \mu & \bar{\mu}+b_{I-1}^j & 0 & & & & g_{I-1}^j \\ & & & 0 & \bar{\mu} & \mu & \ddots & \vdots & g_I^j \\ & & & & \mu & & \ddots & 0 & \vdots \\ \vdots & & & & \ddots & \ddots & \ddots & \mu & g_{2(I-1)}^j \\ 0 & \cdots & & & \cdots & 0 & \mu & \bar{\mu} & 0 \\ 0 & \cdots & & & & & & \cdots & 0 \end{bmatrix}, \tag{3.1.9c}$$

with parameter $\bar{\mu} = 1 - 2\mu$ and vectors

$$b_i^j = \Delta t(1 - v_i^j), \quad i = 1, \ldots, I-1, \tag{3.1.10}$$

$$g_i^j = \begin{cases} -\nu(v_2^j - 1), & i = 1, \\ -2\nu(u_c - v_{I-1}^j), & i = I-1, \\ -2\nu(v_I^j - u_c), & i = I, \\ \nu v_{2(I-1)-1}^j, & i = 2(I-1), \\ -\nu(v_{i+1}^j - v_{i-1}^j), & i \neq 1, I-1, I, 2(I-1), \end{cases} \tag{3.1.11}$$

for each fixed $j \in \mathbb{J}$. The large sparse linear algebraic system (3.1.8) is now solved in an evolutionary manner starting from $j = 0$ using MATLAB's mldivide algorithm. We observe that only the entries in the $(2I-1)^{\text{th}}$ column of the matrices A and B along with the leading diagonal of B vary in time.

3.2 Results

In this section we examine results obtained from numerical solution of the discretised scheme (3.1.6). We choose M to be sufficiently large so that boundary effects imposed by (3.1.6e) are negligible and we set the time step to be $\Delta t = 0.4\Delta y^2$ to ensure the *von Neumann* stability of the explicit method. In Table 3.1 we show the percentage difference between the numerically evaluated approximation to $\lim_{t\to\infty} \dot{s}(t) = v_\infty(u_c)$ and the values obtained when the resolution is doubled (by halving Δy) for decreasing values of Δy. We observe that as we decrease the mesh spacing Δy by a factor of 10, the percentage difference between the numerically calculated value of $v_\infty(u_c)$ and that obtained when the resolution is doubled, also decreases by a factor of 10. This behaviour is evident for the two values of u_c shown (with more values of $u_c \in (0, 1)$ considered but not presented here). Based on these figures, a mesh spacing of $\Delta y = 10^{-2}$ was selected to ensure that the solution is sufficiently well approximated, whilst keeping the computation time required

Δy	v_∞	% difference	time (seconds)
1×10^{-1}	1.184	2.551	0.5935
5×10^{-2}	1.215	1.380	3.518
1×10^{-2}	1.243	0.2406	372.7
5×10^{-3}	1.247	0.1601	3119

(a) $u_c = 0.1$

Δy	v_∞	% difference	time (seconds)
1×10^{-1}	0.5192	3.207	0.8676
5×10^{-2}	0.5364	1.722	5.518
1×10^{-2}	0.5518	0.3791	577.7
5×10^{-3}	0.5539	0.1802	4669

(b) $u_c = 0.5$

Table 3.1: Convergence of the numerical solution $\dot{s}(t)$ of [QIVP] to the constant v_∞ for decreasing Δy. This table shows the percentage difference between the numerically calculated value of v_∞ and the value obtained when the spatial resolution is doubled (by halving Δy). The time, given in seconds, is the calculation time for a typical run. Results are obtained numerically to four significant figures for (a) $u_c = 0.1$ and (b) $u_c = 0.5$.

to solve the numerical scheme (3.1.6) reasonable. Comparison with results obtained for a spatial resolution of $\Delta y = 5 \times 10^{-3}$ resulted in a less than 0.5% difference in $u(y,t)$.

Figures 3.1 - 3.3 represent the numerical solutions for $u(y,t)$ and $s(t)$, to [QIVP], respectively, with cut-off value $u_c = 0.1$, $u_c = 0.5$ and $u_c = 0.9$ obtained for selected values of t. We note that all of the qualitative properties (R1) - (R7) are observed in these figures. Figure 3.1 indicates that for $u_c = 0.1$, $u_c = 0.5$ and $u_c = 0.9$, a permanent form travelling wave develops in the large-time structure of the solution to [QIVP], that is, as $t \to \infty$. However, Figure 3.1(c) shows that for $u_c = 0.9$ we have to extend the period of time over which the solution is evaluated until $t \simeq 400$ to show convergence of the solution to [QIVP] onto the permanent form travelling wave structure. Moreover, this permanent form travelling wave will have propagation speed given by the limit of $\dot{s}(t)$ as

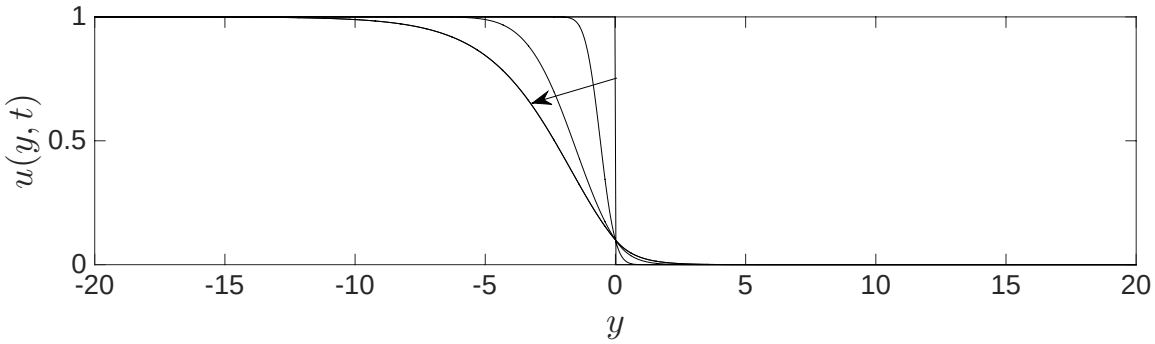

(a) $u_c = 0.1$

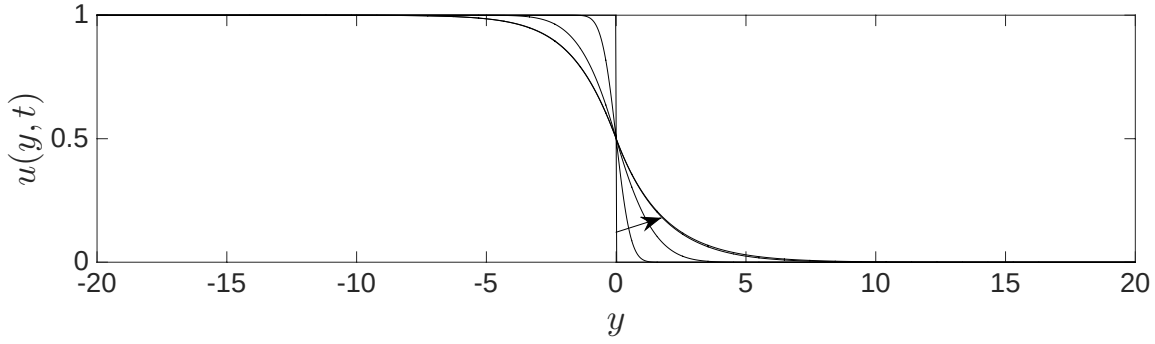

(b) $u_c = 0.5$

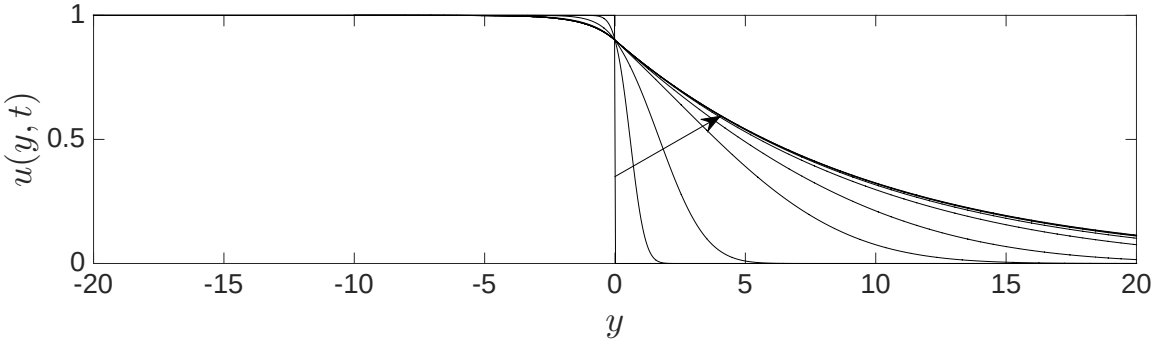

(c) $u_c = 0.9$

Figure 3.1: A plot of the solution $u(y,t)$ to [QIVP] as it evolves over time. Results are obtained numerically for (a) $u_c = 0.1$, (b) $u_c = 0.5$ and (c) $u_c = 0.9$ for $t = 0$, 0.1, 1, 10 and $t = 30$ with the arrow pointing in the direction of increasing t. For panel (c), additional solutions obtained at $t = 100$, 200, 300, 350 and $t = 400$ are plotted.

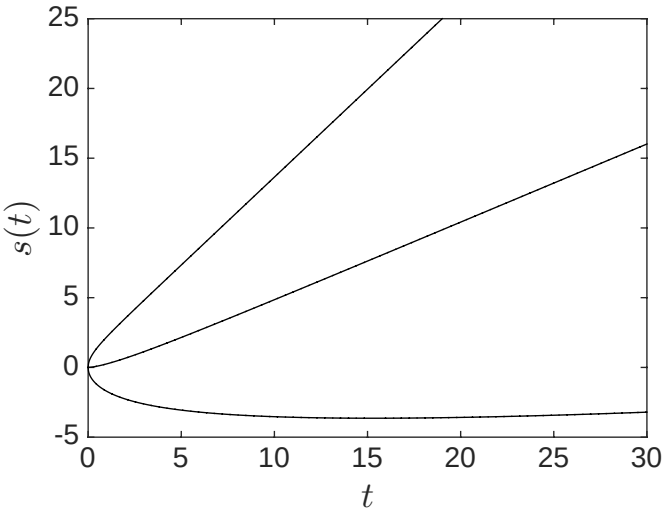

Figure 3.2: A plot of $s(t)$ obtained numerically for $u_c = 0.1$ (top plot), $u_c = 0.5$ (middle plot) and $u_c = 0.9$ (bottom plot).

$t \to \infty$ and in this case, this limit has

$$\lim_{t\to\infty} \dot{s}(t) = \begin{cases} 1.252, & \text{for } u_c = 0.1, \\ 0.5600, & \text{for } u_c = 0.5, \\ 0.1002, & \text{for } u_c = 0.9. \end{cases} \tag{3.2.1}$$

Additionally, we observe via Figure 3.2 and Figure 3.3 that for $u_c = 0.1$ and $u_c = 0.9$, $\dot{s}(t)$ appears to have a (integrable) singularity at $t = 0^+$. These features are persistent for all considered values of $u_c \neq 0.5$ (not shown). For $u_c = 0.5$, $\dot{s}(t)$ is regular in this limit, tending to 0 from above. Figure 3.4 focusses on two values of u_c close to $u_c = 0.5$. It shows the sign of $\dot{s}(t)$ as $t \to 0^+$ depends upon u_c, with $\dot{s}(t)$; initially positive when $0 < u_c < 0.5$ and initially negative when $0.5 < u_c < 1$. Moreover, when $0 < u_c < 0.2$, then $\dot{s}(t)$ is monotonic decreasing for all $t > 0$; when $0.2 < u_c < 0.5$, then $\dot{s}(t)$ decreases to a minimum value, before increasing to $v_\infty(u_c)$; and when $0.5 < u_c < 1$, then $\dot{s}(t)$ is monotonic increasing for all $t > 0$. These situations are illustrated for the specific cut-off values of $u_c = 0.1$, $u_c = 0.45$, $u_c = 0.5$ and $u_c = 0.55$ in Figures 3.3 and 3.4, respectively.

We conclude that the numerical solution of [QIVP] involves the formation of a permanent form travelling wave as $t \to \infty$, which has propagation speed $\dot{s}(t) \to v_\infty(u_c)$ as

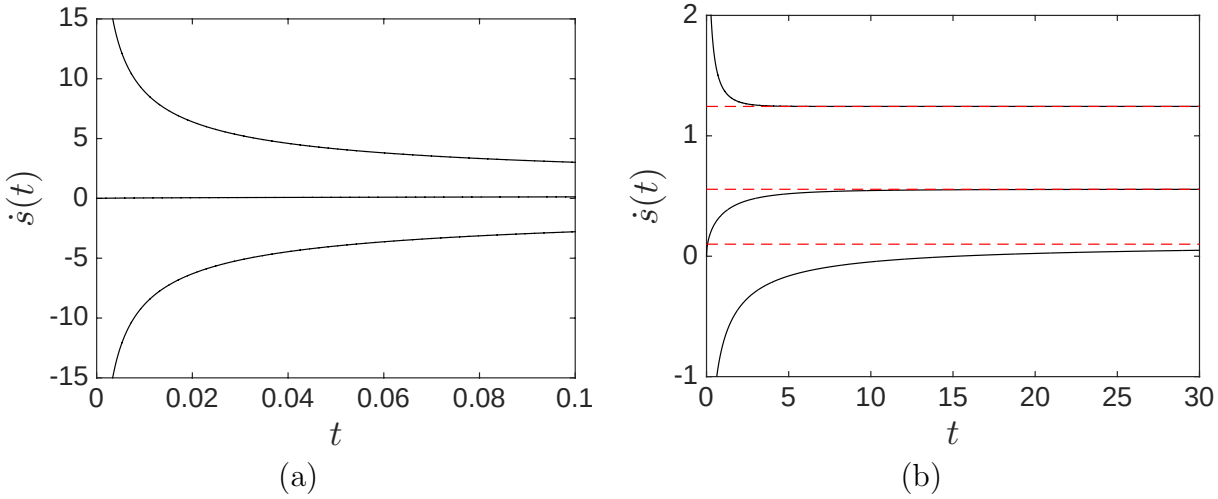

Figure 3.3: Comparison between $\dot{s}(t)$ (solid lines) and $v_\infty(u_c)$ (dashed lines). Results are obtained numerically for $u_c = 0.1$ (top plot), $u_c = 0.5$ (middle plot) and $u_c = 0.9$ (bottom plot) for (a) small time and (b) large time.

$t \to \infty$. The front width, defined as the distance from w_1 to w_2 where $u(w_1, t) = u_c$ and $u(w_2, t) = 1 - \epsilon$ for some small parameter $\epsilon \in (0, u_c)$, is dependent on the specific value of u_c. In particular, the front width is $O((1 - u_c)^{-1})$ in the limit as $u_c \to 1^-$ and $O(1)$ otherwise. We will verify this later. A graph of numerically calculated values $v_\infty(u_c)$ for $u_c \in (0, 1)$ is given in Figure 3.5, which indicates that $v_\infty(u_c)$ is monotone decreasing with $u_c \in (0, 1)$. However, we note that there are numerical issues with obtaining the value of $v_\infty(u_c)$ in both limits. As $u_c \to 0^+$, we require at least $\Delta y \leq u_c/5$ for the front solution to be sufficiently accurately approximated and as $u_c \to 1^-$, the solution $\dot{s}(t)$ does not converge to $v_\infty(u_c)$ until very large values of t. The computational time to obtain $v_\infty(u_c)$ in both limits is extortionate, nonetheless, we expect that $v_\infty(u_c) \to 2$ as $u_c \to 0^+$, whilst, $v_\infty(u_c) \to 0^+$ as $u_c \to 1^-$. In the limit as $u_c \to 1^-$, the front width increases substantially as we are approaching the limit of there being no permanent form travelling wave front (for $u_c = 1$). This is illustrated in Figure 3.1(c) for $u_c = 0.9$. With all this is mind, we next consider the existence and uniqueness of permanent form travelling waves to [QIVP].

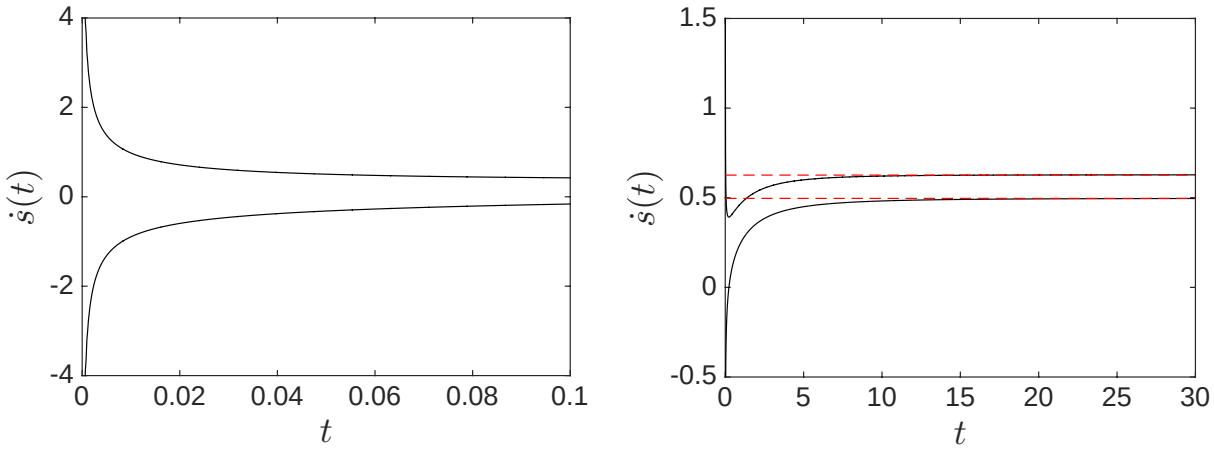

Figure 3.4: Comparison between $\dot{s}(t)$ (solid lines) and $v_\infty(u_c)$ (dashed lines). Results are obtained numerically for $u_c = 0.45$ (top plot) and $u_c = 0.55$ (bottom plot) for (a) small time and (b) large time.

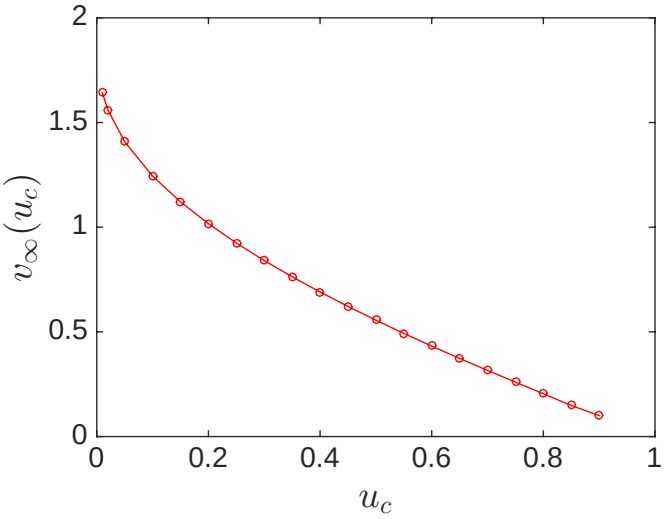

Figure 3.5: A plot of $v_\infty(u_c)$ obtained numerically for selected values of $u_c \in (0, 1)$.

CHAPTER 4

PERMANENT FORM TRAVELLING WAVE SOLUTION TO [QIVP]

In this chapter we study permanent form travelling wave solutions to [QIVP].

4.1 Permanent Form Travelling Waves

We anticipate that as $t \to \infty$, a permanent form travelling wave solution will develop in the solution to [QIVP], advancing with a (non-negative) propagation speed, allowing for the transition between the fully reacted state, $u = 1$ as $y \to -\infty$, to the unreacted state, $u = 0$ as $y \to \infty$. Therefore, in this section we focus attention on the possibility of [QIVP] supporting permanent form travelling wave solutions (henceforth referred to as PTW solutions). We begin by establishing the existence and uniqueness of a PTW to [QIVP] for each fixed $u_c \in (0, 1)$, denoting the unique propagation speed by $v = v^*(u_c)$. We then consider limiting values of $v^*(u_c)$ as $u_c \to 0^+$ and $u_c \to 1^-$.

4.2 The Existence and Uniqueness of a PTW Solution to [QIVP]

A PTW solution to [QIVP], with constant speed of propagation $v \geq 0$, is a steady state solution to [QIVP] with $u : \mathbb{R} \times \mathbb{R}^+ \to \mathbb{R}$ and $s : \overline{\mathbb{R}}^+ \to \mathbb{R}$ such that

$$u(y,t) = U_T(y) \quad \forall (y,t) \in \mathbb{R} \times \mathbb{R}^+, \tag{4.2.1}$$

$$\dot{s}(t) = v \quad \forall t \in \mathbb{R}^+, \tag{4.2.2}$$

where $U_T \in C^1(\mathbb{R}) \cap C^2(\mathbb{R} \setminus \{0\})$ and $v \geq 0$ satisfy the nonlinear boundary value problem,

$$U_T'' + vU_T' + f_c(U_T) = 0, \qquad y \in \mathbb{R} \setminus \{0\}, \tag{4.2.3a}$$

$$U_T \geq u_c \quad \forall y < 0, \qquad 0 \leq U_T \leq u_c \quad \forall y > 0, \tag{4.2.3b}$$

$$U_T(0) = u_c, \tag{4.2.3c}$$

$$U_T(y) \to \begin{cases} 1, & \text{for } y \to -\infty, \\ 0, & \text{for } y \to \infty, \end{cases} \tag{4.2.3d}$$

where the dash denotes differentiation with respect to y. The nonlinear boundary value problem (4.2.3) can be thought of as a nonlinear eigenvalue problem with the eigenvalue being the propagation speed $v \geq 0$.

It is convenient to consider the ordinary differential equation (4.2.3) as the following equivalent autonomous first-order two-dimensional dynamical system, with $\alpha = U_T$ and $\beta = U_T'$, namely,

$$\begin{aligned} \alpha' &= \beta, \\ \beta' &= -v\beta - f_c(\alpha), \end{aligned} \tag{4.2.4}$$

with $y \in \mathbb{R}$. We will analyse this dynamical system in the (α, β) phase plane for $v \geq 0$. In particular, it is straightforward to establish that the existence of a solution to (4.2.3) is equivalent to the existence of a heteroclinic connection in the (α, β) phase plane, for

the dynamical system (4.2.4), which connects the equilibrium point $(1,0)$, as $y \to -\infty$, to the equilibrium point $(0,0)$, as $y \to \infty$ (the translational invariance is then fixed by condition (4.2.3c) which requires that $\alpha(0) = u_c$). From (4.2.3b), this heteroclinic connection must remain in the $\alpha \geq 0$ half plane of the (α, β) phase plane, which we denote by $R^+ = \{(\alpha,\beta) : (\alpha,\beta) \in \overline{\mathbb{R}}^+ \times \mathbb{R}\}$. We henceforth focus on this region of the (α, β) phase plane.

However, before we proceed further, it is first worth considering the effect of introducing the cut-off into the reaction function on the dynamical system (4.2.4). To that end, we introduce the function $\boldsymbol{Q} : \mathbb{R}^2 \to \mathbb{R}^2$ where $\boldsymbol{Q}(\alpha,\beta)$ is given by

$$\boldsymbol{Q}(\alpha,\beta) = (\beta, -v\beta - f_c(\alpha)), \tag{4.2.5}$$

to represent the vector field generating the dynamical system (4.2.4). We observe that, in the (α,β) phase plane, the effect of the discontinuity in $f_c(\alpha)$ across the line $\alpha = u_c$ is simply to *refract* the phase paths passing through this line. In particular, for each $\beta \in \mathbb{R}$, there is exactly one phase path passing through (u_c, β), which has tangent vectors, $\boldsymbol{Q}(u_c^-, \beta) = (\beta, -v\beta)$ and $\boldsymbol{Q}(u_c^+, \beta) = (\beta, -v\beta - f_c^+)$. Thus, the refraction vector for the phase paths which cross the line $\alpha = u_c$ is

$$\begin{aligned} \boldsymbol{R}(u_c,\beta) &= \boldsymbol{Q}(u_c^+,\beta) - \boldsymbol{Q}(u_c^-,\beta) \\ &= (0, -f_c^+). \end{aligned} \tag{4.2.6}$$

We observe that the refraction vector (4.2.6) is independent of $(\beta, v) \in \mathbb{R} \times \overline{\mathbb{R}}^+$ and depends continuously on $u_c \in (0,1)$. It follows that

$$\boldsymbol{R}(u_c,\beta) \to \boldsymbol{0} \quad \text{as} \quad u_c \to 0, \tag{4.2.7}$$

uniformly in $(\beta, v) \in \mathbb{R} \times \overline{\mathbb{R}}^+$. After determining the effect of the discontinuity on the phase paths of the dynamical system (4.2.4) in R^+, we next consider the equilibrium

points of (4.2.4) in R^+. These are readily found to be at locations

$$\boldsymbol{e_a} = (a, 0) \quad \text{for each } a \in [0, u_c], \tag{4.2.8a}$$

$$\boldsymbol{e_1} = (1, 0). \tag{4.2.8b}$$

We begin by examining the local phase portrait in the neighbourhood of the equilibrium point $\boldsymbol{e_1}$. We find that $\boldsymbol{e_1}$ is a hyperbolic equilibrium point. Moreover, $\boldsymbol{e_1}$ is a saddle point with eigenvalues

$$\lambda_{\pm}(v) = \frac{1}{2}\left(-v \pm \sqrt{v^2 + 4|f_c'(1)|}\right). \tag{4.2.9}$$

The associated local straight line paths of $\boldsymbol{e_1}$ are given by

$$\beta(\alpha) = -\lambda_{\pm}(v)(1 - \alpha), \tag{4.2.10}$$

where the negative (positive) eigenvalue corresponds to the local stable (unstable) manifold. We denote the phase path which forms the part of the unstable manifold entering $D_+ = \{(\alpha, \beta) : 0 < \alpha < 1, \beta < 0\}$ as $\mathcal{S}_1^+$. Similarly, we denote $\mathcal{S}_1^-$ as the phase path which forms part of the unstable manifold entering $D_- = \{(\alpha, \beta) : \alpha > 1, \beta > 0\}$.

We next determine the local phase portrait of the equilibrium points $\boldsymbol{e_a}$ for each $a \in [0, u_c]$. For $a \in (0, u_c)$ and $v > 0$, each of the equilibrium points $\boldsymbol{e_a}$ is non-hyperbolic with a single stable manifold in R^+ given by $\{(\alpha, \beta) : \beta = -v(\alpha - a);\ 0 \leq \alpha \leq u_c\}$. Also, the equilibrium point $\boldsymbol{e_0}$ is non-hyperbolic with a single stable manifold in $\mathbb{R}^+$ which we will denote by

$$\mathcal{S}_0 = \{(\alpha, \beta) : \beta = -v\alpha;\ 0 \leq \alpha \leq u_c\}. \tag{4.2.11}$$

Finally, the equilibrium point $\boldsymbol{e_{u_c}}$ is again non-hyperbolic, and, for $0 \leq \alpha \leq u_c$, has a single stable manifold in R^+ given by $\{(\alpha, \beta) : \beta = -v(\alpha - u_c);\ 0 \leq \alpha \leq u_c\}$. In fact, the collection of phase paths of the dynamical system (4.2.4) in the region $\{(\alpha, \beta) : 0 \leq \alpha \leq u_c,\ \beta \leq 0\}$ is given by the family of curves $\beta = c - v\alpha$, for each $c \in \mathbb{R}$. The situation is

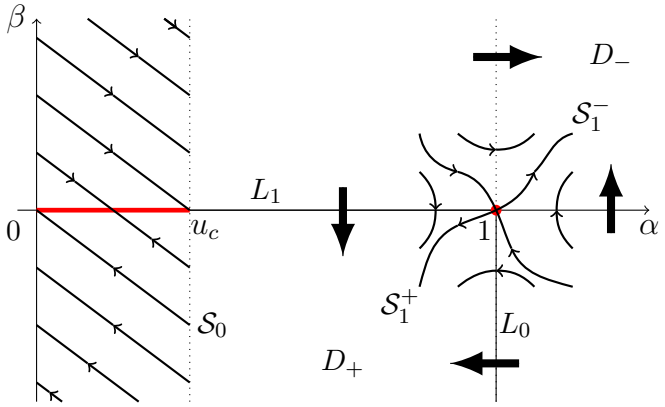

Figure 4.1: The local phase portrait for the equilibrium points of the dynamical system (4.2.4). The thick black arrows denote the direction of the vector field $\boldsymbol{Q}(\alpha, \beta)$ along the line segments L_0, L_1 and on the boundary of D_-.

illustrated in Figure 4.1.

Next, for the line segment $\{(\alpha, \beta) : \alpha = 1,\ \beta > 0\}$, we observe the following,

$$\boldsymbol{Q}(\alpha, \beta) \cdot (1, 0) = \beta > 0. \tag{4.2.12}$$

Similarly, for the line segment $\{(\alpha, \beta) : \alpha > 1,\ \beta = 0\}$, we observe that

$$\boldsymbol{Q}(\alpha, \beta) \cdot (0, 1) = -f_c(\alpha) > 0. \tag{4.2.13}$$

Together with the local structure at the equilibrium point $\boldsymbol{e_1}$, we conclude from (4.2.12) and (4.2.13) that the region D_- is a strictly positively invariant region for the dynamical system (4.2.4). We now examine the line segments $L_0 = \{(\alpha, \beta) : \alpha = 1,\ \beta < 0\}$ and $L_1 = \{(\alpha, \beta) : u_c < \alpha < 1,\ \beta = 0\}$, we observe that

$$\boldsymbol{Q}(\alpha, \beta) \cdot (-1, 0) = -\beta > 0 \quad \forall (\alpha, \beta) \in L_0, \tag{4.2.14}$$

$$\boldsymbol{Q}(\alpha, \beta) \cdot (0, -1) = f_c(\alpha) > 0 \quad \forall (\alpha, \beta) \in L_1. \tag{4.2.15}$$

In addition, for $v > 0$, we observe that for all $(\alpha, \beta) \in R^+$

$$\nabla \cdot \boldsymbol{Q}(\alpha, \beta) = -v < 0. \tag{4.2.16}$$

Thus, for any $v > 0$, it follows from the Bendixson negative criterion (see, for example, [59]) that (4.2.4) has no periodic orbits, homoclinic orbits or heteroclinic cycles in R^+. Finally, we observe that at each $(\alpha, \beta) \in R^+ \setminus (\{\boldsymbol{e_1}\} \cup \{\boldsymbol{e_a} : 0 \leq a \leq u_c\})$ the vector field $\boldsymbol{Q}(\alpha, \beta)$ rotates continuously clockwise for increasing $v \geq 0$. At the equilibrium point $\boldsymbol{e_1}$, the unstable manifold $\mathcal{S}_1^+$ rotates clockwise for increasing $v \geq 0$, as does the stable manifold $\mathcal{S}_0$ at the equilibrium point $\boldsymbol{e_0}$.

As the phase path $\mathcal{S}_1^-$ enters D_- on leaving $\boldsymbol{e_1}$, and we have established that D_- is a strictly positively invariant region for the dynamical system (4.2.4), we conclude that this cannot correspond to a heteroclinic connection between $\boldsymbol{e_1}$ and $\boldsymbol{e_0}$. Thus, at any $v \geq 0$, the existence of a heteroclinic connection in R^+ connecting $\boldsymbol{e_1}$, as $y \to -\infty$, to $\boldsymbol{e_0}$, as $y \to \infty$, is equivalent to the phase path $\mathcal{S}_1^+$, leaving $\boldsymbol{e_1}$, being coincident with the phase path $\mathcal{S}_0$, entering $\boldsymbol{e_0}$. It also follows that, at those $v \geq 0$ when such a heteroclinic connection exists, then it is unique.

We are now in a position to investigate for which values of $v \geq 0$, if any, the required heteroclinic connection exists in R^+. When $v = 0$, it follows directly from (4.2.4) that the phase path $\mathcal{S}_1^+$ has graph $(\alpha, \beta_0(\alpha))$ where

$$\beta_0(\alpha) = -\left(2\int_\alpha^1 f_c(\gamma)d\gamma\right)^{\frac{1}{2}}, \tag{4.2.17}$$

for $\alpha \in [0, 1]$. Thus, $\beta_0(\alpha)$ is (non-positive) non-decreasing for $\alpha \in [0, 1]$ with

$$\beta_0(0) = -\left(2\int_{u_c}^1 f_c(\gamma)d\gamma\right)^{\frac{1}{2}} < 0, \tag{4.2.18a}$$

and, via the vector field (4.2.5) and local straight line paths of $\boldsymbol{e_1}$ (4.2.10),

$$\beta_0'(1) = (-f_c'(1))^{\frac{1}{2}}\,. \tag{4.2.18b}$$

We denote the phase path $\mathcal{S}_1^+|_{v=0}$ as $\mathcal{C}_0$, and note from (4.2.17) that $\mathcal{C}_0 \subset \overline{D}^+$ as illustrated in Figure 4.2. We conclude from (4.2.18a) that when $v = 0$ no heteroclinic connection exists from $\boldsymbol{e_1}$ to $\boldsymbol{e_0}$. Moreover, it follows from the rotational properties of the vector field $\boldsymbol{Q}(\alpha, \beta)$ as discussed earlier, that, for each $v > 0$, we have

$$\boldsymbol{Q}(\alpha, \beta_0(\alpha)) \cdot \boldsymbol{n_0}(\alpha) < 0, \tag{4.2.19}$$

for all $\alpha \in [0, 1)$, where $\boldsymbol{n_0}(\alpha)$ is the unit normal to $\mathcal{C}_0$ as shown in Figure 4.2. We define the line segments $L_2 = \{(\alpha, \beta) : \alpha = 0,\ \beta_0(0) < \beta < 0\}$ and $L_3 = \{(\alpha, \beta) : 0 \leq \alpha \leq 1,\ \beta = 0\}$ and denote the region $\Omega_0 \subset D_+$ as that region bounded by $\partial\Omega_0 = L_2 \cup L_3 \cup \mathcal{C}_0$. We observe, via the rotational properties of $\mathcal{S}_1^+$ at $\boldsymbol{e_1}$, that for any $v > 0$, then $\mathcal{S}_1^+|_v$ enters Ω_0 on leaving $\boldsymbol{e_1}$. Moreover, from (4.2.16), $\overline{\Omega}_0$ contains no periodic orbits, homoclinic orbits or heteroclinic cycles. It then follows from (4.2.14), (4.2.15), (4.2.19) and the Poincaré-Bendixson Theorem (see, for example, [59]), that (recalling that $\overline{\Omega}_0$ contains no periodic or homoclinic orbits, or heteroclinic cycles) $\mathcal{S}_1^+|_v$ must leave Ω_0 through L_2 (at finite y) or connect with $\boldsymbol{e_a}$, for some $a \in [0, u_c]$ (as $y \to \infty$). For each $v \geq 0$, this observation allows us to classify the behaviour of $\mathcal{S}_1^+|_v$, by introducing the following function $\overline{s} : \overline{\mathbb{R}}^+ \to \mathbb{R}$, such that,

$\overline{s}(v) =$ The distance, measured from the origin of the (α, β) plane, to the point of intersection of $\mathcal{S}_1^+|_v$ with L_2 (measuring negative distance) or L_3 (measuring positive distance).

We have immediately that

$$\overline{s}(0) = \beta_0(0) < 0, \tag{4.2.20}$$

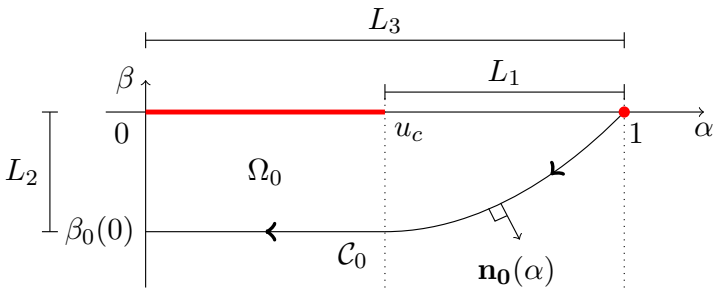

Figure 4.2: The phase path $\mathcal{C}_0 = \mathcal{S}_1^+|_{v=0}$.

and

$$\beta_0(0) < \overline{s}(v) \leq u_c, \tag{4.2.21}$$

for all $v > 0$. Moreover, since $\boldsymbol{Q}(\alpha, \beta)$ depends continuously on $(\alpha, \beta, v) \in \overline{D}_+ \times \overline{\mathbb{R}}^+ \setminus \{(\beta, u_c) : \beta \leq 0\} \times \overline{\mathbb{R}}^+$, the refraction vector (4.2.6) for phase paths crossing the line $\alpha = u_c$ in D_+ is independent of $(\beta, v) \in \mathbb{R}^- \times \overline{\mathbb{R}}^+$, and $\overline{\Omega}_0$ is compact, we may conclude that

$$\overline{s} \in C(\overline{\mathbb{R}}^+). \tag{4.2.22}$$

In addition, from the rotational properties of the vector field $\boldsymbol{Q}(\alpha, \beta)$ in R^+ with increasing $v \geq 0$, we deduce that

$$\overline{s}(v_2) > \overline{s}(v_1) \quad \forall v_2 > v_1 \geq 0. \tag{4.2.23}$$

Therefore, $\overline{s} : \overline{\mathbb{R}}^+ \to \mathbb{R}$ is a continuous and strictly monotone increasing function. Next, take

$$v > v_c(u_c) = \left(\frac{1}{u_c} \sup_{\gamma \in (u_c, 1]} f_c(\gamma) \right)^{\frac{1}{2}}. \tag{4.2.24}$$

Then, with $\beta_c = -v u_c$, we have

$$\begin{aligned} \boldsymbol{Q}(\alpha, \beta_c) \cdot (0, 1) &= v^2 u_c - f_c(\alpha) \\ &> \sup_{\gamma \in (u_c, 1]} f_c(\gamma) - f_c(\alpha) \geq 0, \end{aligned} \tag{4.2.25}$$

for all $\alpha \in (u_c, 1]$, and recall that $\mathcal{S}_0|_v$ is given by $\beta = -v\alpha$ for $\alpha \in [0, u_c]$. It then follows,

from (4.2.25), that

$$\overline{s}(v) > 0 \quad \forall v > v_c(u_c). \tag{4.2.26}$$

We now observe that, at any $v \geq 0$, the dynamical system (4.2.4) has a heteroclinic connection between $\boldsymbol{e_1}$ and $\boldsymbol{e_0}$, in R^+ (which is unique, and is, in fact, contained in $\Omega_0 \subset R^+$) if and only if $\overline{s}(v) = 0$. It follows that since $\overline{s} : \overline{\mathbb{R}}^+ \to \mathbb{R}$ is a continuous and strictly monotone increasing function, which satisfies (4.2.20) and (4.2.26), then, for each $u_c \in (0,1)$, there exists a unique $v^*(u_c) > 0$ such that

$$\overline{s}(v^*(u_c)) = 0, \tag{4.2.27}$$

whilst,

$$\overline{s}(v) < 0 \quad \forall v \in [0, v^*(u_c)), \tag{4.2.28a}$$

$$\overline{s}(v) > 0 \quad \forall v \in (v^*(u_c), \infty). \tag{4.2.28b}$$

We conclude that, for each $u_c \in (0,1)$, [QIVP] has a PTW solution if and only if $v = v^*(u_c)(> 0)$ which we write as $u = U_T(y)$, $y \in \mathbb{R}$. Moreover, this PTW solution is unique. In addition, since the associated heteroclinic connection between $\boldsymbol{e_1}$ and $\boldsymbol{e_0}$ is contained in Ω_0, then we conclude that $U_T : \mathbb{R} \to \mathbb{R}$ satisfies:

$$0 < U_T(y) < 1, \quad U_T'(y) < 0 \qquad \forall y \in \mathbb{R}, \tag{4.2.29a}$$

with $U_T(0) = u_c$, and

$$U_T''(0^+) - U_T''(0^-) = -f_c^+, \tag{4.2.29b}$$

$$U_T(y) = u_c e^{-v^*(u_c)y} \quad \forall y \ \in \overline{\mathbb{R}}^+, \tag{4.2.29c}$$

$$U_T(y) \sim 1 - a_\infty e^{\lambda_+(v^*(u_c))y} \quad \text{as} \quad y \to -\infty, \tag{4.2.29d}$$

for some constant $a_\infty > 0$ (depending upon $u_c \in (0,1)$), and with the eigenvalue $\lambda_+(v)$

given in (4.2.9).

We next consider $u_c \in (0,1)$ as a parameter, regarding v^* as a function of u_c, with $v^* : (0,1) \to \mathbb{R}^+$ such that $v^* = v^*(u_c)$, and associated PTW solution $u = U_T(y, u_c)$ for $(y, u_c) \in \mathbb{R} \times (0,1)$. We recall that the vector field $\boldsymbol{Q}(\alpha, \beta)$ is continuously differentiable on $(\alpha, \beta, v) \in (([0, u_c) \times \mathbb{R}) \cup ((u_c, 1] \times \mathbb{R})) \times \overline{\mathbb{R}}^+$, whilst the refraction vector (4.2.6) depends on $u_c \in (0,1)$ and is continuous. It follows that on fixing $u_c^0 \in (0,1)$, and taking $\varepsilon > 0$, then with $u_c = u_c^0$ and $v = v^*(u_c^0) - \varepsilon$, we have that $\overline{s}(v^*(u_c^0) - \varepsilon)|_{u_c = u_c^0} < 0$, where we have used equation (4.2.27). Hence, there exists $\delta_\varepsilon^- > 0$, which depends on $\varepsilon > 0$, such that for all $u_c \in (u_c^0 - \delta_\varepsilon^-, u_c^0 + \delta_\varepsilon^-) = I_\varepsilon^-$, then

$$\overline{s}(v^*(u_c^0) - \varepsilon)|_{u_c \in I_\varepsilon^-} < 0. \tag{4.2.30}$$

It follows that $v^*(u_c) > v^*(u_c^0) - \varepsilon$ for all $u_c \in I_\varepsilon^-$. Similarly, we establish that there exists $\delta_\varepsilon^+ > 0$, which depends on $\varepsilon > 0$, such that for all $u_c \in (u_c^0 - \delta_\varepsilon^+, u_c^0 + \delta_\varepsilon^+) = I_\varepsilon^+$, then

$$\overline{s}(v^*(u_c^0) + \varepsilon)|_{u_c \in I_\varepsilon^+} > 0. \tag{4.2.31}$$

It follows that $v^*(u_c) < v^*(u_c^0) + \varepsilon$ for all $u_c \in I_\varepsilon^+$. We now set $\delta_\varepsilon = \min(\delta_\varepsilon^-, \delta_\varepsilon^+)$. Thus, for all $u_c \in (u_c^0 - \delta_\varepsilon, u_c^0 + \delta_\varepsilon) = I_\varepsilon$, then

$$|v^*(u_c) - v^*(u_c^0)| < \varepsilon. \tag{4.2.32}$$

We conclude that $v^* : (0,1) \to \mathbb{R}$ is continuous. In addition, we recall that

$$v^*(u_c) > 0 \quad \forall u_c \in (0,1). \tag{4.2.33}$$

Next, let $u_c^0 \in (0,1)$ and consider $\mathcal{S}_1^+|_{(u_c^0, v^*(u_c^0))}$. It follows from the refraction vector (4.2.6) that there exists $\delta > 0$, such that on fixing $v = v^*(u_c^0)$, then for any $u_c \in (u_c^0, u_c^0 + \delta) = P_\delta$, the intersection point of $\mathcal{S}_1^+|_{(u_c, v^*(u_c^0))}$ with the line $\alpha = u_c$ lies above the intersection point

of the line $\beta = -v^*(u_c^0)\alpha$ with the line $\alpha = u_c$. Consequently, $\overline{s}(v^*(u_c^0))|_{u_c \in P_\delta} > 0$, from which we conclude that $v^*(u_c) < v^*(u_c^0)$ for all $u_c \in P_\delta$. Thus, $v^* : (0,1) \to \mathbb{R}$ is locally decreasing, and continuous, and so $v^* : (0,1) \to \mathbb{R}$ is strictly monotone decreasing. It then also follows from (4.2.33) that $v^*(u_c)$ has a finite non-negative limit as $u_c \to 1^-$. Hence, $v^*(u_c) \to v_1^*$ as $u_c \to 1^-$, for some $v_1^* \geq 0$. When $(1 - u_c)$ is sufficiently small, $\mathcal{S}_1^+$ can be approximated in the region $(\alpha, \beta) \in [u_c, 1] \times \mathbb{R}^-$ by its linearised form at the equilibrium point $\boldsymbol{e_1}$; it is then readily established that $v_1^* = 0$, and, moreover, that

$$v^*(u_c) \sim |f_c'(1)|^{\frac{1}{2}}(1 - u_c) \quad \text{as} \quad u_c \to 1^-. \tag{4.2.34}$$

We now investigate $v^*(u_c)$ as $u_c \to 0^+$. To begin with we consider the dynamical system (4.2.4) when $u_c = 0$. In this case, the dynamical system (4.2.4) has a (unique) heteroclinic connection which connects $\boldsymbol{e_1}$, as $y \to -\infty$, to $\boldsymbol{e_0}$, as $y \to \infty$, if and only if $v \in [2, \infty)$, see for example [34, 3, 35, 45]. Moreover, $\overline{s}(v)|_{u_c=0} < 0$ for all $v \in [0, 2)$. From (4.2.6) and (4.2.7), it follows that $\mathcal{S}_1^+$ depends continuously on $u_c \geq 0$. Thus, for $\varepsilon > 0$, there exists $\sigma_\varepsilon > 0$ such that for $u_c \in (0, \sigma_\varepsilon)$, then $\overline{s}(2 - \varepsilon)|_{u_c} < 0$. Therefore, from (4.2.27), we deduce that $v^*(u_c) > 2 - \varepsilon$ for all $u_c \in (0, \sigma_\varepsilon)$. However, it also follows from (4.2.6) and (4.2.7) that $\overline{s}(2)|_{u_c} > 0$ for all $u_c \in (0, 1)$. Thus, $v^*(u_c) < 2$ for all $u_c \in (0, 1)$. We conclude that,

$$2 - \varepsilon < v^*(u_c) < 2 \quad \forall\, u_c \in (0, \sigma_\varepsilon). \tag{4.2.35}$$

Since (4.2.35) holds for all $\varepsilon > 0$, we conclude immediately that $v^*(u_c)$ has limit 2 as $u_c \to 0^+$. We conclude that $v^* : (0,1) \to \mathbb{R}$ is continuous and monotone decreasing, with

$$\lim_{u_c \to 1^-} v^*(u_c) = 0, \qquad \lim_{u_c \to 0^+} v^*(u_c) = 2. \tag{4.2.36}$$

In the next two sections we consider the structure of the PTW solutions in the limits $u_c \to 0^+$ and $u_c \to 1^-$ respectively.

4.3 Asymptotic Structure of the PTW Solution when $u_c \to 0^+$

In this section we investigate the detailed asymptotic form of $v^*(u_c)$ as $u_c \to 0^+$, in the small cut-off limit, via the method of matched asymptotic expansions. To that end, we write $u_c = \varepsilon$ with $0 < \varepsilon \ll 1$. It then follows from equation (4.2.36) that we may write,

$$v^*(\varepsilon) = 2 - \bar{v}(\varepsilon), \tag{4.3.1}$$

where now,

$$\bar{v}(\varepsilon) > 0 \quad \forall\, \varepsilon \in (0,1), \tag{4.3.2}$$

and

$$\bar{v}(\varepsilon) = o(1) \quad \text{as} \quad \varepsilon \to 0^+. \tag{4.3.3}$$

With $U_T : \mathbb{R} \to \mathbb{R}$ being the associated PTW solution, then from (4.2.3),

$$U_{Tyy} + (2 - \bar{v}(\varepsilon))U_{Ty} + f(U_T) = 0, \quad y < 0, \tag{4.3.4a}$$

$$U_T(y) > \varepsilon \quad \forall\, y < 0, \tag{4.3.4b}$$

$$U_T(0) = \varepsilon, \tag{4.3.4c}$$

$$U_{Ty}(0) = -(2 - \bar{v}(\varepsilon))\varepsilon, \tag{4.3.4d}$$

$$U_T(y) \to 1 \quad \text{as} \quad y \to -\infty. \tag{4.3.4e}$$

It is convenient, in what follows, to make a shift of origin by introducing the coordinate $\bar{y}$ via

$$\bar{y} = \bar{y}_c(\varepsilon) + y,$$

where $\bar{y}_c(\varepsilon)$ is chosen so that (4.3.4) becomes,

$$U_{T\bar{y}\bar{y}} + (2 - \bar{v}(\varepsilon))U_{T\bar{y}} + f(U_T(\bar{y})) = 0, \quad \bar{y} < \bar{y}_c(\varepsilon), \tag{4.3.5a}$$

$$U_T(\bar{y}) > \varepsilon \quad \forall\ \bar{y} < \bar{y}_c(\varepsilon), \tag{4.3.5b}$$

$$U_T(\bar{y}_c(\varepsilon)) = \varepsilon, \tag{4.3.5c}$$

$$U_{T\bar{y}}(\bar{y}_c(\varepsilon)) = -(2 - \bar{v}(\varepsilon))\varepsilon, \tag{4.3.5d}$$

$$U_T(\bar{y}) \to 1 \quad \text{as} \quad \bar{y} \to -\infty, \tag{4.3.5e}$$

with now the shift of origin fixing

$$U_T(0) = \frac{1}{2}. \tag{4.3.6}$$

It follows from (4.3.5) and (4.3.6) that

$$\bar{y}_c(\varepsilon) \to +\infty \quad \text{as} \quad \varepsilon \to 0^+. \tag{4.3.7}$$

Our objective is now to examine the boundary value problem (4.3.5) and (4.3.6) as $\varepsilon \to 0^+$, and, in particular, to determine the asymptotic structure of $\bar{v}(\varepsilon)$ as $\varepsilon \to 0^+$. Anticipating the requirement of outer regions, we begin in an inner region when $\bar{y} = O(1)$ and $U_T = O(1)$ as $\varepsilon \to 0^+$, and we label this as region **I**. In region **I** we thus expand as

$$U_T(\bar{y}; \varepsilon) = U_m(\bar{y}) + O(\bar{v}(\varepsilon)) \quad \text{as} \quad \varepsilon \to 0^+, \tag{4.3.8}$$

with $\bar{y} = O(1)$. On substitution from (4.3.8) into (4.3.5) and (4.3.6), and using (4.3.7), we obtain the leading order problem as

$$U_{m\bar{y}\bar{y}} + 2U_{m\bar{y}} + f(U_m) = 0, \quad -\infty < \bar{y} < \infty, \tag{4.3.9a}$$

$$U_m(\bar{y}) > 0, \quad -\infty < \bar{y} < \infty, \tag{4.3.9b}$$

$$U_m(\bar{y}) \to \begin{cases} 1, & \text{as } \bar{y} \to -\infty, \\ 0, & \text{as } \bar{y} \to \infty, \end{cases} \tag{4.3.9c}$$

$$U_m(0) = \frac{1}{2}. \tag{4.3.9d}$$

The leading order problem is immediately recognised as the boundary value problem (4.2.3) for the PTW solution to the corresponding KPP problem without cut-off ($\varepsilon = 0$). Let $U_m : \mathbb{R} \to \mathbb{R}$ be the unique solution to (4.3.9). For use in what follows, we recall (1.1.10) with higher order corrections given by

$$U_m(\bar{y}) = \begin{cases} (A_\infty \bar{y} + B_\infty)\, e^{-\bar{y}} + O(\bar{y}^2 e^{-2\bar{y}}), & \text{as } \bar{y} \to \infty, \\ 1 - A_{-\infty} e^{\gamma \bar{y}} + O(e^{2\gamma \bar{y}}), & \text{as } \bar{y} \to -\infty, \end{cases} \tag{4.3.10}$$

where $\gamma = -1 + \sqrt{1 + |f'(1)|}$ (> 0). On proceeding to $O(\bar{v}(\varepsilon))$ we observe that the inner region expansion (4.3.8) becomes non-uniform when $|\bar{y}| \gg 1$, and in particular when $(-\bar{y}) = O(\bar{v}(\varepsilon)^{-\frac{1}{2}})$ and $\bar{y} = O(\bar{v}(\varepsilon)^{-\frac{1}{2}})$. Therefore, to complete the asymptotic structure of the solution to (4.3.5) as $\varepsilon \to 0^+$, we must introduce two outer regions, namely region $\mathbf{II}^+$ when $\bar{y} = O(\bar{v}(\varepsilon)^{-\frac{1}{2}})$ and region $\mathbf{II}^-$ when $(-\bar{y}) = O(\bar{v}(\varepsilon)^{-\frac{1}{2}})$. We begin in region $\mathbf{II}^-$. To formalise region $\mathbf{II}^-$, we introduce the scaled variable,

$$\hat{y} = \bar{v}(\varepsilon)^{\frac{1}{2}} \bar{y}, \tag{4.3.11}$$

so that $\hat{y} = O(1)^-$ in region $\mathbf{II}^-$ as $\varepsilon \to 0^+$. It then follows from (4.3.8) and (4.3.10) that

$$U_T(\hat{y};\varepsilon) = 1 - O\left(e^{-\bar{v}(\varepsilon)^{-\frac{1}{2}}}\right), \tag{4.3.12}$$

as $\varepsilon \to 0^+$ in region $\mathbf{II}^-$. It is then straightforward to develop an exponential expansion in region $\mathbf{II}^-$, which, after matching (following the Van Dyke matching principle, [58]) with region $\mathbf{I}$, via (4.3.8) and (4.3.10), gives the outer expansion in region $\mathbf{II}^-$ as,

$$\begin{aligned} U_T(\hat{y};\varepsilon) = 1 - A_{-\infty} \exp\left[\gamma\bar{v}(\varepsilon)^{-\frac{1}{2}}\left(1 + O(\bar{v}(\varepsilon))\right)\hat{y}\right] \\ + O\left(\exp\left[2\gamma\bar{v}(\varepsilon)^{-\frac{1}{2}}\left(1 + O(\bar{v}(\varepsilon))\right)\hat{y}\right]\right), \end{aligned} \tag{4.3.13}$$

as $\varepsilon \to 0^+$ with $\hat{y} = O(1)^-$. Thus, the solution in region $\mathbf{II}^-$ is at this order unaffected by the cut-off. We now proceed to region $\mathbf{II}^+$, where $\hat{y} = O(1)^+$ as $\varepsilon \to 0^+$. It is within this region that the conditions at $\bar{y} = \bar{y}_c(\varepsilon)$ must be satisfied, which then requires $\bar{y}_c(\varepsilon) = O(\bar{v}(\varepsilon)^{-\frac{1}{2}})$ as $\varepsilon \to 0^+$, which is consistent with (4.3.7). Thus, we write

$$\bar{y}_c(\varepsilon) = \bar{v}(\varepsilon)^{-\frac{1}{2}}\hat{y}_c(\varepsilon), \tag{4.3.14}$$

so that now,

$$\hat{y}_c(\varepsilon) = O(1)^+ \quad \text{as} \quad \varepsilon \to 0^+. \tag{4.3.15}$$

In region $\mathbf{II}^+$ it follows from (4.3.8) and (4.3.10) that

$$U_T(\hat{y};\varepsilon) = O\left(\bar{v}(\varepsilon)^{-\frac{1}{2}}e^{-\bar{v}(\varepsilon)^{-\frac{1}{2}}}\right),$$

as $\varepsilon \to 0^+$. Again, it is then straightforward to develop an exponential expansion in region $\mathbf{II}^+$, which, after matching with region $\mathbf{I}$, via (4.3.8) and (4.3.10), gives the outer

expansion in region $\mathbf{II}^+$ as,

$$\begin{aligned} U_T(\hat{y};\varepsilon) = &\left(A_\infty \bar{v}(\varepsilon)^{-\frac{1}{2}} \sin\left(\hat{y}(1+O(\bar{v}(\varepsilon)))\right) + B_\infty \cos\left(\hat{y}(1+O(\bar{v}(\varepsilon)))\right)\right) \\ &\times \exp\left[-\bar{v}(\varepsilon)^{-\frac{1}{2}}\left(1+O(\bar{v}(\varepsilon))\right)\hat{y}\right] \\ &+ O\left(\exp\left[-2\bar{v}(\varepsilon)^{-\frac{1}{2}}\left(1+O(\bar{v}(\varepsilon))\right)\hat{y}\right]\right), \end{aligned} \tag{4.3.16}$$

as $\varepsilon \to 0^+$ with $\hat{y} = O(1)^+$. It now remains to apply conditions (4.3.5b), (4.3.5c) and (4.3.5d) to (4.3.16). In the outer region $\mathbf{II}^+$, these conditions become,

$$U_T(\hat{y};\varepsilon) > \varepsilon \quad \forall\, O\left(\bar{v}(\varepsilon)^{-\frac{1}{2}}\right)^+ < \hat{y} < \hat{y}_c(\varepsilon), \tag{4.3.17a}$$

$$U_T(\hat{y}_c(\varepsilon);\varepsilon) = \varepsilon, \tag{4.3.17b}$$

$$u_{T\hat{y}}(\hat{y}_c(\varepsilon);\varepsilon) = -\varepsilon\bar{v}(\varepsilon)^{-\frac{1}{2}}(2-\bar{v}(\varepsilon)). \tag{4.3.17c}$$

We now turn to conditions (4.3.17b) and (4.3.17c). It is convenient to first eliminate ε explicitly between (4.3.17b) and (4.3.17c) to give,

$$u_{T\hat{y}}(\hat{y}_c(\varepsilon);\varepsilon) = -\bar{v}(\varepsilon)^{-\frac{1}{2}}(2-\bar{v}(\varepsilon))U_T(\hat{y}_c(\varepsilon);\varepsilon), \tag{4.3.18}$$

which replaces (4.3.17c). On substitution from (4.3.16) into (4.3.18) and expanding, using (4.3.2), (4.3.3) and (4.3.15), we obtain,

$$A_\infty \sin\omega = -\bar{v}(\varepsilon)^{\frac{1}{2}}(A_\infty + B_\infty)\cos\omega, \qquad \omega = \hat{y}_c(\varepsilon)(1+O(\bar{v}(\varepsilon))), \tag{4.3.19}$$

as $\varepsilon \to 0^+$. Following (4.3.15) and (4.3.19), we now expand,

$$\hat{y}_c(\varepsilon) = \hat{y}_c^0 + \hat{y}_c^1\bar{v}(\varepsilon)^{\frac{1}{2}} + O(\bar{v}(\varepsilon)), \tag{4.3.20}$$

as $\varepsilon \to 0^+$, with the constants $\hat{y}_c^0$ (> 0) and $\hat{y}_c^1$ to be determined. On substitution from (4.3.20) into (4.3.19), we obtain, at $O(1)$,

$$A_\infty \sin \hat{y}_c^0 = 0.$$

Since $A_\infty > 0$, then we must have (recalling $\hat{y}_c^0 > 0$) $\hat{y}_c^0 = k\pi$, for some $k \in \mathbb{N}$. However, condition (4.3.17a), with (4.3.16), then requires $k = 1$, and so

$$\hat{y}_c^0 = \pi. \tag{4.3.21}$$

Proceeding to $O(\bar{v}(\varepsilon)^{\frac{1}{2}})$, we find that, on using (4.3.21),

$$\hat{y}_c^1 = -\frac{(A_\infty + B_\infty)}{A_\infty}. \tag{4.3.22}$$

Thus, via (4.3.20), (4.3.21) and (4.3.22) we have,

$$\hat{y}_c(\varepsilon) = \pi - \frac{(A_\infty + B_\infty)}{A_\infty}\bar{v}(\varepsilon)^{\frac{1}{2}} + O(\bar{v}(\varepsilon)), \tag{4.3.23}$$

as $\varepsilon \to 0^+$. It remains to apply condition (4.3.17b). On using (4.3.16) and (4.3.23), condition (4.3.17b) becomes

$$\ln \varepsilon = -\frac{\pi}{\bar{v}(\varepsilon)^{\frac{1}{2}}} + \left(\frac{(A_\infty + B_\infty)}{A_\infty} + \ln A_\infty\right) + o(1), \tag{4.3.24}$$

as $\varepsilon \to 0^+$. A re-arrangement of (4.3.24) then gives,

$$\bar{v}(\varepsilon) = \frac{\pi^2}{(\ln \varepsilon)^2} + \frac{2\pi^2\left((A_\infty + B_\infty)A_\infty^{-1} + \ln A_\infty\right)}{(\ln \varepsilon)^3} + o\left(\frac{1}{(\ln \varepsilon)^3}\right), \tag{4.3.25}$$

as $\varepsilon \to 0^+$. It then follows from (4.3.23) and (4.3.25) that,

$$\hat{y}_c(\varepsilon) = \pi + \frac{(A_\infty + B_\infty)\pi}{A_\infty}\frac{1}{\ln \varepsilon} + O\left(\frac{1}{(\ln \varepsilon)^2}\right), \tag{4.3.26}$$

as $\varepsilon \to 0^+$. Finally, via (4.3.1) and (4.3.25), we can construct $v^*(\varepsilon)$ as,

$$v^*(\varepsilon) = 2 - \frac{\pi^2}{(\ln \varepsilon)^2} - \frac{2\pi^2 \left((A_\infty + B_\infty)A_\infty^{-1} + \ln A_\infty\right)}{(\ln \varepsilon)^3} + o\left(\frac{1}{(\ln \varepsilon)^3}\right), \tag{4.3.27}$$

as $\varepsilon \to 0^+$. We observe that (4.3.27) is decreasing in ε as $\varepsilon \to 0^+$, and is in full accord with the rigorous results established in Section 4.2. We see immediately that the result derived here, via a rational application of the method of matched asymptotic expansions, agrees in the first two terms with the results that Brunet and Derrida [14] and Dumortier, Popovic and Kaper [19] obtained. However, the method of matched asymptotic expansions has enabled us to obtain the next correction term in (4.3.27), and higher order terms could be obtained by systematically following this approach. We now consider the asymptotic structure of the PTW solution to [QIVP] as $u_c \to 1^-$.

4.4 Asymptotic Structure of the PTW Solution when $u_c \to 1^-$

In this section we investigate the asymptotic form of $v^*(u_c)$ in the large cut-off limit $u_c \to 1^-$. To this end, we write $u_c = 1 - \delta$ with $0 < \delta \ll 1$. Section 4.2 guarantees the existence and uniqueness of a PTW solution, whose speed $v^*(\delta) = o(1)$ as $\delta \to 0^+$. In this case, it is most convenient to consider the problem in the (α, β) phase plane corresponding to the phase path representing the PTW when $u_c = 1 - \delta$ and $v = v^*(\delta)$. Via (4.2.4), (4.2.9), (4.2.10) and (4.2.11), this is given by the phase path $\beta = \beta(\alpha; \delta)$, which satisfies the boundary value problem

$$\frac{d\beta}{d\alpha} = -v^*(\delta) - \frac{f(\alpha)}{\beta}, \quad \alpha \in (1-\delta, 1), \tag{4.4.1a}$$

$$\beta(\alpha; \delta) \sim -\lambda_+(v^*(\delta))(1-\alpha) \quad \text{as} \quad \alpha \to 1^-, \tag{4.4.1b}$$

$$\beta(1-\delta; \delta) = -v^*(\delta)(1-\delta). \tag{4.4.1c}$$

We now examine the boundary value problem (4.4.1) as $\delta \to 0^+$. Since $v^*(\delta) = o(1)$ as $\delta \to 0^+$, we expand $\lambda_+(v^*(\delta))$, via (4.2.9), which determines that $\lambda_+(v^*(\delta)) = O(1)$ as $\delta \to 0^+$. It follows from the boundary condition (4.4.1b), that $\beta = O(\delta)$ as $\delta \to 0^+$. We therefore introduce the following re-scalings

$$\beta = \delta Y, \quad \alpha = 1 - \delta X, \tag{4.4.2}$$

with $Y, X = O(1)$ as $\delta \to 0^+$. The form of the boundary condition (4.4.1c) then necessitates that $v^*(\delta) = O(\delta)$ as $\delta \to 0^+$. Thus, we write

$$v^*(\delta) = \delta V(\delta), \tag{4.4.3}$$

where $V(\delta) = O(1)$ as $\delta \to 0^+$. These re-scalings transform the boundary value problem (4.4.1) into,

$$\frac{dY}{dX} = \delta V(\delta) + \frac{f(1-\delta X)}{\delta Y}, \quad X \in (0,1), \tag{4.4.4a}$$

$$Y(X;\delta) \sim -\lambda_+(\delta V(\delta))X \quad \text{as} \quad X \to 0^+, \tag{4.4.4b}$$

$$Y(1;\delta) = -V(\delta)(1-\delta). \tag{4.4.4c}$$

We now expand $Y(X;\delta)$ and $V(\delta)$ according to,

$$Y(X;\delta) = Y_0(X) + \delta Y_1(X) + o(\delta), \quad X \in [0,1], \tag{4.4.5a}$$

$$V(\delta) = V_0 + \delta V_1 + o(\delta), \tag{4.4.5b}$$

as $\delta \to 0^+$. Substituting the expansions from (4.4.5) into the boundary value problem (4.4.4) and expanding, at $O(1)$, we obtain the following boundary value problem for

$Y_0(X)$, namely,

$$\frac{dY_0}{dX} = -f'(1)\frac{X}{Y_0}, \quad X \in (0,1), \tag{4.4.6a}$$

$$Y_0(X) \sim -|f'(1)|^{\frac{1}{2}}X \quad \text{as} \quad X \to 0^+, \tag{4.4.6b}$$

$$Y_0(1) = -V_0. \tag{4.4.6c}$$

The general solution to (4.4.6a) is $Y_0^2(X) = c_1 - f'(1)X^2$, for $X \in [0,1]$, where c_1 is an arbitrary constant of integration. Applying the boundary condition (4.4.6b) determines $c_1 = 0$. Therefore,

$$Y_0(X) = -|f'(1)|^{\frac{1}{2}}X, \quad X \in [0,1]. \tag{4.4.7}$$

Application of the boundary condition (4.4.6c) then determines

$$V_0 = |f'(1)|^{\frac{1}{2}}. \tag{4.4.8}$$

At $O(\delta)$, we obtain the following boundary value problem for $Y_1(X)$, namely,

$$\frac{dY_1}{dX} - \frac{Y_1}{Y_0(X)^2}f'(1)X = V_0 + \frac{1}{2}f''(1)\frac{X^2}{Y_0(X)}, \quad X \in (0,1), \tag{4.4.9a}$$

$$Y_1(X) \sim \frac{1}{2}V_0X \quad \text{as} \quad X \to 0^+, \tag{4.4.9b}$$

$$Y_1(1) = V_0 - V_1. \tag{4.4.9c}$$

On substituting $Y_0(X)$, given by (4.4.7), into equation (4.4.9a) and solving, we find that the general solution is

$$Y_1(X) = \frac{1}{2}V_0X - \frac{1}{6}\frac{f''(1)}{|f'(1)|^{\frac{1}{2}}}X^2 + \frac{c_2}{X}, \quad X \in (0,1], \tag{4.4.10}$$

where c_2 is an arbitrary constant of integration. From the boundary condition (4.4.9b), $Y_1(X)$ remains bounded as $X \to 0^+$. Therefore, we require $c_2 = 0$. Thus, we obtain the

solution for $Y_1(X)$ as

$$Y_1(X) = \frac{1}{6}|f'(1)|^{\frac{1}{2}} X \left(3 - \frac{f''(1)}{|f'(1)|} X\right), \quad X \in [0,1]. \tag{4.4.11}$$

Finally, an application of the boundary condition (4.4.12) determines

$$V_1 = \frac{1}{6}|f'(1)|^{\frac{1}{2}} \left(3 + \frac{f''(1)}{|f'(1)|}\right). \tag{4.4.12}$$

On collecting expressions (4.4.5a), (4.4.7) and (4.4.11), we have established that

$$\begin{aligned} Y(X;\delta) = -|f'(1)|^{\frac{1}{2}} X + \frac{1}{6}\delta |f'(1)|^{\frac{1}{2}} X \left(3 - \frac{f''(1)}{|f'(1)|} X\right) \\ + o(\delta) \quad \text{as} \quad \delta \to 0^+, \end{aligned} \tag{4.4.13}$$

uniformly for $X \in [0,1]$. Similarly, on collecting expressions (4.4.5b), (4.4.8) and (4.4.12), we obtain,

$$V(\delta) = |f'(1)|^{\frac{1}{2}} + \frac{1}{6}\delta |f'(1)|^{\frac{1}{2}} \left(3 + \frac{f''(1)}{|f'(1)|}\right) + o(\delta) \quad \text{as} \quad \delta \to 0^+. \tag{4.4.14}$$

Using (4.4.3), the propagation speed of the PTW solution to [QIVP] is given by

$$v^*(\delta) = \delta |f'(1)|^{\frac{1}{2}} + \frac{1}{6}\delta^2 |f'(1)|^{\frac{1}{2}} \left(3 + \frac{f''(1)}{|f'(1)|}\right) + o(\delta^2) \quad \text{as} \quad \delta \to 0^+. \tag{4.4.15}$$

We use (4.4.2) to express the PTW solution to [QIVP] in terms of the cut-off u_c as

$$\begin{aligned} \beta(\alpha) = -\frac{1}{2}|f'(1)|^{\frac{1}{2}}(1+u_c)(1-\alpha) - \frac{1}{6}\frac{f''(1)}{|f'(1)|^{\frac{1}{2}}}(1-\alpha)^2 \\ + o((1-u_c)^2) \quad \text{as} \quad u_c \to 1^-. \end{aligned} \tag{4.4.16}$$

Its speed of propagation is given by

$$v^*(u_c) = (1-u_c)|f'(1)|^{\frac{1}{2}} + \frac{1}{6}(1-u_c)^2|f'(1)|^{\frac{1}{2}}\left(3 + \frac{f''(1)}{|f'(1)|}\right) + o((1-u_c)^2) \quad \text{as } u_c \to 1^-. \tag{4.4.17}$$

In the next section we consider the specific case of cut-off Fisher reaction, determining $v^* : (0,1) \to \mathbb{R}$ via numerical integration.

4.5 Numerical Example

We here compare our predictions for the PTW solutions $U_T(y)$ and the speed $v^*(u_c)$ derived in the limits of small and large cut-off u_c with the corresponding values obtained from the numerical evaluation of (4.2.3) (or (4.3.5) when u_c is small) carried out for the particular case of the cut-off Fisher reaction function, namely,

$$f_c(u) = \begin{cases} u(1-u), & u \in (u_c, \infty), \\ 0, & u \in (-\infty, u_c], \end{cases} \tag{4.5.1}$$

where $u_c \in (0,1)$.

For our numerical calculations we adopt a shooting method that combines a standard fourth order Runge-Kutta discretisation scheme with a bisection method. We use (4.2.10) to approximate the unstable manifold near the unstable fixed point $(U_T, U_T') = (1,0)$, taking $U_T = 1-\epsilon$ and $U_T' = -\lambda_+(v)\epsilon$ where $\epsilon = 10^{-10}$. We choose $\Delta\alpha = 10^{-12}$ to ensure that the values of $U_T(y)$ (or $U_T(\bar{y})$ when u_c is small) and $v^*(u_c)$ are obtained to ten decimal places of accuracy.

The asymptotic predictions for the PTW solutions $U_T(\bar{y})$ and the speed $v^*(u_c)$ obtained for small values of u_c rely on the global constants A_∞ and B_∞ (see equations (4.3.16) and (4.3.27)) associated with the leading edge behaviour of $U_m(\bar{y})$ (see expression (4.3.10)).

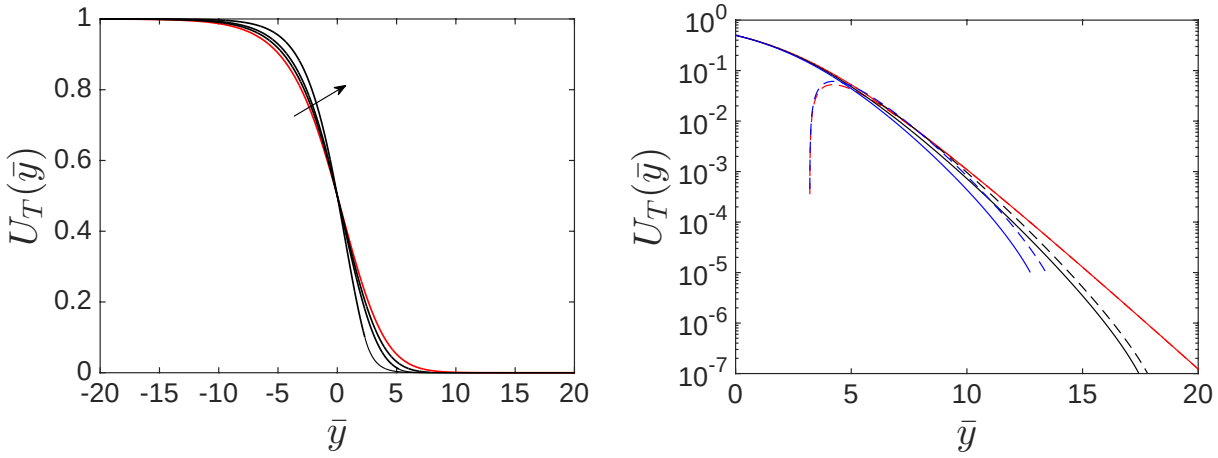

(a) (b)

Figure 4.3: (a) Numerical solutions of $U_T(\bar{y})$ obtained from (4.3.5) for $u_c = 0.001, 0.01$ and 0.1, with the arrow pointing in the direction of increasing u_c (thick black lines), and exact solution derived from (4.2.29c) (thin black lines). These are plotted against the numerical solution of $U_m(\bar{y})$ (in red) obtained from (4.3.9). (b) Comparison between numerical and asymptotic results for $U_T(\bar{y})$ obtained for $\bar{y} \leq \bar{y}_c(u_c)$ for $u_c = 10^{-7}$ (in black) and $u_c = 10^{-5}$ (in blue). The numerical results are juxtaposed against the asymptotic expression (4.3.16) valid for $u_c \to 0^+$ and $\bar{y} \gg 1$ (dashed black and blue lines, respectively). These are plotted against the numerical solution of $U_m(\bar{y})$ (in solid red) and the large-$\bar{y}$ asymptotic expression (4.3.10) (dashed red line).

We determine the values of A_∞ and B_∞ from the numerical evaluation of (4.3.9) where we use the MATLAB solver *ode*45 carried out for the particular case of the Fisher reaction function (1.1.6). We use (4.3.10) to approximate the unstable manifold near the unstable fixed point $(U_m, U_m') = (1, 0)$, taking $U_m = 1 - \varepsilon$ and $U_m' = -\gamma\epsilon$ where $\epsilon = 10^{-10}$. We choose the same resolution as before and use a standard linear least squares fit on $U_m e^{\bar{y}}$ for $\bar{y} \gtrsim 10$ to obtain $A_\infty \approx 3.521$ and $B_\infty \approx -11.15$ to four significant figures.

Figure 4.3 is devoted to the structure of $U_m(\bar{y})$ and that of $U_T(\bar{y})$ obtained for small cut-off u_c. For $\bar{y} \leq \bar{y}_c(u_c)$ this is numerically determined from (4.3.5). For $\bar{y} > \bar{y}_c(u_c)$ the solution is exact (see equation (4.2.29c)). Figure 4.3(a) contrasts the behaviour of $U_T(\bar{y})$ against that of $U_m(\bar{y})$. It is clear that when $\bar{y} = O(1)$, $U_T(\bar{y})$ remains close to $U_m(\bar{y})$ while when $|\bar{y}| \gg 1$, $U_T(\bar{y})$ approaches 1^- and u_c exponentially fast. This behaviour is consistent with expressions (4.3.8), (4.3.13) and (4.3.16) (with $\varepsilon = u_c$). Figure 4.3(b) focuses on the behaviour of $U_m(\bar{y})$ and $U_T(\bar{y})$ when the value of $\bar{y}$ is large. It shows that as long as $\bar{y} \gtrsim 5$, the numerical solution of $U_m(\bar{y})$ and the leading edge asymptotics given

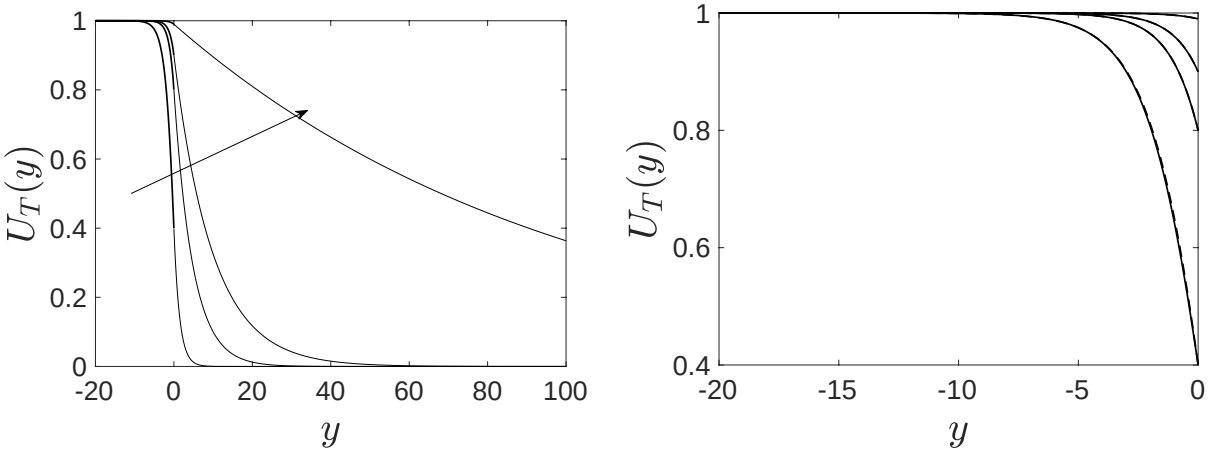

Figure 4.4: (a) Numerical solutions of $U_T(y)$ obtained from (4.2.3) for $u_c = 0.4$, 0.8, 0.9 and 0.99 (thick lines), with the arrow pointing in the direction of increasing u_c, and exact solution given by (4.2.29c) (thin lines). (b) Comparison between the numerical solutions of $U_T(y)$ and the asymptotic expression for $u_c \to 1^-$ derived from (4.4.16) (dashed black lines).

by (4.3.10) (with numerical values of A_∞ and B_∞ given above) are in excellent agreement.

The same figure compares the numerical solution of $U_T(\bar{y})$ with the leading edge asymptotics given by (4.3.16) which applies for $\bar{y}_c(u_c) \geq \bar{y} \gg 1$ (which is the case for $u_c \gg 0.05$). It confirms that the asymptotic expression (4.3.16) describing $U_T(\bar{y})$ becomes increasingly accurate as the value of u_c decreases.

Figure 4.4 focuses on the structure of $U_T(y)$ obtained for larger cut-off u_c. For $y \leq 0$, this is numerically determined from (4.2.3); for $y > 0$ it is exactly given by (4.2.29c). It is clear that the asymptotic prediction associated with (4.4.16) is an excellent approximation of $U_T(y)$ for all values of u_c considered (see Figure 4.4(b)).

We now examine the behaviour of the speed $v^*(u_c)$. Figure 4.5 illustrates that the numerical results for the speed $v_\infty(u_c)$ to [QIVP], obtained in Chapter 3, are in excellent agreement with the speed of propagation of the PTW with $v_\infty(u_c) = v^*(u_c)$. Figure 4.5(a) focuses on speed values $v^*(u_c)$ obtained for small values of u_c. It shows that expression (1.1.15) of Brunet and Derrida [14] is very good as long as $u_c \lesssim 0.02$. Higher order corrections are captured by the asymptotic expression (4.3.27) which remains good (though only marginally better than expression (1.1.15)) as long as $u_c \lesssim 0.05$ (when

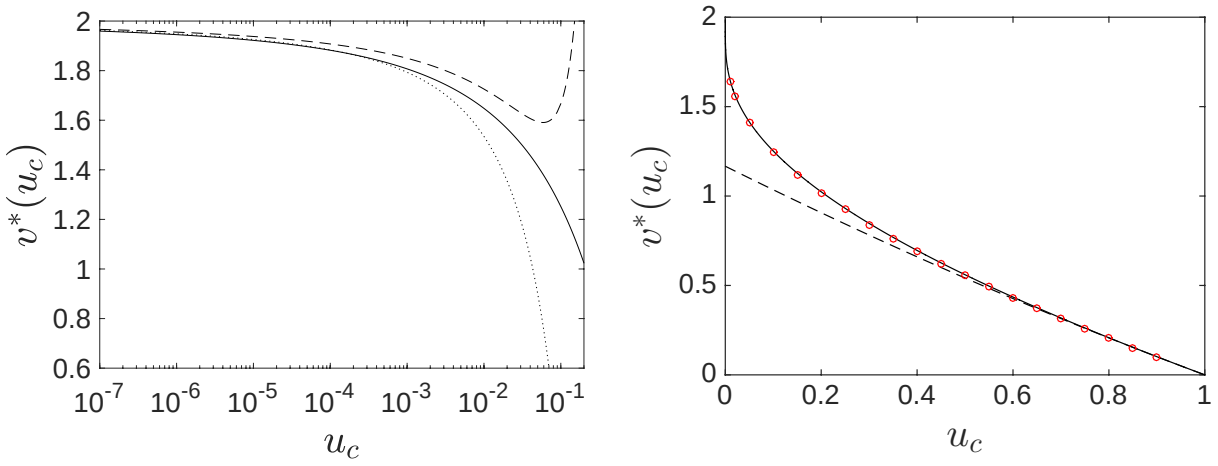

Figure 4.5: Comparison between asymptotic and numerical results of the speed for (a) small and (b) large cut-off values u_c. Numerical solutions of $v^*(u_c)$ derived from the boundary value problem (4.2.3) with f_c given by (4.5.1) are shown as solid lines. The dashed lines are the asymptotic predictions (4.3.27) and (4.4.17) of $v^*(u_c)$. In (a) the dotted line is expression (1.1.15) of Brunet and Derrida [14] and in (b) the red circles are the numerical solutions of $v_\infty(u_c)$ to [QIVP].

$u_c = 0.05$, $\bar{v} \approx 1$ associated with expansion (4.3.8) is no longer small).

Figure 4.5(b) shifts the focus to larger values of u_c. It shows that the asymptotic expression (4.4.17) accurately captures the speed $v^*(u_c)$ for a wide range of values given by $0.4 \lesssim u_c < 1$ (when $u_c = 0.4$, $\delta = 1 - u_c = 0.6$ associated with expansions (4.4.5) is no longer small). Our numerical results for the speed $v^*(u_c)$, obtained for a range of values of $u_c \in (0, 1)$, combined with the asymptotic expressions (4.2.29c), (4.3.27) and (4.4.17) confirms that the the front width of the PTW solution is $O((1 - u_c)^{-1})$ in the limit as $u_c \to 1^-$ and $O(1)$ otherwise.

4.6 Discussion and Conclusions

In this chapter we have concentrated on examining the existence of PTW solutions to [QIVP] with propagation speed $v \geq 0$, which effect the transition from the unreacted state $u = 0$ (ahead of the wave-front) to the fully reacted state $u = 1$ (at the rear of the wave-front). We employ a phase plane analysis of the nonlinear boundary value problem

(4.2.3) to establish that (i) for each $u_c \in (0,1)$, then [QIVP] has a unique PTW solution, with propagation speed $v = v^*(u_c) > 0$ and (ii) $v^* : (0,1) \to \mathbb{R}^+$ is continuous and monotone decreasing, with $v^*(u_c) \to 0^+$ as $u_c \to 1^-$, and $v^*(u_c) \to 2^-$ as $u_c \to 0^+$. It should be noted that 2 is the minimum propagation speed of PTW solutions for the related KPP-type function in the absence of cut-off. Furthermore, we have developed asymptotic methods to determine the asymptotic forms of $v^*(u_c)$ as $u_c \to 0^+$ and $u_c \to 1^-$. The first limit was previously considered by Brunet and Derrida [14] and Dumortier, Popovic and Kaper [19]. The latter employed matched asymptotic expansions in the phase plane to determine the order of the error in [14]. We have here used matched asymptotic expansions on the direct problem (4.2.3) to obtain higher order corrections in a systematic manner. We show that these are controlled by the detailed structure ahead of the wave-front solution travelling with speed 2 for the related KPP problem obtained in the absence of a cut-off. For larger values of u_c, the asymptotic behaviour is obtained via the use of regular asymptotic expansions in the phase plane. The front width of the PTW solution is obtained in both asymptotic limits.

We anticipate that the approach developed in this chapter, for considering PTW solutions to [QIVP], will be readily adaptable to corresponding problems, when the KPP-type cut-off reaction function is replaced by a broader class of cut-off reaction functions. In comparing the PTW theory for the cut-off KPP-type reaction function studied here, and its associated KPP-type reaction function without cut-off, we make the observation that, in the absence of cut-off, a PTW solution exists for each propagation speed $v \in [2, \infty)$, whilst at each fixed cut-off value $u_c \in (0,1)$, a PTW solution exists only at the single propagation speed $v = v^*(u_c)$, with $0 < v^*(u_c) < 2$. This will have implications for the development of PTW solutions as large-t structures in [QIVP], with more general classes of initial data. In the next chapter we consider the evolution problem [QIVP] in more detail. Specifically we establish that, as $t \to \infty$, the solution to [QIVP] does indeed involve the formation of the PTW solution considered in this chapter, and we give the detailed asymptotic structure of the solution to [QIVP] as $t \to \infty$.

CHAPTER 5

ASYMPTOTIC SOLUTION TO [QIVP]

In this chapter we develop the asymptotic structure of the solution to [QIVP] as $t \to 0^+$, as $|y| \to \infty$ and as $t \to \infty$. We begin by examining the asymptotic structure of the solution to [QIVP] as $t \to 0^+$.

5.1 Asymptotic Solution to [QIVP] as $t \to 0^+$

We develop the asymptotic structure to [QIVP] as $t \to 0^+$ via the method of matched asymptotic coordinate expansions. We anticipate that the structure of the solution to [QIVP] as $t \to 0^+$ will have two asymptotic regions in $y < 0$, and two asymptotic regions in $y > 0$. An examination of the leading order balances in equation (2.0.8a), together with the initial condition (2.0.8c) and the connection conditions (2.0.8e), (2.0.8f) determine the asymptotic structure as:

$$\text{region } \mathbf{I_L}: \quad y = O(t^{\frac{1}{2}}) < 0 \text{ with } u = O(1) \text{ as } t \to 0^+, \tag{5.1.1a}$$

$$\text{region } \mathbf{I_R}: \quad y = O(t^{\frac{1}{2}}) > 0 \text{ with } u = O(1) \text{ as } t \to 0^+, \tag{5.1.1b}$$

$$\text{region } \mathbf{II_L}: \quad y = O(1) < 0 \text{ with } u = 1 - o(1) \text{ as } t \to 0^+, \tag{5.1.1c}$$

$$\text{region } \mathbf{II_R}: \quad y = O(1) > 0 \text{ with } u = o(1) \text{ as } t \to 0^+. \tag{5.1.1d}$$

The situation is illustrated in Figure 5.1. For any variable λ, we will henceforth write $\lambda = O(1) > 0$ as $\lambda = O(1)^+$, and correspondingly, $\lambda = O(1) < 0$ as $\lambda = O(1)^-$. It follows from the small-time asymptotic structure (5.1.1) of [QIVP], that we anticipate an asymptotic expansion for $s(t)$ of the form

$$s(t) = s_0 t^\alpha + s_1 t^\beta + o(t^\beta) \quad \text{as} \quad t \to 0^+, \tag{5.1.2}$$

where the constants s_0, s_1, α and $\beta(> \alpha)$ are to be found. The initial condition (2.0.8g), together with a leading order balance in equation (2.0.8a) determines

$$\alpha = \frac{1}{2}. \tag{5.1.3}$$

We begin in region $\mathbf{I_L}$, following (5.1.1a), where we introduce the coordinate $\eta = yt^{-\frac{1}{2}} = O(1)^-$ as $t \to 0^+$ with $u(\eta, t) = u(y, t)$ and where $u(\eta, t)$ satisfies

$$u_t - \frac{1}{t}\frac{\eta}{2}u_\eta - \frac{\dot{s}(t)}{t^{\frac{1}{2}}}u_\eta = \frac{1}{t}u_{\eta\eta} + f(u), \quad \eta < 0. \tag{5.1.4}$$

We expand $u(\eta, t)$ in the form,

$$u(\eta, t) = u_{L0}(\eta) + \phi_L(t)u_{L1}(\eta) + o(\phi_L(t)) \quad \text{as} \quad t \to 0^+, \tag{5.1.5}$$

with $\eta = O(1)^-$ and $\phi_L(t) = o(1)$ as $t \to 0^+$ to be determined. As we are interested in the small-time solution our gauge function ϕ_L depends only on the small-t. On substituting from expansions (5.1.2) and (5.1.5) into equation (5.1.4), we obtain at leading order as $t \to 0^+$,

$$u''_{L0} + \frac{1}{2}(\eta + s_0)u'_{L0} = 0, \quad \eta < 0, \tag{5.1.6a}$$

which must be solved subject to the boundary condition (2.0.8e) at $\eta = 0$, together with the matching condition with region $\mathbf{II_L}$ as $\eta \to -\infty$. Using (5.1.1c) and (5.1.5), these conditions require,

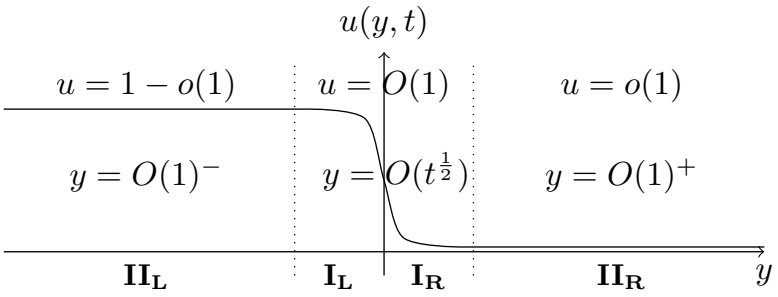

Figure 5.1: A sketch of the structure of the solution to [QIVP] as $t \to 0^+$.

$$u_{L0}(0) = u_c, \tag{5.1.6b}$$

$$u_{L0}(\eta) \to 1 \quad \text{as} \quad \eta \to -\infty. \tag{5.1.6c}$$

Due to the coupling condition (2.0.8f) at $\eta = 0$, it is necessary now to consider region $\mathbf{I_R}$, in which, via (5.1.1b), $\eta = O(1)^+$ and $u = O(1)$ as $t \to 0^+$ with $u(\eta, t) = u(y, t)$ and where $u(\eta, t)$ satisfies

$$u_t - \frac{1}{t}\frac{\eta}{2}u_\eta - \frac{\dot{s}(t)}{t^{\frac{1}{2}}}u_\eta = \frac{1}{t}u_{\eta\eta}, \quad \eta > 0. \tag{5.1.7}$$

We expand $u(\eta, t)$ in the form,

$$u(\eta, t) = u_{R0}(\eta) + \phi_R(t)u_{R1}(\eta) + o(\phi_R(t)) \quad \text{as} \quad t \to 0^+, \tag{5.1.8}$$

with $\eta = O(1)^+$ as $t \to 0^+$. Here $\phi_R = o(1)$ as $t \to 0^+$, and is to be determined. Now, substituting from expansions (5.1.2) and (5.1.8) into equation (5.1.7), we obtain at leading order as $t \to 0^+$,

$$u''_{R0} + \frac{1}{2}(\eta + s_0)u'_{R0} = 0, \quad \eta > 0, \tag{5.1.9a}$$

which must be solved subject to the boundary condition (2.0.8e) at $\eta = 0$, together with the matching condition with region $\mathbf{II_R}$ as $\eta \to \infty$, which requires,

$$u_{R0}(0) = u_c, \tag{5.1.9b}$$

$$u_{R0}(\eta) \to 0 \quad \text{as} \quad \eta \to \infty. \tag{5.1.9c}$$

Finally, the boundary value problems (5.1.6) and (5.1.9) must be solved subject to the coupling condition (2.0.8f) across $\eta = 0$, which requires

$$u'_{L0}(0) = u'_{R0}(0). \tag{5.1.10}$$

The solutions to (5.1.6) and (5.1.9) respectively, are readily obtained as

$$u_{L0}(\eta) = \frac{u_c\left(1 + \operatorname{erf}(\frac{\eta+s_0}{2})\right) - \operatorname{erf}(\frac{\eta+s_0}{2}) + \operatorname{erf}(\frac{s_0}{2})}{\left(1 + \operatorname{erf}(\frac{s_0}{2})\right)}, \quad \eta \leq 0, \tag{5.1.11a}$$

$$u_{R0}(\eta) = u_c\frac{\left(1 - \operatorname{erf}(\frac{\eta+s_0}{2})\right)}{\left(1 - \operatorname{erf}(\frac{s_0}{2})\right)}, \quad \eta \geq 0. \tag{5.1.11b}$$

Finally, an application of condition (5.1.10) to (5.1.11) determines

$$s_0 = 2\operatorname{erf}^{-1}(1 - 2u_c), \tag{5.1.12}$$

and thus, the leading order solutions in region $\mathbf{I_L}$ and region $\mathbf{I_R}$, respectively, are given by

$$u_{L0}(\eta) = \frac{1}{2}\left[1 - \operatorname{erf}\left(\frac{\eta}{2} + \operatorname{erf}^{-1}(1 - 2u_c)\right)\right], \quad \eta \leq 0, \tag{5.1.13a}$$

$$u_{R0}(\eta) = \frac{1}{2}\left[1 - \operatorname{erf}\left(\frac{\eta}{2} + \operatorname{erf}^{-1}(1 - 2u_c)\right)\right], \quad \eta \geq 0. \tag{5.1.13b}$$

We now proceed to the correction terms in expansions (5.1.2), (5.1.5) and (5.1.8). A balancing of terms requires $\phi_L(t) = \phi_R(t) = O(t)$ as $t \to 0^+$ and $\beta = \frac{3}{2}$. Thus, we set $\phi_L(t) = \phi_R(t) = t$, without loss of generality. On substitution from expansions (5.1.2), (5.1.5) and (5.1.8) into equations (5.1.4) and (5.1.7), we obtain the coupled problem for $u_{L1}(\eta)(\eta < 0)$, $u_{R1}(\eta)(\eta > 0)$ and s_1, namely,

$$u''_{L1} + \frac{1}{2}(\eta + s_0)u'_{L1} - u_{L1} = -\frac{3}{2}s_1u'_{L0} - f(u_{L0}(\eta)), \quad \eta < 0, \tag{5.1.14a}$$

$$u''_{R1} + \frac{1}{2}(\eta + s_0)u'_{R1} - u_{R1} = -\frac{3}{2}s_1u'_{R0}, \quad \eta > 0, \tag{5.1.14b}$$

subject to the coupling conditions

$$u_{L1}(0) = u_{R1}(0) = 0, \tag{5.1.14c}$$

$$u'_{L1}(0) = u'_{R1}(0), \tag{5.1.14d}$$

and the matching conditions to region $\mathbf{II_L}$ and to region $\mathbf{II_R}$, respectively, which are readily obtained as,

$$u_{L1}(\eta) \to 0 \quad \text{as} \quad \eta \to -\infty, \tag{5.1.14e}$$

$$u_{R1}(\eta) \to 0 \quad \text{as} \quad \eta \to \infty. \tag{5.1.14f}$$

In considering the coupled problem (5.1.14), we first observe that $1 + \frac{1}{2}(\eta + s_0)^2$ is a solution to the homogeneous part of both (5.1.14a) and (5.1.14b). With this observation, together with the methods of reduction of order and variation of parameters, we can write the general solutions to (5.1.14a) and (5.1.14b) as,

$$u_{L1}(\eta) = d_1\hat{u}(\eta) + d_2\bar{u}(\eta) - \frac{s_1}{2\sqrt{\pi}} \exp\left(-\left(\frac{\eta + s_0}{2}\right)^2\right) + u_{p2}(\eta), \quad \eta \leq 0, \tag{5.1.15a}$$

$$u_{R1}(\eta) = \bar{d}_1\hat{u}(\eta) + \bar{d}_2\bar{u}(\eta) - \frac{s_1}{2\sqrt{\pi}} \exp\left(-\left(\frac{\eta + s_0}{2}\right)^2\right), \quad \eta \geq 0, \tag{5.1.15b}$$

where $d_1, d_2, \bar{d}_1$ and $\bar{d}_2$ are arbitrary constants to be determined and the particular solution $u_{p2}(\eta)$ is given by

$$u_{p2}(\eta) = \frac{\hat{u}(\eta)}{2} \int_\eta^0 I_1(\lambda)d\lambda - \frac{\bar{u}(\eta)}{2} \int_\eta^0 I_2(\lambda)d\lambda, \quad \eta \leq 0, \tag{5.1.16}$$

with functions

$$\hat{u}(\eta) = \sqrt{\pi}\left(1 + \frac{(\eta+s_0)^2}{2}\right)\operatorname{erf}\left(\frac{\eta+s_0}{2}\right) + (\eta+s_0)\exp\left(-\left(\frac{\eta+s_0}{2}\right)^2\right), \tag{5.1.17a}$$

$$\bar{u}(\eta) = 1 + \frac{(\eta+s_0)^2}{2}, \tag{5.1.17b}$$

$$I_1(\eta) = \exp\left(\left(\frac{\eta+s_0}{2}\right)^2\right)\bar{u}(\eta)f(u_{L0}(\eta)), \tag{5.1.17c}$$

$$I_2(\eta) = \exp\left(\left(\frac{\eta+s_0}{2}\right)^2\right)\hat{u}(\eta)f(u_{L0}(\eta)). \tag{5.1.17d}$$

As an aside we remark that on fixing $\eta = O(1)^-$ and varying u_c, we find

$$u_{p2}(\eta) = O(1) \quad \text{as} \quad u_c \to 0^+ \qquad \text{and} \qquad u_{p2}(\eta) = o(1) \quad \text{as} \quad u_c \to 1^-. \tag{5.1.18}$$

This illustrates how $u_{L0}(\eta)$ dominates the solution in region $\mathbf{I_L}$ for large u_c with $u_{p2}(\eta)$, and therefore $u_{L1}(\eta)$, having an increasingly significant impact as u_c decreases. Returning to our analysis of the boundary value problem (5.1.14), for arbitrary $u_c \in (0,1)$, an application of condition (5.1.14c) determines

$$d_2 = \left(\frac{s_1}{\sqrt{\pi}} - 2d_1 s_0\right)\frac{e^{-\frac{{s_0}^2}{4}}}{({s_0}^2+2)} - d_1\sqrt{\pi}\operatorname{erf}\left(\frac{s_0}{2}\right), \tag{5.1.19}$$

$$\bar{d}_2 = \left(\frac{s_1}{\sqrt{\pi}} - 2\bar{d}_1 s_0\right)\frac{e^{-\frac{{s_0}^2}{4}}}{({s_0}^2+2)} - d_1\sqrt{\pi}\operatorname{erf}\left(\frac{s_0}{2}\right). \tag{5.1.20}$$

Moreover, applying the matching conditions (5.1.14e) and (5.1.14f) determines

$$d_1 = \frac{1}{\left(\sqrt{\pi}({s_0}^2+2)\left(\operatorname{erf}\left(\frac{s_0}{2}\right)+1\right) + 2s_0 e^{-\frac{{s_0}^2}{4}}\right)}\left(\frac{s_1}{\sqrt{\pi}}e^{-\frac{{s_0}^2}{4}} - \frac{({s_0}^2+2)}{2}\hat{d}_1\right), \tag{5.1.21}$$

$$\bar{d}_1 = -\frac{1}{\left(\sqrt{\pi}({s_0}^2+2)\left(1-\operatorname{erf}\left(\frac{s_0}{2}\right)\right) - 2s_0 e^{-\frac{{s_0}^2}{4}}\right)}\left[\frac{s_1}{\sqrt{\pi}}e^{-\frac{{s_0}^2}{4}}\right], \tag{5.1.22}$$

with the constant $\hat{d}_1$ given by

$$\hat{d}_1 = \left(\sqrt{\pi} \int_{-\infty}^{0} I_1(\lambda) d\lambda + \int_{-\infty}^{0} I_2(\lambda) d\lambda \right). \tag{5.1.23}$$

As $u'_{p2}(0) = 0$, an application of the coupling condition (5.1.14d) determines $d_1 = \bar{d}_1$ (and thus $d_2 = \bar{d}_2$) which finally requires that

$$s_1 = \frac{1}{4} \left(\sqrt{\pi} ({s_0}^2 + 2) \left(1 - \operatorname{erf} \left(\frac{s_0}{2} \right) \right) e^{\frac{{s_0}^2}{4}} - 2 s_0 \right) \hat{d}_1. \tag{5.1.24}$$

Thus, we have determined that the two-term expansions for $u(\eta, t)$ in region $\mathbf{I_L}$ and region $\mathbf{I_R}$ are given by

$$\begin{aligned} u(\eta, t) = {} & \frac{1}{2} \left[1 - \operatorname{erf} \left(\frac{\eta + s_0}{2} \right) \right] \\ & + t \left(d_1 \hat{u}(\eta) + d_2 \bar{u}(\eta) - \frac{s_1}{2\sqrt{\pi}} \exp \left[- \left(\frac{\eta + s_0}{2} \right)^2 \right] + u_{p2}(\eta) \right) + o(t), \end{aligned} \tag{5.1.25a}$$

as $t \to 0^+$ with $\eta = O(1)^-$, and

$$\begin{aligned} u(\eta, t) = {} & \frac{1}{2} \left[1 - \operatorname{erf} \left(\frac{\eta + s_0}{2} \right) \right] \\ & + t \left(d_1 \hat{u}(\eta) + d_2 \bar{u}(\eta) - \frac{s_1}{2\sqrt{\pi}} \exp \left[- \left(\frac{\eta + s_0}{2} \right)^2 \right] \right) + o(t), \end{aligned} \tag{5.1.25b}$$

as $t \to 0^+$ with $\eta = O(1)^+$; we have also deduced the following two-term expansion for $s(t)$

$$s(t) = s_0 t^{\frac{1}{2}} + s_1 t^{\frac{3}{2}} + o(t^{\frac{3}{2}}), \tag{5.1.26}$$

as $t \to 0^+$. Here the constants d_1, d_2, s_0 and s_1 are given by (5.1.21), (5.1.19), (5.1.12) and (5.1.24), respectively, and the functions $u_{p2}(\eta)$, $\hat{u}(\eta)$, $\bar{u}(\eta)$, $I_1(\lambda)$ and $I_2(\lambda)$ are given by (5.1.16) and (5.1.17), respectively. It is worth noting that we have obtained the two term small-time expansion for $s(t)$ without needing to know the precise asymptotic structure of the solution in regions $\mathbf{II_L}$ and $\mathbf{II_R}$. Their leading order form described by (5.1.1c) and

(5.1.1d), respectively, was sufficient. The asymptotic expansion in regions $\mathbf{II_L}$ and $\mathbf{II_R}$ are obtained for completeness of the small-time regime. From (5.1.25a) and (5.1.25b), we observe that for $(-\eta) \gg 1$,

$$u(\eta, t) \sim 1 - \frac{1}{\sqrt{\pi}} \frac{1}{|\eta + s_0|} \exp\left(- \left(\frac{\eta + s_0}{2} \right)^2 \right) (1 - O((\eta + s_0)^{-2})), \tag{5.1.27}$$

as $t \to 0^+$, and for $\eta \gg 1$,

$$u(\eta, t) \sim \frac{1}{\sqrt{\pi}} \frac{1}{(\eta + s_0)} \exp\left(- \left(\frac{\eta + s_0}{2} \right)^2 \right) (1 - O((\eta + s_0)^{-2})), \tag{5.1.28}$$

as $t \to 0^+$.

Now, as $\eta \to -\infty$ we move out of region $\mathbf{I_L}$ and into region $\mathbf{II_L}$, in which, via (5.1.1c), $y = O(1)^-$ and $u(y, t) = 1 - o(1)$ as $t \to 0^+$. The structure of the expansion in region $\mathbf{I_L}$, for $(-\eta) \gg 1$, (given by (5.1.27)) suggests that in region $\mathbf{II_L}$ we write

$$u(y, t) = 1 - e^{-\frac{H(y,t)}{t}}, \tag{5.1.29}$$

and expand in the form,

$$H(y, t) = H_0(y) + t^{\frac{1}{2}} H_1(y) + t \ln t H_2(y) + t H_3(y) + o(t), \tag{5.1.30}$$

as $t \to 0^+$ with $y = O(1)^-$ and $H_0(y) > 0$. We substitute expansions (5.1.29) and (5.1.30) into equation (2.0.8a) to obtain (on solving at each order of t in turn)

$$\begin{aligned} u(y, t) = \; 1 - \exp\Bigg(& - \frac{1}{t} \left(\frac{y + D_0}{2} \right)^2 - \frac{1}{t^{\frac{1}{2}}} \left(\frac{s_0}{2} (y + D_0) + D_1 (y + D_0)^{\frac{1}{2}} \right) \\ & - D_2 \ln t - \Bigg(\frac{(1 - 2D_2)}{2} \ln|y + D_0| + \frac{s_0 D_1}{2} \frac{1}{(y + D_0)^{\frac{1}{2}}} \\ & + \frac{{D_1}^2}{4} \frac{1}{(y + D_0)} + D_3 \Bigg) + o(1) \Bigg), \end{aligned} \tag{5.1.31}$$

as $t \to 0^+$, with $y = O(1)^-$, and where D_0, D_1, D_2 and D_3 are arbitrary constants to

be determined. It remains to match expansion (5.1.31) in region $\mathbf{II_L}$ (as $y \to 0^-$) with expansion (5.1.27) in region $\mathbf{I_L}$ (as $\eta \to -\infty$). On applying Van Dyke's matching principle [58], we readily obtain that

$$D_0 = 0, \qquad D_1 = 0, \qquad D_2 = -\frac{1}{2}, \qquad D_3 = \frac{1}{2}\ln\pi + \frac{{s_0}^2}{4}. \tag{5.1.32}$$

Thus, the expansion in region $\mathbf{II_L}$ is given by

$$\begin{aligned} u(y,t) = 1 - \exp\Bigg(& -\frac{y^2}{4t} - \frac{y s_0}{2t^{\frac{1}{2}}} + \frac{1}{2}\ln t \\ & - \left(\ln(-y) + \frac{1}{2}\ln\pi + \frac{{s_0}^2}{4}\right) + o(1)\Bigg), \end{aligned} \tag{5.1.33}$$

as $t \to 0^+$ and with $y = O(1)^-$. Furthermore, this expansion remains uniform for $(-y) \gg 1$ as $t \to 0^+$.

Next, as $\eta \to \infty$, we move out of region $\mathbf{I_R}$ and into region $\mathbf{II_R}$, in which, via (5.1.1d), $y = O(1)^+$ and $u(y,t) = o(1)$ as $t \to 0^+$. The structure of the expansion in region $\mathbf{I_R}$, for $\eta \gg 1$, (given by (5.1.28)) suggests that in region $\mathbf{II_R}$ we write

$$u(y,t) = e^{-\frac{\bar{H}(y,t)}{t}}, \tag{5.1.34}$$

and expand in the form,

$$\bar{H}(y,t) = \bar{H}_0(y) + t^{\frac{1}{2}}\bar{H}_1(y) + t\ln t\bar{H}_2(y) + t\bar{H}_3(y) + o(t), \tag{5.1.35}$$

as $t \to 0^+$ with $y = O(1)^+$ and $\bar{H}_0(y) > 0$. Substitution of (5.1.34) and (5.1.35) into

equation (2.0.8a) gives (on solving at each order of t in turn)

$$u(y,t) = \exp\left(-\frac{1}{t}\left(\frac{y+\bar{D}_0}{2}\right)^2 - \frac{1}{t^{\frac{1}{2}}}\left(\frac{s_0}{2}(y+\bar{D}_0) + \bar{D}_1\left(y+\bar{D}_0\right)^{\frac{1}{2}}\right) - \bar{D}_2 \ln t - \left(\frac{\left(1-2\bar{D}_2\right)}{2}\ln|y+\bar{D}_0| + \frac{s_0\bar{D}_1}{2}\frac{1}{\left(y+\bar{D}_0\right)^{\frac{1}{2}}} + \frac{\bar{D}_1^2}{4}\frac{1}{\left(y+\bar{D}_0\right)} + \bar{D}_3\right) + o(1)\right), \tag{5.1.36}$$

as $t \to 0^+$, with $y = O(1)^+$, and where $\bar{D}_0,\ \bar{D}_1,\ \bar{D}_2$ and $\bar{D}_3$ are arbitrary constants to be determined. It remains to match expansion (5.1.36) in region $\mathbf{II_R}$ (as $y \to 0^+$) with expansion (5.1.28) in region $\mathbf{I_R}$ (as $\eta \to \infty$). On applying Van Dyke's matching principle [58], we readily obtain that

$$\bar{D}_0 = 0, \qquad \bar{D}_1 = 0, \qquad \bar{D}_2 = -\frac{1}{2}, \qquad \bar{D}_3 = \frac{1}{2}\ln\pi + \frac{{s_0}^2}{4}. \tag{5.1.37}$$

Thus, the expansion in region $\mathbf{II_R}$ is given by

$$u(y,t) = \exp\left(-\frac{y^2}{4t} - \frac{ys_0}{2t^{\frac{1}{2}}} + \frac{1}{2}\ln t - \left(\ln y + \frac{1}{2}\ln\pi + \frac{{s_0}^2}{4}\right) + o(1)\right), \tag{5.1.38}$$

as $t \to 0^+$ and with $y = O(1)^+$. Furthermore, this expansion remains uniform for $y \gg 1$ as $t \to 0^+$.

The asymptotic structure as $t \to 0^+$ is now complete with the expansions in regions $\mathbf{II_L}$, $\mathbf{I_L}$, $\mathbf{I_R}$ and $\mathbf{II_R}$ providing a uniform approximation to the solution of [QIVP] as $t \to 0^+$. We next use this information to enable us to develop the asymptotic structure of the solution to [QIVP] as $|y| \to \infty$ with $t = O(1)$. However, before proceeding to this, it is of interest to examine the form of $\dot{s}(t)$ in the small-time regime for all $u_c \in (0,1)$. It follows from the expression (5.1.26) that

$$\dot{s}(t) \sim \frac{1}{2}s_0 t^{-\frac{1}{2}} + \frac{3}{2}s_1 t^{\frac{1}{2}} \quad \text{as} \quad t \to 0^+, \tag{5.1.39}$$

with s_0 and s_1 given by equations (5.1.12) and (5.1.24) respectively. In particular, we observe from (5.1.12) that s_0 is monotonic decreasing in u_c with

$$s_0 \to \infty \ \text{ as } \ u_c \to 0^+, \quad s_0 = 0 \ \text{ when } \ u_c = \frac{1}{2} \quad \text{and} \quad s_0 \to -\infty \ \text{ as } \ u_c \to 1^-. \tag{5.1.40}$$

Thus, the leading term in (5.1.39) reveals that $\dot{s}(t)$ has an integrable singularity as $t \to 0^+$, with

$$\dot{s}(t) \to +\infty \quad \text{as} \quad t \to 0^+, \tag{5.1.41}$$

when $u_c \in (0, 1/2)$, whilst,

$$\dot{s}(t) \to -\infty \quad \text{as} \quad t \to 0^+, \tag{5.1.42}$$

when $u_c \in (1/2, 1)$. When $u_c = 1/2$, there is a transition, and in this case, we determine

$$s_1 = \frac{1}{8}\sqrt{\pi}e^{\frac{1}{4}} \int_{-\infty}^{0} e^{\frac{\lambda^2}{4}} \left[1 - \text{erf}^2\left(\frac{\lambda}{2}\right)\right] \times \left(\sqrt{\pi}\left(1 + \frac{\lambda^2}{2}\right)\left(1 + \text{erf}\left(\frac{\lambda}{2}\right)\right) + \lambda e^{-\frac{\lambda^2}{4}}\right) d\lambda, \tag{5.1.43}$$

via (5.1.24). Additionally, we observe that the integrand is positive for all $\lambda < 0$, and, therefore, $s_1 > 0$. On asymptotic expansion of the error function, we determine s_1 approaches zero from above exponentially slowly as $\lambda \to -\infty$. Thus, in this transition case,

$$\dot{s}(t) \to 0^+ \quad \text{as} \quad t \to 0^+. \tag{5.1.44}$$

We observe that (5.1.41), (5.1.42) and (5.1.44) above confirm the numerical solutions for [QIVP] obtained in Section 3.2, as illustrated in Figure 3.2.

5.2 Asymptotic Solution to [QIVP] as $|y| \to \infty$

We now develop the structure of the solution to [QIVP] as $|y| \to \infty$ with $t = O(1)$. We begin in region $\mathbf{III_L}$, where $y \to -\infty$ with $t = O(1)$. The structure of the expansion in

region $\mathbf{II_L}$, for $(-y) \gg 1$, (given by (5.1.33)) suggests that in region $\mathbf{III_L}$ we write

$$u(y,t) = 1 - e^{-y^2\Phi(y,t)}, \tag{5.2.1}$$

and expand in the form,

$$\Phi(y,t) = \Phi_0(t) + \frac{1}{y}\Phi_1(t) + \frac{\ln(-y)}{y^2}\Phi_2(t) + \frac{1}{y^2}\Phi_3(t) + o\left(y^{-2}\right), \tag{5.2.2}$$

as $y \to -\infty$ with $t = O(1)$ and $\Phi_0(t) > 0$. On substitution of expansions (5.2.1) and (5.2.2) into equation (2.0.8a) we obtain a system of equations at successive orders of y which we solve in turn to give:

$$\Phi_0(t) = \frac{1}{(4t + C_0)}, \qquad \Phi_1(t) = \frac{(2s(t) + C_1)}{(4t + C_0)}, \qquad \Phi_2(t) = C_2, \tag{5.2.3a}$$

$$\dot{\Phi}_3(t) = \dot{s}(t)\left(\frac{2s(t) + C_1}{4t + C_0}\right) + \frac{(2 - 4C_2)}{(4t + C_0)} - \left(\frac{2s(t) + C_1}{4t + C_0}\right)^2 - f'(1), \tag{5.2.3b}$$

with $t = O(1)$, and where $C_0,\ C_1,\ C_2$ and the constant associated with integrating equation (5.2.3b) (C_3) are arbitrary constants to be determined. Note that $\Phi_1(t)$ and $\Phi_3(t)$ both depend on the function $s(t)$ which is unknown when $t = O(1)$. We now match the expansion in region $\mathbf{III_L}$, given by substituting expressions (5.2.3) and (5.2.2) into (5.2.1) (as $t \to 0^+$), with expansion (5.1.33) in region $\mathbf{II_L}$ (as $y \to -\infty$). On applying Van Dyke's matching principle [58] we find

$$C_0 = 0, \qquad C_1 = 0, \qquad C_2 = 1, \qquad C_3 = \frac{1}{2}\ln\pi. \tag{5.2.4}$$

Thus, the expansion in region $\mathbf{III_L}$ is given by

$$u(y,t) = 1 - \exp\Bigg(- \frac{y^2}{4t} - y\frac{s(t)}{2t} - \ln(-y) \\ - \left(\frac{s(t)^2}{4t} - \frac{1}{2}\ln t - f'(1)t + \frac{1}{2}\ln\pi\right) + o(1)\Bigg), \tag{5.2.5}$$

as $y \to -\infty$ with $t = O(1)$. Furthermore, we note that the uniformity of expansion (5.2.5) when $t \gg 1$ as $y \to -\infty$ is dependent on the order of $s(t)$ when $t \gg 1$. This will be discussed further in Section 5.3 when we investigate the asymptotic solution to [QIVP] as $t \to \infty$.

We next consider the corresponding region $\mathbf{III_R}$ where we investigate the structure of the solution to [QIVP] as $y \to \infty$ with $t = O(1)$. The structure of the expansion in region $\mathbf{II_R}$, for $y \gg 1$, (given by (5.1.38)) suggests that in region $\mathbf{III_R}$ we write

$$u(y,t) = e^{-y^2\bar{\Phi}(y,t)}, \tag{5.2.6}$$

and expand in the form,

$$\bar{\Phi}(y,t) = \bar{\Phi}_0(t) + \frac{1}{y}\bar{\Phi}_1(t) + \frac{\ln y}{y^2}\bar{\Phi}_2(t) + \frac{1}{y^2}\bar{\Phi}_3(t) + o\left(y^{-2}\right), \tag{5.2.7}$$

as $y \to \infty$ with $t = O(1)$ and $\bar{\Phi}_0(t) > 0$. On substitution of expansions (5.2.6) and (5.2.7) into equation (2.0.8a) we obtain a system of equations at successive orders of y which we solve in turn to give:

$$\bar{\Phi}_0(t) = \frac{1}{(4t + \bar{C}_0)}, \qquad \bar{\Phi}_1(t) = \frac{(2s(t) + \bar{C}_1)}{(4t + \bar{C}_0)}, \qquad \bar{\Phi}_2(t) = \bar{C}_2, \tag{5.2.8a}$$

$$\dot{\bar{\Phi}}_3(t) = \dot{s}(t)\left(\frac{2s(t) + \bar{C}_1}{4t + \bar{C}_0}\right) + \frac{(2 - 4\bar{C}_2)}{(4t + \bar{C}_0)} - \left(\frac{2s(t) + \bar{C}_1}{4t + \bar{C}_0}\right)^2, \tag{5.2.8b}$$

with $t = O(1)$, and where $\bar{C}_0,\ \bar{C}_1,\ \bar{C}_2$ and the constant associated with integrating equation (5.2.8b) ($\bar{C}_3$) are arbitrary constants to be determined. As in region $\mathbf{III_L}$, we note that $\bar{\Phi}_1(t)$ and $\bar{\Phi}_3(t)$ both depend on the function $s(t)$ which is unknown when $t = O(1)$. We now match the expansion in region $\mathbf{III_R}$, given by substituting expressions (5.2.8) and (5.2.7) into (5.2.6) (as $t \to 0^+$), with expansion (5.1.38) in region $\mathbf{II_R}$ (as $y \to \infty$). On applying Van Dyke's matching principle [58] we find

$$\bar{C}_0 = 0, \qquad \bar{C}_1 = 0, \qquad \bar{C}_2 = 1, \qquad \bar{C}_3 = \frac{1}{2}\ln \pi. \tag{5.2.9}$$

Thus, the expansion in region $\mathbf{III_R}$ is given by

$$u(y,t) = \exp\left(-\frac{y^2}{4t} - y\frac{s(t)}{2t} - \ln y - \left(\frac{s(t)^2}{4t} - \frac{1}{2}\ln t + \frac{1}{2}\ln \pi\right) + o(1)\right), \qquad (5.2.10)$$

as $y \to \infty$ with $t = O(1)$. As before, the uniformity of expansion (5.2.10) when $t \gg 1$ as $y \to \infty$ is dependent on the order of $s(t)$ when $t \gg 1$.

5.3 Asymptotic Solution to [QIVP] as $t \to \infty$

We now develop the structure of the solution to [QIVP] as $t \to \infty$. Guided by the numerical results in Section 3.2, we anticipate that

$$s(t) = \sum_{i=0}^{3} c_i \phi_i(t) + o(\phi_3(t)) \quad \text{as} \quad t \to \infty, \qquad (5.3.1)$$

where $\phi_0(t) = t$, $\phi_1(t)$, $\phi_2(t) = 1$ and $\phi_3(t)$ are a gauge sequence as $t \to \infty$, and the constants c_0, c_1, c_2, c_3 are to be determined, with $c_0 > 0$. We begin by developing the structure of the solution to [QIVP] as $t \to \infty$ at leading order, uniform for $y \in \mathbb{R}$. We anticipate that the structure of the solution to [QIVP] as $t \to \infty$ will have two principal asymptotic regions in $y < 0$, and two principal asymptotic regions in $y > 0$. An examination of the leading order balances in the exponent of expansions (5.2.5) and (5.2.10) when $t \gg 1$ (via (5.3.1)), together with the connection conditions (2.0.8e) and (2.0.8f) determine the principal asymptotic structure as:

$$\text{region } \mathbf{IV_L}: \quad y = O(t)^- \text{ with } u = 1 - o(1) \text{ as } t \to \infty, \qquad (5.3.2a)$$

$$\text{region } \mathbf{IV_R}: \quad y = O(t)^+ \text{ with } u = o(1) \text{ as } t \to \infty, \qquad (5.3.2b)$$

$$\text{region } \mathbf{V_L}: \quad y = O(1)^- \text{ with } u = O(1) \text{ as } t \to \infty, \qquad (5.3.2c)$$

$$\text{region } \mathbf{V_R}: \quad y = O(1)^+ \text{ with } u = O(1) \text{ as } t \to \infty. \qquad (5.3.2d)$$

The expansion (5.2.5) in region $\mathbf{III_L}$ will remain uniform for $t \gg 1$ provided that $(-y) \gg t$, but fails when $y = O(t)$ as $t \to \infty$. Hence, we begin in region $\mathbf{IV_L}$, in which, via (5.3.2a), we introduce the scaled coordinate $w = \frac{y}{t} = O(1)^-$ as $t \to \infty$ with $u(w,t) = u(y,t)$ and where $u(w,t)$ satisfies

$$t^2 u_t - t\left(w + c_0 + c_1\dot{\phi}_1 + c_3\dot{\phi}_3 + o(\dot{\phi}_3)\right)u_w = u_{ww} + t^2 f(u), \quad w < 0. \tag{5.3.3}$$

The structure of the expansion in region $\mathbf{III_L}$, for $t \gg 1$, (given by (5.2.5)) suggests that in region $\mathbf{IV_L}$, at leading order, we write

$$u(w,t) = 1 - \exp\Big(- t\left(G_0(w) + o(1)\right)\Big), \tag{5.3.4}$$

as $t \to \infty$ with $w = O(1)^-$ and $G_0(w) > 0$. On substitution of expansion (5.3.4) into equation (5.3.3), we obtain the following boundary value problem, namely,

$$(G_0')^2 - (w + c_0)G_0' + G_0 = -f'(1), \quad w < 0, \tag{5.3.5a}$$

$$G_0(w) > 0 \quad \forall w < 0, \tag{5.3.5b}$$

$$G_0(w) \sim \left(\frac{w + c_0}{2}\right)^2 - f'(1) \quad \text{as} \quad w \to -\infty, \tag{5.3.5c}$$

$$G_0(w) = O(w) \quad \text{as} \quad w \to 0^-. \tag{5.3.5d}$$

Here condition (5.3.5c) represents the matching condition between expansion (5.3.4) in region $\mathbf{IV_L}$ when $(-w) \gg 1$, and expansion (5.2.5) in region $\mathbf{III_L}$ when $t \gg 1$ whilst condition (5.3.5d) represents the matching condition between expansion (5.3.4) in region $\mathbf{IV_L}$ when $w = O(t^{-1})^-$, and region $\mathbf{V_L}$ when $y = O(t)^-$ via (5.3.2c). Equation (5.3.5a) has a family of linear solutions

$$G_0(w) = a_1(w + c_0 - a_1) - f'(1) \quad \forall w < 0, \tag{5.3.6}$$

for any $a_1 \in \mathbb{R}$, and an envelope solution

$$G_0(w) = \left(\frac{w+c_0}{2}\right)^2 - f'(1) \quad \forall w < 0. \tag{5.3.7}$$

It is also possible for a combination of (5.3.6) and (5.3.7) to represent 'envelope-linear' solutions to equation (5.3.5a), which also remain continuous and differentiable. Applying the matching conditions (5.3.5c) and (5.3.5d) determines that for each $c_0 > 0$, the solution to the boundary value problem (5.3.5) is given by the 'envelope-linear' solution

$$G_0(w) = \begin{cases} \left(\frac{w+c_0}{2}\right)^2 - f'(1), & w < -\sqrt{c_0^2 - 4f'(1)}, \\ \left(\frac{c_0 - \sqrt{c_0^2-4f'(1)}}{2}\right) w, & -\sqrt{c_0^2 - 4f'(1)} \leq w < 0. \end{cases} \tag{5.3.8}$$

A sketch of $G_0(w)$, for a fixed $c_0 > 0$, is given in Figure 5.2. For completeness we note that although $G_0(w)$ and $G_0'(w)$ are continuous, $G_0''(w)$ is discontinuous at the point $w = -\sqrt{c_0^2 - 4f'(1)}$. Therefore, a thin transition region must exist about the point $w = -\sqrt{c_0^2 - 4f'(1)}$ where second derivatives are retained at leading order to smooth out this discontinuity. Moreover, region $\mathbf{IV_L}$ will then be replaced by three regions; region $\mathbf{IV_L^a}$, with $-\infty < w < -\sqrt{c_0^2 - 4f'(1)} - o(1)$; region $\mathbf{T_L}$, a thin transition region about the point $w = -\sqrt{c_0^2 - 4f'(1)}$; region $\mathbf{IV_L^b}$, with $-\sqrt{c_0^2 - 4f'(1)} + o(1) < w < 0$. We are only interested in the leading order structure in each expansion for now and will return to consider these regions in more detail later.

Now, as $w \to 0^-$ we move out of region $\mathbf{IV_L}$ and into region $\mathbf{V_L}$, in which, via (5.3.2c), $u = O(1)$ and $y = O(1)^-$ as $t \to \infty$. In this region we therefore expand as

$$u(y,t) = \hat{u}_{L0}(y) + O(\psi_L(t)) \quad \text{as} \quad t \to \infty, \tag{5.3.9}$$

with $y = O(1)^-$, $\hat{u}_{L0}(y) > 0$ and where $\psi_L(t) = o(1)$ as $t \to \infty$. On substitution from expansions (5.3.1) and (5.3.9) into equation (2.0.8a), we obtain at leading order as $t \to \infty$,

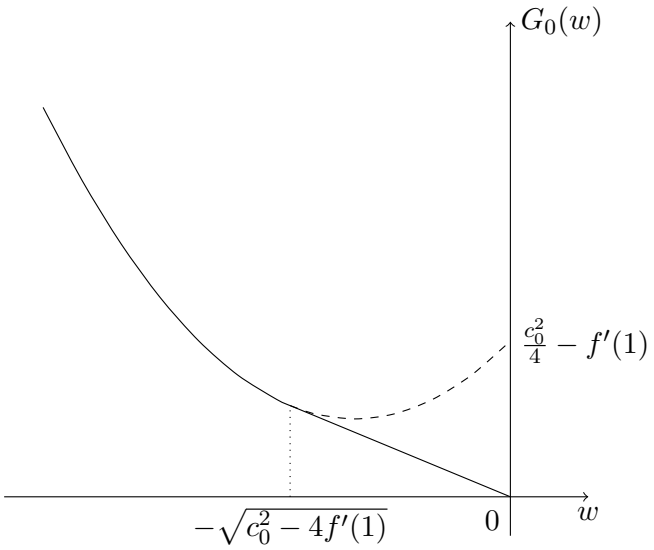

Figure 5.2: A sketch of $G_0(w)$.

$$\hat{u}''_{L0} + c_0\hat{u}'_{L0} + f(\hat{u}_{L0}) = 0 \quad \forall y < 0, \tag{5.3.10a}$$

which must be solved subject to the boundary condition (2.0.8e) at $y = 0$, together with the matching condition with region $\mathbf{IV_L}$ as $y \to -\infty$. Using (5.3.8) and (5.3.9), these conditions require,

$$\hat{u}_{L0}(0^-) = u_c, \tag{5.3.10b}$$

$$\hat{u}_{L0}(y) \to 1 \quad \text{as} \quad y \to -\infty. \tag{5.3.10c}$$

Due to the coupling condition (2.0.8f) across $y = 0$, it is necessary now to formulate the leading order problem in the corresponding regions when $y > 0$ as $t \to \infty$.

The expansion (5.2.10) in region $\mathbf{III_R}$ will remain uniform for $t \gg 1$ provided that $y \gg t$, but fails when $y = O(t)$ as $t \to \infty$. Hence, we now consider region $\mathbf{IV_R}$, in which, via (5.3.2b), we introduce the scaled coordinate $w = \frac{y}{t} = O(1)^+$ as $t \to \infty$ with $u(w,t) = u(y,t)$ and where $u(w,t)$ satisfies

$$t^2 u_t - t\left(w + c_0 + c_1\dot{\phi}_1 + c_3\dot{\phi}_3 + o(\dot{\phi}_3)\right)u_w = u_{ww}, \quad w > 0. \tag{5.3.11}$$

The structure of the expansion in region $\mathbf{III_R}$, for $t \gg 1$, (given by (5.2.10)) suggests that in region $\mathbf{IV_R}$, at leading order, we write

$$u(w,t) = \exp\Big(- t \left(\bar{G}_0(w) + o(1)\right) \Big), \tag{5.3.12}$$

as $t \to \infty$ with $w = O(1)^+$ and $\bar{G}_0(w) > 0$. On substitution of expansion (5.3.12) into equation (5.3.11), we obtain the following boundary value problem, namely,

$$\left(\bar{G}_0'\right)^2 - (w + c_0)\bar{G}_0' + \bar{G}_0 = 0, \quad w > 0, \tag{5.3.13a}$$

$$\bar{G}_0(w) > 0 \quad \forall w > 0, \tag{5.3.13b}$$

$$\bar{G}_0(w) \sim \left(\frac{w + c_0}{2}\right)^2 \quad \text{as} \quad w \to \infty, \tag{5.3.13c}$$

$$\bar{G}_0(w) = O(w) \quad \text{as} \quad w \to 0^+. \tag{5.3.13d}$$

Here condition (5.3.13c) represents the matching condition between expansion (5.3.12) in region $\mathbf{IV_R}$ when $w \gg 1$, and expansion (5.2.10) in region $\mathbf{III_R}$ when $t \gg 1$ whilst condition (5.3.13d) represents the matching condition between expansion (5.3.12) in region $\mathbf{IV_R}$ when $w = O(t^{-1})^+$, and region $\mathbf{V_R}$ when $y = O(t)^+$ via (5.3.2d). For each $c_0 > 0$, the boundary value problem (5.3.13) has the unique solution

$$\bar{G}_0(w) = \begin{cases} \left(\frac{w+c_0}{2}\right)^2, & w > c_0, \\ c_0 w, & 0 < w \leq c_0. \end{cases} \tag{5.3.14}$$

A sketch of $\bar{G}_0(w)$ for a fixed $c_0 > 0$ is given in Figure 5.3. For completeness we note that although $\bar{G}_0(w)$ and $\bar{G}_0'(w)$ are continuous for all $w = O(1)^+$, $\bar{G}_0''(w)$ is discontinuous at the point $w = c_0$. Hence, a thin transition region about the point $w = c_0$ is required in which the second derivatives are retained at leading order to smooth out the discontinuity. This requires that region $\mathbf{IV_R}$ is replaced by three regions; region $\mathbf{IV_R^a}$, with $c_0 + o(1) < w < \infty$; region $\mathbf{T_R}$, a thin transition region about the point $w = c_0$; region $\mathbf{IV_R^b}$, with

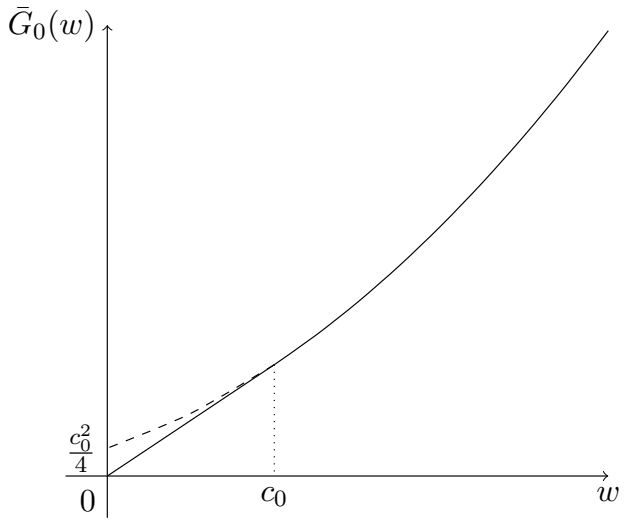

Figure 5.3: A sketch of $\bar{G}_0(w)$.

$0 < w < c_0 - o(1)$. As before, we will consider these regions in more detail later.

Now, as $w \to 0^+$ we move out of region $\mathbf{IV_R}$ and into region $\mathbf{V_R}$, in which, via (5.3.2d), $u = O(1)$ and $y = O(1)^+$ as $t \to \infty$. In this region we must therefore expand as

$$u(y,t) = \hat{u}_{R0}(y) + O(\psi_R(t)) \quad \text{as} \quad t \to \infty, \tag{5.3.15}$$

with $y = O(1)^+$, $\hat{u}_{R0}(y) > 0$ and $\psi_R(t) = o(1)$ as $t \to \infty$. On substitution from expansions (5.3.1) and (5.3.15) into equation (2.0.8a), we obtain at leading order as $t \to \infty$,

$$\hat{u}''_{R0} + c_0 \hat{u}'_{R0} = 0 \quad \forall y > 0, \tag{5.3.16a}$$

which must be solved subject to the boundary condition (2.0.8e) at $y = 0$, together with the matching condition with region $\mathbf{IV_R}$ as $y \to \infty$. Using (5.3.14) and (5.3.15), these conditions require,

$$\hat{u}_{R0}(0^+) = u_c, \tag{5.3.16b}$$

$$\hat{u}_{R0}(y) \to 0 \quad \text{as} \quad y \to \infty. \tag{5.3.16c}$$

Finally, the boundary value problems (5.3.10) and (5.3.16) must be solved subject to the

coupling condition (2.0.8f) across $y = 0$, which requires

$$\hat{u}'_{L0}(0^-) = \hat{u}'_{R0}(0^+). \tag{5.3.17}$$

The coupled nonlinear boundary value problem, given by (5.3.10), (5.3.16) and (5.3.17), across regions $\mathbf{V_L}$ and $\mathbf{V_R}$ is precisely the nonlinear boundary value problem (4.2.3) with v replaced by c_0. Thus, we immediately conclude that

$$\hat{u}_{R0}(y) = U_T(y), \quad y \geq 0, \tag{5.3.18a}$$

$$\hat{u}_{L0}(y) = U_T(y), \quad y < 0, \tag{5.3.18b}$$

and that c_0 is now determined as,

$$c_0 = v^*(u_c), \tag{5.3.18c}$$

where $U_T : \mathbb{R} \to \mathbb{R}$ is the PTW solution to [QIVP] at cut-off $u_c \in (0, 1)$, which has propagation speed $v^*(u_c)$. In Section 4.2, an exact expression for the PTW solution for non-negative y was given by equation (4.2.29c) with its asymptotic form in the limit of $y \to -\infty$ given by (4.2.29d). This completes the asymptotic structure of the solution to [QIVP] as $t \to \infty$ at leading order.

To develop the solution to [QIVP] to higher order we must first return to region $\mathbf{T_R}$, the localised transition region in which $w = v^*(u_c) + o(1)$ as $t \to \infty$. It follows from the leading order term in the expansion in region $\mathbf{IV_R}$ (given by (5.3.14)) that to examine region $\mathbf{T_R}$ we must introduce the scaled coordinate $\zeta = (w - v^*(u_c))t^{\frac{1}{2}}$ with $u(\zeta, t) = u(w, t)$ and where $u(\zeta, t)$ satisfies

$$tu_t - t^{\frac{1}{2}} \left(2v^*(u_c) + \frac{1}{2}\zeta t^{-\frac{1}{2}} + c_1\dot{\phi}_1 + c_3\dot{\phi}_3 + o(\dot{\phi}_3) \right) u_\zeta = u_{\zeta\zeta}, \quad \zeta > 0. \tag{5.3.19}$$

We expand $u(\zeta, t)$ in the form

$$u(\zeta, t) = \big(\bar{F}_0(\zeta) + o(1)\big) \exp\bigg(- tv^*(u_c)^2 - t^{\frac{1}{2}}\zeta v^*(u_c) \bigg), \tag{5.3.20}$$

as $t \to \infty$ with $\zeta = O(1)$ and $\bar{F}_0(\zeta) > 0$. On substitution of expansion (5.3.20) into equation (5.3.19) we obtain

$$t\phi_1'(t)\left(v^*(u_c)c_1\bar{F}_0\right) + \left(-\frac{1}{2}\zeta\bar{F}_0' - \bar{F}_0''\right) + o(1) = 0. \tag{5.3.21}$$

The only non-trivial dominant balance requires that we set, without loss of generality

$$\phi_1(t) = \ln t. \tag{5.3.22}$$

Thus, the leading order equation in region $\mathbf{T_R}$ is given by

$$\bar{F}_0'' + \frac{1}{2}\zeta\bar{F}_0' - \gamma\bar{F}_0 = 0, \qquad -\infty < \zeta < \infty, \tag{5.3.23}$$

with $\gamma = v^*(u_c)c_1$. To obtain the full boundary value problem for $\bar{F}_0(\zeta)$ we require matching conditions as $\zeta \to -\infty$ with region $\mathbf{IV_R^b}$ and as $\zeta \to \infty$ with region $\mathbf{IV_R^a}$. Therefore, we next return to region $\mathbf{IV_R^b}$. The structure of the expansion in region $\mathbf{V_R}$, for $y \gg 1$, (given by (5.3.15), (5.3.18a) and (4.2.29c)) dictates that in region $\mathbf{IV_R^b}$ we expand in the form

$$u(w,t) = \exp\left(-t\left(v^*(u_c)w - \frac{1}{t}\hat{G}(w) + o\left(\frac{1}{t}\right)\right)\right), \tag{5.3.24}$$

as $t \to \infty$ with $O(t^{-1}) < w < v^*(u_c) - O(t^{-\frac{1}{2}})$. We substitute expansion (5.3.24) into equation (5.3.11) to obtain (on solving at each order of t in turn)

$$u(w,t) = \exp\Big(-tv^*(u_c)w + v^*(u_c)c_1\ln\left(v^*(u_c) - w\right) + \bar{d} + o\left(1\right)\Big), \tag{5.3.25}$$

as $t \to \infty$ with $O(t^{-1}) < w < v^*(u_c) - O(t^{-\frac{1}{2}})$ and where the constants c_1 and $\bar{d}$ are to be determined. On matching expansion (5.3.25) in region $\mathbf{IV_R^b}$ (as $w \to v^*(u_c)^-$) with expansion (5.3.20) in region $\mathbf{T_R}$ (as $\zeta \to -\infty$), via Van Dyke's matching principle [58],

we readily obtain that

$$c_1 = 0, \tag{5.3.26}$$

after which we must have

$$\bar{F}_0(\zeta) = e^{\bar{d}} + o(1) \quad \text{as} \quad \zeta \to -\infty. \tag{5.3.27}$$

To determine $\bar{d}$ we next match expansion (5.3.25) (with (5.3.26)) in region $\mathbf{IV_R^b}$ (as $w \to 0^+$) with expansion (4.2.29c) in region $\mathbf{V_R}$ (as $y \to \infty$). On applying Van Dyke's matching principle [58], we require that

$$\bar{d} = \ln u_c. \tag{5.3.28}$$

Thus, via (5.3.25), (5.3.26) and (5.3.28), the expansion in region $\mathbf{IV_R^b}$ is given by

$$u(w,t) = \exp\bigg(- tv^*(u_c)w + \ln u_c + o(1)\bigg), \tag{5.3.29}$$

as $t \to \infty$ with $O(t^{-1}) < w < v^*(u_c) - O(t^{-\frac{1}{2}})$. In addition (5.3.27) becomes

$$\bar{F}_0(\zeta) = u_c + o(1) \quad \text{as} \quad \zeta \to -\infty. \tag{5.3.30}$$

We next consider region $\mathbf{IV_R^a}$. The structure of the expansion in region $\mathbf{III_R}$, for $t \gg 1$, (given by (5.2.10)) and the form of $s(t)$ as $t \to \infty$ (given by (5.3.1) with c_1 now determined by (5.3.26)), suggests that in region $\mathbf{IV_R^a}$ we write

$$u(w,t) = e^{-t\bar{G}(w)}, \tag{5.3.31}$$

and expand in the form,

$$\bar{G}(w,t) = \left(\frac{w + v^*(u_c)}{2}\right)^2 + \frac{\ln t}{t}\bar{G}_1(w) + \frac{1}{t}\bar{G}_2(w) + o(t^{-1}), \tag{5.3.32}$$

as $t \to \infty$ with $w > v^*(u_c) + O(t^{-\frac{1}{2}})$. On substitution of (5.3.31) and (5.3.32) into equation

(5.3.11) we obtain a series of boundary value problems which we solve at each order of t in turn to obtain

$$u(w,t) = \exp\left(-t\left(\frac{w+v^*(u_c)}{2}\right)^2 - \frac{1}{2}\ln t - \bar{G}_2(w) + o(1)\right), \tag{5.3.33}$$

as $t \to \infty$ with $w > v^*(u_c) + O(t^{-\frac{1}{2}})$ and where the function $\bar{G}_2(w)$ is indeterminate, being globally dependent on the evolution at earlier stages when $t = O(1)$ and $y = O(1)$. However, to match with expansion $\mathbf{III_R}$ (when $t \gg 1$) as $w \to \infty$, we require

$$\bar{G}_2(w) \sim c_2\left(\frac{w+v^*(u_c)}{2}\right) + \ln w + \frac{1}{2}\ln\pi \quad \text{as} \quad w \to \infty. \tag{5.3.34}$$

In addition, the structure of the expansion in region $\mathbf{T_R}$, as given by (5.3.20), requires, for matching to be possible, that,

$$\bar{G}_2(w) \sim \bar{\alpha}_1 \ln\big(w - v^*(u_c)\big) + \bar{\alpha}_2 \quad \text{as} \quad w \to v^*(u_c), \tag{5.3.35}$$

for some constants $\bar{\alpha}_1, \bar{\alpha}_2$ to be determined. We now match in detail the expansion in region $\mathbf{IV^a_R}$, given by (5.3.33) and (5.3.35) (as $w \to v^*(u_c)^+$), with expansion (5.3.20) in region $\mathbf{T_R}$ (as $\zeta \to \infty$). On applying Van Dyke's matching principle [58] we find that

$$\bar{\alpha}_1 = 1, \tag{5.3.36}$$

after which,

$$\bar{F}_0(\zeta) = \bar{\sigma}\zeta^{-1}e^{-\frac{\zeta^2}{4}}\left(1 + o(1)\right) \quad \text{as} \quad \zeta \to \infty, \tag{5.3.37}$$

where $\bar{\sigma} = e^{-\bar{\alpha}_2}$. Hence, on collecting (5.3.23), (5.3.26), (5.3.30) and (5.3.37) we obtain

the boundary value problem in region $\mathbf{T_R}$ for $\bar{F}_0(\zeta)$ as,

$$\bar{F}_0'' + \frac{1}{2}\zeta \bar{F}_0' = 0, \qquad -\infty < \zeta < \infty, \tag{5.3.38a}$$

$$\bar{F}_0(\zeta) > 0, \qquad -\infty < \zeta < \infty, \tag{5.3.38b}$$

$$\bar{F}_0(\zeta) = \bar{\sigma}\zeta^{-1} e^{-\frac{\zeta^2}{4}} \left(1 + o(1)\right) \quad \text{as} \quad \zeta \to \infty, \tag{5.3.38c}$$

$$\bar{F}_0(\zeta) = u_c + o(1) \quad \text{as} \quad \zeta \to -\infty. \tag{5.3.38d}$$

This boundary value problem has a solution only when

$$\bar{\sigma} = \frac{u_c}{\sqrt{\pi}}, \tag{5.3.39}$$

with the solution being unique, and given by,

$$\bar{F}_0(\zeta) = \frac{1}{2} u_c \operatorname{erfc}\left(\frac{\zeta}{2}\right), \qquad -\infty < \zeta < \infty. \tag{5.3.40}$$

It follows from (5.3.39) that

$$\bar{\alpha}_2 = -\ln \frac{u_c}{\sqrt{\pi}}. \tag{5.3.41}$$

It is now instructive to summarise the structure in regions $\mathbf{IV_R^a}, \mathbf{T_R}$ and $\mathbf{IV_R^b}$. The expansion in region $\mathbf{IV_R^a}$ is given by (5.3.33) together with the asymptotic conditions

$$\bar{G}_2(w) \sim \begin{cases} \ln\left(w - v^*(u_c)\right) - \ln \frac{u_c}{\sqrt{\pi}}, & \text{as} \quad w \to v^*(u_c), \\ c_2\left(\frac{w + v^*(u_c)}{2}\right) + \ln w + \frac{1}{2}\ln \pi, & \text{as} \quad w \to \infty, \end{cases} \tag{5.3.42}$$

whilst in region $\mathbf{T_R}$

$$u(\zeta, t) = \left(\frac{1}{2} u_c \operatorname{erfc}\left(\frac{\zeta}{2}\right) + o(1)\right) \exp\left(- t v^*(u_c)^2 - t^{\frac{1}{2}} \zeta v^*(u_c)\right), \tag{5.3.43}$$

as $t \to \infty$ with $\zeta = O(1)$, and in region $\mathbf{IV_R^b}$

$$u(w,t) = \exp\bigg(- tv^*(u_c)w + \ln u_c + o(1)\bigg), \tag{5.3.44}$$

as $t \to \infty$ with $O(t^{-1}) < w < v^*(u_c) - O(t^{-\frac{1}{2}})$.

We next consider the structure of the expansion in region $\mathbf{T_R}$ in closer detail. Via (5.3.43), we observe that for $(-\zeta) \gg 1$,

$$u(\zeta,t) \sim \exp\left(-tv^*(u_c)^2 - t^{\frac{1}{2}}v^*(u_c)\zeta + \ln u_c - \frac{1}{\sqrt{\pi}}\frac{1}{\zeta}e^{-\frac{\zeta^2}{4}}\right), \tag{5.3.45}$$

as $t \to \infty$, which demands that in region $\mathbf{IV_R^b}$, to continue the expansion in (5.3.44), we must write

$$u(w,t) = u_c e^{-twv^*(u_c)} + t^{-\frac{1}{2}}\bar{T}(w,t)\exp\left(-\frac{t(w+v^*(u_c))^2}{4}\right), \tag{5.3.46}$$

as $t \to \infty$ with $O(t^{-1}) < w < v^*(u_c) - O(t^{-\frac{1}{2}})$ and $\bar{T}(w,t) = O(1)$ as $t \to \infty$. On substituting from expansion (5.3.46) into equation (5.3.11), and simplifying, we obtain

$$\begin{aligned}\bar{T}_t - t^{-2}\bar{T}_{ww} \\ = O\left(t^{\frac{1}{2}}\phi_3'(t)\exp\left(-t\left(wv^*(u_c) - \frac{(w+v^*(u_c))^2}{4}\right)\right)\right),\end{aligned} \tag{5.3.47}$$

as $t \to \infty$ with $O(t^{-1}) < w < v^*(u_c) - O(t^{-\frac{1}{2}})$. We will later verify that the right-hand side of equation (5.3.47) is exponentially small as $t \to \infty$ in this region. Hence, to obtain a structured balance in (5.3.47), we must expand $\bar{T}(w,t)$ in the form

$$\bar{T}(w,t) = \bar{T}_0(w) + t^{-1}\bar{T}_1(w) + o\left(t^{-1}\right), \tag{5.3.48}$$

as $t \to \infty$ with $O(t^{-1}) < w < v^*(u_c) - O(t^{-\frac{1}{2}})$ and on substitution into (5.3.47) we obtain the leading order equation

$$\bar{T}_0'' + \bar{T}_1 = 0, \tag{5.3.49}$$

with $O(t^{-1}) < w < v^*(u_c) - O(t^{-\frac{1}{2}})$. We conclude that $\bar{T}_0(w)$ is indeterminate and represents a further globally determined function. Therefore, the expansion in region $\mathbf{IV_R^b}$ is developed to,

$$u(w,t) = u_c e^{-twv^*(u_c)} + t^{-\frac{1}{2}}\bar{T}_0(w)(1+O(t^{-1}))\exp\left(-\frac{t(w+v^*(u_c))^2}{4}\right), \tag{5.3.50}$$

as $t \to \infty$ with $O(t^{-1}) < w < v^*(u_c) - O(t^{-\frac{1}{2}})$. We now match the expansion (5.3.50) in region $\mathbf{IV_R^b}$ (as $w \to v^*(u_c)^-$), with expansion (5.3.45) in region $\mathbf{T_R}$ (as $\zeta \to -\infty$), in detail. On applying Van Dyke's matching principle [58] we obtain the condition

$$\bar{T}_0(w) = -\frac{u_c}{\sqrt{\pi}}(w - v^*(u_c))^{-1} + o(w - v^*(u_c))^{-1} \quad \text{as} \quad w \to v^*(u_c)^-. \tag{5.3.51}$$

We next return to region $\mathbf{V_R}$. First, a balance between expansion (5.3.9) in region $\mathbf{V_L}$ and expansion (5.3.15) in region $\mathbf{V_R}$, across the connection at $y = 0$, gives

$$\psi_L(t) = \psi_R(t) = \psi(t), \tag{5.3.52}$$

where $\psi(t) = o(1)$ as $t \to \infty$. In order for the expansion in region $\mathbf{V_R}$ (as $y \to \infty$) to match with the expansion in region $\mathbf{IV_R^b}$ (as $w \to 0^+$), via (5.3.50), we require

$$\psi(t) = O\left(t^\gamma e^{-\frac{v^*(u_c)^2 t}{4}}\right), \tag{5.3.53}$$

as $t \to \infty$ and with constant γ to be determined. Thus, without loss of generality we set

$$\psi(t) = t^\gamma e^{-\frac{v^*(u_c)^2 t}{4}}. \tag{5.3.54}$$

Hence, in region $\mathbf{V_R}$ we develop expansion (5.3.15) in the form

$$u(y,t) = U_T(y) + t^\gamma e^{-\frac{v^*(u_c)^2 t}{4}} u_1(y)(1+o(1)), \tag{5.3.55}$$

as $t \to \infty$ with $y = O(1)^+$. On substitution of expansion (5.3.55) into equation (2.0.8a), and cancelling at leading order, we obtain

$$-\frac{1}{4}v^*(u_c)^2 u_1 - v^*(u_c)u_1' - u_1'' + o(1) \\ = -v^*(u_c)c_3 u_c e^{-v^*(u_c)y} t^{-\gamma}\phi_3'(t)e^{\frac{v^*(u_c)^2 t}{4}}, \tag{5.3.56}$$

as $t \to \infty$ with $y = O(1)^+$. The non-trivial balance in (5.3.56) requires that we set, without loss of generality

$$\phi_3'(t) = t^\gamma e^{-\frac{v^*(u_c)^2 t}{4}}, \tag{5.3.57}$$

and we note that this now confirms that the right-hand side of equation (5.3.47) is exponentially small as $t \to \infty$. The problem for $u_1(y)$ is then given by

$$u_1'' + v^*(u_c)u_1' + \frac{1}{4}v^*(u_c)^2 u_1 = -c_3 U_T'(y), \quad y > 0, \tag{5.3.58a}$$

$$u_1(0^+) = 0, \tag{5.3.58b}$$

where the condition (5.3.58b) is obtained from the boundary condition (2.0.8e). The boundary value problem for $u_1(y)$ must be solved subject to the matching condition with region $\mathbf{IV_R^b}$, however, before formulating this matching condition, we consider the asymptotic solution in regions $\mathbf{IV_L^a}, \mathbf{T_L}, \mathbf{IV_L^b}$ and $\mathbf{V_L}$. We begin in region $\mathbf{IV_L^a}$.

The structure of the expansion in region $\mathbf{III_L}$ for $t \gg 1$ (given by (5.2.5)), the structure of $s(t)$ as $t \to \infty$ (with c_0 and c_1 given by (5.3.18c) and (5.3.26) respectively) and the leading order behaviour in regions $\mathbf{IV_L^a}$ and $\mathbf{IV_L^b}$ (given by (5.3.8)), suggests that in region $\mathbf{IV_L^a}$ we write

$$u(w,t) = 1 - e^{-tG(w,t)}, \tag{5.3.59}$$

and expand in the form,

$$G(w,t) = \left(\frac{w + v^*(u_c)}{2}\right)^2 - f'(1) + \frac{\ln t}{t}G_1(w) + \frac{1}{t}G_2(w) + o(t^{-1}), \tag{5.3.60}$$

as $t \to \infty$ with $w < -\sqrt{v^*(u_c)^2 - 4f'(1)} - O(t^{-\frac{1}{2}})$. On substitution of (5.3.59) and expansion (5.3.60) into equation (5.3.3) we obtain a series of boundary value problems which we solve at each order of t in turn to obtain

$$u(w,t) = 1 - \exp\left(-t\left(\left(\frac{w+v^*(u_c)}{2}\right)^2 - f'(1)\right) - \frac{1}{2}\ln t - G_2(w) + o(1)\right), \quad (5.3.61)$$

as $t \to \infty$ with $w < -\sqrt{v^*(u_c)^2 - 4f'(1)} - O(t^{-\frac{1}{2}})$, and where the function $G_2(w)$ is indeterminate, being globally dependent on the evolution at earlier stages when $t = O(1)$ and $y = O(1)$. However, to match with expansion $\mathbf{III_L}$ (when $t \gg 1$) as $w \to -\infty$, we require

$$G_2(w) \sim c_2\left(\frac{w+v^*(u_c)}{2}\right) + \ln(-w) + \frac{1}{2}\ln\pi \quad \text{as} \quad w \to -\infty. \quad (5.3.62)$$

We next examine region $\mathbf{T_L}$. It follows from the structure of the expansion in region $\mathbf{IV_L^a}$, as $w \to (-\sqrt{v^*(u_c)^2 - 4f'(1)})^-$, that in region $\mathbf{T_L}$ we must introduce the scaled coordinate $\zeta = \left(w + \sqrt{v^*(u_c)^2 - 4f'(1)}\right)t^{\frac{1}{2}}$, with $u(\zeta,t) = u(w,t)$ and where $u(\zeta,t)$ satisfies

$$tu_t - \left[t^{\frac{1}{2}}\left(v^*(u_c) - \sqrt{v^*(u_c)^2 - 4f'(1)} + c_3\dot{\phi}_3 + o(\dot{\phi}_3)\right) + \frac{1}{2}\zeta\right]u_\zeta = u_{\zeta\zeta} + tf(u), \quad (5.3.63)$$

with $\zeta < 0$. We expand $u(\zeta,t)$ in the form

$$u(\zeta,t) = 1 - (F_0(\zeta) + o(1))\exp\left(-t\left(\left(\frac{v^*(u_c) - \sqrt{v^*(u_c)^2 - 4f'(1)}}{2}\right)^2 - f'(1)\right) - t^{\frac{1}{2}}\zeta\left(\frac{v^*(u_c) - \sqrt{v^*(u_c)^2 - 4f'(1)}}{2}\right)\right), \quad (5.3.64)$$

as $t \to \infty$ with $\zeta = O(1)$. On substitution of expansion (5.3.64) into equation (5.3.63) we obtain at leading order

$$F_0'' + \frac{1}{2}\zeta F_0' = 0, \qquad -\infty < \zeta < \infty. \quad (5.3.65)$$

To obtain the full boundary value problem for $F_0(\zeta)$ we require matching conditions as $\zeta \to \pm\infty$. To that end, the structure of the expansion in region $\mathbf{T_L}$, as given by (5.3.64), requires, for matching to be possible, that,

$$G_2(w) \sim \alpha_1 \ln \left| \left(w + \sqrt{v^*(u_c)^2 - 4f'(1)} \right) \right| + \alpha_2, \tag{5.3.66}$$

as $w \to (-\sqrt{v^*(u_c)^2 - 4f'(1)})^-$ for some real constants α_1, α_2 to be determined. We now match in detail the expansion in region $\mathbf{IV_L^a}$, given by (5.3.61) and (5.3.66), as $w \to (-\sqrt{v^*(u_c)^2 - 4f'(1)})^-$, with expansion (5.3.64) in region $\mathbf{T_L}$, as $\zeta \to -\infty$. On applying Van Dyke's matching principle [58], it immediately follows that

$$\alpha_1 = 1, \tag{5.3.67}$$

after which we must have

$$F_0(\zeta) = \sigma \zeta^{-1} e^{-\frac{\zeta^2}{4}} \left(1 + o(1)\right) \quad \text{as} \quad \zeta \to -\infty, \tag{5.3.68}$$

where $\sigma = e^{-\alpha_2}$. We next consider the matching condition as $\zeta \to \infty$. The structure of the expansion in region $\mathbf{V_L}$, for $(-y) \gg 1$, (given by (5.3.9), (5.3.18b) and (4.2.29d)) dictates that in region $\mathbf{IV_L^b}$ we must expand in the form

$$\begin{aligned} u(w,t) = 1 - \exp \Bigg(-t \left(\frac{v^*(u_c) - \sqrt{v^*(u_c)^2 - 4f'(1)}}{2} \right) w \\ + \tilde{G}(w) + o\left(1\right) \Bigg), \end{aligned} \tag{5.3.69}$$

as $t \to \infty$ with $-\sqrt{v^*(u_c)^2 - 4f'(1)} + O(t^{-\frac{1}{2}}) < w < O(t^{-1})^-$. We substitute expansion (5.3.69) into equation (5.3.3) to obtain (on solving at each order of t in turn)

$$u(w,t) = 1 - \exp \left(-t \left(\frac{v^*(u_c) - \sqrt{v^*(u_c)^2 - 4f'(1)}}{2} \right) w + d + o\left(1\right) \right), \tag{5.3.70}$$

as $t \to \infty$ with $-\sqrt{v^*(u_c)^2 - 4f'(1)} + O(t^{-\frac{1}{2}}) < w < O(t^{-1})^-$ and where the constant d is to be determined. On matching expansion (5.3.70) in region $\mathbf{IV_L^b}$ (as $w \to 0^-$) with expansion (5.3.18b) in region $\mathbf{V_L}$ (as $y \to -\infty$), via Van Dyke's matching principle [58], we readily obtain that

$$d = \ln a_\infty, \tag{5.3.71}$$

where, for fixed $u_c \in (0,1)$, a_∞ is the global constant associated with the leading edge behaviour of $U_T(y)$ (see equation (4.2.29d)). Thus, via (5.3.70) and (5.3.71), the expansion in region $\mathbf{IV_L^b}$ is given by

$$u(w,t) = 1 - \exp\left(-t\left(\frac{v^*(u_c) - \sqrt{v^*(u_c)^2 - 4f'(1)}}{2}\right)w + \ln a_\infty + o\left(1\right)\right), \tag{5.3.72}$$

as $t \to \infty$ with $-\sqrt{v^*(u_c)^2 - 4f'(1)} + O(t^{-\frac{1}{2}}) < w < O(t^{-1})^-$. On matching expansion (5.3.72) in region $\mathbf{IV_L^b}$ (as $w \to (-\sqrt{v^*(u_c)^2 - 4f'(1)})^-$) with expansion (5.3.64) in region $\mathbf{T_L}$ (as $\zeta \to \infty$), we obtain the condition

$$F_0(\zeta) = a_\infty + o(1) \quad \text{as} \quad \zeta \to \infty. \tag{5.3.73}$$

Hence, on collecting (5.3.65), (5.3.68) and (5.3.73) we obtain the boundary value problem in region $\mathbf{T_L}$ for $F_0(\zeta)$ as,

$$F_0'' + \frac{1}{2}\zeta F_0' = 0, \qquad -\infty < \zeta < \infty, \tag{5.3.74a}$$

$$F_0(\zeta) > 0, \qquad -\infty < \zeta < \infty, \tag{5.3.74b}$$

$$F_0(\zeta) = \sigma\zeta^{-1}e^{-\frac{\zeta^2}{4}}\left(1 + o(1)\right) \quad \text{as} \quad \zeta \to -\infty, \tag{5.3.74c}$$

$$F_0(\zeta) = a_\infty + o(1) \quad \text{as} \quad \zeta \to \infty. \tag{5.3.74d}$$

This boundary value problem has a solution only when

$$\sigma = \frac{a_\infty}{\sqrt{\pi}}, \tag{5.3.75}$$

with the solution being unique, and given by,

$$F_0(\zeta) = \frac{1}{2}a_\infty \left(1 + \text{erf}\left(\frac{\zeta}{2}\right)\right), \qquad -\infty < \zeta < \infty. \tag{5.3.76}$$

It follows from (5.3.75) that

$$\alpha_2 = -\ln \frac{a_\infty}{\sqrt{\pi}}. \tag{5.3.77}$$

It is again instructive to summarise the structure in regions $\mathbf{IV_L^a}, \mathbf{T_L}$ and $\mathbf{IV_L^b}$. The expansion in region $\mathbf{IV_L^a}$ is given by (5.3.61) together with the asymptotic conditions

$$G_2(w) \sim \begin{cases} G_{21}(w), & \text{as } w \to \left(-\sqrt{v^*(u_c)^2 - 4f'(1)}\right)^-, \\ G_{22}(w), & \text{as } w \to -\infty, \end{cases} \tag{5.3.78a}$$

with

$$\begin{aligned} G_{21}(w) &= \ln|w| + \sqrt{v^*(u_c)^2 - 4f'(1)}| - \ln \frac{a_\infty}{\sqrt{\pi}}, \\ G_{22}(w) &= c_2\left(\frac{w + v^*(u_c)}{2}\right) + \ln|w| + \frac{1}{2}\ln \pi \end{aligned} \tag{5.3.78b}$$

whilst in region $\mathbf{T_L}$,

$$\begin{aligned} u(\zeta, t) = 1 - \Bigg(&\frac{1}{2}a_\infty \left(1 + \text{erf}\left(\frac{\zeta}{2}\right)\right) + o(1)\Bigg) \\ &\times \exp\left(-t\left(\left(\frac{v^*(u_c) - \sqrt{v^*(u_c)^2 - 4f'(1)}}{2}\right)^2 - f'(1)\right)\right. \\ &\left.-t^{\frac{1}{2}}\zeta\left(\frac{v^*(u_c) - \sqrt{v^*(u_c)^2 - 4f'(1)}}{2}\right)\right), \end{aligned} \tag{5.3.79}$$

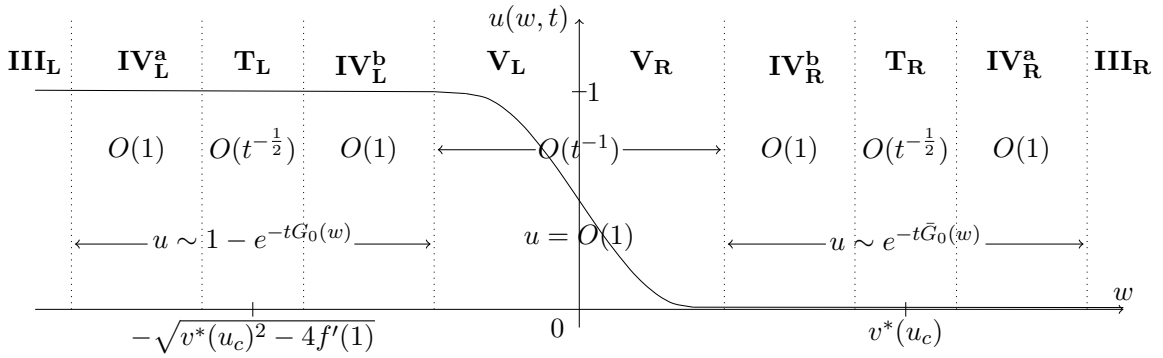

Figure 5.4: A schematic representation of the location and thickness of the asymptotic regions in the solution to [QIVP] as $t \to \infty$. Here the exponents $G_0(w)$ and $\bar{G}_0(w)$ are given by (5.3.8) and (5.3.14), and there are thin transition regions at $w = -\sqrt{v^*(u_c)^2 - 4f'(1)}$ and at $w = v^*(u_c)$, respectively. Note that regions $\mathbf{III_L}$ and $\mathbf{III_R}$ are far field regions for $|w| \gg 1$ as $t \to \infty$.

as $t \to \infty$ with $\zeta = O(1)$, and in region $\mathbf{IV_L^b}$

$$u(w,t) = 1 - \exp\left(- t \left(\frac{v^*(u_c) - \sqrt{v^*(u_c)^2 - 4f'(1)}}{2} \right) + \ln a_\infty + o(1) \right), \tag{5.3.80}$$

as $t \to \infty$ with $-\sqrt{v^*(u_c)^2 - 4f'(1)} + O(t^{-\frac{1}{2}}) < w < O(t^{-1})^-$. A schematic representation of the location and thickness of the asymptotic regions as $t \to \infty$ is given in Figure 5.4.

We next consider the structure of the expansion in region $\mathbf{T_L}$ in closer detail. Via (5.3.79), we observe that for $\zeta \gg 1$,

$$u(\zeta,t) \sim 1 - \exp\left(-t \left(\left(\frac{v^*(u_c) - \sqrt{v^*(u_c)^2 - 4f'(1)}}{2} \right)^2 - f'(1) \right) - t^{\frac{1}{2}} \zeta \left(\frac{v^*(u_c) - \sqrt{v^*(u_c)^2 - 4f'(1)}}{2} \right) + \ln a_\infty - \frac{1}{\sqrt{\pi}} \frac{1}{\zeta} e^{-\frac{\zeta^2}{4}} \right), \tag{5.3.81}$$

as $t \to \infty$, which demands that in region $\mathbf{IV_L^b}$, to continue the expansion in (5.3.80), we

must write

$$u(w,t) = 1 - a_\infty \exp\left[-t\left(\frac{v^*(u_c) - \sqrt{v^*(u_c)^2 - 4f'(1)}}{2}\right) w\right] + t^{-\hat{\beta}} T(w,t) e^{-tH(w)}, \tag{5.3.82}$$

as $t \to \infty$ with $-\sqrt{v^*(u_c)^2 - 4f'(1)} + O(t^{-\frac{1}{2}}) < w < O(t^{-1})^-$ and $T(w,t) = O(1)$ as $t \to \infty$. Here $\hat{\beta}$ is a constant to be determined and

$$H(w) > \frac{1}{2}\left(v^*(u_c) - \sqrt{v^*(u_c)^2 - 4f'(1)}\right) w, \tag{5.3.83}$$

for all $-\sqrt{v^*(u_c)^2 - 4f'(1)} < w < 0$. On substituting from expansion (5.3.82) with (5.3.83) into equation (5.3.3) we obtain

$$\begin{aligned} &T\left(H_w^2 - (w + v^*(u_c)H_w + H + f'(1)\right) + O(t^{-1}) \\ &\quad = O\left(t^{\gamma+\hat{\beta}} \exp\left(-t\left(\left(\frac{v^*(u_c) - \sqrt{v^*(u_c)^2 - 4f'(1)}}{2}\right) w \right.\right.\right. \\ &\quad \left.\left.\left. + \frac{1}{4}v^*(u_c)^2 - H(w)\right)\right)\right), \end{aligned} \tag{5.3.84}$$

as $t \to \infty$ with $-\sqrt{v^*(u_c)^2 - 4f'(1)} + O(t^{-\frac{1}{2}}) < w < O(t^{-1})^-$. To obtain a non-trivial balance at leading order as $t \to \infty$, we suppose that the function $H(w)$ is such that the right-hand side of equation (5.3.84) is exponentially small as $t \to \infty$, and we will later verify this as consistent. Thus, at leading order, we obtain the following boundary value problem in region $\mathbf{IV_L^b}$ for $H(w)$,

$$H_w^2 - (w + v^*(u_c))H_w + H + f'(1) = 0, \tag{5.3.85a}$$

$$0 < H(w) - \frac{1}{2}\left(v^*(u_c) - \sqrt{v^*(u_c)^2 - 4f'(1)}\right) w < \frac{1}{4}v^*(u_c)^2, \tag{5.3.85b}$$

with $-\sqrt{v^*(u_c)^2-4f'(1)}<w<0$ and which must be solved subject to

$$H(w)\to\frac{1}{4}v^*(u_c)^2 \quad \text{as} \quad w\to 0^-, \tag{5.3.85c}$$

$$\begin{aligned} H(w)\sim&\left(\frac{v^*(u_c)-\sqrt{v^*(u_c)^2-4f'(1)}}{2}-v^*(u_c)\right)\sqrt{v^*(u_c)^2-4f'(1)}\\ &-\left(\frac{v^*(u_c)-\sqrt{v^*(u_c)^2-4f'(1)}}{2}\right)\left(w+\sqrt{v^*(u_c)^2-4f'(1)}\right)\\ &+\frac{1}{4}\left(w+\sqrt{v^*(u_c)^2-4f'(1)}\right)^2, \end{aligned} \tag{5.3.85d}$$

as $w\to(-\sqrt{v^*(u_c)^2-4f'(1)})^+$. Here the lower bound of inequality (5.3.85b) follows from (5.3.83), whilst the upper bound ensures the right-hand side of equation (5.3.84) is exponentially small as $t\to\infty$. Condition (5.3.85c) is required so that the correction term in expansion (5.3.82) is of the appropriate order to enable matching of (5.3.82) in region $\mathbf{IV_L^b}$ (as $w\to 0^-$) with expansion (5.3.9), (5.3.18b), (4.2.29d), (5.3.52) and (5.3.54), in region $\mathbf{V_L}$ (as $y\to-\infty$). Condition (5.3.85d) represents the matching condition between the expansion in region $\mathbf{IV_L^b}$ as $w\to(-\sqrt{v^*(u_c)^2-4f'(1)})^+$ (given by (5.3.82)) and the expansion in region $\mathbf{T_L}$ as $\zeta\to\infty$ (given by (5.3.81)). Recalling that for each $u_c\in(0,1)$ then $v^*(u_c)\in(0,2)$, the boundary value problem (5.3.85) has the unique solution

$$H(w)=\begin{cases} H_{L1}(w), & -\sqrt{v^*(u_c)^2-4f'(1)}<w<-2\sqrt{-f'(1)},\\ H_{L2}(w), & -2\sqrt{-f'(1)}<w<0, \end{cases} \tag{5.3.86}$$

with

$$\begin{aligned} H_{L1}(w)&=\frac{1}{4}(w+v^*(u_c))^2-f'(1),\\ H_{L2}(w)&=\frac{1}{4}v^*(u_c)^2+\left(\frac{1}{2}v^*(u_c)-\sqrt{-f'(1)}\right)w, \end{aligned} \tag{5.3.87}$$

and where we also determine, via asymptotic matching, that

$$\hat{\beta} = \frac{1}{2}, \tag{5.3.88}$$

for $-\sqrt{v^*(u_c)^2 - 4f'(1)} + O(t^{-\frac{1}{2}}) < w < -2\sqrt{-f'(1)} - O(t^{-\frac{1}{2}})$. A sketch of the exponents in expansions (5.3.33) and (5.3.44), (5.3.61) and (5.3.80) in regions $\mathbf{IV_R^a}, \mathbf{IV_R^b}$, $\mathbf{IV_L^a}$ and $\mathbf{IV_L^b}$, respectively, is given in Figure 5.5. We note that although $H(w)$ and $H'(w)$ are continuous for all $-\sqrt{v^*(u_c)^2 - 4f'(1)} < w < 0$, the second derivative $H''(w)$ is discontinuous at the point $w = -2\sqrt{-f'(1)}$. Hence, a thin transition region about the point $w = -2\sqrt{-f'(1)}$ is required in which the second derivatives are retained to leading order to smooth out the discontinuity. However, this region is passive, and for brevity will not be considered here. It remains to determine $T(w,t)$ in region $\mathbf{IV_L^b}$. To that end, we expand $T(w,t)$ in the form

$$T(w,t) = T_0(w) + t^{-\lambda} T_1(w) + o\left(t^{-\lambda}\right), \tag{5.3.89}$$

as $t \to \infty$ with $-\sqrt{v^*(u_c)^2 - 4f'(1)} + O(t^{-\frac{1}{2}}) < w < O(t^{-1})$ and substitute from expansion (5.3.82) (with (5.3.86) and (5.3.89)) into equation (2.0.8a). When $-\sqrt{v^*(u_c)^2 - 4f'(1)} < w < -2\sqrt{-f'(1)}$, we find $\lambda = 1$ and obtain at leading order

$$T_0'' + T_1 = 0. \tag{5.3.90}$$

Therefore, $T_0(w)$ is indeterminate when $-\sqrt{v^*(u_c)^2 - 4f'(1)} < w < -2\sqrt{-f'(1)}$ and represents a further globally determined function. However, when $-2\sqrt{-f'(1)} < w < 0$, we obtain at leading order

$$\left(w + 2\sqrt{-f'(1)}\right) T_0' = -\hat{\beta} T_0, \tag{5.3.91}$$

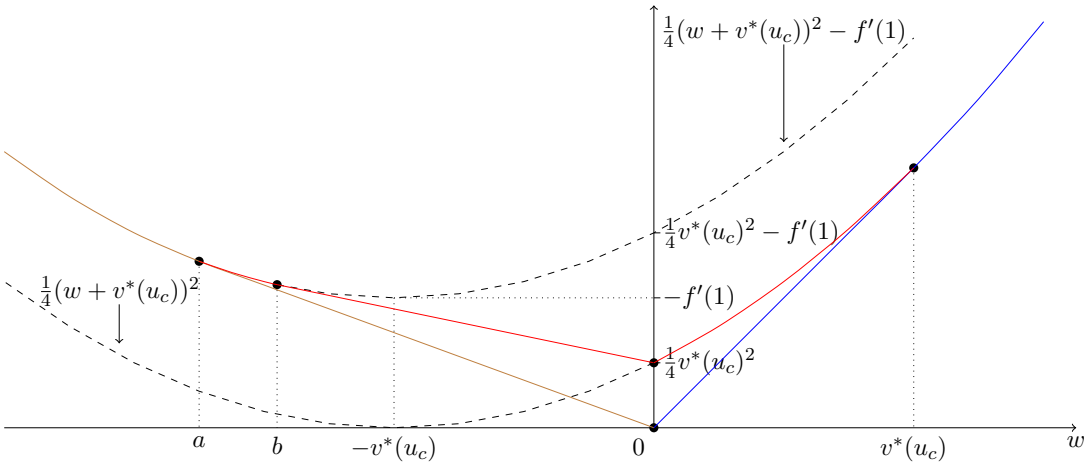

Figure 5.5: Sketches of the exponent in expansions (5.3.61) and (5.3.80), in regions $\mathbf{IV_L^a}$ and $\mathbf{IV_L^b}$, respectively, in brown; sketches of the exponent in expansions (5.3.33) and (5.3.44), in regions $\mathbf{IV_R^a}$ and $\mathbf{IV_R^b}$, respectively in blue; and sketches of the exponential corrections in regions $\mathbf{IV_L^b}$ ($a < w < 0$) and $\mathbf{IV_R^b}$ ($0 < w < v^*(u_c)$), respectively, in red. We have used the notation $a = -\sqrt{v^*(u_c)^2 - f'(1)}$ and $b = -2\sqrt{-f'(1)}$.

which gives, on integration,

$$T_0(w) = \frac{\left(2\sqrt{-f'(1)}\right)^{\hat{\beta}} A_L}{\left(w + 2\sqrt{-f'(1)}\right)^{\hat{\beta}}}, \tag{5.3.92}$$

with $-2\sqrt{-f'(1)} < w < 0$ and where $A_L \neq 0$ is a globally determined constant. Therefore, the expansion in region $\mathbf{IV_L^b}$ is developed to,

$$u(w,t) = 1 - a_\infty \exp\left(-t \left(\frac{v^*(u_c) - \sqrt{v^*(u_c)^2 - 4f'(1)}}{2} \right) w \right) + \hat{u}(w,t), \tag{5.3.93}$$

as $t \to \infty$. Here

$$\hat{u}(w,t) = t^{-\beta_1}\big(T_0(w) + o(1)\big) \exp\left(-t \left(\frac{1}{4}\left(w + v^*(u_c)\right)^2 - f'(1) \right) \right), \tag{5.3.94}$$

when $-\sqrt{v^*(u_c)^2 - 4f'(1)} + O(t^{-\frac{1}{2}}) < w < -2\sqrt{-f'(1)} - O(t^{-\frac{1}{2}})$, with

$$T_0(w) \sim \frac{a_\infty}{\sqrt{\pi}} \left(w + \sqrt{v^*(u_c)^2 - 4f'(1)} \right)^{-1} \quad \text{as } w \to (-\sqrt{v^*(u_c)^2 - 4f'(1)})^+, \tag{5.3.95}$$

and

$$\beta_1 = \frac{1}{2}. \tag{5.3.96}$$

However,

$$\begin{aligned}\hat{u}(w,t) =& \frac{\left(2\sqrt{-f'(1)}\right)^{\beta_2} A_L}{\left(w + 2\sqrt{-f'(1)}\right)^{\beta_2}} t^{-\beta_2}\big(1 + o(1)\big) \\ & \times \exp\left(-t\left(\frac{1}{4}v^*(u_c)^2 + \left(\frac{1}{2}v^*(u_c) - \sqrt{-f'(1)}\right)w\right)\right),\end{aligned} \tag{5.3.97}$$

when $-2\sqrt{-f'(1)} + O(t^{-\frac{1}{2}}) < w < O(t^{-1})^-$, and with β_2 undetermined at this stage. It is important to note that the change in structure of $\hat{u}(w,t)$ across $w = -2\sqrt{-f'(1)}$ is accommodated in a transition region when $w = -2\sqrt{-f'(1)} \pm O(t^{-\frac{1}{2}})$. This region is passive and its details may be omitted here.

We can now return to region $\mathbf{V_L}$. It follows from (5.3.9) with (5.3.18b), (4.2.29d), (5.3.52) and (5.3.54), that in region $\mathbf{V_L}$ we must develop expansion (5.3.9) in the form

$$u(y,t) = U_T(y) + t^{\gamma}\exp\left(-\frac{1}{4}v^*(u_c)^2 t\right)u_1(y)(1 + o(1)), \tag{5.3.98}$$

as $t \to \infty$ with $y = O(1)^-$. On substituting from expansions (5.3.1) and (5.3.98) into equation (2.0.8a), and cancelling at leading order, we obtain

$$u_1'' + v^*(u_c)u_1' + \left(\frac{1}{4}v^*(u_c)^2 + f'(U_T(y))\right)u_1 = -c_3 U_T'(y), \quad y < 0, \tag{5.3.99a}$$

$$u_1(0^-) = 0, \tag{5.3.99b}$$

where the condition (5.3.99b) is obtained from the boundary condition (2.0.8e). It remains to match expansion (5.3.98) in region $\mathbf{V_L}$ (as $y \to -\infty$) with expansion (5.3.93) in region $\mathbf{IV_L^b}$ (as $w \to 0^-$). On applying Van Dyke's matching principle [58], we readily obtain

this matching condition as

$$u_1(y) \sim A_L \exp\left(\left(\sqrt{-f'(1)} - \frac{1}{2}v^*(u_c)\right)y\right) \quad \text{as} \quad y \to -\infty, \tag{5.3.99c}$$

with β_2 now determined as

$$\beta_2 = -\gamma. \tag{5.3.100}$$

On collecting the boundary value problems (5.3.58) and (5.3.99), in addition to the derivative continuity condition (2.0.8f) at $y = 0$, we obtain the following boundary value problem for $u_1(y)$,

$$u_1'' + v^*(u_c)u_1' + \frac{1}{4}v^*(u_c)^2 u_1 = -c_3 U_T'(y), \quad y > 0, \tag{5.3.101a}$$

$$u_1'' + v^*(u_c)u_1' + \left(\frac{1}{4}v^*(u_c)^2 + f'(U_T(y))\right)u_1 = -c_3 U_T'(y), \quad y < 0, \tag{5.3.101b}$$

$$u_1(y) \sim A_L \exp\left(\left(\sqrt{-f'(1)} - \frac{1}{2}v^*(u_c)\right)y\right) \quad \text{as} \quad y \to -\infty, \tag{5.3.101c}$$

$$u_1(0^-) = u_1(0^+) = 0, \tag{5.3.101d}$$

$$u_1'(0^-) = u_1'(0^+), \tag{5.3.101e}$$

which must be solved subject to the matching condition on $u_1(y)$ (as $y \to \infty$) with expansion (5.3.50) in region $\mathbf{IV_R^b}$ (as $w \to 0^+$). We begin in $y < 0$, with the inhomogeneous linear equation (5.3.101b). It follows from equation (4.2.3a) for $U_T(y)$ that a particular integral for (5.3.101b) is readily deduced to be proportional to $U_T'(y)$. Moreover, the general solution to (5.3.101b) may be written as

$$u_1(y) = E_0\phi_+(y) + E_1\phi_-(y) - 4\frac{c_3}{v^*(u_c)^2}U_T'(y), \quad y \leq 0, \tag{5.3.102}$$

with $\phi_+(y), \phi_-(y) : (-\infty, 0] \to \mathbb{R}$ basis functions for the homogeneous part of equation

(5.3.101b) chosen so that

$$\phi_+(y) \sim \exp\left(\left(\sqrt{-f'(1)} - \frac{1}{2}v^*(u_c)\right)y\right), \tag{5.3.103a}$$

$$\phi_-(y) \sim \exp\left(-\left(\sqrt{-f'(1)} + \frac{1}{2}v^*(u_c)\right)y\right), \tag{5.3.103b}$$

as $y \to -\infty$, whilst E_0 and E_1 are arbitrary real constants to be determined. It follows from (4.2.29d), (5.3.103) and an application of condition (5.3.101c), that we must have

$$E_0 = A_L, \qquad E_1 = 0. \tag{5.3.104}$$

Moreover, on applying condition (5.3.101d) (where we have evaluated $U_T'(0)$ via (4.2.29c)), we obtain

$$c_3 = -\frac{A_L v^*(u_c)\phi_+(0)}{4u_c}. \tag{5.3.105}$$

Thus, on collecting expressions (5.3.102), (5.3.104) and (5.3.105) we have

$$u_1(y) = A_L\phi_+(y) + \frac{A_L\phi_+(0)}{v^*(u_c)u_c}U_T'(y), \quad y < 0. \tag{5.3.106}$$

We next consider $u_1(y)$ with $y > 0$. The general solution to the inhomogeneous linear equation (5.3.101a) (using equations (4.2.29c) and (5.3.105)) is readily found to be

$$u_1(y) = (E_3 + E_4 y)\, e^{-\frac{1}{2}v^*(u_c)y} - A_L\phi_+(0)e^{-v^*(u_c)y}, \quad y \geq 0, \tag{5.3.107}$$

with arbitrary real constants E_3 and E_4 determined, via application of the coupling conditions (5.3.101d) and (5.3.101e), as

$$E_3 = A_L\phi_+(0), \tag{5.3.108}$$

$$E_4 = A_L\left(\phi_+'(0) + \phi_+(0)\left(\frac{1}{2}v^*(u_c) - \frac{f_c^+}{v^*(u_c)u_c}\right)\right), \tag{5.3.109}$$

with $A_L \neq 0$. Finally, we match the expansion in region $\mathbf{V_R}$ (as $y \to \infty$) with the

expansion in region $\mathbf{IV_R^b}$ (as $w \to 0^+$). Now, when $E_4 = 0$, we obtain the matching condition

$$\bar{G}_0(w) \sim A_L \phi_+(0) \quad \text{as} \quad w \to 0^+, \tag{5.3.110}$$

and

$$\gamma = -\frac{1}{2} (= -\beta_2). \tag{5.3.111}$$

However, when $E_4 \neq 0$, we obtain the matching condition

$$\bar{G}_0(w) \sim E_4 w \quad \text{as} \quad w \to 0^+, \tag{5.3.112}$$

and

$$\gamma = -\frac{3}{2} (= -\beta_2). \tag{5.3.113}$$

Also, it follows from expression (5.3.105) (since $A_L \neq 0$) that $c_3 = 0$ if and only if $\phi_+(0) = 0$. Therefore, we have the following cases. Firstly,

$$\underline{\phi_+(0) \neq 0}. \tag{I}$$

In this case

$$c_3 \neq 0,$$

and

$$E_4 = 0 \text{ with } \gamma = -\frac{1}{2} (= -\beta_2) \quad \text{or} \quad E_4 \neq 0 \text{ with } \gamma = -\frac{3}{2} (= -\beta_2).$$

Secondly,

$$\underline{\phi_+(0) = 0}. \tag{II}$$

In this case $\phi'_+(0) \neq 0$ and

$$c_3 = 0,$$

whilst $E_4 \neq 0$, and so

$$\gamma = -\frac{3}{2} (= -\beta_2).$$

We next consider the basis function $\phi_+ : (-\infty, 0] \to \mathbb{R}$. For fixed $u_c \in (0,1)$ the initial value problem for $\phi_+ : (-\infty, 0] \to \mathbb{R}$ is given by

$$\phi_+'' + v^*(u_c)\phi_+' + \left(\frac{1}{4}v^*(u_c)^2 + f'(U_T(y))\right)\phi_+ = 0, \quad y < 0, \tag{5.3.116a}$$

$$\phi_+(y) \sim \exp\left(\left(\sqrt{-f'(1)} - \frac{1}{2}v^*(u_c)\right)y\right) \quad \text{as} \quad y \to -\infty. \tag{5.3.116b}$$

We reduce (5.3.116) to normal form by setting $\phi_+(y) = \psi_+(y)\exp\left(-\frac{1}{2}v^*(u_c)y\right)$ with $\psi_+ : (-\infty, 0] \to \mathbb{R}$ now satisfying the initial value problem

$$\psi_+'' + f'(U_T(y))\psi_+ = 0, \quad y < 0, \tag{5.3.117a}$$

$$\psi_+(y) \sim \exp\left(\sqrt{-f'(1)}y\right) \quad \text{as} \quad y \to -\infty. \tag{5.3.117b}$$

This can now be solved numerically to find $\psi_+(0)$ and $\psi_+'(0)$ which we then use to obtain $\phi_+(0)$ and $\phi_+'(0)$, after which the occurrence of case (I) or case (II) is determined.

The asymptotic structure of the solution to [QIVP] as $t \to \infty$ is now complete with the expansions in regions $\mathbf{IV_L^a}$, $\mathbf{T_L}$, $\mathbf{IV_L^b}$, $\mathbf{V_L}$, $\mathbf{V_R}$, $\mathbf{IV_R^b}$, $\mathbf{T_R}$ and $\mathbf{IV_R^a}$ providing a uniform approximation to the solution of [QIVP] as $t \to \infty$. On collecting expressions (5.3.1), (5.3.18c), (5.3.22), (5.3.26) and (5.3.57) we have obtained, in particular, that

$$\begin{aligned}\dot{s}(t) \;=\; & v^*(u_c) + c_3 t^\gamma \exp\left(-\frac{1}{4}v^*(u_c)^2 t\right) \\ & + o\left(t^\gamma \exp\left(-\frac{1}{4}v^*(u_c)^2 t\right)\right) \quad \text{as} \quad t \to \infty,\end{aligned} \tag{5.3.118}$$

where the constants c_3 and γ depend upon whether case (I) or case (II) is pertaining for the given KPP reaction function and the cut-off value $u_c \in (0,1)$. Hence, via the method of matched asymptotic coordinate expansions, we have been able to obtain the correction term to the asymptotic propagation speed $v^*(u_c)$ of the developing PTW structure in the solution to [QIVP] as $t \to \infty$. In addition, with $u : \mathbb{R} \times [0, \infty) \to \mathbb{R}$ being the solution to [QIVP], it follows from expansions (5.3.33), (5.3.42), (5.3.43), (5.3.50), (5.3.55), (5.3.61),

(5.3.78a), (5.3.79), (5.3.93), (5.3.98) in regions $\mathbf{IV_L^a}$, $\mathbf{IV_L^b}$, $\mathbf{IV_R^a}$, $\mathbf{IV_R^b}$, $\mathbf{T_L}$, $\mathbf{T_R}$, $\mathbf{V_L}$ and $\mathbf{V_R}$ that,

$$u(y,t) = U_T(y) + E(y,t), \tag{5.3.119}$$

as $t \to \infty$ for $y \in \mathbb{R}$, with $E(y,t)$ linearly exponentially small in t as $t \to \infty$, uniformly for $y \in \mathbb{R}$. In particular, on any closed bounded interval I,

$$E(y,t) = O\left(t^{\gamma} e^{-\frac{1}{4}v^{*2}(u_c)t}\right), \tag{5.3.120}$$

as $t \to \infty$ uniformly for $y \in$ I. A significant point to note here, is that, for KPP reaction functions satisfying (1.1.5), in the absence of cut-off, the corresponding correction terms in (5.3.118), (5.3.119) and (5.3.120) are only algebraically small in t as $t \to \infty$, being of $O(t^{-1})$ (see, for example, Leach and Needham [36]).

To illustrate these results we consider a simple example of KPP reaction function $f : \mathbb{R} \to \mathbb{R}$ which satisfies (1.1.5), and has

$$f(u) = \lambda(1-u), \quad u \geq \frac{1}{2}\left(1 + \frac{\lambda}{(1+\lambda)}\right), \tag{5.3.121}$$

with $\lambda > 0$ fixed. With the cut-off value

$$u_c \in \left[\frac{1}{2}\left(1 + \frac{\lambda}{(1+\lambda)}\right), 1\right), \tag{5.3.122}$$

then, in this example, $f_c : \mathbb{R} \to \mathbb{R}$ is given by

$$f_c(u) = \begin{cases} 0, & u \in (-\infty, u_c], \\ \lambda(1-u), & u \in (u_c, \infty), \end{cases} \tag{5.3.123}$$

and

$$f'(1) = -\lambda, \quad f_c^+ = \lambda(1-u_c). \tag{5.3.124}$$

For this example, we can readily obtain the PTW explicitly with $U_T : \mathbb{R} \to \mathbb{R}$ given by

$$U_T(y) = \begin{cases} 1 - (1 - u_c) \exp\left(\left(\frac{\sqrt{v^*(u_c)^2 + 4\lambda} - v^*(u_c)}{2} \right) y \right), & y \leq 0, \\ u_c e^{-v^*(u_c) y}, & y > 0, \end{cases} \tag{5.3.125}$$

with propagation speed

$$v^*(u_c) = \sqrt{\lambda} \frac{(1 - u_c)}{\sqrt{u_c}}. \tag{5.3.126}$$

Now, via (5.3.116), the basis function $\phi_+ : (-\infty, 0] \to \mathbb{R}$ satisfies

$$\phi_+'' + v^*(u_c)\phi_+' + \left(\frac{1}{4} v^*(u_c)^2 - \lambda \right) \phi_+ = 0, \quad y < 0, \tag{5.3.127a}$$

$$\phi_+(y) \sim \exp\left(\left(\sqrt{\lambda} - \frac{1}{2} v^*(u_c) \right) y \right) \quad \text{as} \quad y \to -\infty, \tag{5.3.127b}$$

which has solution

$$\phi_+(y) = \exp\left(\left(\sqrt{\lambda} - \frac{1}{2} v^*(u_c) \right) y \right), \quad y \leq 0. \tag{5.3.128}$$

Thus, via (5.3.128), we obtain

$$\phi_+(0) = 1, \quad \phi_+'(0) = \sqrt{\lambda} - \frac{1}{2} v^*(u_c), \tag{5.3.129}$$

and so,

$$E_4 = A_L \sqrt{\lambda} \left(1 - \sqrt{u_c} \right) \neq 0. \tag{5.3.130}$$

Therefore, the particular reaction function (5.3.123) falls into case (I) which has

$$\begin{aligned} \dot{s}(t) \ &= v^*(u_c) + c_3 t^{-\frac{3}{2}} \exp\left(-\frac{1}{4} v^*(u_c)^2 t \right) \\ &\quad + o\left(t^{-\frac{3}{2}} \exp\left(-\frac{1}{4} v^*(u_c)^2 t \right) \right) \quad \text{as} \quad t \to \infty, \end{aligned} \tag{5.3.131}$$

with $c_3 \neq 0$, and $v^*(u_c)$ given by (5.3.126). Similarly, in this example, both (5.3.119) and

(5.3.120) have $\gamma = -3/2$.

5.4 Comparison with KPP asymptotics

In this section we contrast our asymptotic results obtained for the cut-off KPP model to those obtained for the KPP model (1.1.4) (with no cut-off). Although similar results have been obtained by Leach and Needham [36], these have focused on slightly different compact initial conditions. To enable a direct comparison, we work with the KPP model translated so that $u(0,t) = u_c$ where $u_c \in (0,1)$ is some arbitrary value of u.

5.4.1 Formulation of the Problem

On taking $y = x - s(t)$ the moving boundary problem for the KPP model is then formulated as follows,

$$u_t - \dot{s}(t)u_y = u_{yy} + f(u), \quad (y,t) \in \mathbb{R} \times \mathbb{R}^+, \tag{5.4.1a}$$

$$u \geq u_c \text{ in } \overline{Q}^L, \quad u \leq u_c \text{ in } \overline{Q}^R, \tag{5.4.1b}$$

$$u(y,0) = \begin{cases} 1, & y < 0, \\ 0, & y \geq 0, \end{cases} \tag{5.4.1c}$$

$$u(y,t) \to \begin{cases} 1, & \text{as} \quad y \to -\infty, \\ 0, & \text{as} \quad y \to \infty, \end{cases} \quad \text{uniformly for } t \in [0,T] \text{ for all } T > 0, \tag{5.4.1d}$$

$$u(0,t) = u_c, \quad t \in \mathbb{R}^+, \tag{5.4.1e}$$

$$u_y(0^+,t) = u_y(0^-,t), \quad t \in \mathbb{R}^+, \tag{5.4.1f}$$

$$s(0^+) = 0. \tag{5.4.1g}$$

This initial-boundary value problem will henceforth be referred to as [MIVP]. Clearly, the difference between [QIVP] and [MIVP] is that

$$\text{(M1)} \qquad \left[u_{yy}(y,t)\right]_{y=0^-}^{y=0^+} = 0 \quad \forall\, t \in \mathbb{R}^+,$$

and of course, like before, it is easy to establish that

$$\text{(M2)} \qquad u_y(y,t) < 0 \quad \forall\, (y,t) \in \mathbb{R} \times \mathbb{R}^+.$$

The crucial point with regards to comparison of asymptotic solutions to [QIVP], is that for all *right* regions (where $y > 0$), the governing equation for [MIVP] includes a reaction term $f(u)$.

5.4.2 Asymptotic Solution as $t \to 0^+$

An examination of the leading order balances in [MIVP] determine the asymptotic structure of solution as $t \to 0^+$ to be the same as that in the solution to [QIVP] as $t \to 0^+$. That is, we observe the same two principal asymptotic regions in $y < 0$ and the same two principal asymptotic regions in $y > 0$. For KPP reaction, the leading order solutions in regions $\mathbf{I_L}$ and $\mathbf{I_R}$ are not affected as the reaction function appears at second order in t. At second order, a particular solution

$$u_{p1}(\eta) = \frac{\hat{u}(\eta)}{2} \int_0^\eta I_1(\lambda) d\lambda - \frac{\bar{u}(\eta)}{2} \int_0^\eta I_2(\lambda) d\lambda, \quad \eta \geq 0, \tag{5.4.3}$$

(of the same form as the particular solution (5.1.16) for $u_{L1}(\eta)$ with the limits of integration reversed) is introduced into the expansion for $u_{R1}(\eta)$ and, therefore, d_1, d_2 and s_1 in the expansions for $u_{L1}(\eta)$, $u_{R1}(\eta)$ and $s(t)$ are altered. As these are constants that only appear at lower order, we will not present them here.

In regions $\mathbf{II_R}$ and $\mathbf{II_L}$ the reaction function $f(u)$ is of lower order and, hence, the

structure of the expansions in these regions is not affected. We perform asymptotic matching with regions $\mathbf{I_R}$ and $\mathbf{I_L}$ respectively, to leading order, hence, the asymptotic expansions in regions $\mathbf{II_R}$ and $\mathbf{II_L}$ do not change.

5.4.3 Asymptotic Solution as $|y| \to \infty$

In region $\mathbf{III_L}$, the governing equation is the same for [MIVP] as for [QIVP], hence, we obtain the same asymptotic solution in this region. It follows from the unchanged expansion in region $\mathbf{II_R}$, that the general structure of the solution in region $\mathbf{III_R}$ is again given by the expansion (5.2.2). However, the introduction of the reaction function at lower order in y in the governing equation (5.4.1a), adds a t term into the solution as follows,

$$u(y,t) = \exp\left(-\frac{y^2}{4t} - y\frac{s(t)}{2t} - \ln y - \left(\frac{s(t)^2}{4t} - \frac{1}{2}\ln t + \frac{1}{2}\ln \pi - t\right) + o(1)\right), \qquad (5.4.4)$$

with $t = O(1)$.

5.4.4 Asymptotic Solution as $t \to \infty$

The principal asymptotic structure of the solution $u(y,t)$ and $s(t)$ to [MIVP] is again given by (5.3.2) and (5.3.1) as obtained for [QIVP]. As before we begin by developing the structure of the solution to [MIVP] to leading order, uniform for $y \in \mathbb{R}$. While the additional t term is of lower order in region $\mathbf{III_R}$ (as $t = O(1)$), it impacts the leading order problem in region $\mathbf{IV_R}$ (as $t \gg 1$). In region $\mathbf{IV_R}$ for [QIVP], the leading order exponent is given by the 'envelope-linear' solution (5.3.14), however, for [MIVP] a linear solution is also possible. We will return to this later. There is no change in the governing equation for $y < 0$, hence, the 'envelope-linear' solution is again taken in region $\mathbf{IV_L}$. Furthermore, we obtain a PTW solution at leading order in regions $\mathbf{V_L}$ and $\mathbf{V_R}$ with speed c_0. For [QIVP] there exists a unique PTW solution with propagation speed $v^*(u_c)$,

thus fixing c_0, whereas, for [MIVP] there exists a continuum of PTW solutions with propagation speed $c_0 \in [2, \infty)$ which may be selected. The asymptotic form of the PTW in the limit as $y \to \infty$, is dependent on whether $c_0 = 2$ or $c_0 > 2$ and is given by (1.1.10a). On performing asymptotic matching between regions $\mathbf{IV_R}$ and $\mathbf{V_R}$, we find that it is the PTW solution with minimum speed $c_0 = 2$ that is selected and with the leading order exponent in region $\mathbf{IV_R}$ given by

$$\bar{G}_0(w) = \frac{w}{4}(w+4), \quad w = \frac{y}{t} = O(1)^+. \tag{5.4.5}$$

In contrast with the 'envelope-linear' solution (5.3.14), the linear solution (5.4.5) tends to zero as we approach region $\mathbf{V_R}$ (as $w \to 0^+$) and, hence, no additional subregions are required and the solution to [MIVP] at leading order as $t \to \infty$ is complete. As was the case for [QIVP], the full large-time solution is complex, we will skip the finer details here and merely illustrate how the well established result of McKean and Bramson (1.1.12) is obtained as well as state how the asymptotic expansions in each region are affected.

The asymptotic structure in region $\mathbf{IV_L^\flat}$ is guided by the asymptotic form of $U(y)$ as $y \to -\infty$ which is described by (1.1.10b) (and crucially does not contain a factor of y in front of the exponent). Therefore, a balance at second order in region $\mathbf{IV_L^\flat}$ sets $\phi_1(t) = \ln t$. We can now consider the exponent in region $\mathbf{IV_R}$ up to $O(1)$ and on performing rigorous asymptotic matching with region $\mathbf{V_R}$, we find that $c_1 = -3/2$. Moreover,

$$\dot{s}(t) = 2t - \frac{3}{2t} + o(t^{-1}), \tag{5.4.6}$$

with the rate of convergence of the PTW solution (with $y \in \mathbb{R}$) onto the solution to [MIVP] being $O(t^{-1})$ (as obtained by Leach and Needham [36]), in contrast to the linearly exponential convergence obtained for [QIVP].

For completeness we summarise the rest of our findings in the large-time regime as

follows. In region $\mathbf{IV_R}$

$$u(w,t) = \exp\left(-\frac{1}{4}tw(w+4) - \left(\frac{3w}{4}+1\right)\ln t + F_1(w) + o\left(1\right)\right), \tag{5.4.7}$$

with $w > 0$ and where $F_1(w) \sim \ln Aw$ as $w \to 0^+$. In region $\mathbf{IV_L^a}$

$$u(w,t) = 1 - \exp\left(-t\left(\left(\frac{w+2}{2}\right)^2 - f'(1)\right) + \left(\frac{3w}{4}+1\right)\ln t - F_2(w) + o\left(1\right)\right), \tag{5.4.8}$$

with $w < -2\sqrt{1-f'(1)}$ and where $F_2(w) \sim \ln(-w) - 3(w/2+1)/2 + \ln\pi/2$ as $w \to -\infty$. In region $\mathbf{IV_L^b}$

$$\begin{aligned} u(w,t) = 1 - \exp\Bigg(& -t\left(1-\sqrt{1-f'(1)}\right)w \\ & -\frac{3}{2}\left(1-\sqrt{1-f'(1)}\right)\ln\left(\frac{w+2\sqrt{1-f'(1)}}{2\sqrt{1-f'(1)}}\right) + \ln B + o(1)\Bigg), \end{aligned} \tag{5.4.9}$$

with $-2\sqrt{1-f'(1)} \leq w < 0$. On comparison with the appropriate expansions for [QIVP], the main difference is the introduction of a logarithmic term in the exponent of each expansion due to c_1 being non-zero. There is a transition region $\mathbf{T_L}$ about $w = -2\sqrt{1-f'(1)}$ where second order derivatives are retained but as it was not required to obtain the two-term expression (5.4.6), we do not consider that here.

5.5 Numerical Example

In this section we present a comparison between numerical determined solution and the asymptotic expressions which together provide a uniform approximation to the solution of [QIVP] as $t \to 0^+$ and as $t \to \infty$. No numerical comparison is provided for the asymptotic expansions in the solution of [QIVP] as $|y| \to \infty$ as these regions are passive and their asymptotic form is dependent on the unknown global function $s(t) = O(1)$ with $t = O(1)$. We focus on the particular case of the cut-off Fisher reaction function (3.0.1) for fixed

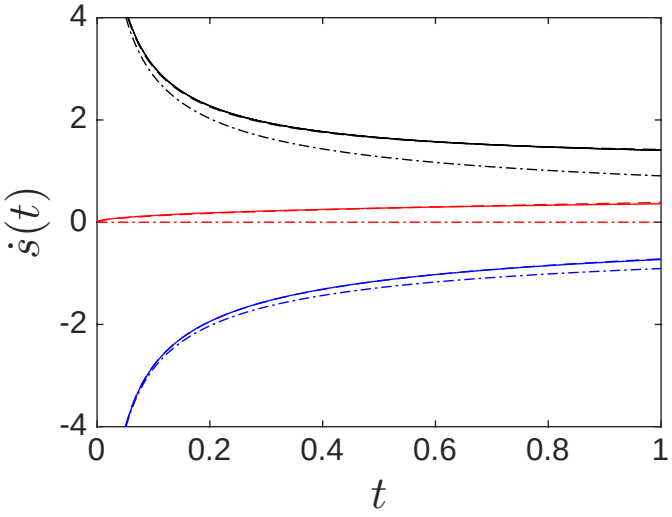

Figure 5.6: Comparison between numerical solutions of $\dot{s}(t)$ (solid lines) and the asymptotic expression (5.1.39) valid in small-time to leading order (dot-dashed lines) and to second order (dashed lines). Results are obtained for $u_c = 0.1$ (in black), $u_c = 0.5$ (in red) and $u_c = 0.9$ (in blue).

cut-off threshold $u_c \in (0, 1)$. Numerical results are obtained via numerical solution of the discretised scheme (3.1.6) described in detail in Section 3.1. We begin with the small time solution to [QIVP].

5.5.1 Small time

Figure 5.6 is devoted to the structure of $\dot{s}(t)$. It contrasts the leading order and two-term behaviour of the asymptotic expression $\dot{s}(t)$ given by (5.1.39) against the numerically determined solution to (3.1.6) for a selection of cut-off values in small-time. It is clear that the two-term expansion (5.1.39) provides an excellent approximation to $\dot{s}(t)$, for each u_c value checked, with the agreement remaining good for $t \simeq 1$. In Figure 5.7 we examine the structure of $u(y, t)$ in small-time. In particular, in Figure 5.7 we present results for the specific cut-off values $u_c = 0.1$, $u_c = 0.5$ and $u_c = 0.9$ at three fixed values of t, respectively. Taken together the asymptotic expressions (5.1.25), (5.1.33) and (5.1.38) valid for arbitrary u_c become increasingly accurate as time decreases. At $t \simeq 1$, our small-time approximations are no longer as accurate. We note that this behaviour is consistent for other cut-off values checked.

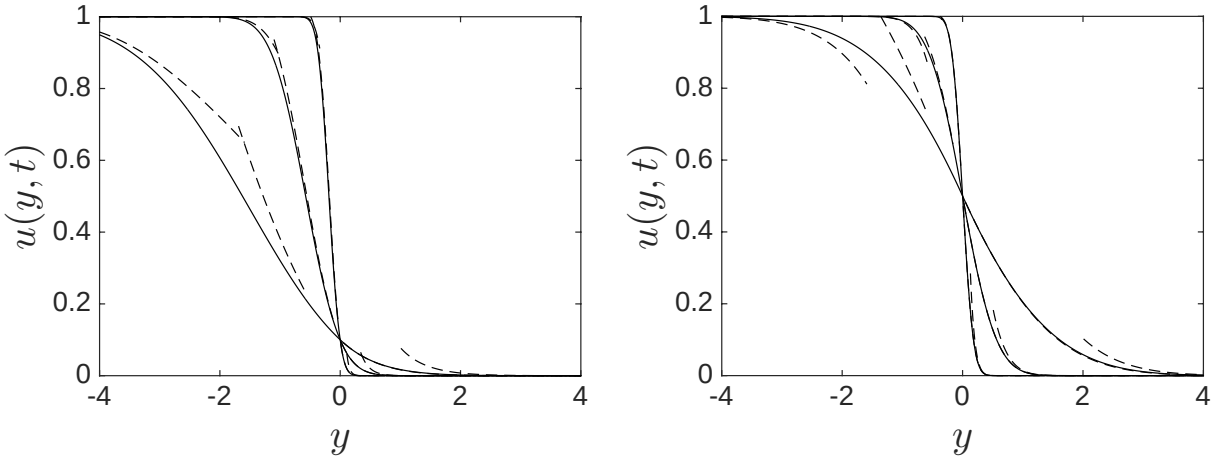

(a) $u_c = 0.1$

(b) $u_c = 0.5$

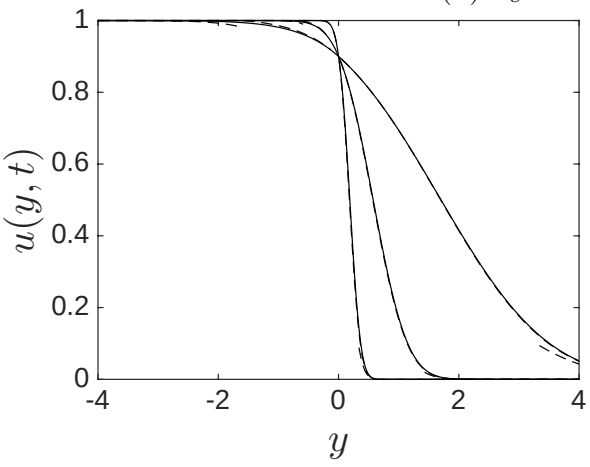

(c) $u_c = 0.9$

Figure 5.7: Comparison between numerical solutions of $u(y,t)$ (solid lines) and the asymptotic expressions (5.1.25), (5.1.33) and (5.1.38) valid in small-time (dashed lines). Results are obtained at time $t = 0.01$, $t = 0.1$ and $t = 1$ for (a) $u_c = 0.1$, (b) $u_c = 0.5$ and (c) $u_c = 0.9$

5.5.2 Large time

We next consider the solution of [QIVP] as $t \to \infty$. For each fixed $u_c \in (0,1)$, the large-time asymptotic structure of $u(y,t)$ and $\dot{s}(t)$ relies on the value of the parameters γ, $\phi_+(0)$, $\phi'_+(0)$, a_∞, A_L and $v^*(u_c)$ which must be determined for the particular case of cut-off Fisher reaction function (3.0.1) before we can proceed. Now, via (5.3.117), the function $\psi_+ : (-\infty, 0] \to \mathbb{R}$ satisfies

$$\psi''_+ + (1 - 2U_T(y))\,\psi_+ = 0, \quad y < 0, \tag{5.5.1a}$$

$$\psi_+(y) \sim e^y \quad \text{as} \quad y \to -\infty. \tag{5.5.1b}$$

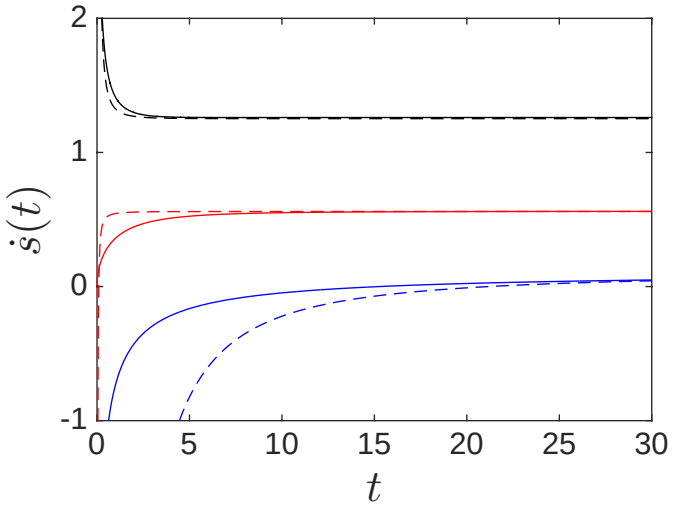

Figure 5.8: Comparison between numerical solutions of $\dot{s}(t)$ (solid lines) and the two-term asymptotic expression (5.3.118) valid in large-time. Results are obtained for $u_c = 0.1$ (in black), $u_c = 0.5$ (in red) and $u_c = 0.9$ (in blue).

We adopt a fourth order Runge-Kutta discretisation scheme to numerically evaluate the equivalent autonomous first-order two-dimensional dynamical system with

$$\phi_+(0) = \psi_+(0), \quad \phi'_+(0) = \psi'_+(0) - \frac{1}{2}v^*(u_c)\psi_+(0). \tag{5.5.2}$$

For a range of values of $u_c \in (0,1)$ considered, we find $\phi_+(0) \neq 0$. Thus the particular reaction function (3.0.1) falls into case (I) where $c_3 \neq 0$, $\gamma = -3/2$ and with $\dot{s}(t)$ satisfying the asymptotic expression

$$\dot{s}(t) \sim v^*(u_c) - \frac{A_L v^*(u_c)\phi_+(0)}{4u_c} t^{-\frac{3}{2}} \exp\left(-\frac{1}{4}v^*(u_c)^2 t\right) \quad \text{as} \quad t \to \infty. \tag{5.5.3}$$

The global constant a_∞ is associated with the leading edge behaviour of the PTW solution $U_T(y)$ (see expression (4.2.29d)). For each $u_c \in (0,1)$, we determine the values of a_∞ and $v^*(u_c)$ from the numerical evaluation of (4.2.3) via the shooting method described in Section 4.5. For each $u_c \in (0,1)$, the value of the global constant A_L can now be determined from numerical calculation of expression (5.5.3).

We now present our numerical results for the large-time solution to [QIVP] with Figure 5.8 devoted to the structure of $\dot{s}(t)$. It contrasts the two-term behaviour of the asymptotic

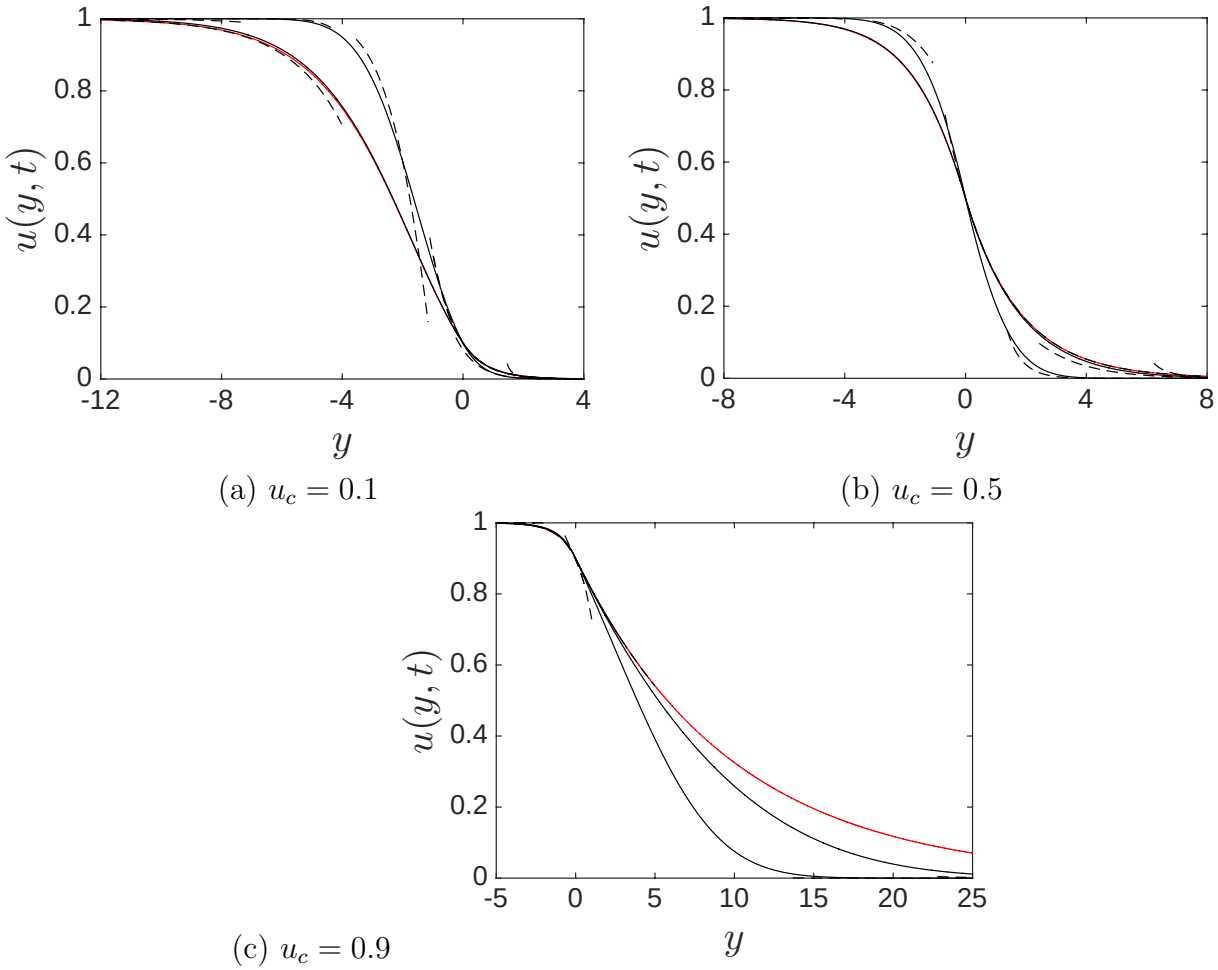

(a) $u_c = 0.1$

(b) $u_c = 0.5$

(c) $u_c = 0.9$

Figure 5.9: Comparison between numerical solutions of $u(y,t)$ (black solid lines), numerical solutions of the PTW solution $U_T(y)$ (red solid lines) and the asymptotic expressions (5.3.33), (5.3.43), (5.3.50), (5.3.61), (5.3.79) and (5.3.93) valid in large-time (dashed lines). (a) Results are obtained at time $t = 1$ and $t = 5$ for $u_c = 0.1$, (b) at time $t = 1$ and $t = 10$ for $u_c = 0.5$ and (c) at time $t = 10$ and $t = 50$ for $u_c = 0.9$.

expression $\dot{s}(t)$ given by (5.5.3) against the numerically determined solution to (3.1.6) for a selection of cut-off values in large-time. It is clear that the two-term expansion (5.5.3) provides an excellent approximation to $\dot{s}(t)$, in large-time, for each u_c value checked. The smaller the value of u_c, the better the agreement as we decrease t from large-time. In Figure 5.9 we examine the structure of $u(y,t)$ in large-time. In particular, we contrast the two-term asymptotic expression against the numerically determined solution to (3.1.6) and the numerically determined PTW profile $U_T(y)$ (obtained in Section 4.5) for a range of cut-off values. In Figure 5.9 we present results for the specific cut-off values $u_c = 0.1$, $u_c = 0.5$ and $u_c = 0.9$ at three fixed values of t, respectively. Taken together the asymptotic expressions (5.3.33), (5.3.43), (5.3.50), (5.3.61), (5.3.79) and (5.3.93), valid for arbitrary u_c, become increasingly accurate as time increases.

5.6 Discussion and Conclusions

In this chapter we examine the solution to [QIVP]. In particular, we use the method of matched asymptotic expansions to develop the detailed asymptotic structure of the small-time, large-space and large-time solutions to [QIVP] for arbitrary $u_c \in (0,1)$. First, we focus on the small-time regime where we determine that, the asymptotic structure of $u(y,t)$ will have two asymptotic regions in $y < 0$, and two asymptotic regions in $y > 0$. The two-term expression for the function $s(t)$ can be determined from the inner left and inner right regions, where $y = o(1)^-$ and $y = o(1)^+$ respectively, in addition to the leading order matching conditions as $|y|$ increases to $O(1)$. The asymptotic structure of $\dot{s}(t)$ as $t \to 0^+$ reveals an integrable singularity which depends on the cut-off threshold value. Here $\dot{s}(t) \to +\infty$ when $u_c \in (0, 1/2)$, whilst, $\dot{s}(t) \to -\infty$ when $u_c \in (1/2, 1)$ with a transition case where $\dot{s}(t) \to 0^+$ when $u_c = 1/2$. The outer left and outer right small time regions, where $y = O(1)^-$ and $y = O(1)^+$, provide uniform expansions for $(-y) \gg 1$ and $y \gg 1$ respectively. We next examine the asymptotic structure of the solution to [QIVP] for $|y| \to \infty$ with $t = O(1)$. Guided by the asymptotic structure of the solution

in the small-time outer regions, we determine that the large-space solution $u(y,t)$ will have one asymptotic region as $y \to \infty$ and one asymptotic region as $y \to -\infty$ with $t = O(1)$. Both expansions remain uniform for $t \gg 1$ provided $|y| \gg t$. Finally, we focus on the asymptotic structure of the solution to [QIVP] as $t \to \infty$ with $|y| = O(1)$. Guided by an examination of the leading order balances in the asymptotic structure of the solution in the large-space regions together with the connection conditions about $y = 0$, we determine that the asymptotic structure of $u(y,t)$ will have two principal asymptotic regions in $y < 0$, and two principal asymptotic regions in $y > 0$. We determine the asymptotic structure of the expansion in each of these regions. This systematic approach allows the correction to the propagation speed and the rate of convergence of the solution to [QIVP] onto the PTW structure with propagation speed $v = v^*(u_c)$ to be determined. This convergence occurs at a rate that is linearly exponentially small in t, specifically $O(\dot{s}(t) - v^*(u_c))$, where

$$\dot{s}(t) = v^*(u_c) + O\left(t^\gamma \exp\left(-\frac{1}{4}v^*(u_c)^2 t\right)\right), \quad \text{as } t \to \infty, \tag{5.6.1}$$

(with $\gamma = -1/2$ or $-3/2$ depending on properties of $f_c(u)$) so that convergence slows down as u_c increases. All asymptotic results have excellent agreement with results obtained via numerical evaluation of [QIVP] in Chapter 3.

In comparing the theory for the cut-off KPP-type reaction function studied here, and its associated KPP-type reaction function without cut-off, we make the observation that, in the absence of cut-off, a PTW solution exists for each propagation speed $v \in [2, \infty)$. However, it is the unique PTW with minimum speed ($v = 2$) that the solution to the corresponding initial-boundary value problem (to [QIVP] in the absence of cut-off) approaches in large-time. Moreover, it has been established that the corresponding corrections are only algebraically small in t in large-time (see, for example, Leach and Needham [36]). Hence, the rate of convergence onto the PTW structure is much faster in comparison with the solution to [QIVP]. We anticipate that the approach developed

in this thesis, for considering large-time solutions to [QIVP], will be readily adaptable to corresponding problems, when the KPP-type cut-off reaction function is replaced by a broader class of cut-off reaction functions.

This concludes our analysis of [QIVP]. We next consider the the initial-boundary value problem (1.2.11) with a particular focus on how the introduction of a background shear flow influences the profile and propagation of travelling front solutions.

CHAPTER 6

FORMULATION OF THE PROBLEM

Due to the discontinuity in $f_c(u)$ at $u = u_c$, it is convenient to re-structure (1.2.11) as a moving boundary problem. To this end, we introduce the domains:

$$D^L = \{(x, y, t) \in \mathbb{R} \times (0, \pi) \times \mathbb{R}^+ : \ x < s(y, t)\}, \tag{6.0.1a}$$

$$D^R = \{(x, y, t) \in \mathbb{R} \times (0, \pi) \times \mathbb{R}^+ : \ x > s(y, t)\}, \tag{6.0.1b}$$

and the curve

$$\mathcal{L} = \{(x, y, t) \in \mathbb{R} \times (0, \pi) \times \mathbb{R}^+ : \ x = s(y, t)\}, \tag{6.0.1c}$$

that describes the moving boundary between the two domains. The boundary is assumed to be sufficiently smooth, that is, it does not possess any corners, and can be expressed in terms of $s(y, t)$ which satisfies $u(s(y, t), y, t) = u_c$, with $u \geq u_c$ in $\overline{D}^L$ and $u \leq u_c$ in $\overline{D}^R$. The situation is illustrated in Figure 6.1. In this context, a classical solution will

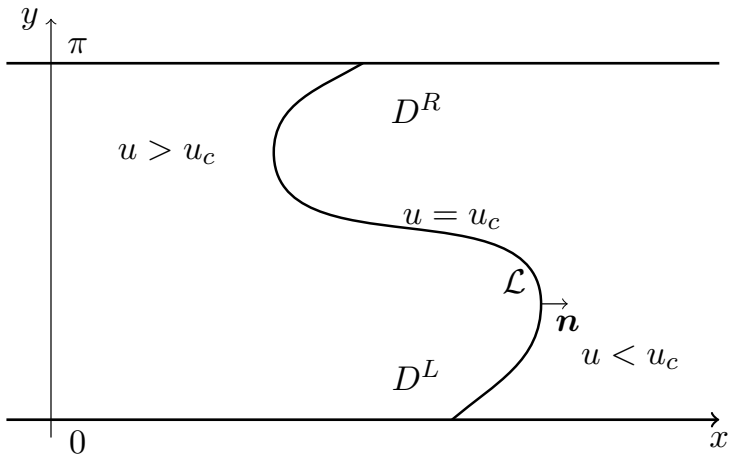

Figure 6.1: A sketch of the moving boundary problem at a fixed time t.

have $u : \mathbb{R} \times [0,\pi] \times \overline{\mathbb{R}}^+ \to \mathbb{R}$ and $s : [0,\pi] \times \overline{\mathbb{R}}^+ \to \mathbb{R}$ such that,

$$u \in C\left((\mathbb{R} \times [0,\pi] \times \overline{\mathbb{R}}^+) \setminus (\{0\} \times [0,\pi] \times \{0\})\right) \cap C^{1,1,1}\left(\mathbb{R} \times [0,\pi] \times \mathbb{R}^+\right) \cap C^{2,2,1}\left(D^L \cup D^R\right), \tag{6.0.2a}$$

$$s \in C^{1,1}\left([0,\pi] \times \mathbb{R}^+\right) \cap C^{2,1}\left((0,\pi) \times \mathbb{R}^+\right), \tag{6.0.2b}$$

$$s(y, 0^+) = 0. \tag{6.0.2c}$$

The moving boundary problem is then formulated as follows,

$$u_t + b(y)u_x = \mathrm{Pe}^{-1}\Delta u + \mathrm{Da} f_c(u), \quad (\boldsymbol{x}, t) \in D^L \cup D^R, \tag{6.0.3a}$$

$$b \in C^1([0,\pi]) \quad \text{and} \quad \int_0^\pi b(y)dy = 0, \tag{6.0.3b}$$

$$u \geq u_c \text{ in } \overline{D}^L, \quad u \leq u_c \text{ in } \overline{D}^R, \tag{6.0.3c}$$

$$u(\boldsymbol{x}, 0) = \begin{cases} 1, & x < 0, \\ 0, & x \geq 0, \end{cases} \quad \forall\ y \in [0,\pi], \tag{6.0.3d}$$

$$u(\boldsymbol{x}, t) \to \begin{cases} 1, & \text{as} \quad x \to -\infty, \\ 0, & \text{as} \quad x \to \infty, \end{cases} \tag{6.0.3e}$$

uniformly for $(y,t) \in [0,\pi] \times [0,T]$ for all $T > 0$,

$$u_y(x,0,t) = u_y(x,\pi,t) = 0, \quad (x,t) \in \mathbb{R} \times \mathbb{R}^+, \tag{6.0.3f}$$

$$u(s(y,t),y,t) = u_c, \quad (y,t) \in [0,\pi] \times \mathbb{R}^+, \tag{6.0.3g}$$

$$\partial_n u|_{\mathcal{X}^+} = \partial_n u|_{\mathcal{X}^-}, \tag{6.0.3h}$$

$$s(y,0^+) = 0, \quad y \in [0,\pi]. \tag{6.0.3i}$$

Here we use the notation $\partial_n = \boldsymbol{n} \cdot \nabla$ where $\boldsymbol{n}$ is the unit normal vector to the zero-level curve $x - s(y,t) = 0$ orientated towards D^R and

$$\begin{aligned} \mathcal{X} = \{(x,y,t) + \boldsymbol{n}h \in \mathbb{R} \times (0,\pi) \times \mathbb{R}^+ :\ & x = s(y,t), \\ & \boldsymbol{n} = (1,-s_y)/|(1,-s_y)| \text{ and } h \in \mathbb{R}\}, \end{aligned} \tag{6.0.4}$$

describes the curves which have been translated in the normal direction, orientated towards D^R, to the boundary, with

$$\mathcal{X}^+ = \lim_{h \to 0^+} \mathcal{X}, \qquad \mathcal{X}^- = \lim_{h \to 0^-} \mathcal{X}. \tag{6.0.5}$$

This initial-boundary value problem will henceforth be referred to as [IVPA]. On using the classical maximum principle and comparison theorem (see also for ignition, Berestycki and Hamel [6] or Xin [61], Section 3.3, and the references therein) together with translational invariance in y, and the regularity in (6.0.2), we can readily establish the following qualitative properties concerning [IVPA], namely,

(A1) $\quad 0 < u(\boldsymbol{x},t) < u_c \quad \forall (\boldsymbol{x},t) \in D^R$,

(A2) $\quad u_c < u(\boldsymbol{x},t) < 1 \quad \forall (\boldsymbol{x},t) \in D^L$,

(A3) $\quad u(\boldsymbol{x},t)$ is strictly monotone decreasing in $x \in \mathbb{R}$ for fixed $y \in [0,\pi]$ for all $t \in \mathbb{R}^+$.

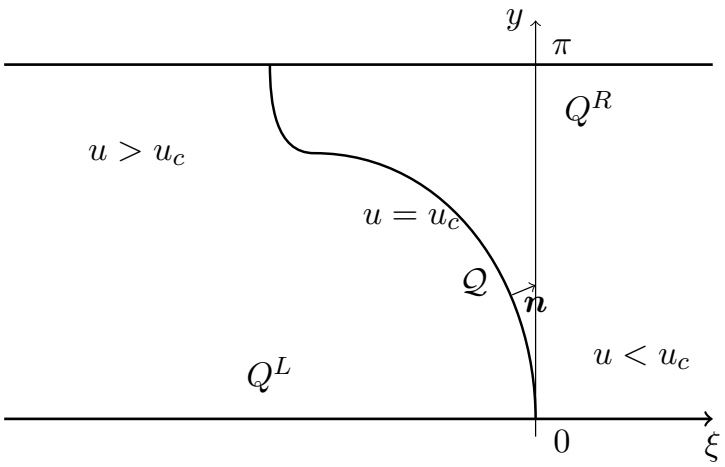

Figure 6.2: A sketch of the moving boundary problem at a fixed time t.

In addition, via the regularity results in [29], the regularity conditions (6.0.2) and the partial differential equation (6.0.3a), we deduce that

(A4) $$\left[\partial_n^2 u\right]_{\mathcal{X}^-}^{\mathcal{X}^+} = \mathrm{PeDa} f_c^+.$$

It is now convenient to make the coordinate transformation $(x, y, t) \to (\xi, y, t)$ with $\xi = x - s_0(t)$ where $s_0(t) = s(0, t)$. To that end, we introduce the domains:

$$Q^L = \{(\xi, y, t) \in \mathbb{R} \times (0, \pi) \times \mathbb{R}^+ : \ \xi < s(y, t) - s_0(t)\}, \tag{6.0.7a}$$

$$Q^R = \{(\xi, y, t) \in \mathbb{R} \times (0, \pi) \times \mathbb{R}^+ : \ \xi > s(y, t) - s_0(t)\}, \tag{6.0.7b}$$

and the curve

$$\mathcal{Q} = \{(\xi, y, t) \in \mathbb{R} \times (0, \pi) \times \mathbb{R}^+ : \ \xi = s(y, t) - s_0(t)\}, \tag{6.0.7c}$$

that describes the moving boundary between the two domains. The boundary is expressed in terms of $s(y, t) - s_0(t)$ which satisfies $u(s(y, t) - s_0(t), y, t) = u_c$, with $u \geq u_c$ in $\overline{Q}^L$ and $u \leq u_c$ in $\overline{Q}^R$. The situation is illustrated in Figure 6.2. A classical solution will have

$u : \mathbb{R} \times [0,\pi] \times \overline{\mathbb{R}}^+ \to \mathbb{R}$ and $s - s_0 : [0,\pi] \times \overline{\mathbb{R}}^+ \to \mathbb{R}$ such that,

$$u \in C\left((\mathbb{R} \times [0,\pi] \times \overline{\mathbb{R}}^+) \setminus (\{0\} \times [0,\pi] \times \{0\})\right) \cap C^{1,1,1}\left(\mathbb{R} \times [0,\pi] \times \mathbb{R}^+\right) \cap C^{2,2,1}\left(Q^L \cup Q^R\right), \tag{6.0.8a}$$

$$s - s_0 \in C^{1,1}\left([0,\pi] \times \mathbb{R}^+\right) \cap C^{2,1}\left((0,\pi) \times \mathbb{R}^+\right). \tag{6.0.8b}$$

The equivalent problem to [IVPA] is then given by

$$u_t + (b(y) - \dot{s}_0(t))\, u_\xi = \mathrm{Pe}^{-1}\left(u_{\xi\xi} + u_{yy}\right) + \mathrm{Da} f_c(u), \quad (\xi, y, t) \in Q^L \cup Q^R, \tag{6.0.9a}$$

$$b \in C^1([0,\pi]) \quad \text{and} \quad \int_0^\pi b(y)dy = 0, \tag{6.0.9b}$$

$$u \geq u_c \text{ in } \overline{Q}^L, \quad u \leq u_c \text{ in } \overline{Q}^R, \tag{6.0.9c}$$

$$u(\xi, y, 0) = \begin{cases} 1, & \xi < 0, \\ 0, & \xi \geq 0, \end{cases} \quad \forall\ y \in [0,\pi], \tag{6.0.9d}$$

$$u(\xi, y, t) \to \begin{cases} 1, & \text{as} \quad \xi \to -\infty, \\ 0, & \text{as} \quad \xi \to \infty, \end{cases} \tag{6.0.9e}$$

uniformly for $(y,t) \in [0,\pi] \times [0,T]$ for all $T > 0$,

$$u_y(\xi, 0, t) = u_y(\xi, \pi, t) = 0, \quad (\xi, t) \in \mathbb{R} \times \mathbb{R}^+, \tag{6.0.9f}$$

$$u(s(y,t) - s_0(t), y, t) = u_c, \quad (y,t) \in [0,\pi] \times \mathbb{R}^+, \tag{6.0.9g}$$

$$\partial_n u|_{\mathcal{P}^+} = \partial_n u|_{\mathcal{P}^-}, \tag{6.0.9h}$$

$$s(y, 0^+) - s_0(0^+) = 0, \quad y \in [0,\pi], \tag{6.0.9i}$$

where the dot denotes differentiation with respect to time, t. Here $\boldsymbol{n}$ is the unit normal vector to the zero-level curve $\xi - s(y,t) + s_0(t) = 0$ orientated towards Q^R and

$$\mathcal{P} = \{(\xi, y, t) + \boldsymbol{n}h \in \mathbb{R} \times (0,\pi) \times \mathbb{R}^+ : \ \xi = s(y,t) - s_0(t), \\ \boldsymbol{n} = (1, -s_y)/|(1, -s_y)| \text{ and } h \in \mathbb{R}\}, \tag{6.0.10}$$

describes the curves which have been translated in the normal direction, orientated towards Q^R, to the boundary, with

$$\mathcal{P}^+ = \lim_{h \to 0^+} \mathcal{P}, \qquad \mathcal{P}^- = \lim_{h \to 0^-} \mathcal{P}. \tag{6.0.11}$$

This initial-boundary value problem will henceforth be referred to as [QIVPA]. On using the classical maximum principle and comparison theorem, together with translational invariance in y, and the regularity in (6.0.8), we can readily establish the following qualitative properties concerning [QIVPA], namely,

(Q1) $\qquad 0 < u(\xi, y, t) < u_c \quad \forall (\xi, y, t) \in Q^R,$

(Q2) $\qquad u_c < u(\xi, y, t) < 1 \quad \forall (\xi, y, t) \in Q^L,$

(Q3) $\qquad u(\xi, y, t)$ is strictly monotone decreasing in $\xi \in \mathbb{R}$
for fixed $y \in [0, \pi]$ for all $t \in \mathbb{R}^+$.

In addition, via the regularity results in [29], the regularity conditions (6.0.8) and the partial differential equation (6.0.9a), we deduce that

(Q4) $\qquad \left[\partial_n^2 u\right]_{\mathcal{P}^-}^{\mathcal{P}^+} = \mathrm{PeDa} f_c^+.$

These problems are equivalent but, for ease of numerical simulation, Chapter 7 concentrates on the analysis of [IVPA] with Chapter 8 concentrating on the analysis of [QIVPA].

CHAPTER 7

NUMERICAL SOLUTION TO [IVPA]

In this chapter we consider a numerical solution to [IVPA]. We present results for the particular case of the cut-off Fisher reaction function (3.0.1) for fixed cut-off threshold $u_c \in (0, 1)$. All our previous results for initial-boundary value problems of reaction–diffusion type have been based on finite difference methods, however, on adding a background flow we must introduce the concept of finite volume methods. Finite volume methods appear similar to finite difference methods, however, their derivation is not as intuitive and will be detailed here.

7.1 Numerical Method

We discretise [IVPA] for the specific case of shear flow using a fractional-step method (also referred to as a time-splitting method) which splits the problem into *subproblems* that can be solved independently. Fractional step methods were first introduced by Chorin to obtain approximations to the incompressible Navier-Stokes equation [15]. The advantage of this method, is that it is easy and comparatively numerically inexpensive to combine a high resolution finite volume method for the advection equation

$$u_t + b(y)u_x = 0, \tag{7.1.1a}$$

with an explicit method for the diffusion equation

$$u_t = \mathrm{Pe}^{-1}\Delta u, \tag{7.1.1b}$$

and an exact solution for the reaction equation

$$u_t = \mathrm{Da} f_c(u), \tag{7.1.1c}$$

in an alternating manner. If the order in which we solve equations (7.1.1a), (7.1.1b) and (7.1.1c) does not impact the final solution, the subproblems are said to *commute* and there is no associated error from performing such a splitting. That is not the case here. The size of the splitting error is dependent on the particular method used to solve each subproblem as well as the associated boundary conditions. The fractional-step method we take is known as the Godunov splitting and is first order accurate (see, for example, Leveque [37] for further details). The reason we use such a numerical method is that it is possible to adapt this technique for more complicated flows where monotonicity in x is not necessarily preserved over one time step.

We first define the evenly spaced numerical grid as

$$x_i = -M + i\Delta x, \quad i \in \mathbb{I}, \tag{7.1.2a}$$

$$y_j = j\Delta y, \quad j \in \mathbb{J}, \tag{7.1.2b}$$

$$t_k = k\Delta t, \quad k \in \mathbb{K}, \tag{7.1.2c}$$

where $\mathbb{I} = \{0, 1, \ldots, I, \ldots, 2I\}$, $\mathbb{J} = \{0, 1, \ldots, J\}$ and $\mathbb{K} = \{0, 1, \ldots, K\}$, with $x_I = 0$, $y_J = \pi$ and $t_K = T$. We approximate $u(x, y, t)$ and $b(y)$ by piecewise linear functions defined on the evenly spaced grid (7.1.2) and we use $U^k_{i,j} \approx u_d(x_i, y_j, t_k)$ and B_j to approximate $u(x_i, y_j, t_k)$ and $b(y_j)$ for all $i \in \mathbb{I}$, $j \in \mathbb{J}$ and $k \in \mathbb{K}$. We solve (7.1.1) in an evolutionary manner starting from $k = 0$. At each time step, the solution to (7.1.1a) is an intermediate solution which we use to obtain a second intermediate solution on solving (7.1.1b), and

from this we obtain the full solution at the next time step on solving (7.1.1c). We illustrate this procedure for arbitrary fixed $k \in \mathbb{K}$. First, we consider the advection equation.

7.1.1 The Advection Equation

We derive a finite volume method for the general two-dimensional advection equation

$$u_t + \boldsymbol{b} \cdot \nabla u = 0, \tag{7.1.3}$$

where $\boldsymbol{b} = (b(x,y), a(x,y))$. We introduce the fundamental concepts behind finite volume methods with a specific focus on first order accurate upwind methods, which we then implement for the case of shear flow given by (7.1.1a).

Finite Volume Methods

First, we split up the two-dimensional spatial domain into grid cells and calculate the average concentration of $u(x,y,t)$ in each grid cell at a given time. Assuming a uniformly spaced grid, we denote each grid cell centred about (x_i, y_j) by $\Omega_{i,j} = [x_{i-1/2}, x_{i+1/2}] \times [y_{j-1/2}, y_{j+1/2}]$ with $\Delta x = x_{i+1/2} - x_{i-1/2}$ and $\Delta y = y_{i+1/2} - y_{j-1/2}$. We approximate the average concentration of $u(x,y,t)$ over the grid cell $\Omega_{i,j}$ at time t_k as

$$Q_{i,j}^k \approx \frac{1}{\Delta x \Delta y} \int_{\Omega_{i,j}} u(x,y,t_k) dx dy, \tag{7.1.4}$$

and we approximate the background flow by the piecewise linear functions $\bar{B}_{i,j} \approx b(x_i, y_j)$ and $\bar{A}_{i,j} \approx a(x_i, y_j)$. In each time step we modify the values (7.1.4) based on the flux through the grid cell boundaries at $y = y_{j-1/2}$, $y = y_{j+1/2}$, $x = x_{i-1/2}$ and $x = x_{i+1/2}$. The advantage of working with finite volumes as opposed to finite differences is that it is easier to derive a numerical method which implements important properties of the conservation law. The integral form of a conservation law states, in a finite domain if a substance can neither be created or destroyed, then the rate of change of mass of this substance is

entirely due to fluxes across the domain boundaries. The integral form of the conservation law applied here gives

$$\frac{d}{dt}\int_{\Omega_{i,j}} u(x,y,t)dxdy = \int_{x_{i-1/2}}^{x_{i+1/2}} g(u(x,y_{j-1/2},t))dx - \int_{x_{i-1/2}}^{x_{i+1/2}} g(u(x,y_{j+1/2},t))dx + \int_{y_{j-1/2}}^{y_{j+1/2}} g(u(x_{i-1/2},y,t))dy - \int_{y_{j-1/2}}^{y_{j+1/2}} g(u(x_{i+1/2},y,t))dy, \quad (7.1.5)$$

where $g(u(x,y_{j-1/2},t))$, $-g(u(x,y_{j+1/2},t))$, $g(u(x_{i-1/2},y,t))$ and $-g(u(x_{i+1/2},y,t))$ are the flux coming into the grid cell through $y = y_{j-1/2}$, $y = y_{j+1/2}$, $x = x_{i-1/2}$ and $x = x_{i+1/2}$ respectively. Integrating equation (7.1.5) in time over $t \in [t_k, t_{k+1}]$ and rearranging yields

$$\begin{aligned}\frac{1}{\Delta x\Delta y}\int_{\Omega_{i,j}} u(x,y,t_{k+1})dydx = \frac{1}{\Delta x\Delta y}\int_{\Omega_{i,j}} u(x,y,t_k)dydx \\ - \frac{1}{\Delta x\Delta y}\left(\int_{t_k}^{t_{k+1}}\int_{x_{i-1/2}}^{x_{i+1/2}} \Big(g(u(x,y_{j+1/2},t)) - g(u(x,y_{j-1/2},t))\Big)dxdt\right) \\ - \frac{1}{\Delta x\Delta y}\left(\int_{t_k}^{t_{k+1}}\int_{y_{j-1/2}}^{y_{j+1/2}} \Big(g(u(x_{i+1/2},y,t)) - g(u(x_{i-1/2},y,t))\Big)dydt\right). \quad (7.1.6)\end{aligned}$$

We cannot evaluate the time integrals in equation (7.1.6) exactly, however, this leads us to take a numerical method of the form

$$Q_{i,j}^{k+1} = Q_{i,j}^k - \frac{\Delta t}{\Delta x}\Big(F_{i+1/2,j}^k - F_{i-1/2,j}^k\Big) - \frac{\Delta t}{\Delta y}\Big(F_{i,j+1/2}^k - F_{i,j-1/2}^k\Big), \quad (7.1.7)$$

where $F_{i\pm1/2,j}^k$ and $F_{i,j\pm1/2}^k$ are numerical approximations to the average flux entering the grid cell $\Omega_{i,j}$ through $x = x_{j\pm1/2}$ and $y = y_{i\pm1/2}$,

$$F_{i\pm1/2,j}^k \approx \frac{1}{\Delta t\Delta y}\int_{t_k}^{t_{k+1}}\int_{y_{j-1/2}}^{y_{j+1/2}} g(u(x_{i\pm1/2},y,t))dydt, \quad (7.1.8a)$$

$$F_{i,j\pm1/2}^k \approx \frac{1}{\Delta t\Delta x}\int_{t_k}^{t_{k+1}}\int_{x_{i-1/2}}^{x_{i+1/2}} g(u(x,y_{j\pm1/2},t))dxdt. \quad (7.1.8b)$$

When applied to the numerical method (7.1.7), the sum $\sum_{i,j} Q_{i,j}^{k+1}$ approximates the integral of u over the entire domain and only changes due to flux at the domain boundaries.

Hence, the conservation law is satisfied. The main goal in applying a finite volume method is to determine numerical flux functions that approximate the true flux as accurately as desired.

If we take

$$F^k_{i+1/2,j} = \frac{1}{2}\bar{B}_{i+1,j}\left(Q^k_{i+1,j} + Q^k_{i,j}\right) - \frac{1}{2}\bar{B}^2_{i+1,j}\frac{\Delta t}{\Delta x}\left(Q^k_{i+1,j} - Q^k_{i,j}\right) - \frac{1}{4}\bar{A}_{i+1,j}\bar{B}_{i+1,j}\frac{\Delta t}{\Delta y}\left(Q^k_{i+1,j+1} + Q^k_{i,j+1} - Q^k_{i+1,j-1} - Q^k_{i,j-1}\right), \tag{7.1.9a}$$

$$F^k_{i-1/2,j} = \frac{1}{2}\bar{B}_{i,j}\left(Q^k_{i,j} + Q^k_{i-1,j}\right) - \frac{1}{2}\bar{B}^2_{i,j}\frac{\Delta t}{\Delta x}\left(Q^k_{i,j} - Q^k_{i-1,j}\right) - \frac{1}{4}\bar{A}_{i,j}\bar{B}_{i,j}\frac{\Delta t}{\Delta y}\left(Q^k_{i,j+1} + Q^k_{i-1,j+1} - Q^k_{i,j-1} - Q^k_{i-1,j-1}\right), \tag{7.1.9b}$$

$$F^k_{i,j+1/2} = \frac{1}{2}\bar{A}_{i,j+1}\left(Q^k_{i,j+1} + Q^k_{i,j}\right) - \frac{1}{2}\bar{A}^2_{i,j+1}\frac{\Delta t}{\Delta y}\left(Q^k_{i,j+1} - Q^k_{i,j}\right), \tag{7.1.9c}$$

$$F^k_{i,j-1/2} = \frac{1}{2}\bar{A}_{i,j}\left(Q^k_{i,j} + Q^k_{i,j-1}\right) - \frac{1}{2}\bar{A}^2_{i,j}\frac{\Delta t}{\Delta y}\left(Q^k_{i,j} - Q^k_{i,j-1}\right), \tag{7.1.9d}$$

the numerical method (7.1.7) is second order accurate in space but is dispersive near the leading and trailing edges of the front (where the concentration is no longer bounded between 0 and 1) as illustrated in Figure 7.1(a). Instead we consider upwind methods which are conditionally numerically stable provided the CFL condition (see, for example, Leveque [37]) is satisfied, namely,

$$\frac{|\bar{B}|\Delta t}{\Delta x}, \frac{|\bar{A}|\Delta t}{\Delta y} \leq 1. \tag{7.1.10}$$

For the advection equation, information propagates as waves moving along characteristics which have a constant speed, an upwind method uses information obtained from the direction from which this information should be coming. A first order upwind method for

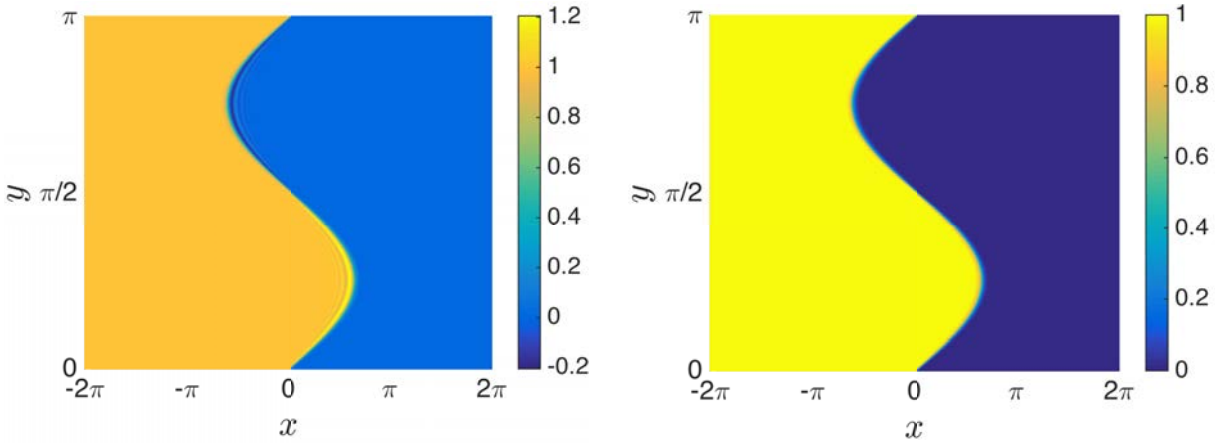

(a) (b)

Figure 7.1: The solution $u(x, y, t)$ to (7.1.3) approximated numerically for shear flow $\boldsymbol{b} = (\sin(2y), 0)$ at time $t = 2$ for (a) a second order accurate flux function (7.1.9) and (b) a first order upwind flux function (7.1.11).

the advection equation (7.1.3) is given by (7.1.7) with

$$F^k_{i+1/2,j} = \left(\bar{B}^-_{i+1,j} Q^k_{i+1,j} + \bar{B}^+_{i+1,j} Q^k_{i,j}\right) + \frac{1}{2}|\bar{B}_{i+1,j}| \left(Q^k_{i+1,j} - Q^k_{i,j}\right), \tag{7.1.11a}$$

$$F^k_{i-1/2,j} = \left(\bar{B}^-_{i,j} Q^k_{i,j} + \bar{B}^+_{i,j} Q^k_{i-1,j}\right) + \frac{1}{2}|\bar{B}_{i,j}| \left(Q^k_{i,j} - Q^k_{i-1,j}\right), \tag{7.1.11b}$$

$$F^k_{i,j+1/2} = \left(\bar{A}^-_{i,j+1} Q^k_{i,j+1} + \bar{A}^+_{i,j+1} Q^k_{i,j}\right) + \frac{1}{2}|\bar{A}_{i,j+1}| \left(Q^k_{i,j+1} - Q^k_{i,j}\right), \tag{7.1.11c}$$

$$F^k_{i,j-1/2} = \left(\bar{A}^-_{i,j} Q^k_{i,j} + \bar{A}^+_{i,j} Q^k_{i,j-1}\right) + \frac{1}{2}|\bar{A}_{i,j}| \left(Q^k_{i,j} - Q^k_{i,j-1}\right), \tag{7.1.11d}$$

where we define

$$C^+_{i,j} = \max(C_{i,j}, 0), \qquad C^-_{i,j} = \min(C_{i,j}, 0), \tag{7.1.12}$$

for any matrix C. The numerical method is only first order accurate but is no longer dispersive as illustrated in Figure 7.1(b). Next we derive a high resolution numerical method to solve the advection equation which we implement for the specific case of shear flow, described by equation (7.1.1a).

Implementation for Shear Flow

It follows from the numerical method (7.1.7), that we approximate the average concentration of $u(x, y, t)$, for the specific case of shear flow, over the grid cell $\Omega_{i,j}$ at time t_k as

$$Q_{i,j}^{k+1} = Q_{i,j}^{k} - \frac{\Delta t}{\Delta x}\Big(F_{i+1/2,j}^{k} - F_{i-1/2,j}^{k}\Big), \tag{7.1.13}$$

for $i \in \mathbb{I} \setminus \{0, 2I\}$ and $j \in \mathbb{J}$. We take the numerical approximation to the average flux entering $\Omega_{i,j}$ through $x = x_{i+1/2}$ and $x = x_{i-1/2}$ as

$$F_{i+1/2,j}^{k} = \Big(B_j^{-} Q_{i+1,j}^{k} + B_j^{+} Q_{i,j}^{k}\Big) + \frac{1}{2}|B_j|\left(I - \frac{\Delta t}{\Delta x}|B_j|\right)\delta_{i+1/2,j}(a_1, a_2), \tag{7.1.14a}$$

$$F_{i-1/2,j}^{k} = \Big(B_j^{-} Q_{i,j}^{k} + B_j^{+} Q_{i-1,j}^{k}\Big) + \frac{1}{2}|B_j|\left(I - \frac{\Delta t}{\Delta x}|B_j|\right)\delta_{i-1/2,j}(a_1, a_2), \tag{7.1.14b}$$

where $\delta_{i+1/2,j}(a_1, a_2)$ and $\delta_{i-1/2,j}(a_3, a_4)$ are upwind minmod limiters

$$\delta_{i+1/2,j}(a_1, a_2) = \begin{cases} a_1, & \text{if } |a_1| < |a_2|,\ a_1 a_2 > 0, \\ a_2, & \text{if } |a_1| > |a_2|,\ a_1 a_2 > 0, \\ 0, & \text{otherwise,} \end{cases} \tag{7.1.14c}$$

$$\delta_{i-1/2,j}(a_3, a_4) = \begin{cases} a_3, & \text{if } |a_3| < |a_4|,\ a_3 a_4 > 0, \\ a_4, & \text{if } |a_3| > |a_4|,\ a_3 a_4 > 0, \\ 0, & \text{otherwise,} \end{cases} \tag{7.1.14d}$$

with $a_1 = Q_{i+1,j}^{k} - Q_{i,j}^{k}$, $a_3 = Q_{i,j}^{k} - Q_{i-1,j}^{k}$ and

$$a_2 = \begin{cases} Q_{i+2,j}^{k} - Q_{i+1,j}^{k}, & \text{if } B_j \le 0, \\ Q_{i,j}^{k} - Q_{i-1,j}^{k}, & \text{if } B_j > 0, \end{cases} \tag{7.1.14e}$$

$$a_4 = \begin{cases} Q_{i+1,j}^{k} - Q_{i,j}^{k}, & \text{if } B_j \le 0, \\ Q_{i-1,j}^{k} - Q_{i-2,j}^{k}, & \text{if } B_j > 0, \end{cases} \tag{7.1.14f}$$

for each $k \in \mathbb{K}$. We take as initial conditions

$$Q^0_{i,j} = \begin{cases} 1, & i = 0, 1, \dots I, \\ 0, & i = I+1, \dots, 2I, \end{cases} \qquad j \in \mathbb{J}, \tag{7.1.14g}$$

and boundary conditions

$$Q^k_{-1,j} = Q^k_{0,j} = Q^k_{1,j}, \quad Q^k_{2I+1,j} = Q^k_{2I,j} = Q^k_{2I-1,j}, \quad j \in \mathbb{J}, \tag{7.1.14h}$$

for fixed $k \in \mathbb{K}$. There are stability issues associated with taking the *ghost* cells (immediately outside our numerical grid) $\Omega_{-1,j}$ and $\Omega_{2I+1,j}$ to have constant value due to the flux across the domain boundaries. Given Heaviside initial conditions (6.0.3d), replacing the travelling wave boundary conditions (6.0.3e), with zero-order extrapolation boundary conditions (7.1.14h), introduces only negligible errors provided the numerical grid in the x-direction is sufficiently large. The numerical flux functions (7.1.14a) and (7.1.14b) can be thought of as an upwind flux term (the first term) with a correction term (the second term) to account for second order corrections. We have applied a limiter that modifies the magnitude of the correction term to take into account how the solution is behaving in the neighbouring grid cells (from the direction information is flowing). We next solve the diffusion equation (7.1.1b). To that end, we make the assumption that the concentration in each cell $\Omega_{i,j}$ is uniform across the whole cell for all $i \in \mathbb{I}$, $j \in \mathbb{J}$ and $k \in \mathbb{K}$. As the solution to the advection equation (7.1.1a) is only an intermediate solution to (7.1.1), at time step $k \in \mathbb{K}$, we take $U^k_{i,j} = Q^{k+1}_{i,j}$ as the initial value of the concentration when solving the diffusion equation (7.1.1b).

7.1.2 The Diffusion Equation

We use finite differences to approximate the derivatives in (7.1.1b) with our choice of finite difference method determined by the location of the level curve $u = u_c$ at each

time step. If $U_{i,j}^k > u_c$ ($U_{i,j}^k < u_c$), then the concentration at this grid point at next time step must be calculated from other concentrations $U_{\hat{i},\hat{j}}^k$ such that $U_{\hat{i},\hat{j}}^k > u_c$ ($U_{\hat{i},\hat{j}}^k < u_c$). Any implicit method, such as an alternating direction implicit method which is often used for multidimensional diffusion problems (see, for example, Tzella and Vanneste [57] with the method described in detail in Chapter 3 of Morton and Mayers [41]), relies on a discretisation at the current time step where the location of the level curve $u = u_c$ is yet to be determined and, therefore, cannot be used here. Instead, we use explicit finite differences to approximate the derivatives in equation (7.1.1b) and then solve the resulting differential equation. We use first order forward differences to approximate the time derivative, namely,

$$\frac{\partial}{\partial t} U_{i,j}^k \approx \frac{U_{i,j}^{k+1} - U_{i,j}^k}{\Delta t}, \quad i \in \mathbb{I},\ j \in \mathbb{J}, \tag{7.1.15}$$

for all $k \in \mathbb{K}$. In order to accurately approximate the space derivatives we must first locate the level curve $u = u_c$ for each $k \in \mathbb{K}$. It follows from the monotonicity property (A3) that, for fixed $y \in [0, \pi]$ and $t > 0$, there exists a unique value of x such that $u(x, y, t) = u_c$. On returning to our discretised problem, we denote the horizontal pair of grid points which the level curve $u = u_c$ is located between as $(H(j) - 1, j) - (H(j), j)$ for all $j \in \mathbb{J}$. Using linear interpolation, we find the horizontal distance from $U_{H(j)-1,j}^k$ to $u = u_c$, which we refer to as $a_0(j)$, via

$$a_0(j) = \Delta x \left(\frac{u_c - U_{H(j)-1,j}^k}{U_{H(j),j}^k - U_{H(j)-1,j}^k} \right). \tag{7.1.16}$$

The situation is illustrated in Figure 7.2. We use centred second differences to approximate the second space derivative in the x-direction for $i \in \mathbb{I} \setminus \{0, 2I\}$ and adapt the method when $i = H(j) - 1, H(j)$ for all $j \in \mathbb{J}$ to ensure the level curve $u = u_c$ is not crossed. To

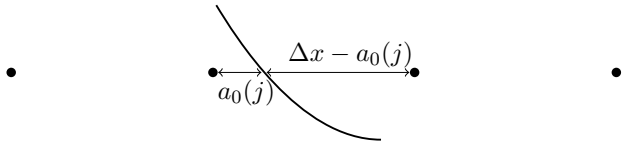

Figure 7.2: A sketch to illustrate which discrete mesh points are horizontally adjacent to the level curve $u = u_c$.

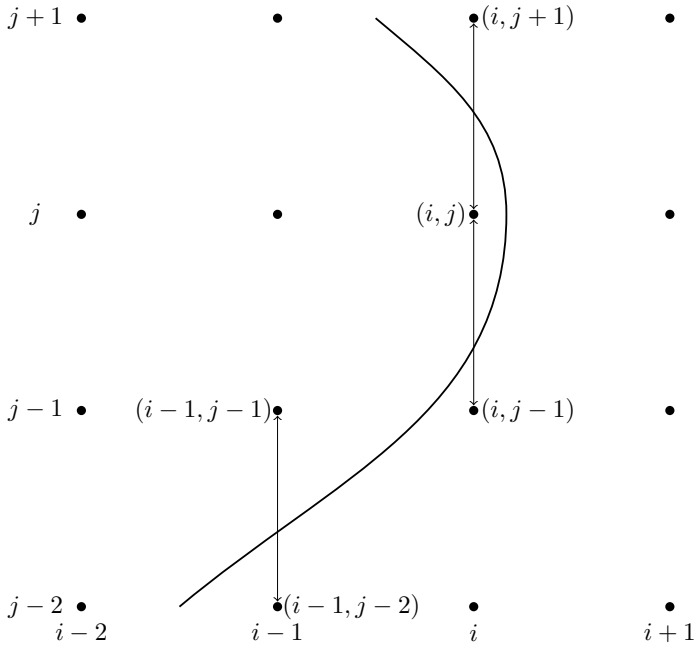

Figure 7.3: A sketch to illustrate which discrete mesh points are vertically adjacent to the level curve $u = u_c$.

that end, we obtain the following first-order accurate approximations

$$\frac{\partial^2}{\partial x^2} U^k_{i,j} \approx \frac{U^k_{i+1,j} - 2U^k_{i,j} + U^k_{i-1,j}}{\Delta x^2}, \quad i \in \mathbb{I} \setminus \{0, H(j) - 1, H(j), 2I\}, \tag{7.1.17a}$$

$$\frac{\partial^2}{\partial x^2} U^k_{H(j)-1,j} \approx \frac{2\Delta x u_c - 2(a_0(j) + \Delta x) U^k_{H(j)-1,j} + 2a_0(j) U^k_{H(j)-2,j}}{a_0(j)\Delta x(a_0(j) + \Delta x)}, \tag{7.1.17b}$$

$$\frac{\partial^2}{\partial x^2} U^k_{H(j),j} \approx \frac{2\left(\Delta x - a_0(j)\right) U^k_{H(j)+1,j} - 2(2\Delta x - a_0(j)) U^k_{H(j),j} + 2\Delta x u_c}{\left(\Delta x - a_0(j)\right)\Delta x(2\Delta x - a_0(j))}, \tag{7.1.17c}$$

for all $j \in \mathbb{J}$ and $k \in \mathbb{K}$.

We next locate all vertical pairs of grid points the level curve $u = u_c$ is located

between. Motivated by results for related problems where the reaction nonlinearity is of ignition-type [6], for fixed x, we do not expect that the solution $u(x, y, t)$ to [IVPA] will be monotonic in y at time $t > 0$, due to the impact of the shear flow. For fixed $x \in [-M, M]$ and $t > 0$, there could exist multiple values, a unique value or zero values of y such that $u(x, y, t) = u_c$. On returning to our discretised problem, we must find all vertical pairs of grid points $(i, j) - (i, j + 1)$ such that $U^k_{i,j} > u_c$ with $U^k_{i,j+1} < u_c$ or $U^k_{i,j} < u_c$ with $U^k_{i,j+1} > u_c$ for each fixed $k \in \mathbb{K}$. These situations are illustrated in Figure 7.3. To that end, we make the following definitions:

$$\begin{aligned} G_1 =&\{(i_1, j_1) \in \mathbb{I} \times (\mathbb{J} \setminus \{0, J\}) : U^k_{i_1,j_1} > u_c \text{ and } U^k_{i_1,j_1+1}, U^k_{i_1,j_1-1} < u_c, \\ &\text{or, } U^k_{i_1,j_1} < u_c \text{ and } U^k_{i_1,j_1+1}, U^k_{i_1,j_1-1} > u_c\}, \end{aligned} \tag{7.1.18a}$$

$$\begin{aligned} G_2 =&\{(i_2, j_2) \in \mathbb{I} \times (\mathbb{J} \setminus \{0, J\}) : U^k_{i_2,j_2} < u_c \text{ and } U^k_{i_2,j_2+1} > u_c, \\ &\text{or, } U^k_{i_2,j_2} > u_c \text{ and } U^k_{i_2,j_2+1} < u_c\} \setminus G_1, \end{aligned} \tag{7.1.18b}$$

for each fixed $k \in \mathbb{K}$. Using linear interpolation, we find the following vertical distances: from $U^k_{i_1,j_1}$ up to $u = u_c$ which we refer to as $a_1(j_1)$, from $U^k_{i_1,j_1-1}$ up to $u = u_c$ which we refer to as $\bar{a}_1(j_1)$ and from $U^k_{i_2,j_2}$ up to $u = u_c$ which we refer to as $a_2(j_2)$, via

$$a_1(j_1) = \Delta y \left(\frac{u_c - U^k_{i_1,j_1}}{U^k_{i_1,j_1+1} - U^k_{i_1,j_1}} \right), \tag{7.1.19a}$$

$$\bar{a}_1(j_1) = \Delta y \left(\frac{u_c - U^k_{i_1,j_1-1}}{U^k_{i_1,j_1} - U^k_{i_1,j_1-1}} \right), \tag{7.1.19b}$$

$$a_2(j_2) = \Delta y \left(\frac{u_c - U^k_{i_2,j_2}}{U^k_{i_2,j_2+1} - U^k_{i_2,j_2}} \right). \tag{7.1.19c}$$

The situation is illustrated in Figure 7.4. We use centred second differences to approximate the second space derivative in the y-direction for $j \in \mathbb{J} \setminus \{0, J\}$ and adapt the method when $(i, j) = (i_1, j_1)$, $(i_1, j_1 \pm 1)$, (i_2, j_2) and $(i_2, j_2 + 1)$ to ensure that the finite difference approximation does not take values from both sides of the level curve $u = u_c$.

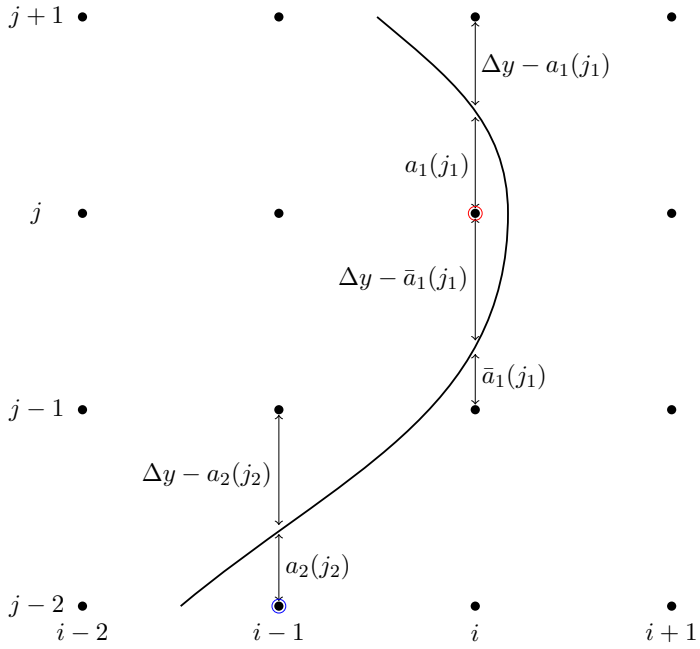

Figure 7.4: A sketch of the discrete mesh points that are part of the set G_1 (circled in red) with $(i_1, j_1) = (i, j)$ and part of the set G_2 (circled in blue) with $(i_2, j_2) = (i-1, j-2)$.

To that end, we obtain the following first-order accurate approximations

$$\frac{\partial^2}{\partial y^2} U^k_{i,j} \approx \frac{U^k_{i,j+1} - 2U^k_{i,j} + U^k_{i,j-1}}{\Delta y^2}, \tag{7.1.20a}$$

$$\frac{\partial^2}{\partial y^2} U^k_{i_1,j_1+1} \approx \frac{2\left(\Delta y - a_1(j_1)\right) U^k_{i_1,j_1+2} - 2(2\Delta y - a_1(j_1)) U^k_{i_1,j_1+1} + 2\Delta y u_c}{\left(\Delta y - a_1(j_1)\right) \Delta y (2\Delta y - a_1(j_1))}, \tag{7.1.20b}$$

$$\frac{\partial^2}{\partial y^2} U^k_{i_1,j_1} \approx \frac{2\left(u_c - U^k_{i_1,j_1}\right)}{a_1(j_1)\left(\Delta y - \bar{a}_1(j_1)\right)}, \tag{7.1.20c}$$

$$\frac{\partial^2}{\partial y^2} U^k_{i_1,j_1-1} \approx \frac{2\Delta y u_c - 2(\bar{a}_1(j_1) + \Delta y) U^k_{i_1,j_1-1} + 2\bar{a}_1(j_1) U^k_{i_1,j_1-2}}{\bar{a}_1(j_1)\Delta y(\bar{a}_1(j_1) + \Delta y)}, \tag{7.1.20d}$$

$$\frac{\partial^2}{\partial y^2} U^k_{i_2,j_2+1} \approx \frac{2\left(\Delta y - a_2(j_2)\right) U^k_{i_2,j_2+2} - 2(2\Delta y - a_2(j_2)) U^k_{i_2,j_2+1} + 2\Delta y u_c}{\left(\Delta y - a_2(j)\right) \Delta y (2\Delta y - a_2(j_2))}, \tag{7.1.20e}$$

$$\frac{\partial^2}{\partial y^2} U^k_{i_2,j_2} \approx \frac{2\Delta y u_c - 2(a_2(j_2) + \Delta y) U^k_{i_2,j_2} + 2a_2(j_2) U^k_{i_2,j_2-1}}{a_2(j_2)\Delta y(a_2(j_2) + \Delta y)}, \tag{7.1.20f}$$

for all $(i, j) \in \mathbb{I} \times (\mathbb{J} \setminus \{0, J\}) \setminus (G_1 \cup G_2)$, $(i_1, j_1) \in G_1$ and $(i_2, j_2) \in G_2$, respectively, and for fixed $k \in \mathbb{K}$.

These approximations lead to the following numerical scheme

$$U_{i,j}^{k+1} = U_{i,j}^{k} + \frac{\Delta t}{\mathrm{Pe}} \left[\frac{U_{i+1,j}^{k} - 2U_{i,j}^{k} + U_{i-1,j}^{k}}{\Delta x^2} + \frac{U_{i,j+1}^{k} - 2U_{i,j}^{k} + U_{i,j-1}^{k}}{\Delta y^2} \right], \tag{7.1.21a}$$

wrote for convenience when the values of i, j and k place $U_{i,j}^{k}$ away from the level curve $u = u_c$. When $U_{i,j}^{k}$ is evaluated at a mesh point directly next to the boundary, the discretised second spatial derivative approximations in the square brackets must be replaced by the appropriate version of (7.1.17) and (7.1.20) respectively. We have

$$U_{i,j}^{k} > u_c, \quad i = 0, 1, \ldots, H(j) - 1, \qquad U_{i,j}^{k} < u_c, \quad i = H(j), \ldots, 2I, \tag{7.1.21b}$$

for all $j \in \mathbb{J}$ and $k \in \mathbb{K}$. Using (6.0.3f), we set absorbing boundary conditions

$$U_{i,0}^{k} = U_{i,1}^{k}, \quad U_{i,J+1}^{k} = U_{i,J}^{k}, \quad i \in \mathbb{I}, \tag{7.1.21c}$$

and, similarly, impose absorbing boundary conditions

$$U_{0,j}^{k} = U_{1,j}^{k}, \quad U_{2I,j}^{k} = U_{2I-1,j}^{k}, \quad j \in \mathbb{J}, \tag{7.1.21d}$$

for consistency with the boundary conditions (7.1.14h) in the advective scheme for each fixed $k \in \mathbb{K}$. The continuity of first spatial derivative is explicitly used to find the precise location of level curve $u = u_c$ via linear interpolation in the x-direction (7.1.16) and in y-direction (7.1.19), respectively. The explicit finite difference scheme (7.1.21) consists of $2I - 1 \times J - 1$ linear equations and $2I - 1 \times J - 1$ unknowns $U_{i,j}^{k}$ ($i \in \mathbb{I} \setminus \{0, 2I\}$; $j \in \mathbb{J} \setminus \{0, J\}$). As the solution to the diffusion equation (7.1.1b) is only an intermediate solution to (7.1.1), at time step $k \in \mathbb{K}$, we set $U_{i,j}^{k} = U_{i,j}^{k+1}$.

7.1.3 The Reaction Equation

We next consider the reaction equation (7.1.1c) which can be solved exactly over $[t_k, t_{k+1}]$. On integrating directly we find

$$U_{i,j}^{k+1} = \begin{cases} \frac{U_{i,j}^k e^{\mathrm{Da}\Delta t}}{1-U_{i,j}^k\left(1-e^{\mathrm{Da}\Delta t}\right)}, & \text{if } U_{i,j}^k > u_c, \\ U_{i,j}^k, & \text{otherwise,} \end{cases}$$

for all $i \in \mathbb{I}$, $j \in \mathbb{J}$ and $k \in \mathbb{K}$.

7.1.4 Further Details

This completes our numerical approximation to the concentration $U_{i,j}^{k+1}$ at this time step but before moving on to examine the next time step there are a few matters left to consider. The level curve $u(s(y,t),y,t) = u_c$ uniquely determines the numerical scheme employed in sections 7.1.2 - 7.1.3 and, as such, is of paramount importance to this problem. We approximate $s(y,t)$ by the piecewise linear function $S_j^k \approx s_d(y_j, t_k)$ defined on the evenly spaced numerical grid (7.1.2). As in the diffusive step, we obtain the value of S_j^{k+1} using linear interpolation for each $j \in \mathbb{J}$.

Additionally, if the concentration at $x = (M-1)\pi$ becomes larger than $\epsilon = 10^{-5}$, we modify the computational domain by eliminating the mesh points with $-M\pi \leq x \leq (-M+1)\pi$, far behind the boundary where the concentration is approximately 1, and add new mesh points with $M\pi \leq x \leq (M+1)\pi$, well in advance of the boundary where we set the concentration to be equal to 0. Results are not sensitive to the precise value of ϵ provided $\epsilon \ll 1$ with this *cut-domain* procedure allowing us track the evolution of $U_{i,j}^k$ and S_j^{k+1} for large-time. We repeat the procedure illustrated in Sections 7.1.1 - 7.1.4 for each value of $k \in \mathbb{K}$ in an evolutionary manner. For $k_1 \in \mathbb{K}$ such that the profile of S_j^k remains approximately constant in time for all $k > k_1$, we calculate its speed based on a linear fitting obtained for such values $k > k_1$. Results for the speed are not sensitive to the particular level curve chosen to track, with the speed of the level curve $u = a$ the

same for each $a \in (0,1)$. Hence, this speed corresponds to the speed of propagation of the solution $U_{i,j}^k$ in the positive x-direction.

7.2 Results

In this section we examine results obtained from numerical solution of [IVPA] for shear flow $\boldsymbol{b} = (\sin(2y), 0)$ using the fractional step method described in detail in Section 7.1. We choose artificial domain boundary M to be sufficiently large so that boundary effects imposed by the absorbing boundary conditions (7.1.14h) and (7.1.21d) are negligible. We set spatial resolution to be equal in both directions $\Delta x = \Delta y = \Delta$ and we set the time step to be

$$\Delta t = \min\left(\frac{1}{2}\Delta^2, \Delta\right), \tag{7.2.1}$$

to ensure the *von Neumann* stability of the explicit method for diffusion and that the upwind scheme for advection satisfies the CFL condition (see, for example, [37]).

In Table 7.1 we show the percentage difference between the numerically evaluated approximation to $\lim_{t\to\infty} s_t(y,t)$ and that obtained when the resolution is doubled (by halving Δ) for decreasing values of Δ. The results are not sensitive to the precise value of y with comparison for results obtained with any fixed $y \in [0,\pi]$ resulting in less than 0.05% difference in $\lim_{t\to\infty} s_t(y,t)$, hence, without loss of generality we consider results for $y = 0$. It is evident from Figure 7.5 that $\lim_{t\to\infty} s_0(t)$ is linear in t, thus, $\lim_{t\to\infty} \dot{s}_0(t)$ converges to a constant value c_∞. The particular value of c_∞ is dependent on the parameters u_c, Pe and Da, however, we write $c_\infty(u_c)$ for ease of notation as we are mainly interested in how our solution for fixed Pe and Da changes as we vary $u_c \in (0,1)$. We observe that as we decrease the mesh spacing Δ by a factor of 2, the percentage difference between the numerically calculated value of $c_\infty(u_c)$ and that obtained when the resolution is doubled, also decreases by a factor of 2. This behaviour is evident for the two values of u_c shown for Pe = 4 and Da = 1/64 (with more values of Pe, Da and $u_c \in (0,1)$ considered but not presented here). Based on these figures, a mesh spacing of $\Delta = \pi/200$ was selected to ensure

Δ	$c_\infty(0.1)$	% difference	time (seconds)
$\pi/50$	0.2117	3.713×10^{-1}	69.91
$\pi/100$	0.2125	1.851×10^{-1}	744.6
$\pi/150$	0.2127	1.399×10^{-1}	$3,392$
$\pi/200$	0.2129	7.088×10^{-2}	$6,798$
$\pi/250$	0.2129	4.694×10^{-2}	$13,014$

(a) $u_c = 0.1$

Δ	$c_\infty(0.5)$	% difference	time (seconds)
$\pi/50$	7.636×10^{-2}	5.852×10^{-1}	124.1
$\pi/100$	7.681×10^{-2}	3.020×10^{-1}	$1,245$
$\pi/150$	7.698×10^{-2}	1.958×10^{-1}	$4,949$
$\pi/200$	7.704×10^{-2}	1.585×10^{-1}	$12,880$
$\pi/250$	7.706×10^{-2}	1.361×10^{-1}	$24,130$

(b) $u_c = 0.5$

Table 7.1: Convergence of the numerical approximation to $\dot{s}_0(t)$ of [IVPA] onto the constant $c_\infty(u_c)$ for decreasing Δ. This table shows the percentage difference between the numerically calculated value of $c_\infty(u_c)$ and the value obtained when the spatial resolution is doubled. The time, given in seconds, is the calculation time for a typical run. Results are obtained numerically to four significant figures for Pe = 4, Da = 1/64 with (a) $u_c = 0.1$ and (b) $u_c = 0.5$.

that the solution is sufficiently well approximated for a large range of parameter values whilst keeping the computation time required to solve the numerical scheme in Section 7.1 reasonable. Comparison with results obtained for a spatial resolution of $\Delta = \pi/300$ resulted in a less than 0.5% difference in $u(x, y, t)$.

Figures 7.5 - 7.11 represent the numerical solutions for $u(x, y, t)$ and $s(y, t)$, to [IVPA], respectively, with cut-off value $u_c = 0.1$, 0.5 and 0.9 and parameter values Pe = 50 and Da = 50, 1 and 1/50 obtained at selected values of t. They indicate that for all combinations of parameter values, a permanent form travelling wave-front develops in the large-time structure of the solution to [IVPA], that is, as $t \to \infty$. We first consider $s(y, t)$ for Pe fixed as we vary u_c and Da. Figure 7.5(c) shows that extremely large values of t are required to observe the linear behaviour of $\lim_{t\to\infty} s_0(t)$ for small-Da and large-Pe and u_c. This point is further illustrated by Figures 7.7(c) and 7.8(c), which show that for $u_c = 0.9$, with Da = 1 and 1/50 respectively, we have to extend the period of time over

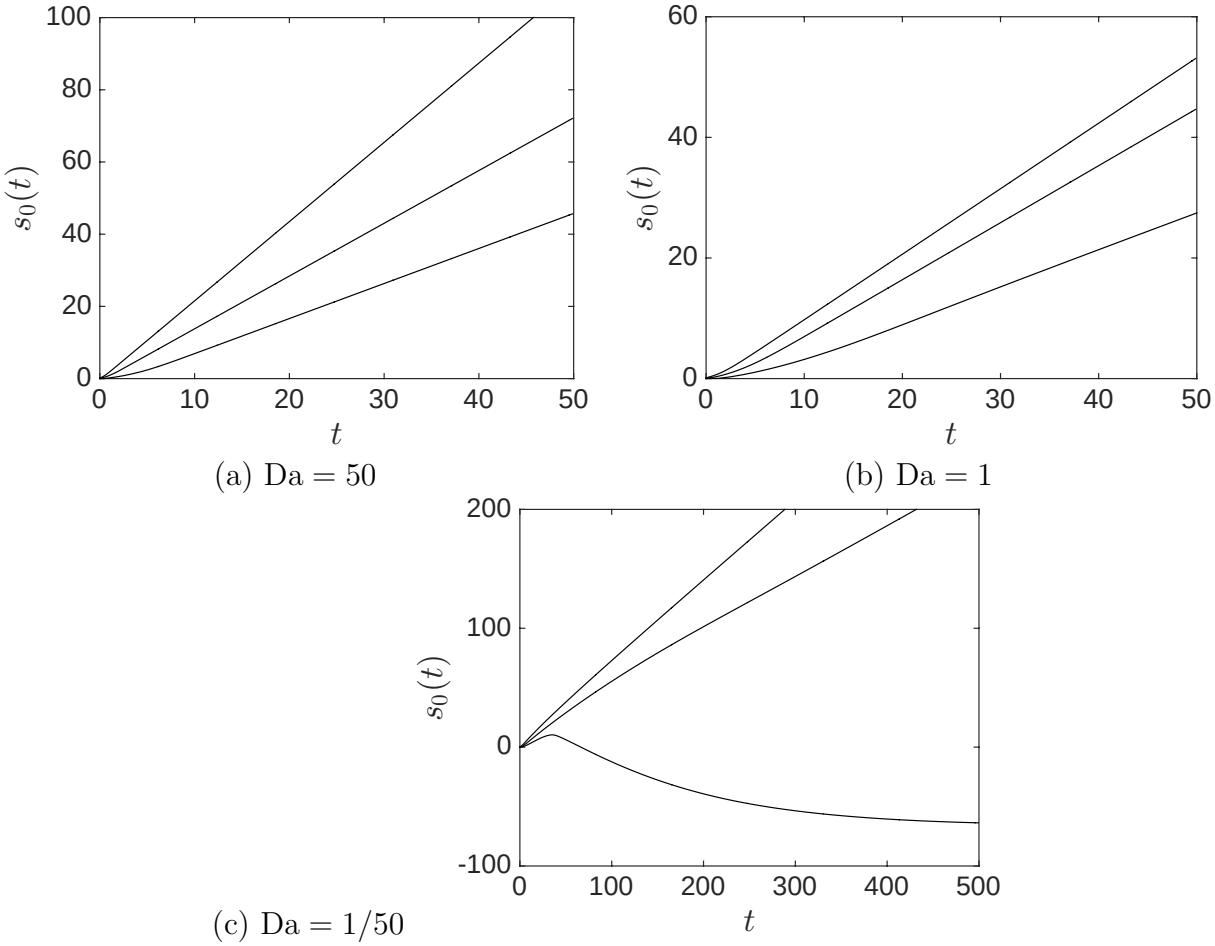

(a) Da = 50

(b) Da = 1

(c) Da = 1/50

Figure 7.5: Numerical approximation of $s_0(t)$ as it evolves over time for $u_c = 0.1$ (top plot), $u_c = 0.5$ (middle plot) and $u_c = 0.9$ (bottom plot). Results are obtained for Pe = 50 with (a) Da = 50, (b) Da = 1 and (c) Da = 1/50.

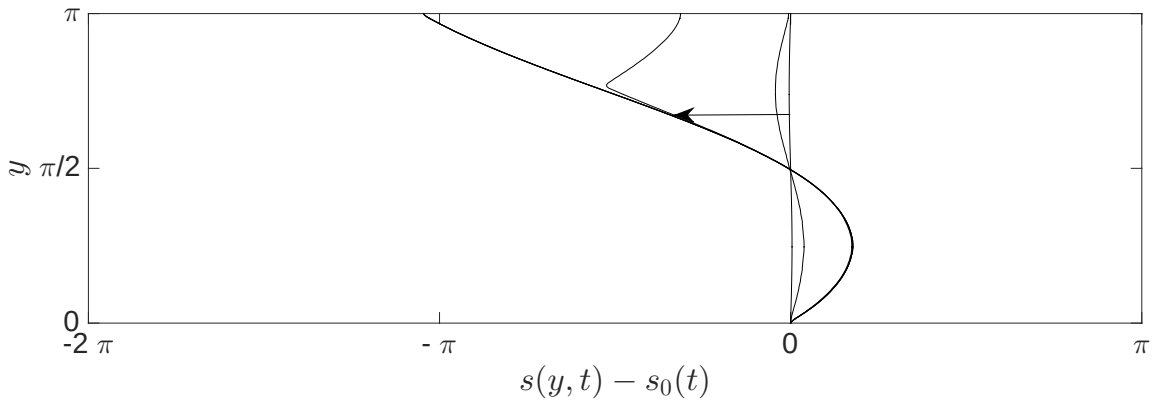

$s(y,t) - s_0(t)$

(a) $u_c = 0.1$

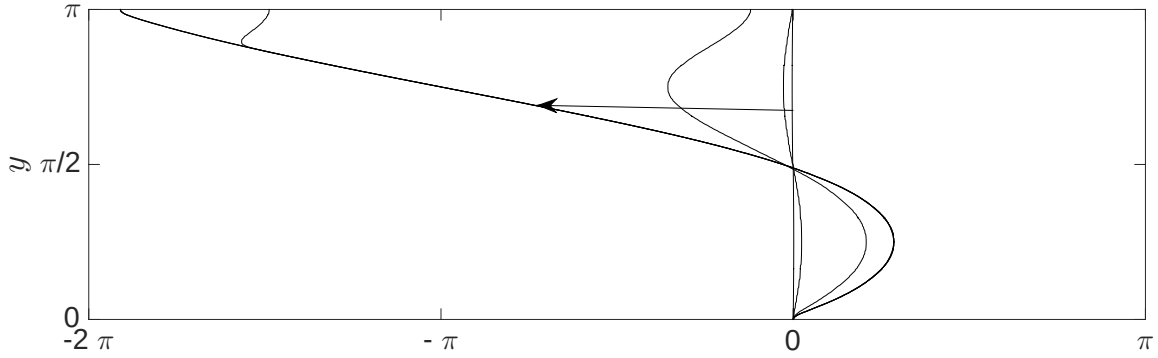

$s(y,t) - s_0(t)$

(b) $u_c = 0.5$

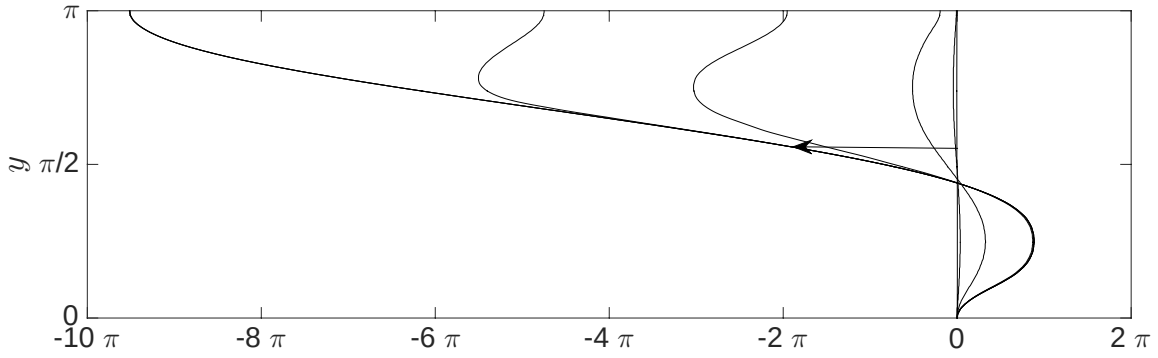

$s(y,t) - s_0(t)$

(c) $u_c = 0.9$

Figure 7.6: Numerical approximation of the profile of the moving boundary $s(y,t)$ as it evolves over time for Pe = 50 and Da = 50. Results are obtained for (a) $u_c = 0.1$, (b) $u_c = 0.5$ and (c) $u_c = 0.9$ for $t = 0$, $t = 0.1$, 1, 5, 10, 20 and $t = 30$ with the arrow pointing in the direction of increasing t. For panel (c), the axes have been increased so convergence can be observed.

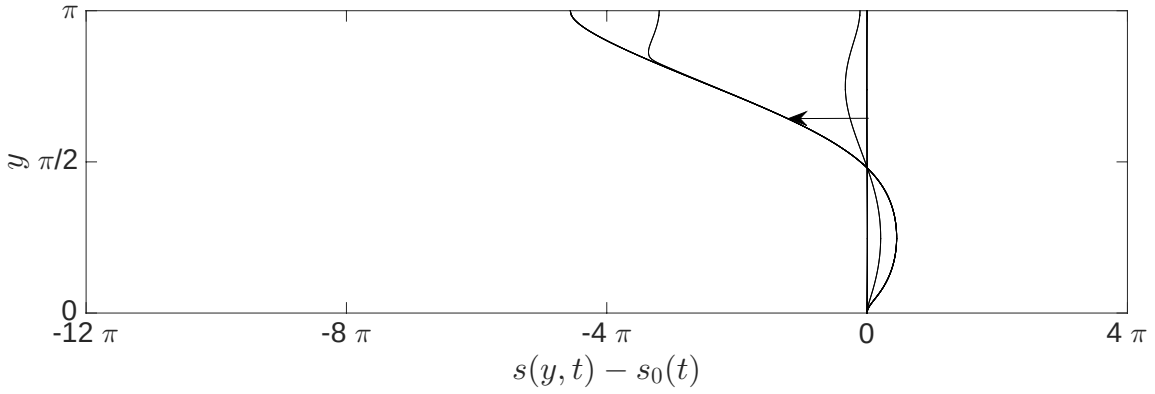

(a) $u_c = 0.1$

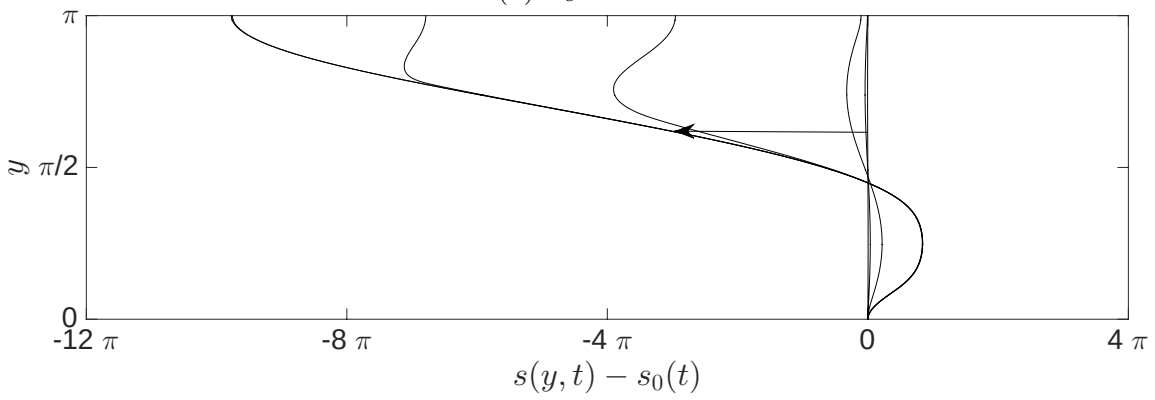

(b) $u_c = 0.5$

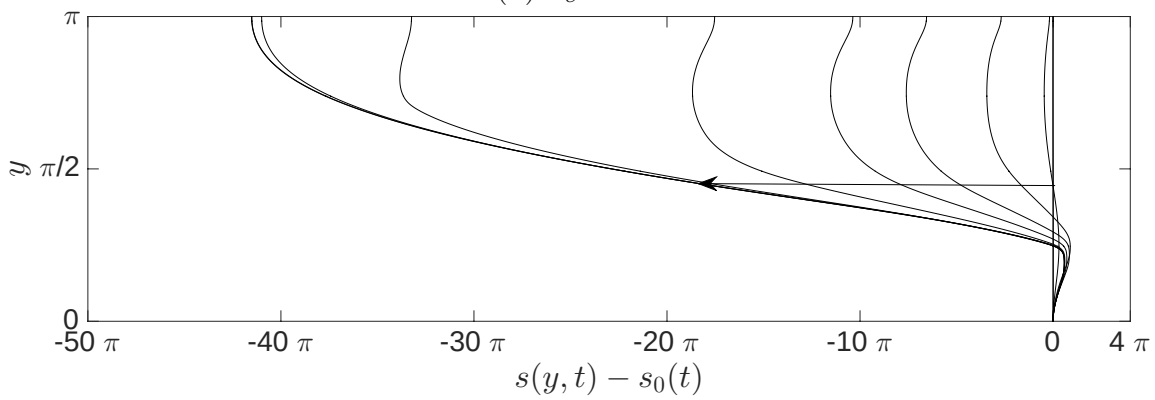

(c) $u_c = 0.9$

Figure 7.7: Numerical approximation of the profile of the moving boundary $s(y,t)$ as it evolves over time for Pe = 50 and Da = 1. Results are obtained for (a) $u_c = 0.1$, (b) $u_c = 0.5$ and (c) $u_c = 0.9$ for $t = 0$, 0.1, 1, 10, 20, 30 and $t = 50$ with the arrow pointing in the direction of increasing t. For panel (c), additional solutions obtained at $t = 100$, 150, 200 and $t = 250$ are plotted and the axes have been increased so convergence can be observed.

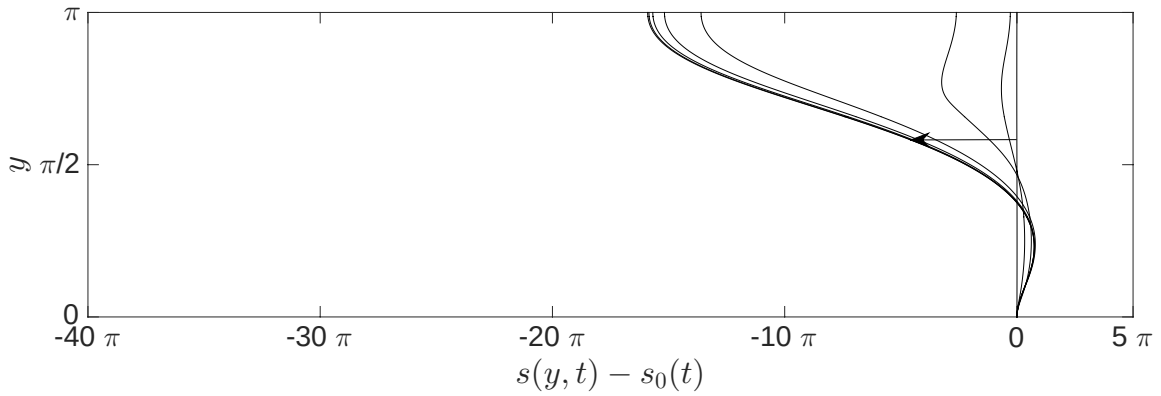

(a) $u_c = 0.1$

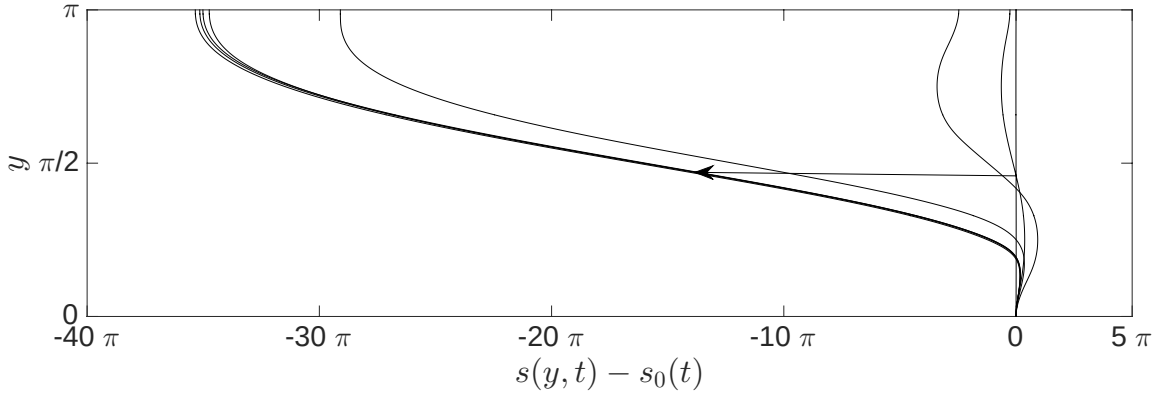

(b) $u_c = 0.5$

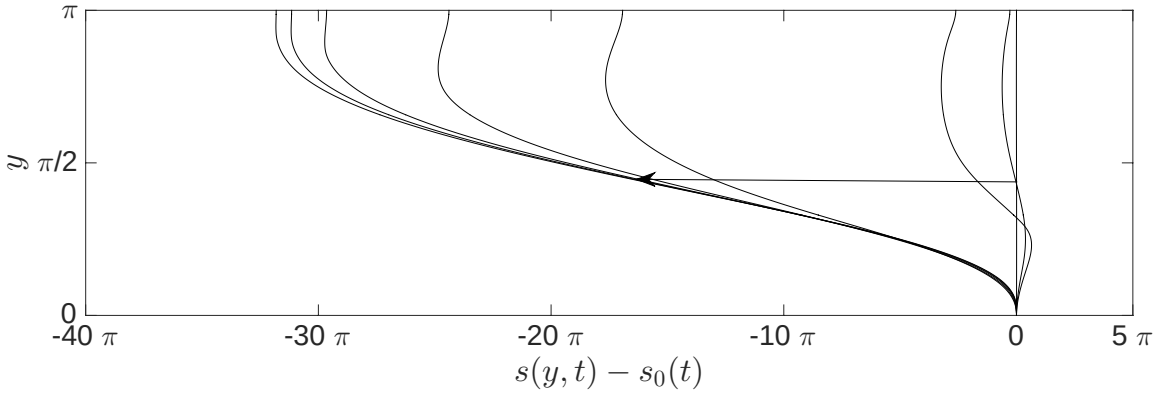

(c) $u_c = 0.9$

Figure 7.8: Numerical approximation of the profile of the moving boundary $s(y,t)$ as it evolves over time for Pe $= 50$ and Da $= 1/50$. Results are obtained for (a) $u_c = 0.1$, (b) $u_c = 0.5$ and (c) $u_c = 0.9$ for $t = 0$, $t = 1$, 10, 100, 200, 300, 400 and $t = 500$ with the arrow pointing in the direction of increasing t.

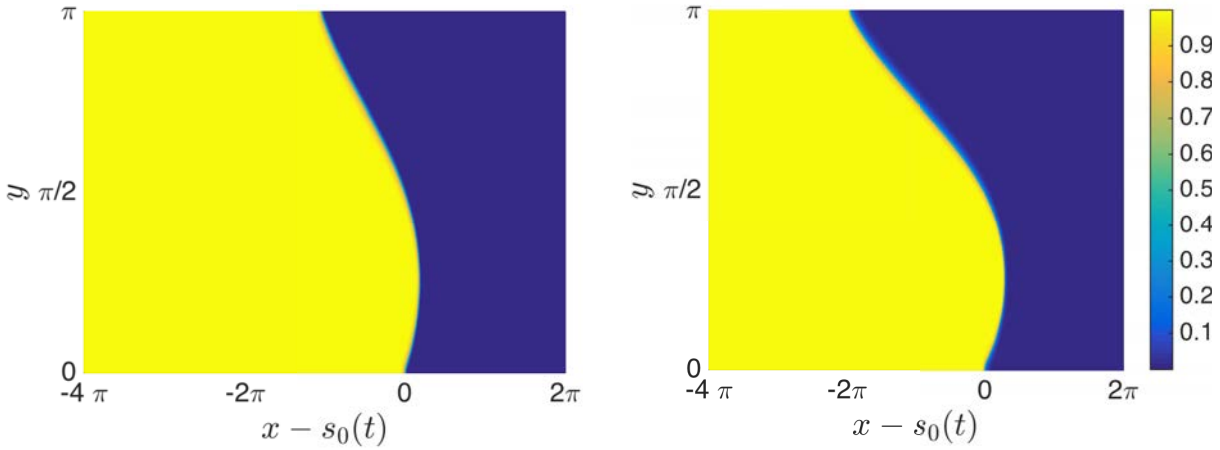

(a) $u_c = 0.1$ (b) $u_c = 0.5$

Figure 7.9: Numerical approximation of the large-time solution $u(x, y, t)$ to [IVPA] for $\mathrm{Pe} = 50$ and $\mathrm{Da} = 50$. Results are obtained for (a) $u_c = 0.1$ and (b) $u_c = 0.5$.

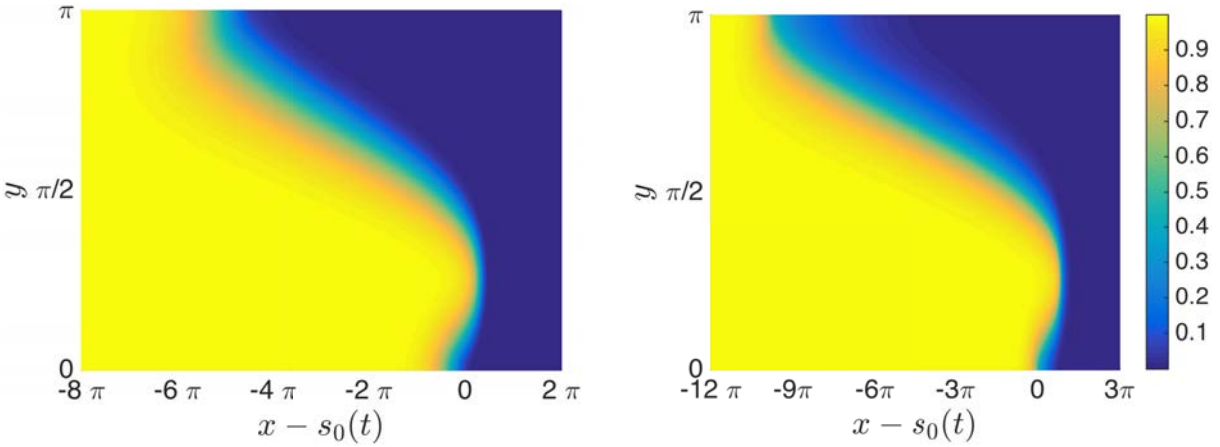

(a) $u_c = 0.1$ (b) $u_c = 0.5$

Figure 7.10: Numerical approximation of the large-time solution $u(x, y, t)$ to [IVPA] for $\mathrm{Pe} = 50$ and $\mathrm{Da} = 1$. Results are obtained for (a) $u_c = 0.1$ and (b) $u_c = 0.5$.

which the solution is evaluated to show convergence of $s(y, t) - s_0(t)$ onto a permanent form structure which we will refer to as $\lim_{t\to\infty}[s(y, t) - s_0(t)] = \phi_\infty(y)$. For Figure 7.7(c), we have to extend the period of time until $t \simeq 250$, whereas, for Figure 7.8(c), it is not possible to observe convergence onto the permanent form structure $\phi_\infty(y)$ for any reasonable value of t as the computational time required becomes far too expensive. Based on comparison of results for $u_c = 0.5$ and $u_c = 0.9$ in Figure 7.6 for $\mathrm{Da} = 50$ and in Figure 7.7 for $\mathrm{Da} = 1$, we expect that for fixed Pe and Da that the width of $\phi_\infty(y)$ for $u_c = 0.9$ to be approximately 5 times as large as the width of $\phi_\infty(y)$ for $u_c = 0.5$. This

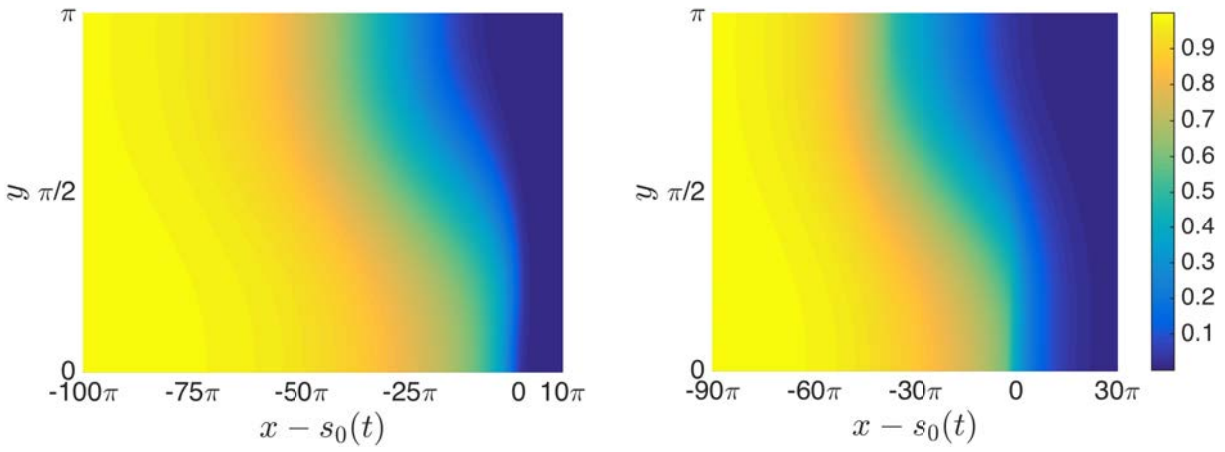

(a) $u_c = 0.1$ (b) $u_c = 0.5$

Figure 7.11: Numerical approximation of the large-time solution $u(x, y, t)$ to [IVPA] for $\mathrm{Pe} = 50$ and $\mathrm{Da} = 1/50$. Results are obtained for (a) $u_c = 0.1$ and (b) $u_c = 0.5$.

illustrates how far away convergence is from occurring for $\mathrm{Da} = 1/50$ and $u_c = 0.9$. For parameter values such that convergence onto a permanent form travelling wave-front has occurred, the profile of $\phi_\infty(y)$ appears similar in shape, however, it is *stretched* based on the values of Pe, Da and u_c.

Figures 7.9 - 7.11 illustrate the large-time form of $u(x - s_0(t), y, t)$. We find this is time-independent and, hence, introduce the notation $\lim_{t\to\infty} u(x - s_0(t), y, t) = u_\infty(\xi, y)$ with $\xi = x - s_0(t)$. We consider how the width of $u_\infty(\xi, y)$, which we define as maximum distance from $u_\infty(\xi, y) = 1 - \varepsilon$ to $u_\infty(\xi, y) = \varepsilon$ for $\varepsilon = 10^{-2}$, is affected as we vary Da and u_c for Pe fixed. For fixed u_c, we observe that the transition from $u_\infty \approx 1$ to $u_\infty \approx 0$ occurs quickly for larger values of Da with the width of $u_\infty(\xi, y)$ being closely related to the width of $\phi_\infty(y)$. The transition is much more gradual for small values of Da. Furthermore, we note that the width of the level curve $u_\infty(\xi, y) = a$ is narrower for $u_c \ll a < 1$ and $0 < a \ll u_c$ in comparison to when $a = u_c$. This is due to the cut-off having a reduced impact in these regions. These features are independent of the particular value of ε chosen provided $\varepsilon \ll 1$. All Figures 7.6 - 7.11 focus on the regime of large-Pe, which corresponds to strong advection relative to diffusion, to illustrate the impact introducing a background shear flow has on the formation of permanent form travelling front solutions considered in Chapters 2 - 5. Stronger advection usually means

$c_\infty(u_c)$	Da		
u_c	50	1	1/50
0.1	2.195	1.086	0.6670
0.5	1.482	0.9455	0.4375
0.9	0.9703	0.6142	–

Table 7.2: A table of numerically obtained values for $c_\infty(u_c)$ for Pe = 50.

the concentration $u(x, y, t)$ is transported faster in the direction of the flow and, hence, the cut-domain technique described in Section 7.1.4 is needed for such problems.

Values of the speed of propagation $c_\infty(u_c)$ of the travelling front solution are given in Table 7.2 for the parameter values considered above. However, we note that there are numerical issues with obtaining the value of $c_\infty(u_c)$. As $u_c \to 0^+$, we require at least $\Delta \leq u_c/5$ for the front solution to be sufficiently accurately approximated. We observe that increasing the value of $u_c \in (0, 1)$ has the effect of increasing the width of $s_\infty(y)$ and means the value of $\dot{s}_0(t)$ does not converge onto the speed $c_\infty(u_c)$ until very large values of t, these results are especially evident as $u_c \to 1^-$. Hence, in this limit, a much larger domain in the x-direction is necessary and we would have to significantly extend the period of time over which the solution is evaluated to show convergence of the solution to [IVPA] onto the travelling front structure $u_\infty(\xi, y)$. Similar behaviour to the large u_c limit is observed for smaller values of Da. As Da $\to 0^+$, a much larger domain is necessary and we have to extend the period of time over which the solution is evaluated in order to observe convergence of the solution. This corresponds to the computational time to obtain $c_\infty(u_c)$ in the combined limit of $u_c \to 1^-$ and Da $\to 0^+$ being extremely extensive and beyond the scope of this thesis. The limits of small Da and large u_c correspond to a weaker reaction and we expect it is the strength of this reaction that drives the evolution of $u(x, y, t)$ and $s(y, t) - s_0(t)$ onto their permanent form structures in large-time.

We conclude that the numerical solution of [IVPA], and hence, [QIVPA], involves the formation of a permanent form travelling wave-front as $t \to \infty$, which has propagation speed $\dot{s}_0(t) \to c_\infty(u_c)$ as $t \to \infty$. A graph of numerically calculated values of $c_\infty(u_c)$ for selected values of Pe, Da and $u_c \in (0.05, 0.8)$ is given in Figure 7.12 which indicates

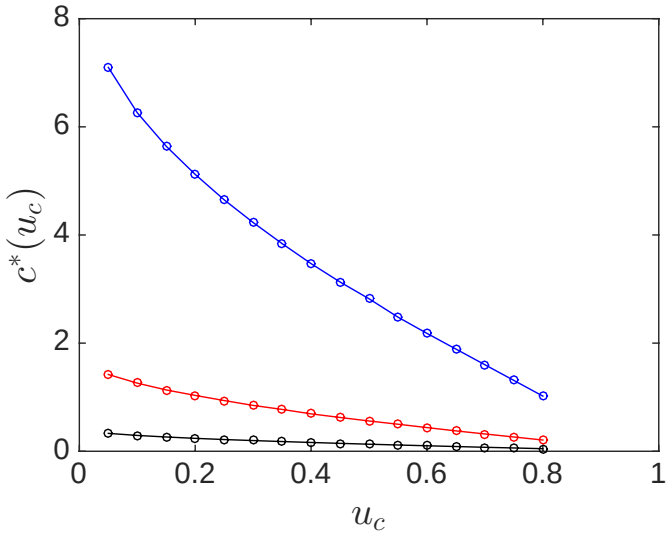

Figure 7.12: A plot of $c_\infty(u_c)$ obtained numerically for selected values of $u_c \in (0.05, 0.8)$. Results for $\mathrm{Pe} = 1$ and $\mathrm{Da} = 1/25$ are shown in black, $\mathrm{Pe} = \mathrm{Da} = 1/10$ are shown in red and $\mathrm{Pe} = 1/25$ and $\mathrm{Da} = 1$ are shown in blue.

that for fixed Pe and Da, $c_\infty(u_c)$ is monotone decreasing with $u_c \in (0.05, 0.8)$. We expect that this monotonicity property will hold for all $u_c \in (0, 1)$. With this is mind, the next chapter focuses on the asymptotic solution to [QIVPA] in a homogenisation limit where asymptotic results follow from the solution to [QIVP].

CHAPTER 8

TRAVELLING WAVE-FRONT SOLUTIONS TO [QIVPA]

In this chapter we study permanent form travelling wave-front solutions to [QIVPA].

8.1 Travelling Wave-Fronts

We anticipate that as $t \to \infty$, a permanent form travelling wave-front solution will develop in the solution to [QIVPA], advancing with a (non-negative) propagation speed, allowing for the transition between the fully reacted state, $u = 1$ as $\xi \to -\infty$, to the unreacted state, $u = 0$ as $\xi \to \infty$. Therefore, in this section we focus attention on the possibility of [QIVPA] supporting permanent form travelling wave-front solutions (henceforth referred to as PTWF solutions). To establish the existence and uniqueness of a permanent form travelling wave solution to [QIVP], we considered the equivalent dynamical system and proved the existence of a heteroclinic connection orbit in phase space. Such an approach is not possible in higher dimensions when we have space-dependent coefficients. Instead, guided by numerical simulations and results for closely related problems where the reaction function is of ignition type (see, for example, Berestycki and Hamel [6]), we will assume the existence and uniqueness of a PTWF solution to [QIVPA] for each fixed $u_c \in (0, 1)$, denoting the unique propagation speed by $c^*(u_c)$.

A PTWF solution to [QIVPA], with constant speed of propagation $c^*(u_c) > 0$, is a

steady state solution to [QIVPA] with $u : \overline{\Omega} \times \mathbb{R} \to \mathbb{R}$, $s_0 : \overline{\mathbb{R}}^+ \to \mathbb{R}$ and $\phi : [0, \pi] \to \mathbb{R}$ such that

$$u(\xi, y, t) = U(\xi, y) \quad \forall\, (\xi, y, t) \in \overline{\Omega} \times \mathbb{R}^+, \tag{8.1.1}$$

$$\dot{s}_0(t) = c^*(u_c) \quad \forall\, t \in \mathbb{R}^+, \tag{8.1.2}$$

$$s(y, t) - s_0(t) = \phi(y) \quad \forall\, (y, t) \in [0, \pi] \times \mathbb{R}^+, \tag{8.1.3}$$

for domain $\Omega = \mathbb{R} \times (0, \pi)$. Here $U \in C^1(\Omega) \cap C^2(\Omega \setminus \mathcal{S})$, $c^*(u_c) > 0$ and $\phi \in C^1([0, \pi])$ satisfy the nonlinear boundary value problem,

$$(b(y) - c^*(u_c))\, \frac{\partial U}{\partial \xi} = \mathrm{Pe}^{-1} \left(\frac{\partial^2 U}{\partial y^2} + \frac{\partial^2 U}{\partial \xi^2} \right) + \mathrm{Da} f_c(U), \quad (\xi, y) \in \Omega \setminus \mathcal{S}, \tag{8.1.4a}$$

$$U(\xi, y) \to \begin{cases} 1, & \text{as} \quad \xi \to -\infty, \\ 0, & \text{as} \quad \xi \to \infty, \end{cases} \quad \text{uniformly for } y \in [0, \pi], \tag{8.1.4b}$$

$$\frac{\partial U}{\partial y}(\xi, 0) = \frac{\partial U}{\partial y}(\xi, \pi) = 0, \quad \xi \in \mathbb{R}, \tag{8.1.4c}$$

$$U(\xi, y) \geq u_c \ \text{ for } \ \xi \leq \phi(y), \quad U(\xi, y) \leq u_c \ \text{ for } \ \xi \geq \phi(y), \quad y \in [0, \pi], \tag{8.1.4d}$$

$$U(\phi(y), y) = u_c, \quad y \in [0, \pi], \tag{8.1.4e}$$

$$\partial_{\boldsymbol{n}} U|_{(\phi(y)^+, y)} = \partial_{\boldsymbol{n}} U|_{(\phi(y)^-, y)}, \quad y \in (0, \pi), \tag{8.1.4f}$$

where $b(y)$ is a shear flow that satisfies

$$b \in C^1([0, \pi]) \quad \text{and} \quad \int_0^\pi b(y) dy = 0. \tag{8.1.5}$$

The set of points which form the level curve $U = u_c$ is given by

$$\mathcal{S} = \{(\xi, y) \in \mathbb{R} \times [0, \pi] : \ \xi = \phi(y)\}, \tag{8.1.6}$$

with $\phi(0) = 0$ fixed through our choice of coordinate $\xi = x - s_0(t)$ and with the following

unit normal vector to the zero-level curve $\xi - \phi(y)$=0,

$$\boldsymbol{n} = \frac{1}{\sqrt{1 + \left(\frac{d\phi}{dy}\right)^2}} \left(1, -\frac{d\phi}{dy}\right). \tag{8.1.7}$$

8.2 Homogenisation Limit

In this chapter we focus on flows that vary on a much faster scale than the width of the PTWF. In this case, one can upscale the faster scale to obtain an effective wave-front. This is achieved by the method of homogenisation (see, for example, Lions et al [1] and Pavliotis and Stuart [49]). Heinze, Papanicolaou and Stevens [53] were the first to employ this method in the context of wave-fronts and describe the effective wave-front for a large class of reactions for which a unique PTWF solution exists. However, all of their reaction functions considered are Lipschitz continuous on $[0, 1]$. We begin by re-scaling

$$\xi \longmapsto \frac{\xi}{\epsilon}, \tag{8.2.1}$$

for some small parameter ϵ which represents the ratio between characteristic length scale of the background flow and the largest length scale of the problem. To emphasize this re-scaling we let $U^\epsilon(\xi, y) = U(\xi/\epsilon, y)$ with this choice of re-scaling meaning the effective speed of propagation of the PTWF solution is re-scaled as follows,

$$c^*(u_c) \longmapsto c^\epsilon = \epsilon c^*(u_c). \tag{8.2.2}$$

The re-scaled field $U^\epsilon \in C^1(\Omega) \cap C^2(\Omega \setminus \mathcal{S}^\epsilon)$ and speed $c^*(u_c) > 0$ satisfy the boundary value problem

$$\frac{\partial^2 U^\epsilon}{\partial y^2} + \epsilon^2 \frac{\partial^2 U^\epsilon}{\partial \xi^2} + \mathrm{Pe}\epsilon \left(\epsilon c^*(u_c) - b(y)\right) \frac{\partial U^\epsilon}{\partial \xi} + \mathrm{PeDa} f_c(U^\epsilon) = 0, \ (\xi, y) \in \Omega \setminus \mathcal{S}^\epsilon, \quad (8.2.3a)$$

$$b \in C^1([0,\pi]) \quad \text{and} \quad \int_0^\pi b(y)dy = 0, \quad (8.2.3b)$$

$$U^\epsilon(\xi, y) \to \begin{cases} 1, & \text{as} \quad \xi \to -\infty, \\ 0, & \text{as} \quad \xi \to \infty, \end{cases} \quad \forall\ y \in [0,\pi], \quad (8.2.3c)$$

$$\frac{\partial U^\epsilon}{\partial y}(\xi, 0) = \frac{\partial U^\epsilon}{\partial y}(\xi, \pi) = 0, \quad \xi \in \mathbb{R}, \quad (8.2.3d)$$

$$U^\epsilon(\xi, y) \geq u_c \ \text{ for } \ \xi \leq \epsilon\phi(y), \quad U^\epsilon(\xi, y) \leq u_c \ \text{ for } \ \xi \geq \epsilon\phi(y), \quad y \in [0,\pi], \quad (8.2.3e)$$

$$U^\epsilon(\epsilon\phi(y), y) = u_c, \quad y \in [0,\pi], \quad (8.2.3f)$$

$$\partial_{\boldsymbol{n}^\epsilon} U^\epsilon|_{(\epsilon\phi(y)^+, y)} = \partial_{\boldsymbol{n}^\epsilon} U^\epsilon|_{(\epsilon\phi(y)^-, y)}, \quad y \in (0,\pi), \quad (8.2.3g)$$

$$\phi(0) = 0, \quad (8.2.3h)$$

where the set of points which form the level curve $U^\epsilon = u_c$ is given by

$$\mathcal{S}^\epsilon = \{(\xi, y) \in \mathbb{R} \times [0,\pi] : \ \xi = \epsilon\phi(y)\}, \quad (8.2.4)$$

and with unit normal vector to the zero-level curve $\xi - \epsilon\phi(y) = 0$,

$$\boldsymbol{n}^\epsilon = \frac{1}{\sqrt{1 + \left(\epsilon \frac{d\phi}{dy}\right)^2}} \left(1, -\epsilon \frac{d\phi}{dy}\right). \quad (8.2.5)$$

We now use a multiple scales approach to obtain an effective medium equation for the boundary value problem (8.2.3). This relies on two scales, one slow (macroscopic) scale and one fast (microscopic) scale. It is clear, for $\epsilon = o(1)$, that the variable y changes rapidly in comparison to the variable ξ and therefore, ξ represents the slow scale and y the fast scale. We treat the variables as independent. This is one of the fundamental assumptions of homogenisation theory (see, for example, Pavliotis and Stuart [49]).

In multiple scales form, $U^\epsilon \in C^1(\Omega) \cap C^2(\Omega \setminus \tilde{\mathcal{S}})$ where the set of points which form the level curve $U^\epsilon = u_c$ is simply

$$\tilde{\mathcal{S}} = \{(0, y) : y \in \times[0, \pi]\}. \tag{8.2.6}$$

Thus

$$U^\epsilon(\epsilon\phi(y)^+, y) = U^\epsilon(0^+, y) + \epsilon\phi(y)\frac{\partial U^\epsilon}{\partial \xi}(0^+, y) + \frac{1}{2}\epsilon^2\phi^2(y)\frac{\partial^2 U^\epsilon}{\partial \xi^2}(0^+, y) + O(\epsilon^3), \tag{8.2.7}$$

and therefore,

$$\begin{aligned}\partial_{\boldsymbol{n}^\epsilon} U^\epsilon|_{(\epsilon\phi(y)^+, y)} &= \left[1 - \frac{1}{2}\epsilon^2\left(\frac{d\phi}{dy}\right)^2 + o(\epsilon^2)\right]\left(\frac{\partial U^\epsilon}{\partial \xi}(\epsilon\phi(y)^+, y) - \epsilon\frac{d\phi}{dy}\frac{\partial U^\epsilon}{\partial y}(\epsilon\phi(y)^+, y)\right) \\ &= \mathcal{L}U^\epsilon(0^+, y),\end{aligned} \tag{8.2.8a}$$

where the operator $\mathcal{L}$ is given by

$$\mathcal{L} = \mathcal{L}_0 + \epsilon\mathcal{L}_1 + \epsilon^2\mathcal{L}_2 + O(\epsilon^3), \tag{8.2.8b}$$

with

$$\mathcal{L}_0 = \frac{\partial}{\partial \xi}, \tag{8.2.8c}$$

$$\mathcal{L}_1 = \phi(y)\frac{\partial^2}{\partial \xi^2} - \frac{d\phi}{dy}\frac{\partial}{\partial y}, \tag{8.2.8d}$$

$$\mathcal{L}_2 = \frac{1}{2}\phi^2(y)\frac{\partial^3}{\partial \xi^3} - \frac{d\phi}{dy}\phi(y)\frac{\partial^2}{\partial y \partial \xi} - \frac{1}{2}\left(\frac{d\phi}{dy}\right)^2\frac{\partial}{\partial \xi}. \tag{8.2.8e}$$

Therefore, in multiple scales form, equations (8.2.3f) and (8.2.3g) become

$$U^\epsilon(0, y) + \epsilon\phi(y)\frac{\partial U^\epsilon}{\partial \xi}(0, y) + o(\epsilon) = u_c, \quad y \in [0, \pi], \tag{8.2.9}$$

and

$$\mathcal{L}U^{\epsilon}(0^{+},y)=\mathcal{L}U^{\epsilon}(0^{-},y),\quad y\in[0,\pi]. \tag{8.2.10}$$

Hence, the boundary value problem (8.2.3) becomes

$$\frac{\partial^2 U^{\epsilon}}{\partial y^2}+\epsilon^2\frac{\partial^2 U^{\epsilon}}{\partial \xi^2}+\mathrm{Pe}\epsilon\left(\epsilon c^{*}(u_c)-b(y)\right)\frac{\partial U^{\epsilon}}{\partial \xi}+\mathrm{PeDa}f_c(U^{\epsilon})=0,\ (\xi,y)\in\Omega\setminus\tilde{\mathcal{S}}, \tag{8.2.11a}$$

$$b\in C^{1}([0,\pi])\quad\text{and}\quad\int_0^{\pi}b(y)dy=0, \tag{8.2.11b}$$

$$U^{\epsilon}(\xi,y)\to\begin{cases}1, & \text{as}\quad \xi\to-\infty,\\ 0, & \text{as}\quad \xi\to\infty,\end{cases}\qquad\forall\ y\in[0,\pi], \tag{8.2.11c}$$

$$\frac{\partial U^{\epsilon}}{\partial y}(\xi,0)=\frac{\partial U^{\epsilon}}{\partial y}(\xi,\pi)=0,\quad \xi\in\mathbb{R}, \tag{8.2.11d}$$

$$U^{\epsilon}(\xi,y)\geq u_c\ \text{ for }\ \xi\leq 0,\quad U^{\epsilon}(\xi,y)\leq u_c\ \text{ for }\ \xi\geq 0,\quad y\in[0,\pi], \tag{8.2.11e}$$

$$U^{\epsilon}(0,y)+\epsilon\phi(y)\frac{\partial U^{\epsilon}}{\partial \xi}(0,y)+o(\epsilon)=u_c,\quad y\in[0,\pi], \tag{8.2.11f}$$

$$\mathcal{L}U^{\epsilon}(0^{+},y)=\mathcal{L}U^{\epsilon}(0^{-},y),\quad y\in[0,\pi], \tag{8.2.11g}$$

$$\phi(0)=0, \tag{8.2.11h}$$

where the set of points which form the level curve $U^{\epsilon}=u_c$ is simply

$$\tilde{\mathcal{S}}=\{(0,y):y\in\times[0,\pi]\}. \tag{8.2.12}$$

8.2.1 Asymptotic solution for $\mathrm{Pe}=O(1)$ and $\mathrm{Da}=O(\epsilon^2)$

We examine the boundary value problem (8.2.11) for the specific regime of Pe and Da where $\mathrm{Pe}=O(1)$ and $\mathrm{Da}=O(\epsilon^2)$, where, without loss of generality, we set

$$\mathrm{Da}=\gamma\epsilon^2, \tag{8.2.13}$$

with parameter $\gamma = O(1)$. The boundary value problem for $(c^*(u_c),\, U^\epsilon)$ in this regime is given by

$$\frac{\partial^2 U^\epsilon}{\partial y^2} - \epsilon \mathrm{Pe}\, b(y) \frac{\partial U^\epsilon}{\partial \xi} + \epsilon^2 \left(\frac{\partial^2 U^\epsilon}{\partial \xi^2} + \mathrm{Pe}\, c^*(u_c) \frac{\partial U^\epsilon}{\partial \xi} + \mathrm{Pe}\, \gamma f_c(U^\epsilon) \right) = 0, \quad (\xi, y) \in \Omega \setminus \tilde{\mathcal{S}}, \tag{8.2.14a}$$

$$b \in C^1([0,\pi]) \quad \text{and} \quad \int_0^\pi b(y)dy = 0, \tag{8.2.14b}$$

$$U^\epsilon(\xi, y) \to \begin{cases} 1, & \text{as} \quad \xi \to -\infty, \\ 0, & \text{as} \quad \xi \to \infty, \end{cases} \qquad \forall\ y \in [0,\pi], \tag{8.2.14c}$$

$$\frac{\partial U^\epsilon}{\partial y}(\xi, 0) = \frac{\partial U^\epsilon}{\partial y}(\xi, \pi) = 0, \quad \xi \in \mathbb{R}. \tag{8.2.14d}$$

$$U^\epsilon(\xi, y) \geq u_c \ \text{ for } \ \xi \leq 0, \quad U^\epsilon(\xi, y) \leq u_c \ \text{ for } \ \xi \geq 0, \quad y \in [0,\pi], \tag{8.2.14e}$$

$$U^\epsilon(0, y) + \epsilon \phi(y) \frac{\partial U^\epsilon}{\partial \xi}(0, y) + o(\epsilon) = u_c, \quad y \in [0,\pi], \tag{8.2.14f}$$

$$\mathcal{L} U^\epsilon(0^+, y) = \mathcal{L} U^\epsilon(0^-, y), \quad y \in (0,\pi), \tag{8.2.14g}$$

$$\phi(0) = 0. \tag{8.2.14h}$$

We take power series asymptotic expansions of the form

$$U^\epsilon(\xi, y) = U_0(\xi, y) + \epsilon U_1(\xi, y) + \epsilon^2 U_2(\xi, y) + O(\epsilon^3), \quad (\xi, y) \in \overline{\Omega}, \tag{8.2.15a}$$

$$c^*(u_c) = c_0(u_c) + O(\epsilon), \tag{8.2.15b}$$

$$\phi(y) = \phi_0(y) + \epsilon \phi_1(y) + O(\epsilon^2), \quad y \in [0,\pi], \tag{8.2.15c}$$

which we substitute into the boundary value problem (8.2.14) to obtain a sequence of problems at three successive orders of ϵ which we solve in turn. We take the shear flow $b(y)$ to satsify the conditions (8.2.14b) at each order. The leading order problem is given

by

$$\frac{\partial^2 U_0}{\partial y^2} = 0, \quad (\xi, y) \in \Omega \setminus \tilde{\mathcal{S}}, \tag{8.2.16a}$$

$$U_0(\xi, y) \to \begin{cases} 1, & \text{as} \quad \xi \to -\infty, \\ 0, & \text{as} \quad \xi \to \infty, \end{cases} \quad \forall\ y \in [0, \pi], \tag{8.2.16b}$$

$$\frac{\partial U_0}{\partial y}(\xi, 0) = \frac{\partial U_0}{\partial y}(\xi, \pi) = 0, \quad \xi \in \mathbb{R}, \tag{8.2.16c}$$

$$U_0(\xi, y) \geq u_c \ \text{ for } \ \xi \leq 0, \quad U_0(\xi, y) \leq u_c \ \text{ for } \ \xi \geq 0, \quad y \in [0, \pi], \tag{8.2.16d}$$

$$U_0(0, y) = u_c, \quad y \in [0, \pi], \tag{8.2.16e}$$

$$\mathcal{L}_0 U_0(0^+, y) = \mathcal{L}_0 U_0(0^-, y), \quad y \in (0, \pi). \tag{8.2.16f}$$

In equation (8.2.16a), y is a variable and ξ is just a parameter. Hence, we conclude that there exists a solution $U_0 = U_0(\xi)$ to (8.2.16) such that

$$U_0(\xi) \to \begin{cases} 1, & \text{as} \quad \xi \to -\infty, \\ 0, & \text{as} \quad \xi \to \infty, \end{cases} \tag{8.2.17a}$$

$$U_0(\xi) \geq u_c \ \text{ for } \ \xi \leq 0, \quad U_0(\xi) \leq u_c \ \text{ for } \ \xi \geq 0, \tag{8.2.17b}$$

$$U_0(0) = u_c, \tag{8.2.17c}$$

$$\left.\frac{dU_0}{d\xi}\right|_{0^-}^{0^+} = 0, \tag{8.2.17d}$$

which will be uniquely determined by the problem at $O(\epsilon^2)$. At $O(\epsilon)$, we obtain the boundary value problem

$$\frac{\partial^2 U_1}{\partial y^2} = \mathrm{Pe} b(y) \frac{dU_0}{d\xi}, \quad (\xi, y) \in \Omega \setminus \tilde{\mathcal{S}}, \tag{8.2.18a}$$

$$U_1(\xi, y) \to 0 \quad \text{as} \quad \xi \to \pm\infty, \quad y \in [0, \pi], \tag{8.2.18b}$$

$$\frac{\partial U_1}{\partial y}(\xi, 0) = \frac{\partial U_1}{\partial y}(\xi, \pi) = 0, \quad \xi \in \mathbb{R}, \tag{8.2.18c}$$

$$U_1(\xi, y) \geq -\phi_0(y) \frac{dU_0}{d\xi}(\xi) \text{ for } \xi \leq 0, \quad y \in [0, \pi], \tag{8.2.18d}$$

$$U_1(\xi, y) \leq -\phi_0(y) \frac{dU_0}{d\xi}(\xi) \text{ for } \xi \geq 0, \quad y \in [0, \pi], \tag{8.2.18e}$$

$$U_1(0, y) = -\phi_0(y) \frac{dU_0}{d\xi}(0), \quad y \in [0, \pi], \tag{8.2.18f}$$

$$\left.\frac{\partial U_1}{\partial \xi}\right|_{(0^-, y)}^{(0^+, y)} = -\phi_0(y) \left.\frac{d^2 U_0}{d\xi^2}\right|_{0^-}^{0^+}, \quad y \in [0, \pi], \tag{8.2.18g}$$

$$\phi_0(0) = 0. \tag{8.2.18h}$$

On applying the Fredholm Alternative, we find this is a well-posed problem, admitting a unique solution which can be determined once the right-hand side of equation (8.2.18a) is known. Equation (8.2.18a) allows us to compute the function $U_1(\xi, y)$ in terms of the function $U_0(\xi)$. As there are only derivatives of $U_1(\xi, y)$ with respect to y present, we conclude $U_1(\xi, y)$ must be separable and we seek a solution to (8.2.18) of the form

$$U_1(\xi, y) = \chi_1(y) \frac{dU_0}{d\xi} + g(\xi), \quad (\xi, y) \in \overline{\Omega}. \tag{8.2.19}$$

On substitution of (8.2.19) into (8.2.18), we obtain the following boundary value problem for the function $\chi_1(y)$,

$$\frac{d^2 \chi_1}{dy^2} = \mathrm{Pe} b(y), \quad y \in [0, \pi], \tag{8.2.20a}$$

$$\frac{d\chi_1}{dy}(0) = \frac{d\chi_1}{dy}(\pi) = 0, \tag{8.2.20b}$$

where we take the function to have zero mean value without loss of generality,

$$\int_0^\pi \chi_1(y)dy = 0, \tag{8.2.20c}$$

to ensure uniqueness of the solution $\chi_1(y)$. In homogenisation theory this is referred to as the first cell problem. Moreover, we obtain the boundary $\phi_0(y)$ as

$$\phi_0(y) = \chi_1(0) - \chi_1(y), \quad y \in [0, \pi], \tag{8.2.21}$$

and, in addition, the function $g(\xi)$ must satisfy the conditions

$$g(\xi) \to 0 \text{ as } \xi \to \pm\infty, \tag{8.2.22a}$$

$$g(\xi) \geq -\chi_1(0)\frac{dU_0}{d\xi}(\xi) \text{ for } \xi \leq 0, \quad g(\xi) \leq -\chi_1(0)\frac{dU_0}{d\xi}(\xi) \text{ for } \xi \geq 0, \tag{8.2.22b}$$

$$g(0) = -\chi_1(0)\frac{dU_0}{d\xi}(0), \tag{8.2.22c}$$

$$\left.\frac{dg}{d\xi}\right|_{0^-}^{0^+} = -\chi_1(0)\left.\frac{d^2U_0}{d\xi^2}\right|_{0^-}^{0^+}. \tag{8.2.22d}$$

At $O(\epsilon^2)$, we obtain

$$\frac{\partial^2 U_2}{\partial y^2} = \mathrm{Pe} b(y)\frac{\partial U_1}{\partial \xi} + \frac{d^2 U_0}{d\xi^2} + \mathrm{Pe} c_0(u_c)\frac{dU_0}{d\xi} + \mathrm{Pe}\gamma f_c(U_0), \quad (\xi, y) \in \Omega \setminus \tilde{\mathcal{S}}, \tag{8.2.23a}$$

$$U_2(\xi, y) \to 0 \quad \text{as} \quad \xi \to \pm\infty, \quad \forall\ y \in [0, \pi], \tag{8.2.23b}$$

$$\frac{\partial U_2}{\partial y}(\xi, 0) = \frac{\partial U_2}{\partial y}(\xi, \pi) = 0, \quad \xi \in \mathbb{R}, \tag{8.2.23c}$$

$$\begin{aligned} U_2(\xi, y) \geq -\phi_0(y)\frac{\partial U_1}{\partial \xi}(\xi, y) - \frac{1}{2}\phi_0^2(y)\frac{d^2 U_0}{d\xi^2}(\xi) \\ - \phi_1(y)\frac{dU_0}{d\xi}(\xi), \ \text{ for } \ \xi < 0, \quad y \in [0, \pi], \end{aligned} \tag{8.2.23d}$$

$$\begin{aligned} U_2(\xi, y) \leq -\phi_0(y)\frac{\partial U_1}{\partial \xi}(\xi, y) - \frac{1}{2}\phi_0^2(y)\frac{d^2 U_0}{d\xi^2}(\xi) \\ - \phi_1(y)\frac{dU_0}{d\xi}(\xi), \ \text{ for } \ \xi > 0, \quad y \in [0, \pi], \end{aligned} \tag{8.2.23e}$$

$$\left.\frac{\partial U_2}{\partial \xi}\right|_{(0^-, y)}^{(0^+, y)} = -\phi_1(y)\left.\frac{d^2 U_0}{d\xi^2}\right|_{0^-}^{0^+} - \frac{1}{2}\phi_1^2(y)\left.\frac{d^3 U_0}{d\xi^3}\right|_{0^-}^{0^+} - \phi_0(y)\left.\frac{\partial^2 U_1}{\partial \xi^2}\right|_{(0^-, y)}^{(0^+, y)}, \quad y \in [0, \pi], \tag{8.2.23f}$$

$$\phi_1(0) = 0. \tag{8.2.23g}$$

On substitution of the expansion (8.2.19) and equation (8.2.21) into the boundary value problem (8.2.23), we obtain

$$\frac{\partial^2 U_2}{\partial y^2} = \mathrm{Pe} b(y) \left(\frac{d^2 U_0}{d\xi^2} \chi_1(y) + \frac{dg}{d\xi} \right) + \frac{d^2 U_0}{d\xi^2} + \mathrm{Pe} c_0(u_c) \frac{dU_0}{d\xi} + \mathrm{Pe} \gamma f_c(U_0), \quad (\xi, y) \in \Omega \setminus \tilde{\mathcal{S}}, \tag{8.2.24a}$$

$$U_2(\xi, y) \to 0 \quad \text{as} \quad \xi \to \pm\infty, \quad \forall\ y \in [0, \pi], \tag{8.2.24b}$$

$$\frac{\partial U_2}{\partial y}(\xi, 0) = \frac{\partial U_2}{\partial y}(\xi, \pi) = 0, \quad \xi \in \mathbb{R}, \tag{8.2.24c}$$

$$U_2(\xi, y) \geq \frac{1}{2} \left(\chi_1^2(y) - \chi_1^2(0) \right) \frac{d^2 U_0}{d\xi}(\xi) + \left(\chi_1(y) - \chi_1(0) \right) \frac{dg}{d\xi}(\xi) - \phi_1(y) \frac{dU_0}{d\xi}(\xi), \ \text{ for } \ \xi < 0, \quad y \in [0, \pi], \tag{8.2.24d}$$

$$U_2(\xi, y) \leq \frac{1}{2} \left(\chi_1^2(y) - \chi_1^2(0) \right) \frac{d^2 U_0}{d\xi}(\xi) + \left(\chi_1(y) - \chi_1(0) \right) \frac{dg}{d\xi}(\xi) - \phi_1(y) \frac{dU_0}{d\xi}(\xi), \ \text{ for } \ \xi > 0, \quad y \in [0, \pi], \tag{8.2.24e}$$

$$\left. \frac{\partial U_2}{\partial \xi} \right|_{(0^-, y)}^{(0^+, y)} = -\phi_1(y) \left. \frac{d^2 U_0}{d\xi^2} \right|_{0^-}^{0^+} + \frac{1}{2} (\chi_1^2(y) - \chi_1^2(0)) \left. \frac{d^3 U_0}{d\xi^3} \right|_{0^-}^{0^+} + (\chi_1(y) - \chi_1(0)) \left. \frac{d^2 g}{d\xi^2} \right|_{0^-}^{0^+}, \quad y \in [0, \pi], \tag{8.2.24f}$$

$$\phi_1(0) = 0. \tag{8.2.24g}$$

Let us assume that the equation (8.2.24a) is well posed, and therefore possess a unique solution. As there are only derivatives of $U_2(\xi, y)$ with respect to y present in equation (8.2.24a), we require $U_2(\xi, y)$ to be separable and specifically of the form,

$$U_2(\xi, y) = \frac{d^2 U_0}{d\xi^2} \chi_2(y) + \frac{dg}{d\xi} \chi_1(y), \quad (\xi, y) \in \overline{\Omega} \setminus \tilde{\mathcal{S}}. \tag{8.2.25}$$

On substitution of the expansion (8.2.25) into (8.2.24), we find that the function $\chi_2(y)$ satisfies the second cell problem

$$\frac{d^2\chi_2}{dy^2} = A_0 - 1 + \mathrm{Pe}\, b(y)\chi_1(y), \quad y \in [0,\pi], \tag{8.2.26a}$$

$$\frac{d\chi_2}{dy}(0) = \frac{d\chi_2}{dy}(\pi) = 0, \tag{8.2.26b}$$

$$\int_0^\pi \chi_2(y)dy = 0, \tag{8.2.26c}$$

where the constant A_0 represents the homogenised diffusion coefficient and we take the zero mean value condition (8.2.26c) to hold, without loss of generality, to ensure uniqueness of the solution $\chi_2(y)$. The right-hand side of equation (8.2.24a) has zero average over $y \in [0,\pi]$, and thus, there exists a unique solution to (8.2.24), provided $U_0(\xi)$ satisfies homogenised travelling wave problem

$$A_0\frac{d^2U_0}{d\xi^2} + \mathrm{Pe}\, c_0\frac{dU_0}{d\xi} + \mathrm{Pe}\,\gamma f_c(U_0) = 0, \quad \xi \in \mathbb{R}\setminus\{0\}. \tag{8.2.27}$$

It then follows from the already established properties of $U_0(\xi)$, given by (8.2.17), that on taking the scalings

$$c_0 = \sqrt{\frac{A_0\gamma}{\mathrm{Pe}}}v^*(u_c), \qquad \xi = \sqrt{\frac{A_0}{\mathrm{Pe}\gamma}}(x - v^*(u_c)t), \tag{8.2.28}$$

and letting $U_0(\xi) = U_T(x - v^*(u_c)t)$, we can relate the leading order solution to (8.2.14) to the PTW solution to [QIVP]. On integrating equation (8.2.26a) once, we obtain the homogenised diffusion coefficient as

$$A_0 = 1 - \frac{\mathrm{Pe}}{\pi}\int_0^\pi b(y)\chi_1(y)dy, \tag{8.2.29}$$

which, via the first cell problem (8.2.20), simplifies to

$$A_0 = 1 + \frac{1}{\pi}\int_0^\pi \left(\frac{d\chi_1}{dy}\right)^2 dy. \tag{8.2.30}$$

It follows from equation (8.2.24f) and (8.2.24g) that

$$\phi_1(y) = -\left(\chi_2(y) - \chi_2(0) + \frac{1}{2}\left[\chi_1^2(0) - \chi_1^2(y)\right]\right) \frac{\left.\frac{d^3U_0}{d\xi^3}\right|_{0-}^{0+}}{\left.\frac{d^2U_0}{d\xi^2}\right|_{0-}^{0+}}, \quad y \in [0, \pi], \tag{8.2.31}$$

and, in addition, we obtain an expression for the jump discontinuity at second order in $g(\xi)$ as

$$\left.\frac{d^2g}{d\xi^2}\right|_{0-}^{0+} = -\frac{\chi_2(0)}{\chi_1(0)}\left.\frac{d^3U_0}{d\xi^3}\right|_{0-}^{0+}, \tag{8.2.32}$$

provided $\chi_1(0) \neq 0$.

In summary, on collecting expressions (8.2.15a), (8.2.19), and (8.2.25), we have established that

$$U(\xi, y) = U_0(\xi) + \epsilon\left(\frac{dU_0}{d\xi}\chi_1(y) + g(\xi)\right) + \epsilon^2\left(\frac{d^2U_0}{d\xi^2}\chi_2(y) + \frac{dg}{d\xi}\chi_1(y)\right) + O(\epsilon^3), \tag{8.2.33}$$

with $U_0(\xi) = U_T(x - v^*(u_c)t)$ and $\epsilon = o(1)$. Similarly, on collecting expressions (8.2.15c), (8.2.21) and (8.2.31), we have deduced

$$\phi(y) = \chi_1(0) - \chi_1(y) - \epsilon\left(\chi_2(y) - \chi_2(0) + \frac{1}{2}\left[\chi_1^2(0) - \chi_1^2(y)\right]\right) \frac{\left.\frac{d^3U_0}{d\xi^3}\right|_{0-}^{0+}}{\left.\frac{d^2U_0}{d\xi^2}\right|_{0-}^{0+}} + O(\epsilon^2), \tag{8.2.34}$$

for $y \in [0, \pi]$. Finally, on collecting expressions (8.2.15b) and (8.2.28), we obtain the speed of propagation of the PTWF solution to (8.2.3) as

$$c^*(u_c) = \sqrt{\frac{A_0\gamma}{\mathrm{Pe}}}v^*(u_c) + O(\epsilon). \tag{8.2.35}$$

The asymptotic expression (8.2.35) can be explicitly stated in the limits of small and large cut-off u_c, via the asymptotic predictions (4.3.27) and (4.4.17) of $v^*(u_c)$, with numerical predictions for obtained in Section 4.5 for all $u_c \in (0, 1)$, for the specific case of cut-off Fisher reaction function (3.0.1).

8.2.2 Numerical Example

In this section we compare asymptotic predictions of $\phi_0(y)$ and $c^*(u_c)$ against the corresponding values $\phi_\infty(y)$ and $c_\infty(u_c)$ obtained from the numerical evaluation of [IVPA] in the homogenisation limit of small Da and $\mathrm{Pe} = O(1)$. We focus on the particular case of the cut-off Fisher reaction function (3.0.1) for fixed cut-off threshold $u_c \in (0,1)$ and shear flow

$$b(y) = \sin(2y). \tag{8.2.36}$$

It follows from the boundary value problem (8.2.20), that

$$\chi_1(y) = \frac{\mathrm{Pe}}{2}\left(y - \frac{1}{2}\left[\pi + \sin(2y)\right]\right), \quad y \in [0,\pi], \tag{8.2.37}$$

therefore,

$$\phi_0(y) = -\frac{1}{2}\mathrm{Pe}\left[y - \frac{1}{2}\sin(2y)\right], \quad y \in [0,\pi]. \tag{8.2.38}$$

The asymptotic structure of $c^*(u_c)$ relies on the constant A_0 which we determine for the particular shear flow (8.2.36) as

$$A_0 = 1 + \frac{3}{8}\mathrm{Pe}^2, \tag{8.2.39}$$

and thus, via the scaling (8.2.2), our asymptotic prediction for the propagation speed $c^*(u_c)$ of the PTWF solution to (8.1.4) is given by

$$c^*(u_c) \sim \sqrt{\frac{\left(1 + \frac{3}{8}\mathrm{Pe}^2\right)}{\mathrm{Pe}}}\, v^*(u_c)\sqrt{\mathrm{Da}}, \tag{8.2.40}$$

as $\mathrm{Da} \to 0^+$. Numerical results are obtained via numerical solution of the fractional-step method described in detail in Section 7.1.

In Figure 8.1 we compare asymptotic and numerical predictions for the profile of the level curve $U = u_c$. We observe that (8.2.40) strongly agrees with the numerically determined value of $\phi_\infty(y)$ in the large-time solution of [IVPA] obtained for $u_c = 0.1$, $\mathrm{Pe} = 1$ and two values of Da. In Figure 8.2 we contrast the behaviour of the asymptotic

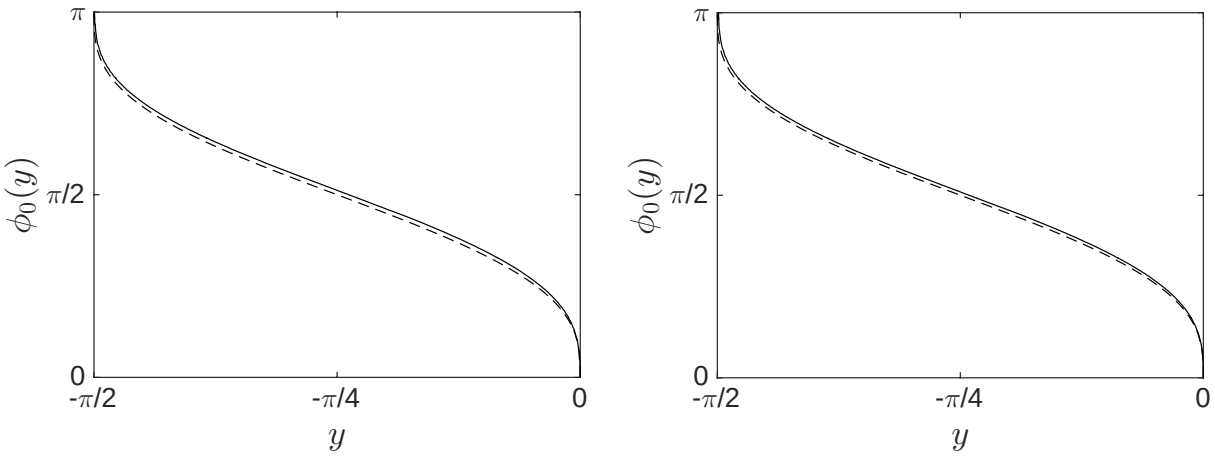

Figure 8.1: Comparison between asymptotic and numerical results of the boundary $\phi_0(y)$ for $u_c = 0.1$ and Pe $= 1$. Numerical solutions derived from the large-time solution to [IVPA] are shown as solid lines with dashed lines representing the asymptotic prediction (8.2.38). Results are obtained for (a) Da $= 1/25$ and (b) Da $= 1/50$.

expression (8.2.40), based on the numerical evaluation of $v^*(u_c)$ for $u_c \in (0, 1)$, obtained in Section 4.5, against the numerically determined solution $c_\infty(u_c)$ to [IVPA] in large-time for a selection of cut-off values. It is clear that the expansion (8.2.40) provides an excellent approximation to the asymptotic speed of propagation for arbitrary u_c.

8.3 Discussion and Conclusions

In chapters 6 - 8 of this thesis we have considered an evolution problem for a reaction–diffusion process in the presence of a shear flow and where the reaction function is of cut-off KPP-type for arbitrary fixed cut-off $u_c \in (0, 1)$. In Chapter 6 we formulated this evolution problem in terms of an initial moving boundary problem [IVPA] and, equivalently, [QIVPA]. In Chapter 7 we obtain a numerical solution to [IVPA] for the particular case of the cut-off Fisher reaction function (3.0.1) for arbitrary $u_c \in (0, 1)$, Pe and Da. Focussing on the specific case of a shear flow (8.2.36), we illustrate the formation of a PTWF in the large-time solution. We observe that the rate of convergence of the solution onto the permanent form travelling wave solution was strongly influenced by the values of Pe, Da and u_c. In particular, we find that the rate of convergence decreases considerably

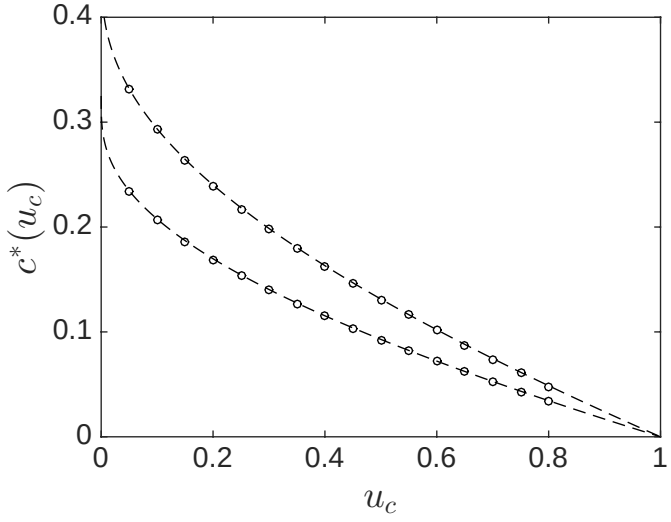

Figure 8.2: Comparison between asymptotic and numerical results of the speed for selected cut-off values $u_c \in (0,1)$ and $\mathrm{Pe} = 1$. Numerical solutions of $c_\infty(u_c)$ derived from the large-time solution to [IVPA] are shown as circles with dashed lines representing the asymptotic prediction (8.2.40) of $c^*(u_c)$. The top plot is obtained for parameters $\mathrm{Da} = 1/25$ and the bottom plot for $\mathrm{Da} = 1/50$.

as u_c increases and Da decreases. In Chapter 8 we have developed the asymptotic structure of the PTWF for the specific case of $\mathrm{Pe} = O(1)$, small Da and arbitrary $u_c \in (0,1)$. It would be interesting to extend the analysis in Section 8.2 to obtain explicit results for the PTWF solution for a wider range of parameters Pe and Da. Chapter 7 showed that the behaviour of the PTWF can drastically vary depending on whether PeDa is small or large.

Exploration of a wider range of parameter values would be facilitated by a more straight forward way to obtain the large-time solution to [IVPA]. Alternatively, since we are interested in PTWF solutions we may focus on determining the solution to the nonlinear boundary value problem (8.1.4) numerically.

We could extend the analysis in Chapter 8 further by considering the effect of different types of shear flow on PTWF solutions. For example plane Couette flow $b(y) = y$ and plane Poiseuille flow $b(y) = \pi^2/3 - y^2$.

Finally, in comparing the theory for the two-dimensional reaction–diffusion–advection problem with shear flow, and the associated one-dimensional reaction–diffusion problem, we make the observation that, in the absence of flow, the rate of convergence onto the

PTW solution is linearly exponentially slow in t with the leading order exponent given by $-v^*(u_c)^2 t/4$. Guided by numerical solutions and asymptotic predictions for the speed, we expect that the rate of convergence of the solution to [IVPA] onto the PTWF solution will be exponentially slow with the leading order exponent $-Ac^*(u_c)^2 t$, where A is dependent on a combination of Pe and Da.

CHAPTER 9

FUTURE WORK

In this thesis we have studied two intimately related problems. The first problem concerns the evolution of PTW solutions arising in a class of scalar homogeneous reaction–diffusion equations that are characterised by an arbitrary cut-off $u_c \in (0,1)$ in a KPP-type reaction function. The second problem considers the impact of a heterogeneous environment enforced by a background shear flow on these PTW structures. With regards to the first problem, there are a number of closely related problems which would provide compelling extensions. Firstly, it would be interesting to contrast the results presented here against those obtained when an arbitrary cut-off $u_c \in (0,1)$ is introduced into other types of reaction–diffusion models, such as the Nagumo model [44] with a bistable reaction function given by

$$f(u) = u(1-u)(u-\theta), \tag{9.0.1}$$

with parameter $\theta \in (0,1)$. The initial-boundary value problem (1.1.4) for the Nagumo equation has a unique permanent form travelling wave solution which propagates with speed $v = \frac{1}{\sqrt{2}} - \sqrt{2}\theta$. The existence and uniqueness of a front solution when a Heaviside cut-off is introduced into the reaction function was established by Dumortier, Popović and Kaper [20] via a rigorous phase plane type analysis. Furthermore, for $\theta \in (0, 1/2)$ (corresponding to positive speed values when $u_c = 0$), Dumortier, Popović and Kaper [20] find that the speed of propagation tends to the speed of propagation in the absence of a cut-off algebraically as $u_c \to 0^+$ (the exact form depending on the value of θ). This is

significantly faster than for the cut-off KPP-type reaction function. It remains an open problem to establish the existence and uniqueness of a PTW solution and its propagation speed for arbitrary $u_c \in (0,1)$. Moreover, it would be interesting to examine the rate of convergence of the solution onto a PTW structure.

Another interesting topic of future work concerns the stochastic randomly perturbed KPP equation, whose dimensional form was given by equation (1.1.28) for the specific case of a Fisher reaction. Results regarding the large-time solution to (1.1.28) have recently been obtained by Mueller, Mytnik and Quastel [42] who proved that the speed of propagation is given by

$$\hat{v}(\hat{u}_c) = \sqrt{\frac{\kappa f'(0)}{\tau}}\left[2 - \frac{\pi^2}{(\ln \hat{u}_c)^2} + O\left(\frac{\ln|\ln \hat{u}_c|}{|\ln \hat{u}_c|^3}\right)\right], \quad \text{as} \quad \hat{u}_c \to 0^+. \tag{9.0.2}$$

The difference between the non-dimensional speed $\tilde{v}(\tilde{u}_c) = \sqrt{\tau/\kappa f'(0)}\hat{v}(\hat{u}_c)$ obtained from this model and $v^*(u_c)$ obtained from the deterministic cut-off model [QIVP], on taking $\tilde{u}_c \sim u_c$, only arises in the order of the error as both u_c and $\tilde{u}_c \to 0^+$. The two models behave very differently when u_c and $\tilde{u}_c$ can no longer be regarded as small, as might be anticipated. In this case, Doering, Mueller and Smereka [18] conjectured that the speed of propagation is given by $\tilde{v}(\tilde{u}_c) \sim 2/\tilde{u}_c$, as $\tilde{u}_c \to \infty$. The behaviour in this limit should be contrasted against expression (4.4.17) obtained for $u_c \to 1^-$. A comparison suggests that $\tilde{u}_c$ and u_c may in this case be related according to $\tilde{u}_c \sim 2/(1-u_c)$ as $u_c \to 1^-$. However, it remains to determine how the asymptotic structure of the solution to (1.1.28) evolves in time and, in particular, what is the rate of convergence onto the travelling front solution in large-time.

With regards to the second problem, the effect of introducing a background flow on PTW solutions to reaction–diffusion models with cut-off type reaction functions is a new topic and, as such, there are many questions that remain to be investigated. To begin, a rigorous proof of the existence and uniqueness of a PTWF solution in the presence of a background shear flow is required. We have already mentioned the need to investigate a

wider range of parameter values and shear flows as an immediate extension to Chapter 8. Furthermore, it would be interesting to examine the rate of convergence of the solution onto the PTWF.

Advection by a shear flow is the simplest example of the impact of a heterogeneous environment on a PTW solution to a homogeneous reaction–diffusion equation. We anticipate that the approach developed in this thesis will be readily adaptable when the shear flow is replaced by more complicated spatially periodic flow such as the ones considered in the review by Majda and Kramer [38]. For such periodic flows, we have to replace the notion of PTWF solutions by pulsating front solutions which change periodically with respect to time. It would be very interesting to examine this in the context of a cut-off reaction function.

LIST OF REFERENCES

[1] A. A. Bensoussan, J. L. Lions, and G. Papanicolaou. *Asymptotic analysis for periodic structures*. North Holland, 1978.

[2] D. G. Aronson and J. Serrin. Local behavior of solutions of quasilinear parabolic equations. *Arch. Rational Mech. Anal.*, 25(2):81–122, 1967.

[3] D. G. Aronson and H. F. Weinberger. *Nonlinear diffusion in population genetics, combustion, and nerve pulse propagation*, volume 446. Springer, Heidelberg, 1975.

[4] D. Bargteil and T. Solomon. Barriers to front propagation in ordered and disordered vortex flows. *Chaos*, 22(3):037103, 2012.

[5] H. Berestycki. The influence of advection on the propagation of fronts in reaction–diffusion equations. In H. Berestycki and Y. Pomeau, editors, *Nonlinear PDEs in Condensed Matter and Reactive Flows*, volume 569 of *NATO Science Series C*. Kluwer, Doordrecht, 2003.

[6] H. Berestycki and F. Hamel. Front propagation in periodic excitable media. *Comm. Pure Appl. Math.*, 55(8):949–1032, 2002.

[7] H. Berestycki, F. Hamel, and N. Nadirashvili. Propagation speed for reaction–diffusion equations in general domains. *C. R. Acad. Sci. Paris*, 339:163–168, 2004.

[8] H. Berestycki, F. Hamel, and N. Nadirashvili. The speed of propagation for KPP type problems. I: Periodic framework. *J. Eur. Math. Soc.*, 7(2):173–213, 2005.

[9] H. Berestycki and L. Nirenberg. Travelling fronts in cyclinders. *Ann. I. H. Poincaré*, 9:497–572, 1992.

[10] J. Billingham and D. J. Needham. The development of travelling waves in quadratic and cubic autocatalysis with unequal diffusion rates. III. Large time development in quadratic autocatalysis. *Q. Appl. Math.*, 2:343–372, 1992.

[11] M. Bramson. Maximal displacement of branching Brownian motion. *Comm. Pure Appl. Math.*, 31(285):531–581, 1978.

[12] M. Bramson. Convergence of solutions of the Kolmogorov equation to travelling waves. *Mem. Am. Math. Soc.*, 44(285), 1983.

[13] N. F. Britton. *Reaction–diffusion equations and their applications to biology.* Academic Press Inc., 1986.

[14] E. Brunet and B. Derrida. Shift in the velocity of a front due to a cut-off. *Phys. Rev. E.*, 56(3):2597 – 2604, 1997.

[15] A. J. Chorin. Numerical solution of the Navier-Stokes equations. *Math. Comp.*, 22:745–762, 1968.

[16] P. Constantin, A. Kiselev, A. Oberman, and L. Ryzhik. Bulk burning rate in passive-reactive diffusion. *Arch. Ration. Mech. An.*, 154:53–91, 2000.

[17] M. Dentz, T. Le Borgne, A. Englert, and B. Bijeljic. Mixing, spreading and reaction in heterogeneous media: A brief review. *J. Contam Hydrol.*, 120-121:1 – 17, 2011. Reactive Transport in the Subsurface: Mixing, Spreading and Reaction in Heterogeneous Media.

[18] C. D. Doering, C. Mueller, and P. Smereka. Interacting particles, the stochastic Fisher-Kolmogorov-Petrovskii-Piscounov equation, and duality. 325:243–259, 2003.

[19] F. Dumortier, N. Popovic, and T. J. Kaper. The critical wave speed for the Fisher-Kolmogorov-Petrovskii-Piscounov equation with cut-off. *Nonlinearity*, 20(4):855–877, 2007.

[20] F. Dumortier, N. Popovic, and T. J. Kaper. A geometric approach to bistable front propagation in scalar reaction–diffusion equations with cut-off. *Phys. D*, 239:1984–1999, 2010.

[21] U. Ebert and W. van Saarloos. Front propagation into unstable states: universal algebraic convergence towards uniformly translating pulled fronts. *Physica D: Nonlinear Phenomena*, 146(1–4):1–99, 2000.

[22] A. Fick. On liquid diffusion - an english reprint of the original 1855 german article. *J. Membr. Sci.*, 100:33–38, 1995.

[23] P. C. Fife. *Mathematical Aspects of Reacting and Diffusing Systems*. Springer-Verlag, Berlin, 1979.

[24] P. C. Fife and J. McLeod. The approach of solutions of nonlinear diffusion equations to traveling front solutions. *Arch. Ration. Mech. Anal.*, 65:335–361, 1977.

[25] R. A. Fisher. The wave of advance of advantageous genes. *Ann. Eugenics*, 7(4):355–369, 1937.

[26] M. I. Friedlin. *Functional Integration and Partial Differential Equations*. Princeton University Press, 1985.

[27] R. A. Gardner. Existence of multidimensional travelling wave solutions of an initial boundary value problem. *J. Differential Equations*, 61:335–379, 1986.

[28] J. Gärtner and M. I. Freidlin. On the propagation of concentration waves in periodic and random media. *Soviet Math. Dokl.*, 20(2):1282–1286, 1979.

[29] D. Gilbarg and N. S. Trudinger. *Elliptic Partial Differential Equations of Second Order*. Springer, 1983.

[30] K. P. Hadeler and F. Rothe. Travelling fronts in nonlinear diffusion equations. *J. Math. Biol.*, 2:251–263, 1975.

[31] F. Hamel, J. Nolen, J-M Roquejoffre, and L. Ryzhik. A short proof of the logarithmic Bramson correction in Fisher–KPP equations. *Networks & Heterogeneous Media*, 8(1):275, 2013.

[32] P. H. Haynes and J. Vanneste. Dispersion in the large-deviation regime. Part 1: shear flows and periodic flows. *J. Fluid Mech.*, 745:321–350, 2014.

[33] D. A. Kessler, Z. Ner, and L. M. Sander. Front propagation: Precursors, cutoffs, and structural stability. *Phys. Rev. E*, 58:107–114, 1998.

[34] A. N. Kolmogorov, I. G. Petrovsky, and N. S. Piskunov. Étude de l'équation de la diffusion avec croissance de la quantité de matière et son application à un problème biologique. *Bull. Univ. Moskov. Ser. Internat. Sect.*, 1:1–25, 1937.

[35] D. A. Larson. Transient bounds and time-asymptotic behaviour of solutions to nonlinear equations of Fisher type. *SIAM J. Appl. Math.*, 34:93–103, 1978.

[36] J. A. Leach and D. J. Needham. *Matched Asymptotic Expansions in Reaction–Diffusion Theory*. Springer Monographs in Mathematics, 2003.

[37] R. J. Leveque. *Finite Volume Methods for Hyperbolic Problems*. Cambridge University Press, 2002.

[38] A. J. Majda and P. R. Kramer. Simplified models for turbulent diffusion: Theory, numerical modelling, and physical phenomena. *Phys. Rep.*, 314(4–5):237 – 574, 1999.

[39] H. P. McKean. Application of brownian motion to the equation of Kolmogorov-Petrovskii-Piskunov. *Comm. Pur. Appl. Math.*, 28(3):323–331, 1975.

[40] H. P. McKean. A correction to "Application of brownian motion to the equation of Kolmogorov-Petrovskii-Piskunov". *Comm. Pur. Appl. Math.*, 29(5):553–554, 1976.

[41] K. W. Morton and D. Mayers. *Numerical solution of partial differential equations*. Cambridge University Press, 2005.

[42] C. Mueller, L. Mytnik, and J. Quastel. Effect of noise on front propagation in reaction–diffusion equations of KPP type. *J. Invent. Math.*, 184(2):405–453, 2011.

[43] J. D. Murray. *Mathematical Biology I: An introduction*. Springer-Verlag, 3rd edition, 2002.

[44] J. Nagumo, S. Arimoto, and S. Yoshiwaza. An active pulse transmission line simulating nerve axon. *Proc. IRE*, 50(10):2061–2070, 1962.

[45] D. J. Needham. A formal theory concerning the generation and propagation of travelling wave-fronts in reaction–diffusion equations. *Quart. J. Mech. Appl. Math.*, 45:469–498, 1992.

[46] Z. Neufeld and E. Hernández-Garcia. *Chemical and Biological Processes in Fluid Flows: A Dynamical Systems Approach*. Imperial College Press, 2009.

[47] J. Nolen, M. Rudd, and J. Xin. Existence of KPP fronts in spatially-temporally periodic advection and variational principle for propagation speeds. *Dyn. Partial Differ. Equ.*, 2:1–24, 2005.

[48] J. Nolen and J. Xin. Reaction–diffusion front speeds in spatially-temporally periodic shear flows. *Multiscale Model. Simul.*, 1:554–570, 2003.

[49] G. A. Pavliotis and A. M. Stuart. *Multiscale Methods: Averaging and Homogenization*. Springer, 2007.

[50] A. Pocheau and F. Harambat. Front propagation in a laminar cellular flow: Shapes, velocities, and least time criterion. *Phys. Rev. E*, 77:036304, 2008.

[51] M. E. Schwartz and T. H. Solomon. Chemical reaction fronts in ordered and disordered cellular flows with opposing winds. *Phys. Rev. Lett.*, 100:028302, Jan 2008.

[52] J. Smoller. *Shock Waves and Reaction–Diffusion equations*. Springer, Berlin, 1989.

[53] A. Stevens, G. Papanicolaou, and S. Heinze. Variational principles for propagation speeds in inhomogeneous media. *SIAM J. Appl. Math.*, 62(1):129–148, 2001.

[54] T. Tél, A. de Moura, C. Grebogi, and G. Károlyi. Chemical and biological activity in open flows: A dynamical systems approach. *Phys. Rep.*, 413:91–196, 2005.

[55] F. Tesser and C. R. Doering. *Discrete and Continuum Dynamics of Reacting and Interacting Individuals. In: Muntean A., Toschi F. (eds) Collective Dynamics from Bacteria to Crowds. CISM International Centre for Mechanical Sciences*, volume 553. Springer, Vienna, 2014.

[56] B. W. Thompson, J. Novak, M. C. T. Wilson, M. M. Britton, and A. F. Taylor. Inward propagating chemical waves in Taylor vortices. *Phys. Rev. E*, 81:047101, 2010.

[57] A. Tzella and J. Vanneste. FKPP fronts in cellular flows: The large-Péclet regime. *SIAM J. Appl. Math*, 75:1789–1816, June 2015.

[58] M. Van Dyke. *Perturbation Methods in Fluid Mechanics*. Parabolic Press, 1975.

[59] F. Verhulst. *Nonlinear Differential Equations and Dynamical Systems*. Springer, 1990.

[60] H. F. Weinberger. On spreading speeds and traveling waves for growth and migration models in a periodic habitat. *J. Math. Biol.*, 46(2):190–190, 2002.

[61] J. Xin. Front propagation in heterogeneous media. *SIAM Rev.*, 42(2):161–230, 2000.

[62] A. Zlatoš. Sharp asymptotics for KPP pulsating front speed-up and diffusion enhancement by flows. *Arch. Ration. Mech. Anal.*, 195(2):441–453, 2010.